ORGANIC MATURATION AND SOURCE ROCK POTENTIAL OF MESOZOIC AND TERTIARY STRATA, QUEEN CHARLOTTE ISLANDS, BRITISH COLUMBIA

BY

DAVID VELLUTINI

B.A.Sc. The University of British Columbia, 1986

A THESIS SUBMITTED IN PARTIAL FULFILLMENT OF THE

REQUIREMENTS FOR THE DEGREE OF MASTER OF APPLIED SCIENCE

IN

THE FACULTY OF GRADUATE STUDIES

(Department of Geological Sciences)

We accept this thesis as conforming to the required standard

THE UNIVERSITY OF BRITISH COLUMBIA

OCTOBER, 1988

Department of _____

The University of British Columbia
Vancouver, Canada

Date _____

ABSTRACT

The level of organic maturation, thermal history, and source rock potential of Mesozoic and Tertiary strata in the Queen Charlotte Islands have been investigated with vitrinite reflectance measurements ($\%Ro_{rand}$), numerical modelling (modified Arrhenius and Lopatin models), and Rock-Eval pyrolysis (source rock potential). The level of organic maturation increases from north to south and is primarily controlled by high heat flow associated with plutonism on Moresby Island. Upper Triassic-Lower Jurassic strata are overmature on Moresby Island with vitrinite reflectance values ranging from 2.40 to 5.80 $\%Ro_{rand}$. Jurassic, Cretaceous, and Tertiary strata are immature to overmature on Graham Island with values ranging from 0.15 $\%Ro_{rand}$ (Skonun Formation) to 2.43 $\%Ro_{rand}$ (Haida Formation).

Constant and variable geothermal gradient thermal regimes were numerically modelled with modified Arrhenius and Lopatin methods. Numerical modelling (assuming constant geothermal gradients) predicts high paleogeothermal gradients (45 to 90 $^{o}C/km$) for up to 180 million years from the Late Triassic to the Tertiary. Variable paleogeothermal gradient modelling (utilizing a 30 $^{o}C/km$ background geothermal gradient) predicts peak geothermal gradients ranging up to 150 $^{o}C/km$ during Yakoun (183-178 Ma) and Masset (35-10 Ma) volcanism.

The timing of hydrocarbon generation was estimated with numerical modelling. The levels of organic maturation for Mesozoic and Tertiary strata reflect the timing of plutonism and associated high heat flow. Triassic strata from west Graham Island and Cretaceous strata from north and south Graham Island entered the oil window during the Early Miocene and are still in the oil window. Jurassic strata in central Graham Island and north Moresby Island entered the oil window during the Bajocian and remain within the oil window. The Skonun Formation is generally immature except for strata at west Graham Island (Port Louis well) and at northeast Graham Island (basal strata in the Tow Hill well) which entered the oil window during the Late Miocene.

Mean total organic carbon (TOC) contents are generally low (0.06 %) to moderately high (3.6 %) for Mesozoic and Tertiary strata. Some organic-rich horizons with TOC values up to 11.2 % occur in Upper Triassic (black limestone member of the Kunga Group) and Lower Jurassic (Sandilands and Ghost Creek Formations) source strata. Mesozoic and Tertiary strata generally contain gas prone Type III organic matter except for the Lower Jurassic Ghost Creek Formation and the Upper Triassic-Lower Jurassic Kunga Group which contain oil and gas prone Type II organic matter and significant amounts of oil prone Type I organic matter.

Lateral variations in TOC and the quality of organic matter (QOM) for Triassic and Jurassic strata are primarily related to the level of organic maturation. The strata have poor to good hydrocarbon source potential on Graham Island. High heat flow associated with plutonism on Moresby Island has overmatured the strata resulting in poor source potential on Moresby Island.

Hydrocarbon source potential for Cretaceous and Tertiary strata is primarily controlled by the level of organic maturation and depositional patterns. The Cretaceous Haida and Honna Formation generally contain terrestrially derived Type III organic matter with poor to fair gas source potential. The Skidegate Formation contains a mixture of Types II and III organic matter with decreased (terrestrial) Type III organic matter input and increased Type II (marine) organic matter input relative to the Haida Formation. Cretaceous strata from Moresby Island are generally overmature and have poor source potential whereas equivalent strata from Graham Island are immature to overmature and have fair to moderate gas source potential. Generally immature coal and lignite from the Tertiary Skonun Formation have poor to fair gas source potential. Resinite horizons containing hydrogen-rich organic matter have good oil and gas source potential where mature. Siltstone and shale facies of the Skonun Formation contain moderate amounts of Type II organic matter and have good hydrocarbon source potential.

TABLE OF CONTENTS

LIST OF FIGURES

LIST OF TABLES

ACKNOWLEDGEMENT

The author is grateful to the thesis supervisor, Dr. R.M. Bustin, for his apt supervision and patience. The author also acknowledges the financial support provided by Energy, Mines, and Resources Canada, NSERC grant (A7337) to R.M. Bustin, Chevron Resources Ltd., and Amoco Canada. Special thanks are also due to B.E.B. Cameron, M. Orchard, and C. Hickson for access to their extensive sample collections. The assistance of the U.B.C. Geology Department Technicians is gratefully appreciated.

INTRODUCTION

Evaluation of the petroleum potential of frontier sedimentary basins is an important part of hydrocarbon exploration and requires knowledge concerning the distribution, quality, and level of organic maturation of potential source and reservoir strata. Factors controlling hydrocarbon source potential include the quality, quantity, and degree of organic maturation (DOM) of the organic matter. The level of organic maturation of the strata is influenced primarily by temperature and time (Dow, 1977; Waples, 1980). In the Queen Charlotte Islands, Bustin and Macauley (1988) have identified Lower Jurassic potential source rocks and oil seeps from outcrop sections and exploration wells. The source rock quality and DOM of the Mesozoic and Tertiary sedimentary succession of the Queen Charlotte Islands and adjacent offshore basins, however, have received only limited study.

The following study is divided into two parts. In the first part, the DOM of the Mesozoic and Tertiary strata is documented and modelled in order to establish thermal histories of the strata and to predict the timing of hydrocarbon generation. In the second part, the abundance and type of organic matter within the strata are investigated in order to establish the petroleum source rock quality.

REGIONAL GEOLOGY OF THE QUEEN CHARLOTTE ISLANDS

The Queen Charlotte Islands consist of two main islands, Graham Island to the north and Moresby Island to the south, along with numerous small islands between 51^{O} N, 131^{O} W, and 54^{O} N, 134^{O} W (Figure 1). Sutherland Brown (1968) published the first comprehensive geologic study of the Queen Charlotte Islands; included in this report were regional geologic maps (1:125 000) and stratigraphic, structural, and economic assessments of the exposed and subsurface lithologic units.

The Queen Charlotte Islands are part of the Wrangellia tectonostratigraphic terrane and share a similar Late Paleozoic (?), Triassic, and Jurassic tectonic and stratigraphic history with Vancouver Island and parts of southern Alaska (Figure 2). The Queen Charlotte Islands include a diverse sequence of

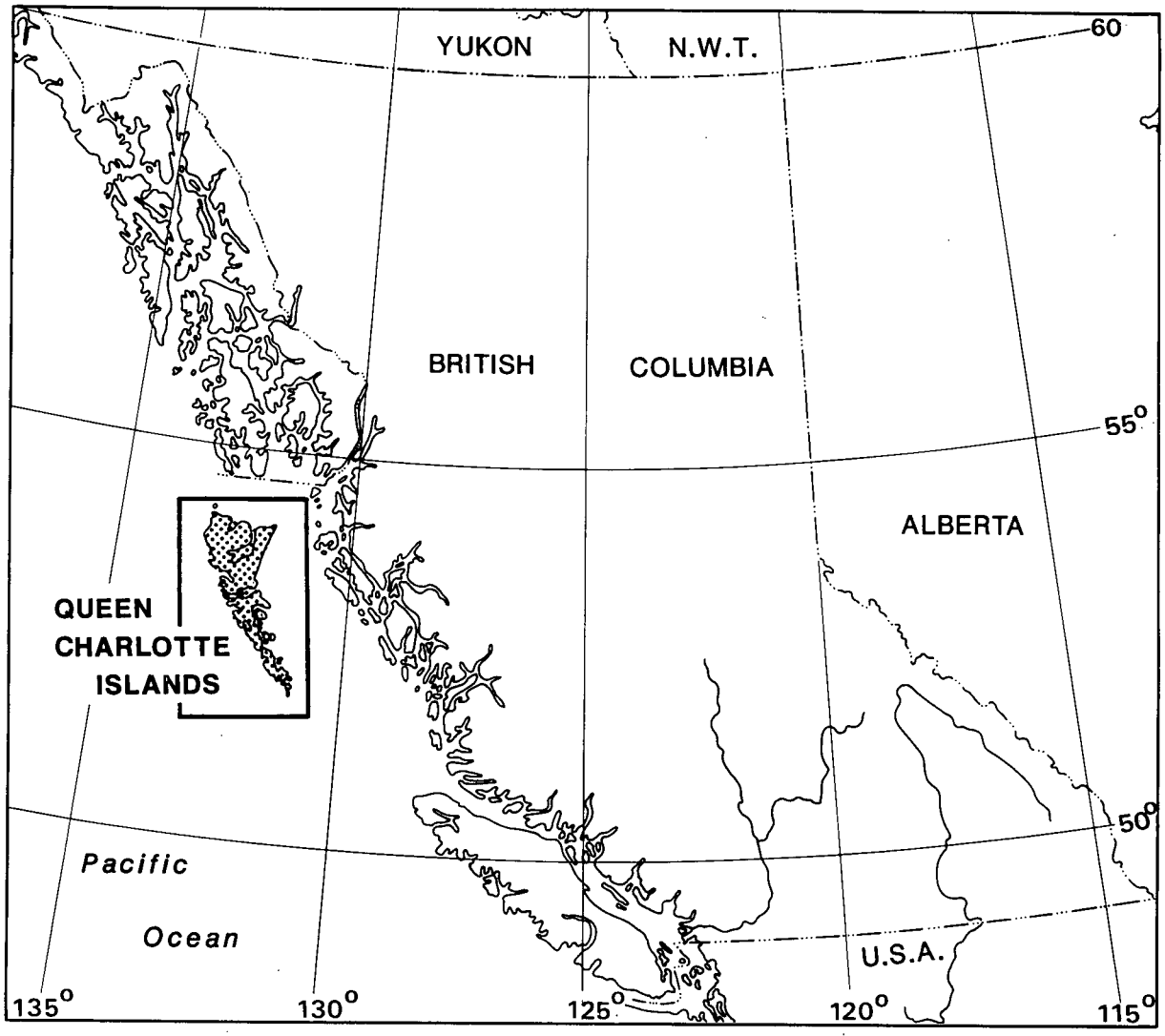

Figure 1. Location map of British Columbia showing the Queen Charlotte Islands study area

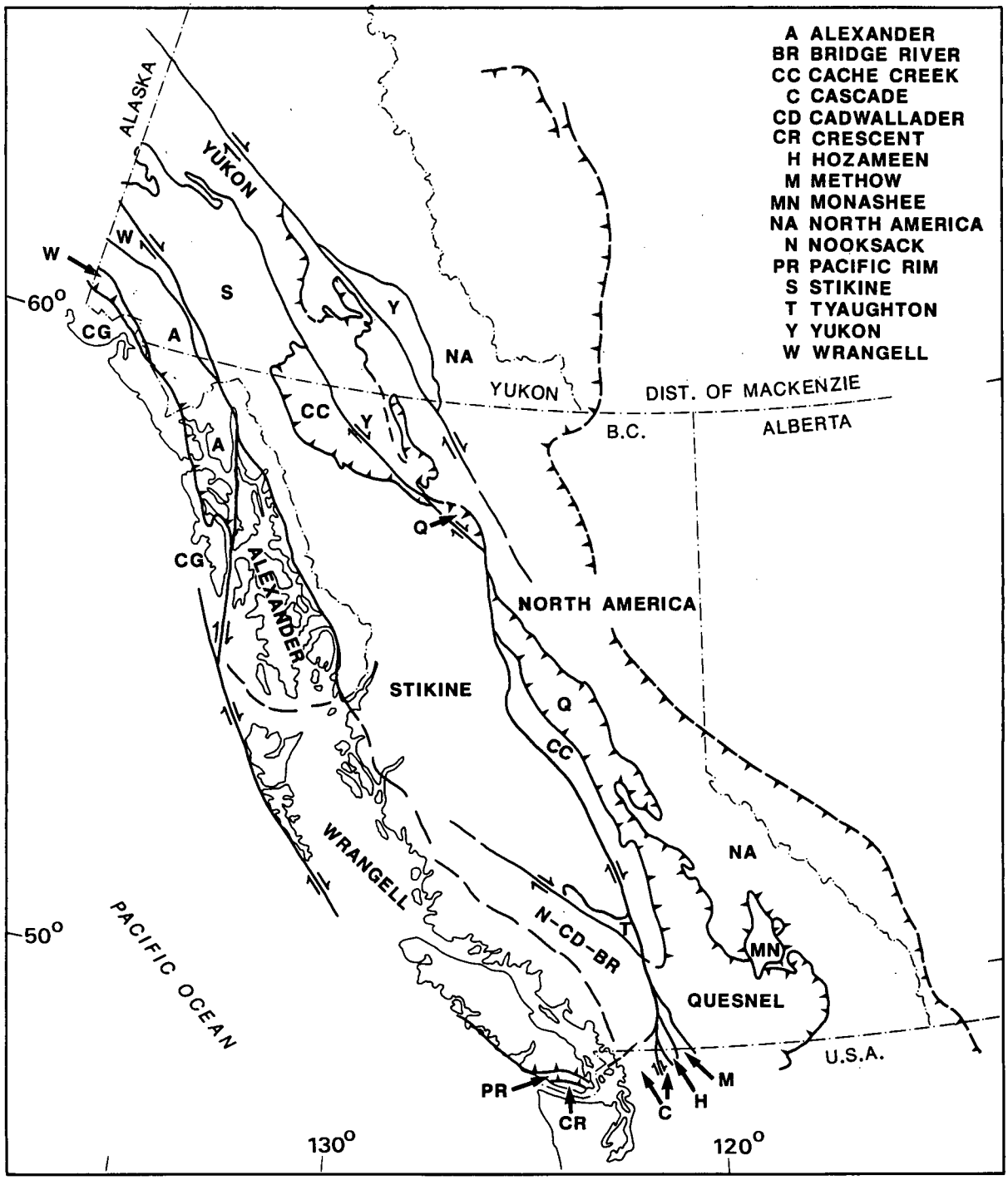

Figure 2. Tectonostratigraphic terrane map of western Canada (Armstrong, 1988)

sedimentary, volcanic, and plutonic rocks which range in age from Triassic to Recent. The plutonic rocks are predominantly exposed on Moresby Island and the western part of Graham Island; the volcanic and sedimentary rocks crop out in most areas of the Queen Charlotte Islands and underlie Hecate Strait. The following tectonic history and stratigraphic summary are based mainly on the work of Sutherland Brown (1968), Cameron and Tipper (1985), and Cameron and Hamilton (1988).

Stratigraphy

Strata of the Queen Charlotte Islands range in age from Late Triassic to Recent. The succession is dominated by volcanic rocks with interbedded marine and terrigenous strata (Figure 3). Triassic through Jurassic deposition was nearly continuous and the strata can be correlated with Wrangellian equivalents on Vancouver Island and southern Alaska. The Cretaceous and Tertiary strata, however are unique to the Queen Charlotte Islands and cannot be correlated with strata of equivalent age on Vancouver Island or southern Alaska. The Mesozoic and Tertiary stratigraphy of the Queen Charlotte Islands are summarized below.

KARMUTSEN FORMATION

The oldest lithologic unit exposed on the Queen Charlotte Islands is the Triassic Karmutsen Formation. The strata consist of more than 4 000 m of tholeiitic lavas comprising chloritized greenstone, amygdaloidal basalt, pillow lava and breccia, aquagene tuff, and minor limestone intercalations (Sutherland Brown, 1968). The Karmutsen Formation also outcrops on Vancouver Island and Bonilla Island (east side of Hecate Strait) and has been correlated with the Nicolai Greenstone of the Wrangell Mountains of southern Alaska (Muller, 1977; Jones et al., 1977; Woodsworth, 1988).

The Karmutsen lavas have been interpreted by various authors as oceanic crust originating from an

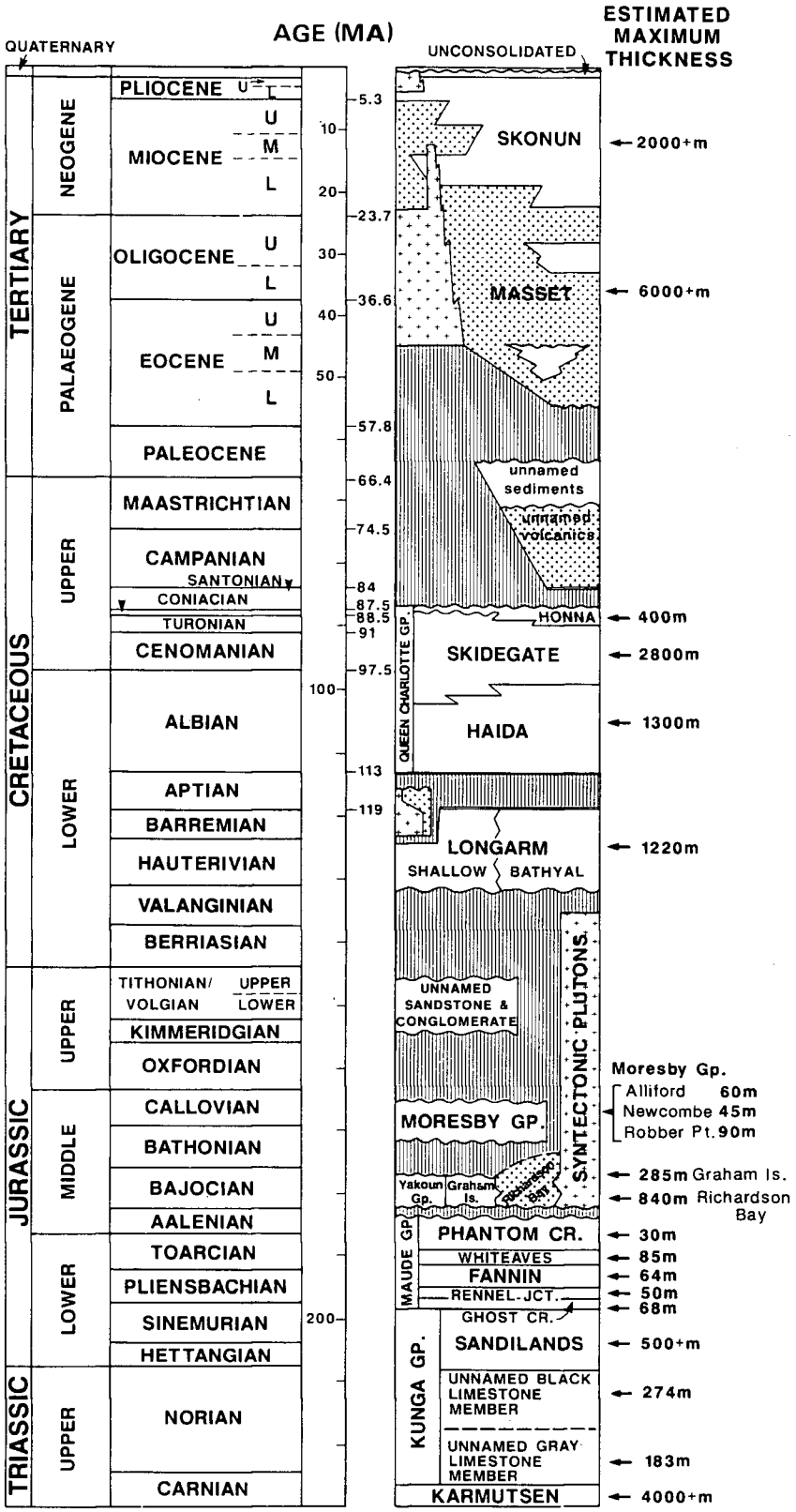

Figure 3. Stratigraphic column of Mesozoic and Tertiary strata for the Queen Charlotte Islands (modified from Cameron and Hamilton, 1988)

oceanic ridge, island arc, or marginal-interarc basin which was erupted subaqueously over a broad, low relief surface (Sutherland Brown, 1968; Monger et al., 1972; Muller et al., 1974; Souther, 1977).

The age of the Karmutsen Formation has not been positively determined. The top of the Formation is overlain conformably by Upper Carnian limestones of the Kunga Group. The base of the Karmutsen Formation is not known on the Queen Charlotte Islands but is probably Early or Middle Triassic, similar to the Karmutsen Formation on Vancouver Island (Sutherland Brown, 1968). Some crinoidal limestone found near the base of the Karmutsen in Hutton Inlet may be as old as Permian (Sutherland Brown, 1968).

KUNGA GROUP

The Kunga Group conformably overlies the Karmutsen Formation and consists primarily of limestone and argillite with some siltstone and sandstone. The strata range in age from Late Carnian to Late Sinemurian (Sutherland Brown, 1968). The Kunga Group was deposited on a stable carbonate platform remote from volcanic sources during a period of initial volcanic quiescence during the Late Triassic followed by arc related volcanism in the Sinemurian (Late Carnian and Norian) (Sutherland Brown, 1968; Cameron and Tipper, 1985). The Kunga Group has been divided by Cameron and Tipper (1985) into the Sandilands Formation and two informal members, a grey limestone member and a black limestone member.

Grey Limestone Member

The Upper Carnian grey limestone member consists of massive, crystalline, limestone with poorly preserved corals, pelecypods, gastropods, and ammonites (Sutherland Brown, 1968). Grainstone interbeds or lenses and silicified burrows are common near the top of the unit. The grey limestone was deposited on a stable carbonate shelf isolated from clastic and volcanic sediments (Sutherland Brown, 1968).

Middle Limestone Member

The Lower to Upper Norian middle limestone member consists of thinly bedded, pyritic, flaggy, black, bituminous limestone with cross-bedded calcarenite and minor argillite, limestone conglomerate, and sandstone (Sutherland Brown, 1968). The beds are finely laminated with abundant *Halobia* and *Monotis* and may contain concretionary horizons. The middle limestone member was deposited in a partly euxinic basin with some clastic input but remote from volcanic tuffaceous sources (Sutherland Brown, 1968).

Sandilands Formation

The Hettangian (?) to Sinemurian Sandilands Formation conformably overlies the middle limestone member and consists of thinly bedded siliceous siltstone and sandstone (or argillite) with interbedded ash-fall tuff, grey-green shale, and thin black shale laminations (Cameron and Tipper, 1985). Thin, interbedded limestone lenses and sedimentary structures (cross-bedding, bioturbation) are rare (Sutherland Brown, 1968). Fauna consist mainly of pelagic pelecypods and ammonites with few foraminifers. Thin, continuous bedding with regular tuffaceous interbeds and abundant pyrite suggest deposition in a relatively deep, partly euxinic basin which received ash-fall tuffs from remote volcanic sources (Cameron and Tipper, 1985).

MAUDE GROUP

The Pliensbachian-Aalenian Maude Group consists of fossiliferous argillite, shale, calcareous shale, lithic sandstone, and minor limestone lenses. The Maude Group, where present, conformably and gradationally overlies the Kunga Group (Sutherland Brown, 1968). Cameron and Tipper (1985) have divided the Maude Group into five formations which from base to top are: Ghost Creek, Rennell Junction, Fannin, Whiteaves, and Phantom Creek Formations.

Ghost Creek Formation

The Lower Pliensbachian Ghost Creek Formation consists of pyritic, bituminous, fetid, dark grey shale with minor silty shale and limestone lenses (Cameron and Tipper, 1985). The Ghost Creek Formation conformably overlies the Sandilands Formation (Kunga Group) from which it is distinguished by the paucity of ash-fall tuff and by a higher proportion of shale in the Ghost Creek Formation (Cameron and Tipper, 1985). Deposition of the Ghost Creek Formation occurred in a deep, partly euxinic basin which was characterized by an abundant pelagic fauna (ammonites, belemnites) and few benthic fauna. Rare ash-fall tuff interbeds suggest decreased volcanism from the Sinemurian to the Early Pliensbachian (Cameron and Tipper, 1985).

Rennell Junction Formation

The Lower Pliensbachian Rennell Junction Formation consists of fine grained, flaggy sandstone, argillaceous siltstone, grey shale, and minor limestone lenses (Cameron and Tipper, 1985). The shale at the base is glauconitic and grades into siltstone and sandstone near the top. The Rennell Junction Formation conformably overlies the Ghost Creek Formation and contains more siltstone and less bituminous grey shale than the Ghost Creek Formation (Cameron and Tipper, 1985). Biostratigraphic studies suggest that the Rennell Junction Formation represented the progressive infilling of a deep marine basin (Cameron and Tipper, 1985).

Fannin Formation

The Upper Pliensbachian-Lower Toarcian Fannin Formation is a heterogeneous sedimentary succession of tuffaceous and calcareous sandstone with minor siltstone and rare shale (Cameron and Tipper, 1985). In the upper part of the Fannin Formation, abundant chamosite ooliths occur in an argillaceous matrix (Cameron and Tipper, 1985). The formation was deposited in a shallow, high energy environment at

the peak of a regressive cycle (Cameron and Tipper, 1985). Cameron and Tipper (1985) suggest that chamosite ooliths reflect deposition near a warm, humid landmass.

Whiteaves Formation

The Middle Toarcian Whiteaves Formation consists of carbonaceous, silty shale with minor interbedded argillaceous sandstone and nodular limestone (Cameron and Tipper, 1985). The Whiteaves Formation unconformably overlies the Fannin Formation which is marked by an abrupt lithologic change from sandstone to shale (Cameron and Tipper, 1985). The base of the Whiteaves Formation contains abundant glauconite and septarian nodules. In the upper half of the unit, glauconite is less abundant and septarian nodules are rare (Cameron and Tipper, 1985). According to biostratigraphic studies, the Whiteaves Formation was deposited following a regression (marked by the erosional hiatus at the top of the Fannin Formation) by rapidly transgressing seas (Cameron and Tipper, 1985).

Phantom Creek Formation

The Upper Toarcian Phantom Creek Formation consists of partly calcareous and argillaceous fine- to coarse-grained sandstone (Cameron and Tipper, 1985). The sandstone is fossiliferous with abundant ammonites, bivalves, and belemnites. The Phantom Creek Formation paraconformably overlies the Whiteaves Formation (Cameron and Tipper, 1985). The lower part of the Phantom Creek Formation was deposited at the peak of a regression which began towards the end of Whiteaves Formation deposition (Cameron and Tipper, 1985). The upper part of the Phantom Creek Formation represents sedimentation during a transgression with very little tuffaceous ash-fall (Cameron and Tipper, 1985).

YAKOUN GROUP

Diverse strata of the Lower Bajocian Yakoun Group reflects greatly increased volcanic activity as a result of amalgamation between the Wrangellia and Alexander terranes (Cameron and Tipper, 1985). The

degree of volcanic input in the strata varies with the proximity to volcanic sources (Cameron and Tipper, 1985). The Yakoun Group is divided into the Graham Island and Richardson Bay Formations (Cameron and Tipper, 1985).

Graham Island Formation

The Lower Bajocian Graham Island Formation is a heterogeneous unit composed of shale, tuff, and volcanic sandstone. The formation comprises a wide range of lithologies which reflect varying proximity to volcanic sources (Cameron and Tipper, 1985). The Graham Island Formation in central Graham Island is divided into two members, the shale tuff and mottled siltstone member. In Skidegate Inlet, the lithologies of the Graham Island Formation are different than in central Graham Island, but they are in part coeval. The formation in Skidegate Inlet is divided informally into the volcanic sandstone and lapilli members (Cameron and Tipper, 1985).

The shale tuff and mottled siltstone members consist of well-bedded bituminous shale, argillaceous and tuffaceous siltstone with minor cross-bedded sandstone (Cameron and Tipper, 1985).

The volcanic sandstone and lapilli tuff members consist of lapilli tuff and andesitic agglomerate in the Skidegate Inlet area and sandstone with minor siltstone in the central Graham Island area (Cameron and Tipper, 1985).

The shale tuff and mottled siltstone members were deposited in a partly euxinic, deep marine environment whereas the volcanic sandstone and lapilli members were deposited in a shallow marine or possibly non-marine environment (Cameron and Tipper, 1985).

Richardson Bay Formation

The Lower Bajocian Richardson Bay Formation is a widespread and thick succession of volcanic rocks. The thickness of the formation varies greatly (180 m to 760 m) depending on proximity to the volcanic source (Cameron and Tipper, 1985). The formation is divided into two informal members, the volcanic breccia member and the dark sandstone member (Cameron and Tipper, 1985). The volcanic breccia member consists of massive, poorly sorted porphyritic andesite breccia and tuff, whereas the dark sandstone member consists of carbonaceous sandstone, siltstone, and shale with abundant bivalves, plant debris, and coalified wood (Cameron and Tipper, 1985). The sediments grade laterally into volcanic detritus or volcanic breccia (Cameron and Tipper, 1985).

MORESBY GROUP

The Upper Bathonian to Lower Callovian Moresby Group contains conglomerate, sandstone, siltstone, and shale which unconformably overlie the Yakoun Group (Cameron and Tipper, 1985). The Moresby Group was deposited on an irregular basin surface after the cessation of Yakoun volcanism and partial erosion of Yakoun and older sediments (Cameron and Tipper, 1985). The sediments were deposited in a relatively shallow basin which supported abundant pelecypods and some ammonites (Cameron and Tipper, 1985).

The Moresby Group has been divided into three formations by Cameron and Tipper (1985) which from base to top are: Robber Point, Newcombe, and Alliford.

Robber Point Formation

The lithology of the Upper Bathonian Robber Point Formation varies from siltstone, tuffaceous siltstone, to volcanic breccia. The sediments contain abundant pelecypods, gastropods, ostracods, and foraminifers (Cameron and Tipper, 1985).

Newcombe Formation

The Upper Bathonian to Lower Callovian Newcombe Formation consists of well-bedded sandstone at the base grading into massive concretionary, volcaniclastic sandstone at the top. Some concretions contain pelecypods and rare belemnites or ammonites (Cameron and Tipper, 1985).

Alliford Formation

The Lower Callovian Alliford Formation consist of laminated siltstone with a fauna comprising pelecypods, ammonites, rare belemnites, ostracods, and foraminifers (Cameron and Tipper, 1985).

LONGARM FORMATION

The Upper Valanginian to Barremian Longarm Formation consists of calcareous siltstone, lithic greywacke, volcaniclastic sandstone, and pebble conglomerate with large *Inoceramus* shell fragments. Minor volcanic tuff and agglomerate occur at scattered localities (Sutherland Brown, 1968). The siltstone and greywacke of the Longarm Formation were deposited in a relatively deep water environment near the present Rennell Sound fold zone; and the sandstone and conglomerate were deposited in a shoreline environment (Sutherland Brown, 1968).

QUEEN CHARLOTTE GROUP

The Albian to Conacian Queen Charlotte Group is a thick succession (1 500 m to 2 000 m) of clastic sedimentary rocks which unconformably overlies the Longarm and older formations (Sutherland Brown, 1968; Haggart, 1987). Cameron and Hamilton (1988) divide the Queen Charlotte Group into the Haida, Skidegate, and Honna Formations (Cameron and Hamilton, 1988).

Haida Formation

The basal unit of the Queen Charlotte Group is composed of granular conglomerate, sandstone, siltstone, and silty shale (Sutherland Brown, 1968; Haggart, 1987). Fogarassy and Barnes (1988) have informally divided the Haida Formation into the basal Haida lithofacies, the lower Haida sandstone lithofacies, and the transitional Haida lithofacies. The basal lithofacies consists of granular conglomerate with interbedded pebbly sandstone, whereas the lower sandstone lithofacies consists of fine to medium grained carbonaceous sandstone, and the transitional lithofacies is composed of interbedded sandstone, siltstone, and silty shale (Fogarassy and Barnes, 1988).

Skidegate Formation

The Cenomanian to Turonian Skidegate Formation is composed of sandstone, siltstone, and shale (Haggart, 1987; Fogarassy and Barnes, 1988). The Skidegate Formation is divided into two informal units: the Skidegate shale lithofacies which consists of concretionary, silty shale; and the Skidegate sandstone-siltstone lithofacies which consists of thinly bedded, fine grained sandstone, siltstone, and shale (Fogarassy, pers. comm. 1988).

Honna Formation

The Conacian Honna Formation is composed of sandstone, siltstone, shale, and conglomerate (Haggart, 1987; Fogarassy and Barnes, 1988). The Honna Formation is divided into the basal Honna lithofacies, the middle Honna lithofacies, and the upper Honna lithofacies by Fogarassy and Barnes (1988).

The basal lithofacies consists of clast supported pebble and cobble conglomerate with lenticular sandstone. The middle lithofacies consists of sandstone, siltstone, and shale with interbedded conglomerate and massive sandstone whereas the upper lithofacies consists of clast supported pebble and cobble conglomerate with interbedded, lenticular sandstone (Fogarassy and Barnes, 1988).

Sutherland Brown (1968) suggests the Queen Charlotte Group was deposited in a marine, near shore environment with considerable submarine topography and an abundant supply of terrestrial organic detritus (Haida Formation). Much of the sediment were sourced from Yakoun volcanics and granitic plutons (Sutherland Brown, 1968). The Skidegate Formation was deposited in a deeper, near shore marine environment during a short transgressive episode. The Queen Charlotte Group was capped by the marine Honna Formation during a period of rapid uplift (Sutherland Brown, 1968).

MASSET FORMATION

The Oligocene to Miocene Masset Formation consists of mixed mafic and felsic volcanic flows with thin interflow breccias and rare diamictite channel deposits containing carbonized wood (Hickson, 1988). The felsic volcanics are predominantly welded lapilli tuffs (Hickson, 1988). Hamilton (1985) described the flows as subalkaline tholeiites, basaltic andesites, dacites, and rhyolites. The climax of Masset volcanism occurred 20 to 25 Ma, during the Late Oligocene to Early Miocene (Hickson, 1988). Hickson (1988) and Souther (1988) suggest that the areal extent of the Masset volcanics probably closely resembles the current outcrop distribution and did not extend appreciably under Hecate Strait.

SKONUN FORMATION

The Miocene to Pliocene Skonun Formation consists of a thick succession (1 800 m onshore and >3 000 m offshore) of alternating marine and non-marine sandstone, siltstone, and shale with some lignite, and coal (Sutherland Brown, 1968). Rare conglomerates occur at the base of the Skonun Formation at the Tow Hill well on northern Graham Island (Sutherland Brown, 1968). The Skonun Formation sediments are generally unconsolidated to poorly consolidated and are chemically and mechanically immature (Sutherland Brown, 1968).

The Skonun Formation was deposited in alternating marine (near shore) and non-marine (fluvial, deltaic) environments. Galloway (1974) suggests that Skonun Formation deposition post-dated the intrusion of the Coast Plutonic Complex and that the sediments, in part, were sourced from the unroofing of the plutons.

Tectonic History

The Karmutsen Formation and the Kunga, Maude, Yakoun, and Moresby Groups can be correlated with similar lithologic and stratigraphic units of Wrangellian affinities found on Vancouver Island and southern Alaska (Figure 2) (Sutherland Brown, 1968; Jones et al., 1977; Coney et al., 1980; Cameron and Tipper, 1985). Paleomagnetic data (Yole and Irving, 1980) from the Karmutsen volcanics suggest that Vancouver Island was located approximately 45^{O} ($\pm$ 15^{O}), or 3 000 km, south of its current position during Karmutsen volcanism in the Triassic. Similar paleomagnetic results from the Late Triassic Nicolai basalts of southern Alaska indicate 30^{O} of northward displacement of Wrangellian terranes (Hillhouse, 1977).

During the Sinemurian, a northwest trending volcanic arc developed offshore of the North American craton which lead to the deposition of interbedded ash-fall tuffs and shales of the Sandilands and Ghost Creek Formations in Early Jurassic shale basins (Cameron and Tipper, 1985). Following the Aalenian, regional uplift (corresponding to rifting between Gondwanaland and Laurasia) resulted in partial erosion of Lower Jurassic Maude Group sediments as represented by a regional unconformity at the top of the Maude Group (Cameron and Hamilton, 1988).

During the early Bajocian, the Yakoun Group volcanics erupted accompanying the amalgamation of Wrangellia and Alexander terranes. Yakoun volcanics may have been sourced from partial melting of Karmutsen volcanics and Upper Paleozoic sediments as a result of high heat flow related to subduction and terrane amalgamation (Sutherland Brown, 1968; Monger et al., 1972; Cameron and Hamilton, 1988).

Four plutonic suites (Figure 4) occur primarily on Moresby Island and on Graham Island (first studied in detail by Sutherland Brown, 1968, and later by Anderson, 1988). The Middle to Late Jurassic San Christoval and Burnaby Island Plutonic Suites are, in part coeval with, and successor to, the Yakoun Group volcanics (Cameron and Tipper, 1985). Skarn alteration (magnetite, chalcopyrite) and dense calcite veining associated with hydrothermal solutions are prevalent in the Burnaby Island Plutonic Suite. The emplacement of the plutonic suites was coeval with the Nevadan Orogeny (Anderson, 1988; Cameron and Hamilton, 1988). The Oligocene Kano and Carpenter Bay Plutonic Suites are possibly related to Masset Volcanism (Anderson, pers. comm., 1988).

During the Early Cretaceous (Valanginian-Aptian), the Longarm Formation was deposited while Wrangellia moved northward with the Farallon plate. Superterrane II (Quesnellia and Stikinia) accreted onto the North American craton during this time period (Cameron and Hamilton, 1988).

Following Aptian time, the Queen Charlotte Islands were in a fore-arc position and the Farallon plate began oblique subduction beneath the North American craton (Cameron and Hamilton, 1988). The Conacian Honna Formation sediments are considered to mark the amalgamation of the Wrangellia-Alexander terrane with the Taku terrane as well as the initiation of Kula-Farallon spreading (Cameron and Hamilton, 1988). During Conacian time, the Queen Charlotte Islands were at a latitude approximate opposite southern California (Irving et al., 1985). Northward movement of the Wrangellia-Alexander-Taku superterrane continued until its final accretion to North America during the Tertiary. Accretion of the Wrangellia-Alexander-Taku superterrane with North America is marked by a regional unconformity at the base of the Tertiary Masset volcanic succession (Cameron and Hamilton, 1988). Deposition of the Skonun Formation occurred syn- and post-Masset volcanism during the Miocene and Pliocene.

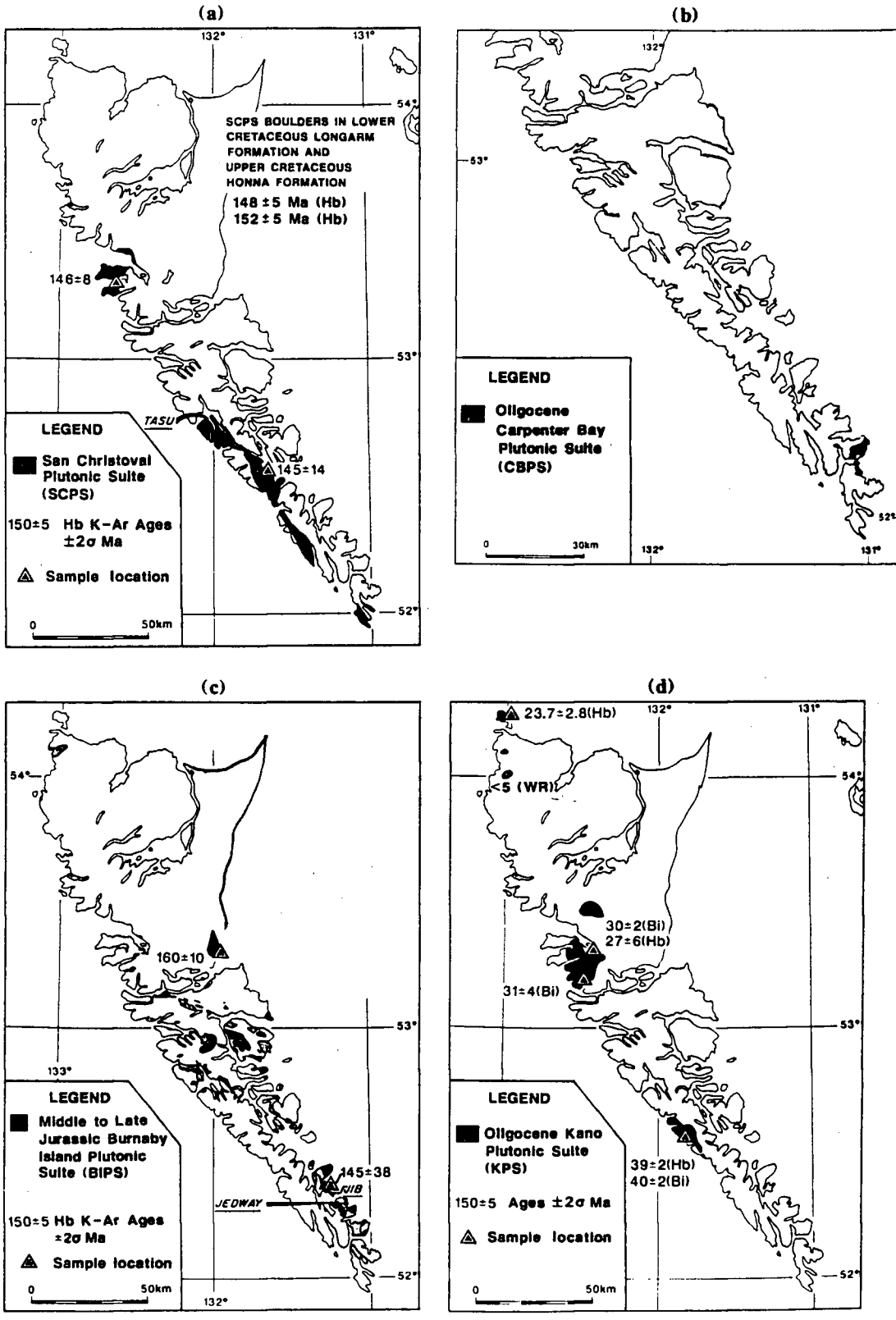

Figure 4. Regional map of the Queen Charlotte Islands showing four plutonic suites (modified from Anderson, 1988): a) Middle to Late Jurassic San Christoval Plutonic Suite (SCPS); b) Oligocene Carpenter Bay Plutonic Suite (CBPS); c) Middle to Late Jurassic Burnaby Island Plutonic Suite (BIPS); d) Oligocene Kano Plutonic Suite

REFERENCES

Anderson, R.G. 1988
Jurassic and Cretaceous-Tertiary plutonic rocks on the Queen Charlotte Islands, British Columbia; in Current Research, Part E, Geological Survey of Canada, Paper 88-1E, p. 213-216.

Armstrong, R.L. 1988
Mesozoic and Early Cenozoic magmatic evolution of the Canadian Cordillera: Special Paper 218, Geological Society of America, p. 55-91

Cameron, B.E.B. 1987
Significance of Lower Jurassic hydrocarbon source rocks in the Cumshewa Inlet area, Queen Charlotte Islands, British Columbia; in Current Research, Part A, Geological Survey of Canada, Paper 87-1A, p. 925-928.

Cameron, B.E.B. and Tipper, H.W. 1985
Jurassic stratigraphy of the Queen Charlotte Islands, British Columbia; Geological Survey of Canada, Bulletin, v. 365, 49 p.

Cameron, B.E.B. and Hamilton, T.S. 1988
Contributions to the stratigraphy and tectonics of the Queen Charlotte Basin, British Columbia; in Current Research, Part E, Geological Survey of Canada, Paper 88-1E, p. 221-227.

Coney, P.J., Jones, D.L., and Monger, J.W.H. 1980
Cordilleran suspect terranes; Nature, v. 288, p. 329-333.

Fogarassy, J.A.S. and Barnes, W.C. 1988
Stratigraphy, diagenesis and petroleum reservoir potential of the mid- to Upper Cretaceous Haida and Honna formations of the Queen Charlotte Islands, British Columbia; in Current Research, Part E, Geological Survey of Canada, Paper 88-1E, p. 265-268.

Galloway, W.E. 1974
Deposition and diagenetic alteration of sandstone in northeast Pacific arc-related basins: implications for greywacke genesis; Geological Society of America Bulletin, v. 85, p. 379-390.

Haggart, J.W. 1987
On the age of the Queen Charlotte Group of British Columbia; Canadian Journal of Earth Sciences, v. 24, p. 2470-2476.

Hamilton, T. 1985
Volcanics of the Cenozoic Masset Formation: implications for geological and tectonic evolution of the Queen Charlotte Islands, British Columbia, Canada; Geological Society of America, Cordilleran Section Annual Meeting, Program with Abstracts, Vancouver, British Columbia, May 8-10, p. 359

Hickson, C.J. 1988
Structure and stratigraphy of the Masset Formation, Queen Charlotte Islands, British Columbia; *in* Current Research, Part E, Geological Survey of Canada, Paper 88-1E, p. 269-274.

Hillhouse, J.W. 1977
Paleomagnetism of the Triassic Nicolai Greenstone, McCarthy Quadrangle, Alaska; Canadian Journal of Earth Sciences, 14, p. 2578-2592.

Irving, E., Woodsworth,G.J., Wynne, P.J., and Morrison, A. 1985
Paleomagnetic evidence for displacement from the south of the Coast Plutonic Complex, British Columbia; Canadian Journal of Earth Sciences, 22, p. 584-598.

Jones, D.L., Silberling, N.J., and Hillhouse, J. 1977
Wrangellia-A displaced terrane in northwestern North America; Canadian Journal of Earth Sciences, 14, p. 2565-2577.

Martin, H.A. and Rouse, G.E. 1966
palynology of Late Tertiary sediments from the Queen Charlotte Islands, British Columbia; Canadian Journal of Botony, 44, p. 171-208.

Monger, J.W.H., Souther, J.G., and Gabrielse, H. 1972
Evolution of the Canadian Cordillera: a plate tectonic model; American Journal of Sciences, 272, p. 577-602.

Muller, J.E., Northcote, K.E., and Carlisle, D. 1974
Geology and mineral deposits of Alert Bay-Cape Scott map-area, Vancouver Island, British Columbia. Geological Survey of Canada, Paper 74-8. 77 pp.

Muller, J.E. 1977
Evolution of the Pacific Margin, Vancouver Island and adjacent areas; Canadian Journal of Earth Sciences, 14, p. 2062-2085.

Souther, J.G. 1977
Volcanism and tectonic environments in the Canadian Cordillera-a second look. *in* Volcanic regimes in Canada. *ed.* W.R.A. Baragar, L.C. Coleman, and M.Hall. Geological Association of Canada, Special Paper 16, p. 3-24.

Souther, J.G. 1988
Implications for hydrocarbon exploration of dyke emplacement in the Queen Charlotte Islands, British Columbia; *in* Current Research, Part E, Geological Survey of Canada, Paper 88-1E, p. 241-245.

Sutherland Brown, A. 1968
Geology of the Queen Charlotte Islands; British Columbia Department of Mines and Petroleum Resources Bulletin 54, 226 pp.

Woodsworth, G.J. 1988
Karmutsen Formation and the east boundary of Wrangellia, Queen Charlotte Basin, British Columbia; *in* Current Research, Part E, Geological Survey of Canada, Paper 88-1E, p. 209-212.

Yole and Irving, 1980
Displacement of Vancouver Island: paleomagnetic evidence from the Karmutsen Formation; Canadian Journal of Earth Sciences, 17 p. 1210-1228.

PART I

ORGANIC MATURATION OF MESOZOIC AND TERTIARY STRATA OF THE QUEEN CHARLOTTE ISLANDS

ABSTRACT

The level of organic maturation and the thermal history of Mesozoic and Tertiary strata in the Queen Charlotte Islands have been determined with vitrinite reflectance ($\%Ro_{rand}$) and numerical modelling (modified Arrhenius and Lopatin models). The degree of organic maturation (DOM) varies from immature to overmature and increases from north to south. The DOM is primarily controlled by high heat flow associated with plutonism on Moresby Island. Upper Triassic-Lower Jurassic Kunga Group strata are immature to overmature (0.45 to 1.75 $\%Ro_{rand}$) on northwest and central Graham Island, and are overmature (2.40 to 5.80 $\%Ro_{rand}$) on Moresby Island south of Cumshewa Inlet. Locally, anomalously high maturation values range up to 3.20 $\%Ro_{rand}$ on Graham Island, and 8.31 $\%Ro_{rand}$ on Moresby Island adjacent igneous intrusives. Lower Jurassic Maude, Yakoun, and Moresby Groups strata (including Lower Jurassic source rocks) are marginally mature to overmature with maturation increasing from central Graham Island (0.43 $\%Ro_{rand}$) to north Moresby Island (1.58 $\%Ro_{rand}$). The DOM of Cretaceous strata (Longarm, Haida, Skidegate, and Honna Formations) increases from northwest Graham Island (0.33 to 1.91 $\%Ro_{rand}$), to south Graham Island (1.53 to 2.43 $\%Ro_{rand}$), to south Moresby Island (2.31 to 4.78 $\%Ro_{rand}$). Tertiary strata are restricted to Graham Island and are generally immature except for the mature succession on western Graham Island (Port Louis well) and northeast Graham Island (basal strata at the Tow Hill well).

Calculated thickness of eroded strata on west Graham Island range from 1040 m at Fredrick Island to 735 m at Kennecott Point. Thicknesses of eroded strata are similar for Jurassic sections in central Graham Island at Rennell Junction (1725 m) and north Moresby Island at Cumshewa Inlet (1985 m). Increased thicknesses of eroded strata on north Moresby Island at Onward Point (1500 m) relative to northwest Graham Island at north Lauder Point (745 m) suggests differential uplift for Cretaceous strata at northwest Graham Island. Thicknesses of eroded strata for the Tertiary Skonun Formation range from 375 m on east Graham Island (Tlell well) to 1685 m on west Graham Island (Port Louis well).

Constant and variable geothermal gradient thermal regimes were modelled with modified Arrhenius and Lopatin methods. Time-temperature modelling (assuming constant geothermal gradients) predicts high paleogeothermal gradients (45 to 90 ^{O}C/km) for up to 180 million years during the Upper Triassic-Tertiary. Variable geothermal gradient modelling (utilizing a 30 ^{O}C/km background geothermal gradient) predicts elevated geothermal gradients ranging from 83 to 150 ^{O}C/km during Yakoun (between 183 and 178 Ma) and Masset (between 35 and 10 Ma) volcanism.

Triassic strata at Fredrick Island are predicted to have entered and exited the oil window during the Early and Late Miocene respectively while strata at Kennecott Point entered the oil window during the Early Miocene and are still in the oil window. Jurassic strata at Rennell Junction and Cumshewa Inlet entered the oil window during the Bajocian and remain within the oil window. Cretaceous strata on north and south Moresby Island entered the oil window during the Early Miocene and are currently within the oil window. The Skonun Formation is generally immature except for strata at west Graham Island (Port Louis well) and northeast Graham Island (Tow Hill well) which entered the oil window in the Late Miocene.

INTRODUCTION

In the Queen Charlotte Islands, a succession of Mesozoic and Tertiary strata up to 14 000 m thick is exposed. These strata are considered to contain potential source and reservoir rocks (Sutherland Brown, 1968) and during the late 1950's and 1960's, eight offshore and six onshore petroleum exploration wells were drilled to test the Tertiary strata for hydrocarbon accumulations. Recent studies have defined the Mesozoic and Tertiary stratigraphy and examined potential hydrocarbon resources and source rocks for selected strata (Sutherland Brown, 1968; Cameron and Tipper, 1985; Haggart, 1986; Cameron, 1987; Bustin and Macauley, 1988). In this study, the degree of organic maturation (DOM) of Mesozoic and Tertiary strata from the Queen Charlotte Islands is quantified with organic petrology (vitrinite reflectance) in order to document vertical (stratigraphic) and areal trends in organic maturation. The maturation data are modelled to establish areas of potential petroleum generation, the timing of hydrocarbon generation, and to predict the location of the oil window in time and space.

The hydrocarbon generative potential of sedimentary strata depends upon the type and abundance of organic matter and the thermal history of the strata (Dow, 1977). The type of organic matter can be determined from geochemical and petrographic analysis (Tissot and Welte, 1984). Organic maturation indices (such as vitrinite reflectance), can be used to infer the time-temperature history of the strata. Maturation data can be used in conjunction with numerical models to predict the timing of hydrocarbon generation, the type of hydrocarbons, the temperatures corresponding to hydrocarbon generation, the fractional conversion of kerogen to liquid hydrocarbons, and other parameters (Tissot and Espitalie, 1975).

METHODS

Approximately 1700 samples were collected in order to establish lateral and vertical (stratigraphic) variations in organic maturation. One hundred thirty three carbonaceous strata and lignite samples were collected from well cuttings and well core in the Tertiary Skonun Formation from the following six onshore exploration wells: Richfield et al. Cape Ball a-41-1; Richfield Mic Mac Homestead Gold Creek #1; Richfield Mic Mac Homestead Nadu River; Richfield Mic Mac Homestead Tlell #1; Richfield Mic Mac Homestead Tow Hill #1; and Union Port Louis c-28-1. In addition, outcrop samples were collected from the Skonun Formation on Graham Island, lignite samples from Skonun Point and Miller Creek, and carbonaceous siltstone from Log Creek.

One hundred and eighty eight lignite and carbonaceous shale outcrop samples were collected from the Cretaceous Longarm, Haida, Skidegate, and Honna Formations. The majority of Cretaceous samples were collected from Graham Island and a few from Moresby Island. Two hundred and forty one limestone, argillite, and carbonaceous sandstone outcrop samples were collected from the Triassic Kunga Group. The majority of Triassic samples were collected from Moresby Island and fewer from Graham and Fredrick Islands.

Additional samples together with stratigraphic data were kindly provided by B.E.B Cameron, M. Orchard, and C. Hickson of the Geological Survey of Canada and by T. Fogarassy of the University of British Columbia. Rock-Eval pyrolysis and organic maturation data for Lower Jurassic strata were supplied by R.M. Bustin of the University of British Columbia.

The degree of organic maturation (DOM) was determined using the vitrinite reflectance techniques outlined in England and Bustin (1986). Samples containing visible coal or lignite were crushed and analyzed as whole rock samples. Samples containing low concentrations of organic matter were crushed (-80 mesh) and demineralized with hydrochloric and hydrofluoric acids. The samples were mounted in transoptic and

heated to 120^{0} C for 5 minutes forming an optically transparent pellet. The pellets were stored in argon or nitrogen gas to prevent oxidation of the organic matter prior to analysis.

The mean random vitrinite reflectance ($\%Ro_{rand}$) in oil (n=1.518 at 546 nm) was measured with the polarizer out using a Leitz R (M.P.V. II) microscope. The mean random vitrinite reflectance was measured rather than the mean maximum vitrinite reflectance ($\%Ro_{max}$) in order to save time and to enable measurement of smaller particles (Davis, 1978; England and Bustin, 1986). Wherever possible, 50 vitrinite reflectance measurements were made on each sample, and the mean and standard deviation were determined.

RESULTS

Lateral maturation trends (Figs. 5-20) and vertical maturation profiles (Figs. 21-24) were determined from vitrinite reflectance measurements of samples collected from all regions of the Queen Charlotte Islands (Table 1). The regional DOM increases markedly from Graham Island to south Moresby Island. Regional elevated maturation levels on Moresby and adjacent islands are in part a result of increased heat flow associated with igneous activity (pluton emplacement) in the Middle-Late Jurassic and Oligocene (Anderson, pers. comm., 1988; Anderson, 1988; Souther, 1988). Local, anomalously high maturation values which result from high heat flow near igneous intrusions or possibly from hydrothermal activity near faults have often obscured regional maturation trends. Due to poor outcrop exposure, large scale intrusion by plutonic complexes, and limited lateral continuity of sedimentary units, interpretation of lateral maturation trends is difficult and in some places impossible. The isomaturity maps presented here will thus ultimately require modification as new data is acquired.

Most of the organic matter found within the strata is either Type II or Type III (see Part II); therefore, the oil window has been defined as between 0.50 $\%Ro_{rand}$ and 1.35 $\%Ro_{rand}$ for this study (Dow, 1977). Strata with maturation values less than 0.50 $\%Ro_{rand}$ are considered to be immature, and

strata with maturation values greater than 1.35 $\%Ro_{rand}$ are considered to be overmature with respect to hydrocarbon generation and preservation.

Lateral Variation In Organic Maturity

The following section outlines the outcrop exposure and maturation values for selected stratigraphic horizons. Local, high maturation levels which deviate from regional trends are considered anomalous. These anomalous maturation values often overprint regional trends. In the following section, local anomalous maturation values are differentiated from regional trends.

KUNGA GROUP

In samples collected from Kunga Group lithologies on Moresby Island, vitrinite reflectances were measured from organic matter which was morphologically and texturally indistinguishable from vitrinite. The organic matter did not have definitive form and often occurs as a groundmass. Internal texture varied from homogeneous to mosaic. The Kunga Group is interpreted to be an offshore carbonate platform deposit (see regional geology) with some clastic input suggesting that the organic matter is of marine origin (hydrogen rich) and may not be vitrinite. It is, therefore, possible that the organic matter is either vitrinite, bituminite, or both.

Grey Limestone Member

The oldest sedimentary unit in the Queen Charlotte Islands is the Late Carnian grey limestone member (informal name from Cameron and Tipper, 1985) of the Kunga Group. The grey limestone member is best exposed on eastern and southern Moresby Island where the strata are overmature (Fig. 5) with regional maturation values ranging from 2.91 $\%Ro_{rand}$ at Huston Inlet (central Moresby Island) to 5.80 $\%Ro_{rand}$ at Breaker Bay (eastern Moresby Island). At Carpenter Bay, maturation values range up to 7.96 $\%Ro_{rand}$ adjacent to the Carpenter Bay Plutonic Suite (southeastern Moresby Island).

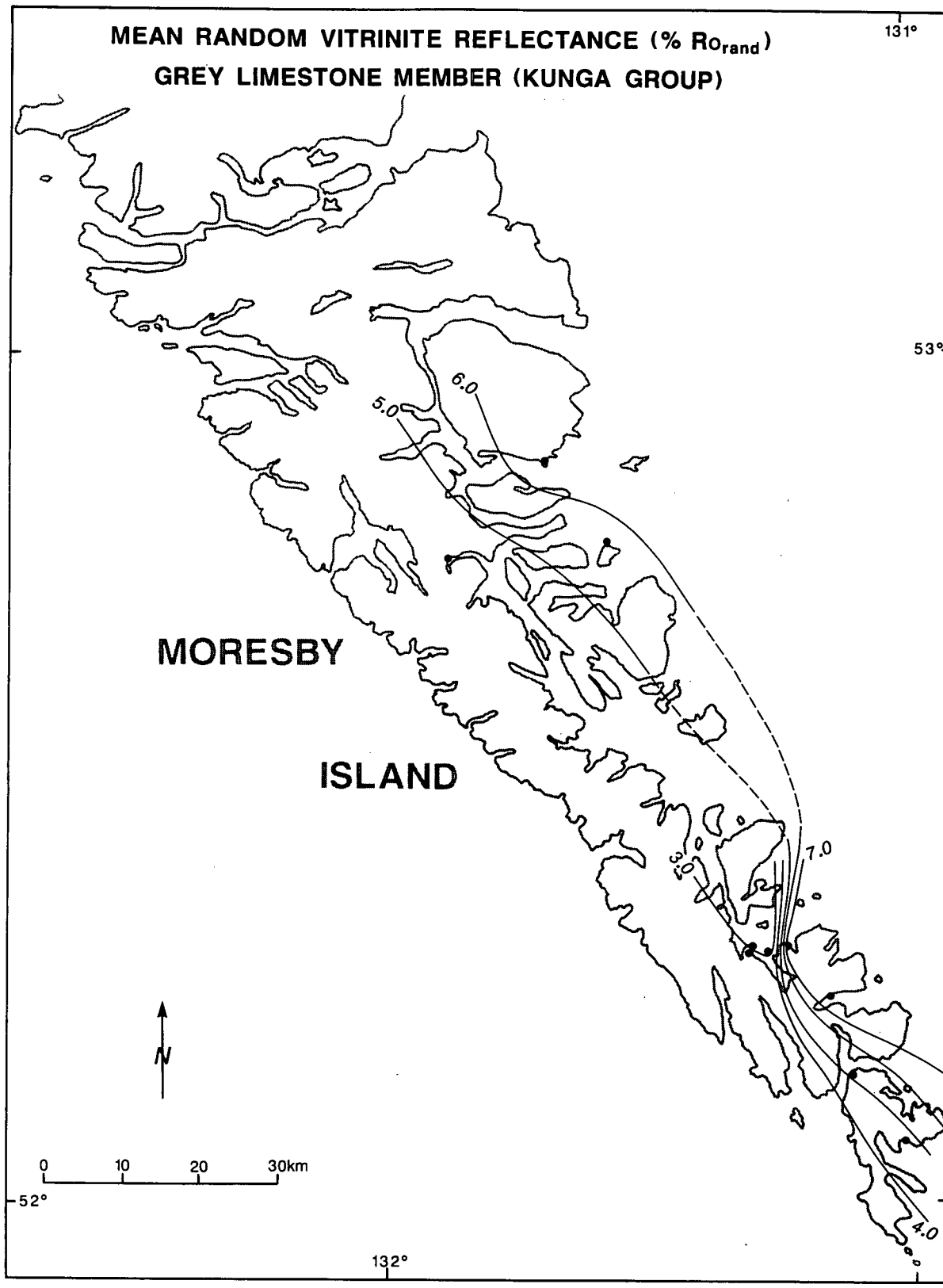

Figure 5. Regional surface maturation patterns (%Ro_{rand}) of the Upper Triassic grey limestone member (Kunga Group). Dashed line represents an inferred contour

Black Limestone Member

The Late Carnian to Late Norian black limestone member (informal name from Cameron and Tipper, 1985) of the Kunga Group crops out predominantly on central and eastern Moresby Island and is overmature (2.40 to 5.80 $\%Ro_{rand}$). The strata are also exposed locally on northwest Graham Island and in Skidegate Inlet where they are mature to overmature. The regional DOM increases from west to east on Moresby Island (Fig. 6) with maturation values ranging from 2.40 $\%Ro_{rand}$ at Huston Inlet (central Moresby Island) to 5.80 $\%Ro_{rand}$ at Howay Island (eastern Moresby Island). Local, anomalously high maturation values range up to 8.31 $\%Ro_{rand}$ at Carpenter Bay.

Black limestone member strata are marginally mature to overmature on northwestern Graham Island with maturation values ranging from 0.51 $\%Ro_{rand}$ at Kennecott Point to 1.59 $\%Ro_{rand}$ at Lauder Point. Local, anomalously high maturation values range up to 3.20 $\%Ro_{rand}$ at Sialun Bay in northwest Graham Island.

Sandilands Formation

Regional maturation values for the Sinemurian Sandilands Formation, which is exposed primarily on Moresby Island and locally on Graham Island, increase from north to south (Figs. 7 and 10). Values range from 0.45 $\%Ro_{rand}$ at Kennecott Point (northwestern Graham Island) to 3.78 $\%Ro_{rand}$ at Kunga Island (central Moresby Island). Locally, values range up to 4.73 $\%Ro_{rand}$ on Moresby Island. Maturation values for central Graham Island and northern Moresby Island range from 0.48 $\%Ro_{rand}$ in central Graham Island to 1.75 $\%Ro_{rand}$ at Cumshewa Inlet (northern Moresby Island).

MAUDE GROUP

The regional level of organic maturation for the Maude Group is illustrated in Figure 8.

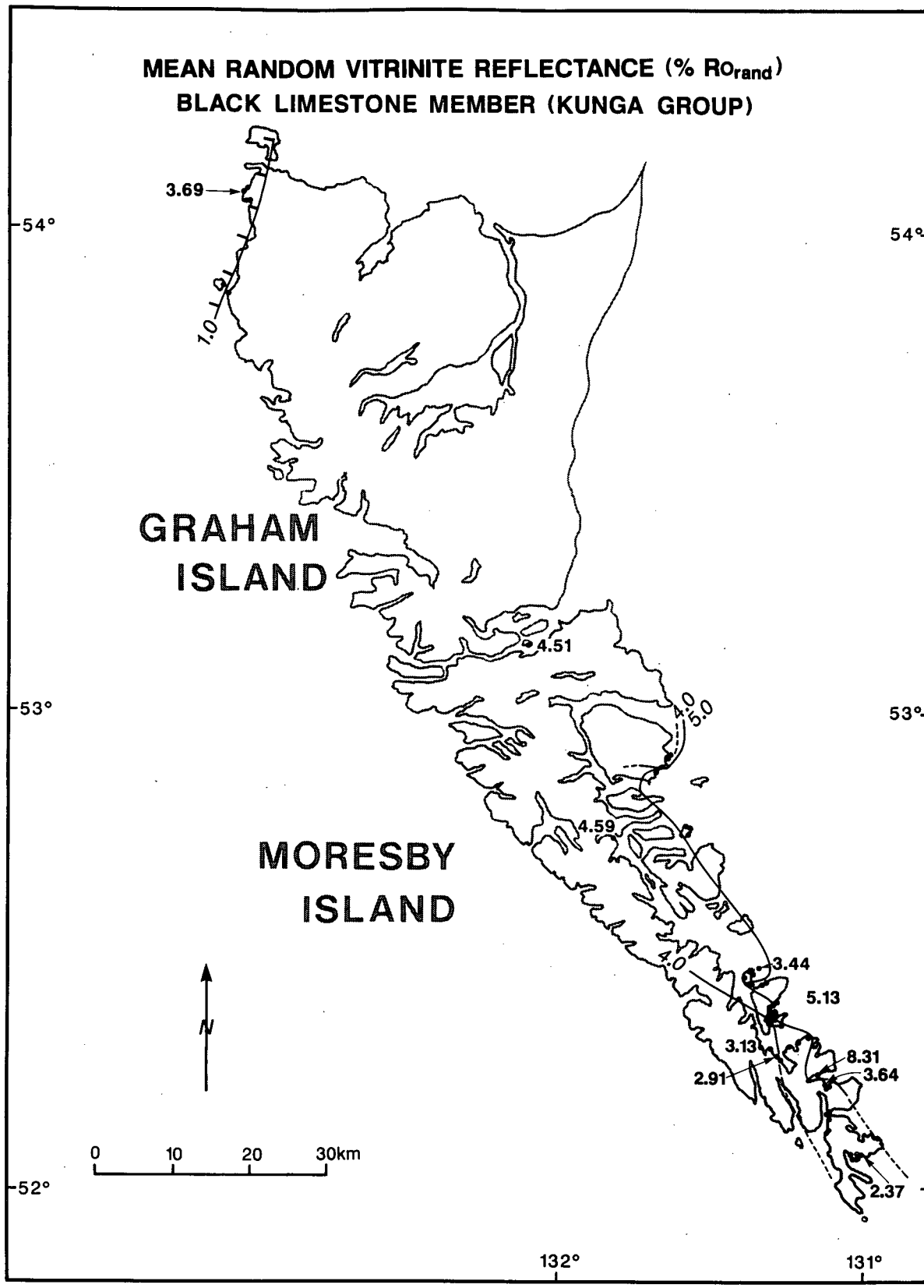

Figure 6. Regional surface maturation patterns (%Ro$_{rand}$) of the Upper Triassic black limestone member (Kunga Group). Dashed line represents an inferred contour. Tick marks on contour indicate decreasing maturation

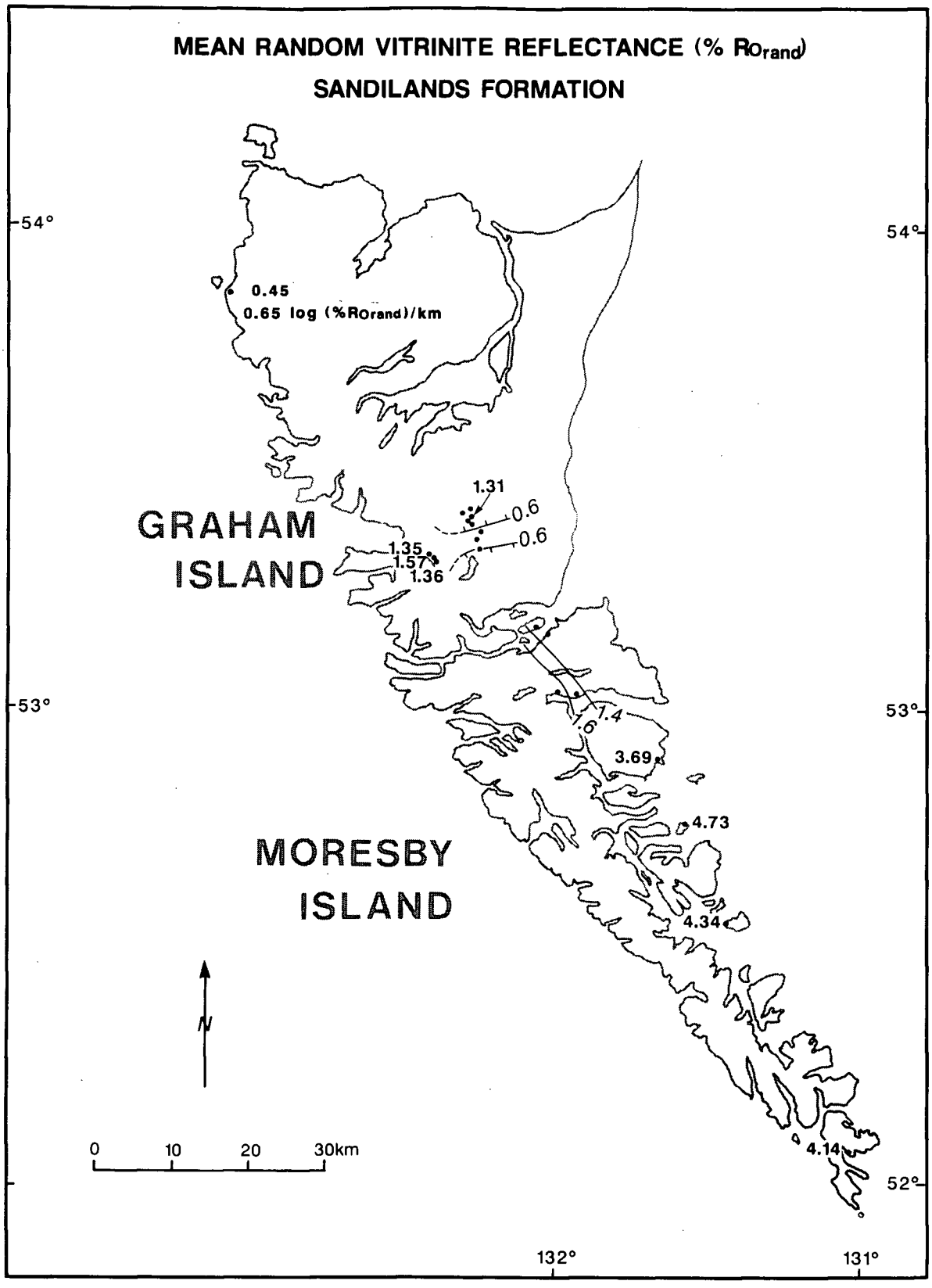

Figure 7. Regional surface maturation patterns (%Ro_{rand}) of the Sinemurian Sandilands Formation. Dashed line represents an inferred contour. Labelled values do not fit regional trends and are not contoured. Tick marks on contour indicate decreasing maturation. Maturation gradient is 0.65 log (%Ro_{rand})/km

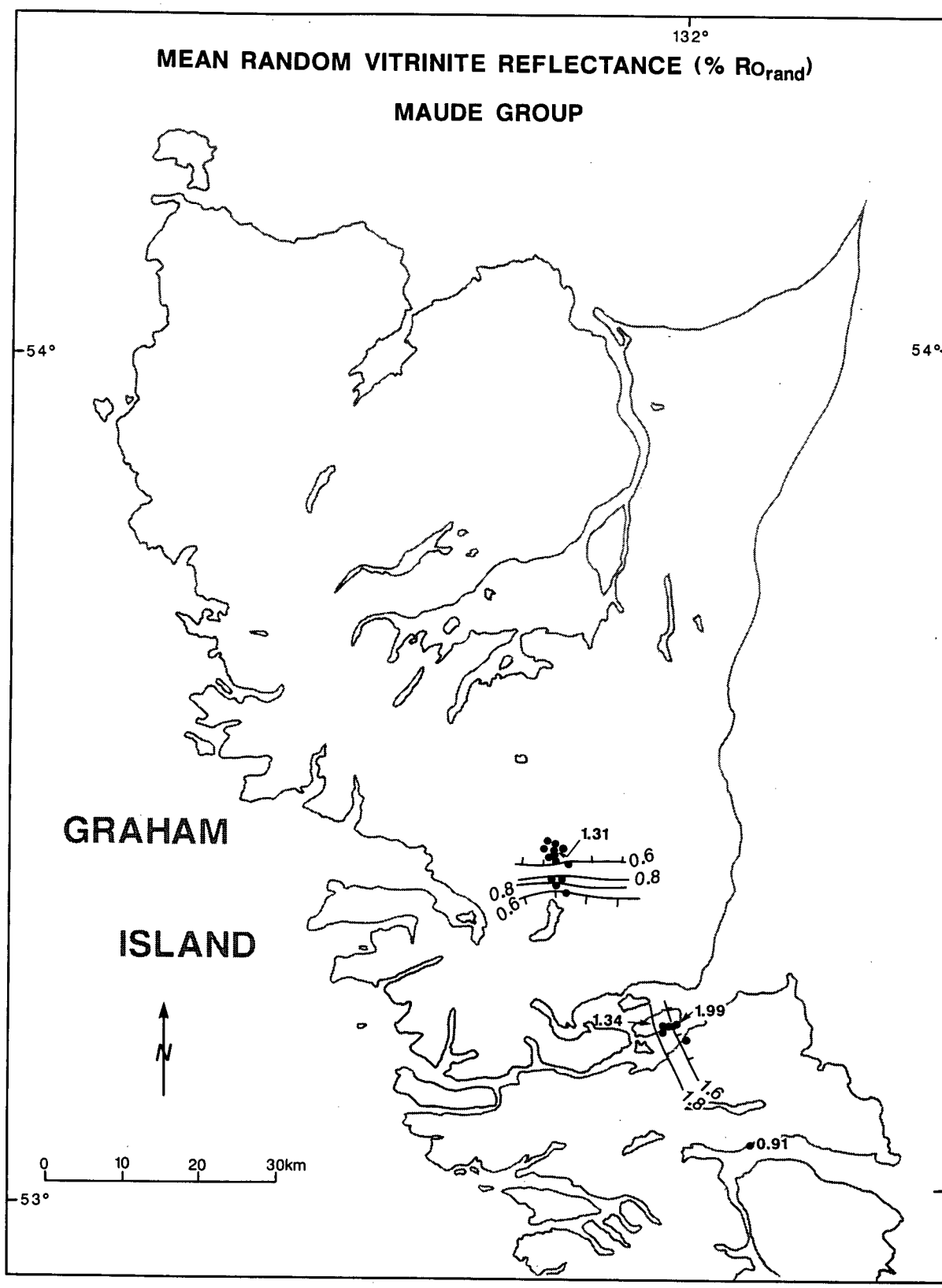

Figure 8. Regional surface maturation patterns (%Ro_{rand}) of the Lower Jurassic Maude Group. Labelled values do not fit regional trends and are not contoured. Tick marks on contour indicate decreasing maturation

Ghost Creek Formation

The Lower Pliensbachian Ghost Creek Formation crops out from central Graham Island to northern Moresby Island where the regional DOM increases from north to south and varies from mature to overmature. Organic maturation values range from 0.50 $\%Ro_{rand}$ on central Graham Island to 1.53 $\%Ro_{rand}$ at Cumshewa Inlet (Figs. 9 and 10). Vitrinite reflectance measurements taken proximal to dikes and sills range up to 1.31 $\%Ro_{rand}$ on the central Graham Island to 1.71 $\%Ro_{rand}$ at Cumshewa Inlet. Similar values were reported by Bustin and Macauley (1988).

Rennell Junction Formation

The mature to marginally overmature Lower Pliensbachian Rennell Junction Formation is exposed locally on central Graham Island, Skidegate Inlet, and northern Moresby Island. The regional level of organic maturation (Fig. 11) ranges from 0.52 $\%Ro_{rand}$ on central Graham Island to 1.50 $\%Ro_{rand}$ on Maude Island (Skidegate Inlet). Local, anomalously high, maturation values range up to 2.12 $\%Ro_{rand}$.

Fannin Formation

Maturation values for the Upper Pliensbachian-Lower Toarcian Fannin Formation (Fig. 12) range from 0.85 $\%Ro_{rand}$ at Cumshewa Inlet to 1.58 $\%Ro_{rand}$ on Maude Island (Skidegate Inlet).

Whiteaves Formation

The regional DOM for the Middle Toarcian Whiteaves Formation increases from west to east with maturation values ranging from 0.43 $\%Ro_{rand}$ on central Graham Island to 1.51 $\%Ro_{max}$ on Skidegate Inlet (Fig. 13).

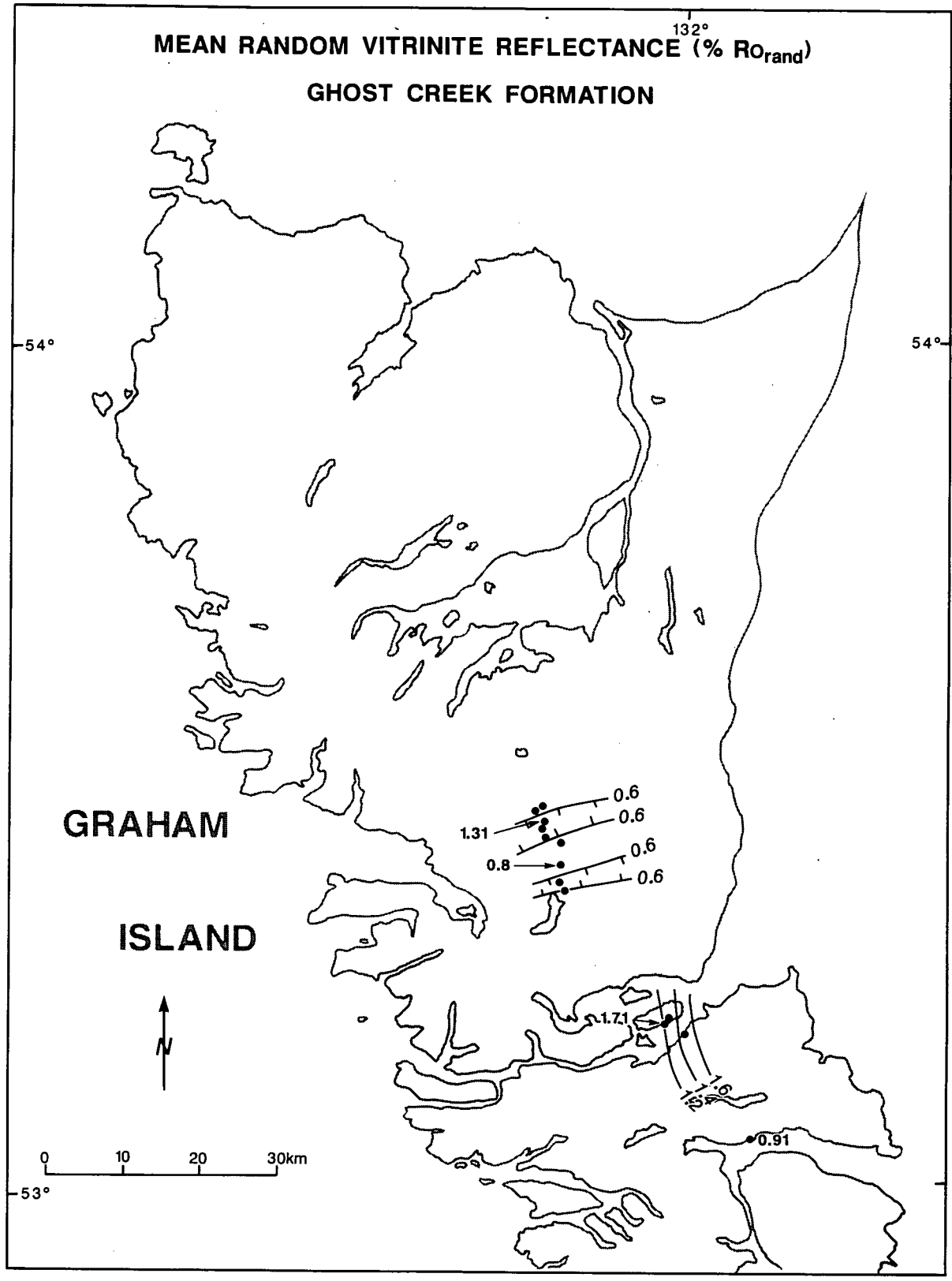

Figure 9. Regional surface maturation patterns (%Ro_{rand}) of the Lower Pliensbachian Ghost Creek Formation. Labelled values do not fit regional trends and are not contoured. Tick marks on contour indicate decreasing maturation

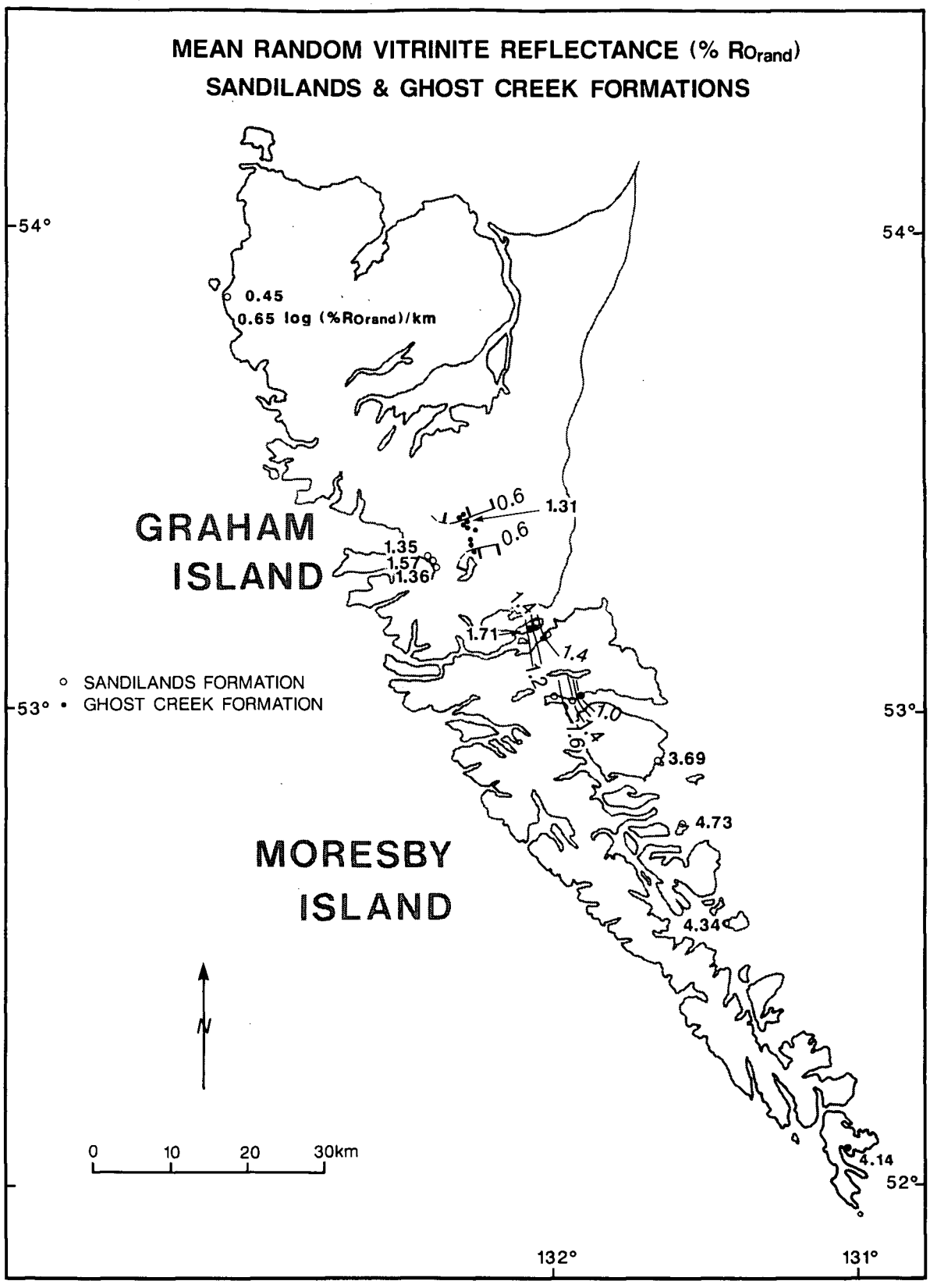

Figure 10. Regional surface maturation patterns (%Ro_{rand}) of the Sinemurian Sandilands and Lower Pliensbachian Ghost Creek Formations. Dashed line represents an inferred contour. Labelled values do not fit regional trends and are not contoured. Tick marks on contour indicate decreasing maturation. Maturation gradient is 0.65 log (%Ro_{rand})/km

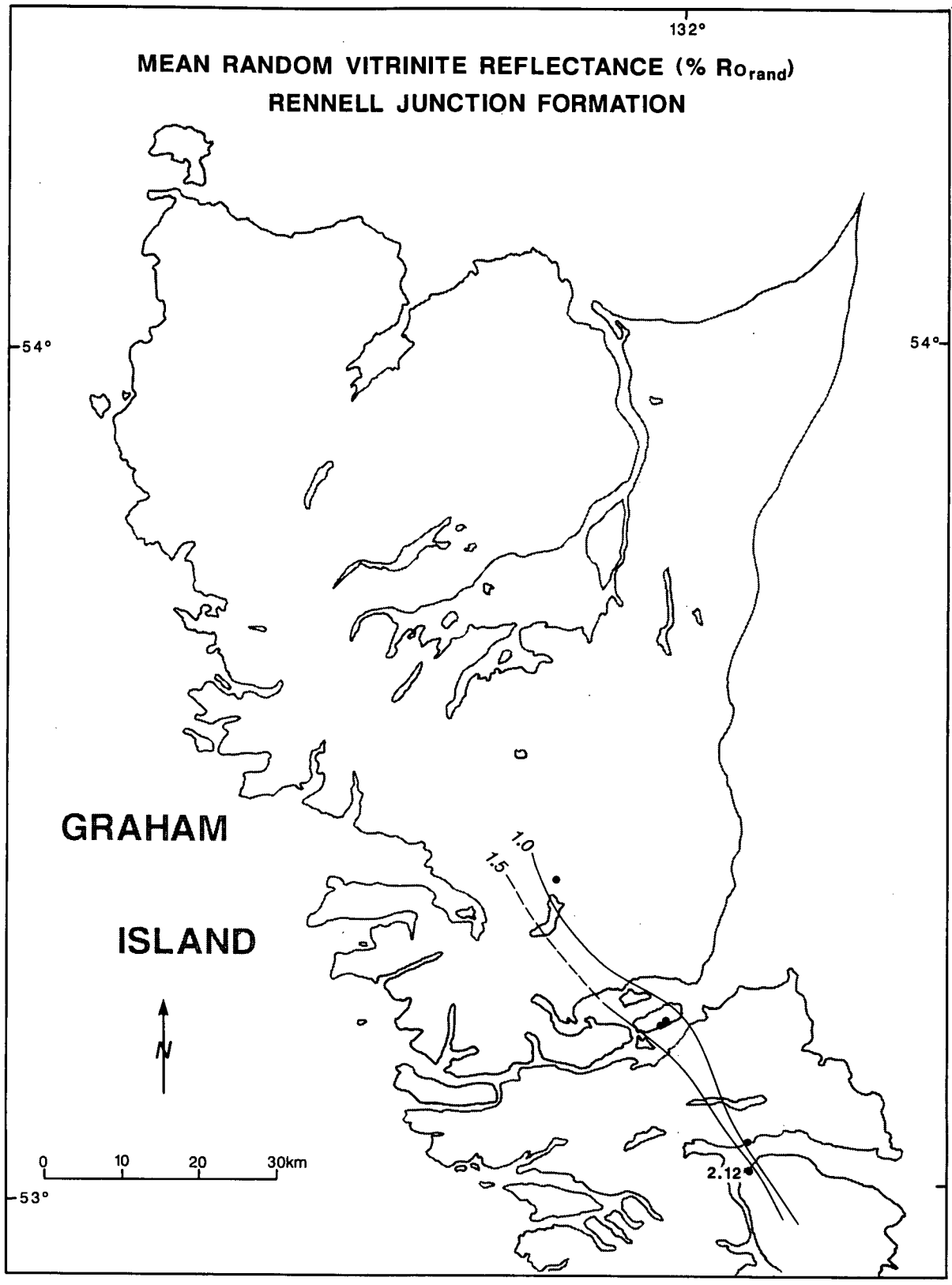

Figure 11. Regional surface maturation patterns (%Ro_{rand}) of the Lower Pliensbachian Rennell Junction Formation. Dashed line represents an inferred contour. Labelled values do not fit regional trends and are not contoured. Tick marks on contour indicate decreasing maturation

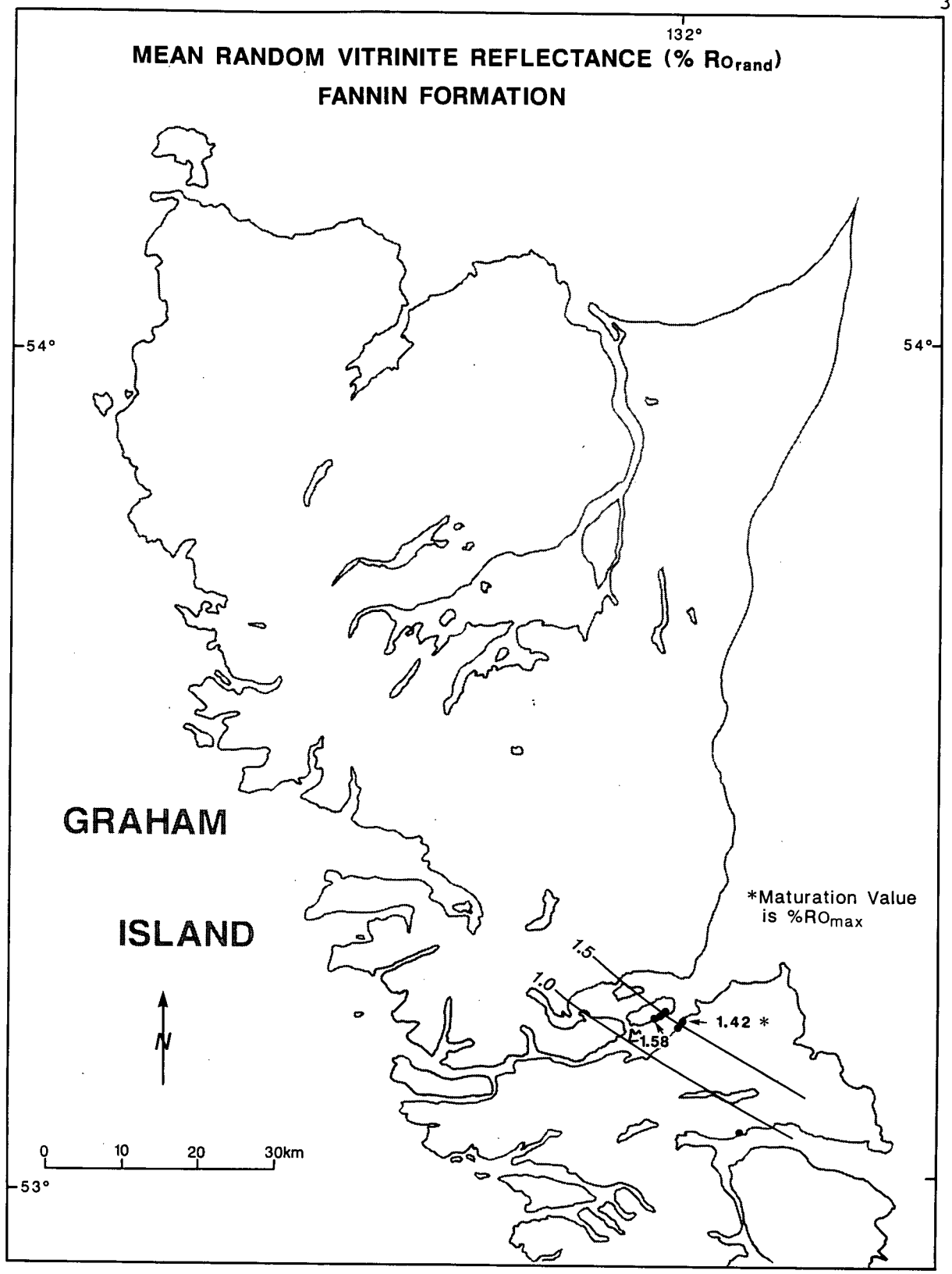

Figure 12. Regional surface maturation patterns (%Ro_{rand}) of the Upper Pliensbachian to Lower Toarcian Fannin Formation. Labelled values do not fit regional trends and are not contoured

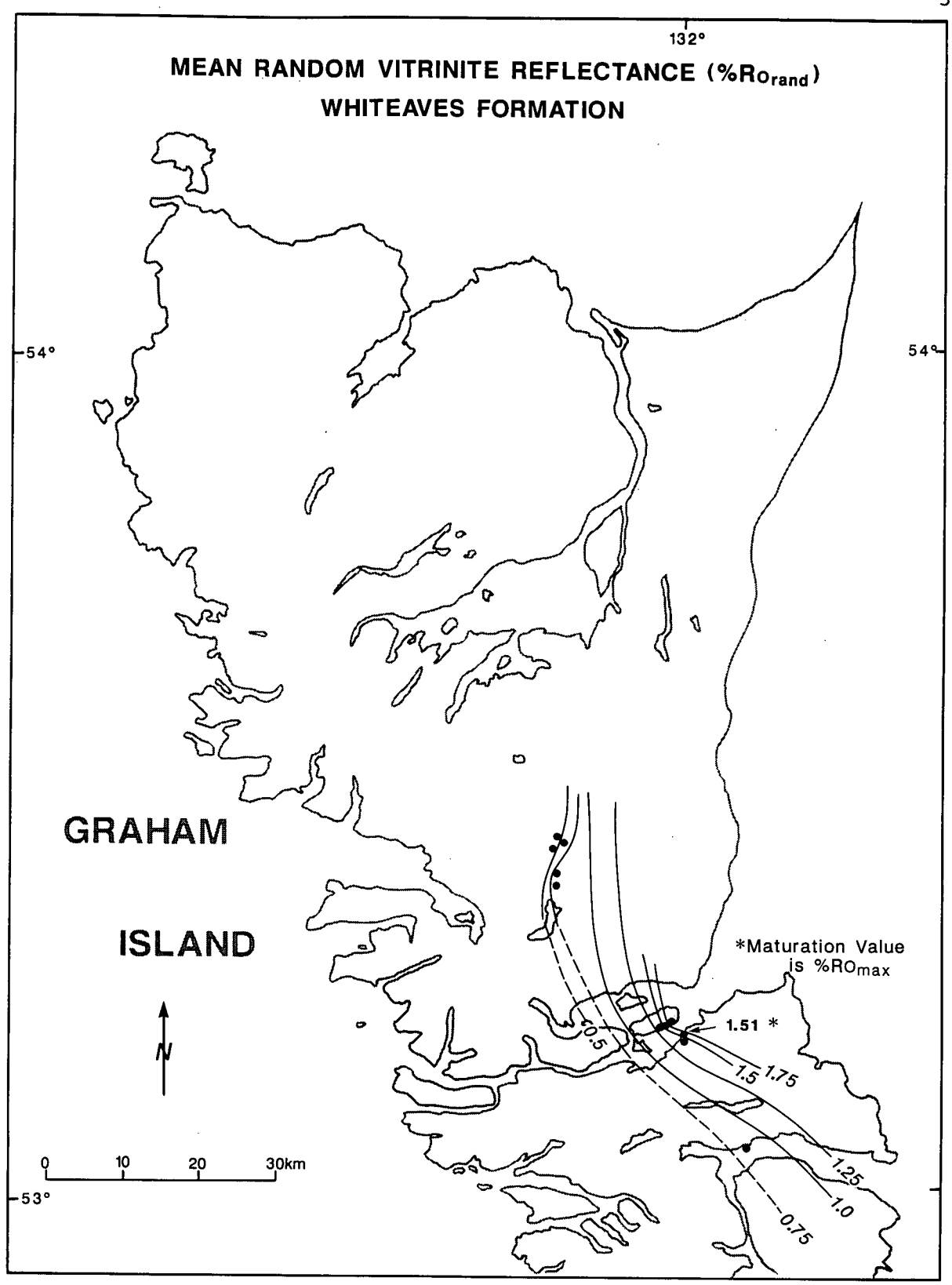

Figure 13. Regional surface maturation patterns (%Ro_{rand}) of the Middle Toarcian Whiteaves Formation. Dashed line represents an inferred contour. Labelled values do not fit regional trends and are not contoured

Phantom Creek Formation

The strata outcrop locally and only one organic maturation value (0.46 $\%Ro_{rand}$) was obtained for the Upper Toarcian Phantom Creek Formation in central Graham Island (Fig. 14).

YAKOUN GROUP

The regional level of organic maturation for the Yakoun and Moresby Groups is illustrated in Fig. 15.

Graham Island Formation

The Lower Bajocian Graham Island Formation is marginally mature to mature (Fig. 15) in central Graham Island (0.48 $\%Ro_{rand}$) and overmature in the Skidegate Inlet area (1.50 $\%Ro_{rand}$).

Richardson Bay Formation

The Lower Bajocian Richardson Bay Formation is exposed locally in Skidegate Inlet (Fig. 15) where the strata are mature (1.13 $\%Ro_{rand}$).

MORESBY GROUP

Robber Point, Newcombe and Alliford Formations

In Skidegate Inlet, the limited maturation data available indicates that the Upper Bathonian Robber Point (1.10 $\%Ro_{rand}$), the Upper Bathonian-Lower Callovian Newcombe (1.08 $\%Ro_{rand}$), and the Lower Callovian Alliford Formations (1.04 $\%Ro_{rand}$) are mature (Fig. 15).

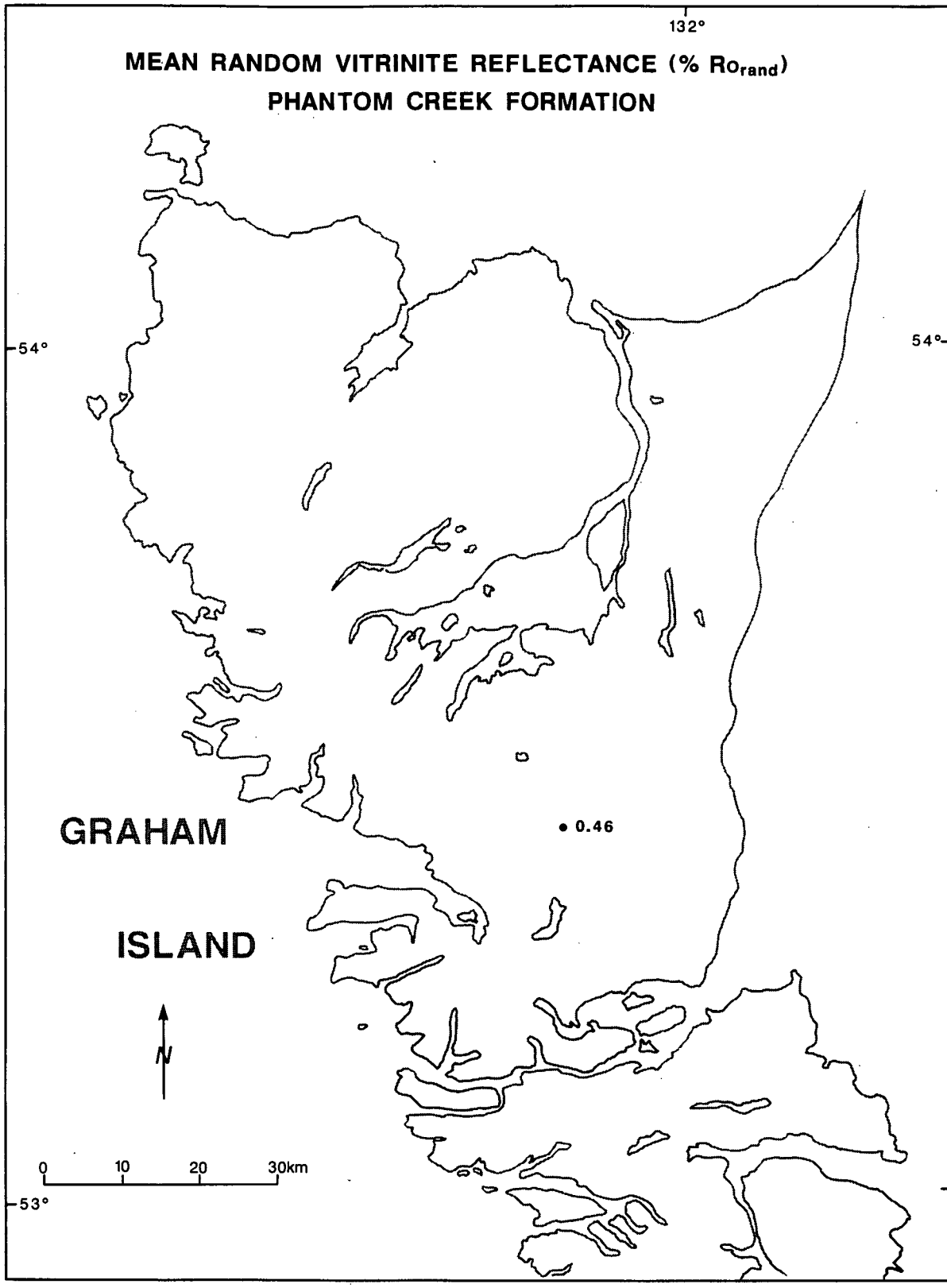

Figure 14. Regional surface maturation patterns (%Ro_{rand}) of the Middle Toarcian to Aalenian Phantom Creek Formation

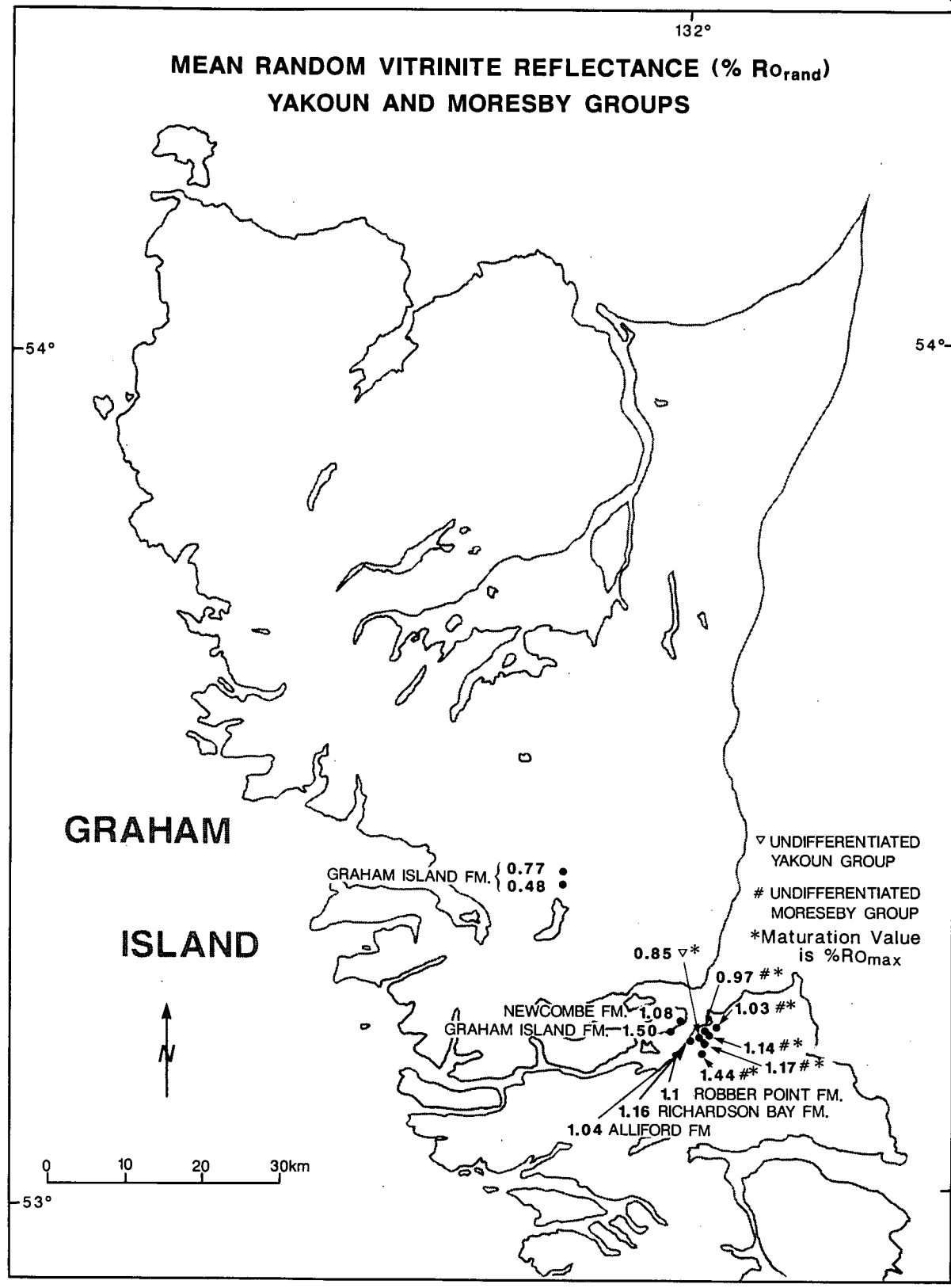

Figure 15. Regional surface maturation patterns (%Ro_{rand}) of the Lower Jurassic Yakoun, and Moresby Groups

LONGARM FORMATION

The Upper Valanginian-Lower Barremian Longarm Formation crops out on Moresby Island and parts of Graham Island. The Longarm Formation is overmature on northern Moresby Island (Fig. 16) with maturation values ranging from 1.53 $\%Ro_{max}$ to 2.43 $\%Ro_{max}$. The strata on eastern Moresby Island are overmature with regional maturation increasing from west (2.31 $\%Ro_{rand}$ at Huston Inlet) to east (4.86 $\%Ro_{rand}$ on Murchison Island).

QUEEN CHARLOTTE GROUP

Haida Formation

The Albian Haida Formation is exposed locally from northwest Graham Island to central Moresby Island. The regional DOM varies from immature to overmature and increases from north to south. Maturation values range from 0.33 $\%Ro_{rand}$ in Beresford Bay (northwest Graham Island), 1.29 $\%Ro_{max}$ in Skidegate Inlet, 2.08 $\%Ro_{rand}$ in Cumshewa Inlet, to 4.18 $\%Ro_{rand}$ in central Moresby Island (Fig. 17). Local, anomalously high vitrinite reflectance values (up to 1.72 $\%Ro_{rand}$) occur on northwest Graham Island.

Skidegate Formation

The Cenomanian-Turonian Skidegate Formation crops out in the Skidegate and Cumshewa Inlet areas, northwest Graham Island, and Langara Island. The Skidegate Formation (Fig. 18) is immature to mature on northwest Graham Island (0.40 $\%Ro_{rand}$) and mature to overmature in Skidegate Inlet (2.21 $\%Ro_{rand}$). Regional organic maturation increases from east to west on northwest Graham Island with anomalously high values near Langara Island. A slight increase in the DOM from west to east occurs in both Skidegate and Cumshewa Inlets. Local, anomalously high vitrinite reflectance values range up to 2.55 $\%Ro_{rand}$ in the Skidegate and Cumshewa Inlet areas.

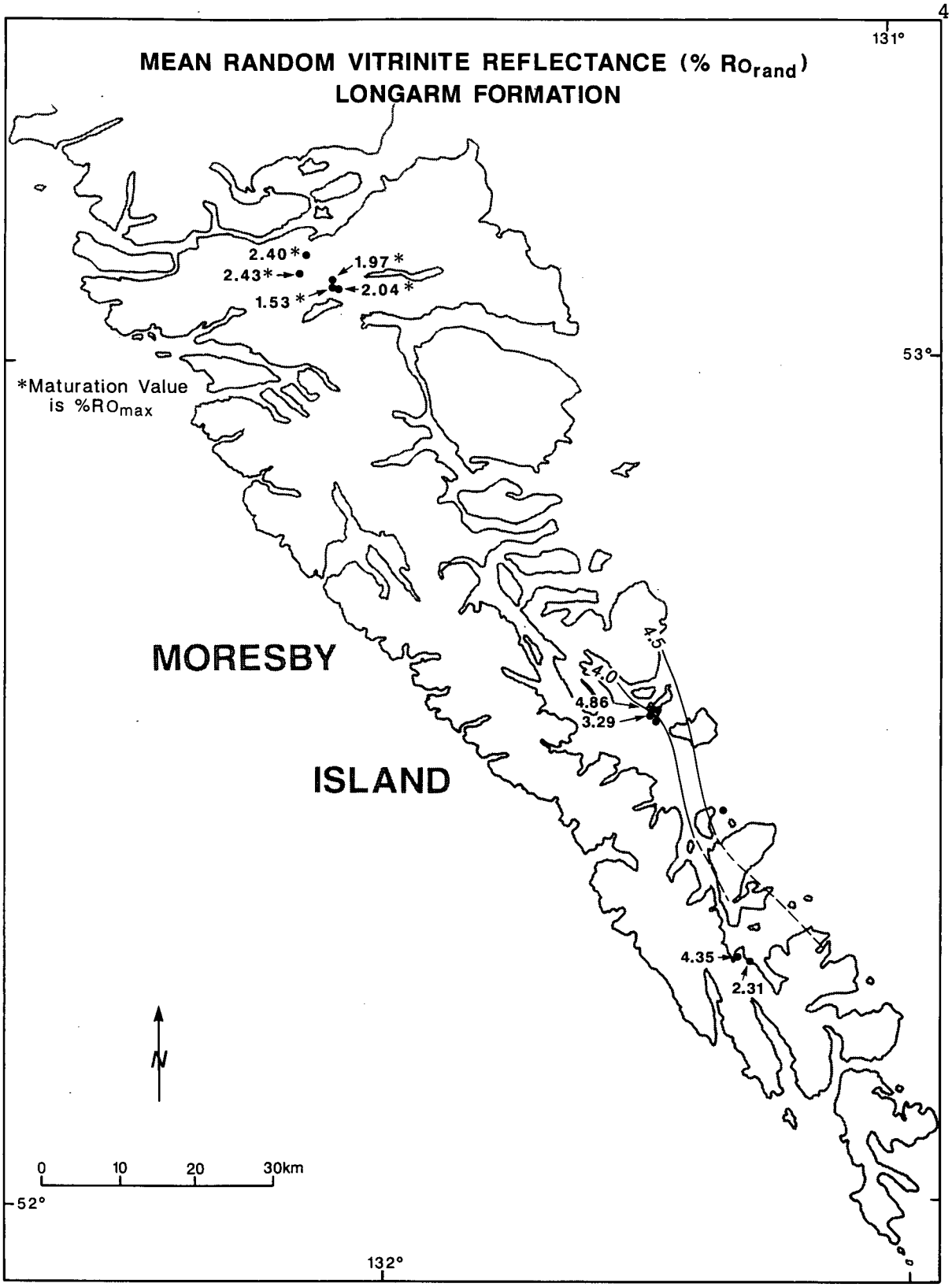

Figure 16. Regional surface maturation patterns (%Ro_{rand}) of the Upper Valanginian to Berremian Longarm Formation. Dashed line represents an inferred contour. Labelled values do not fit regional trends and are not contoured

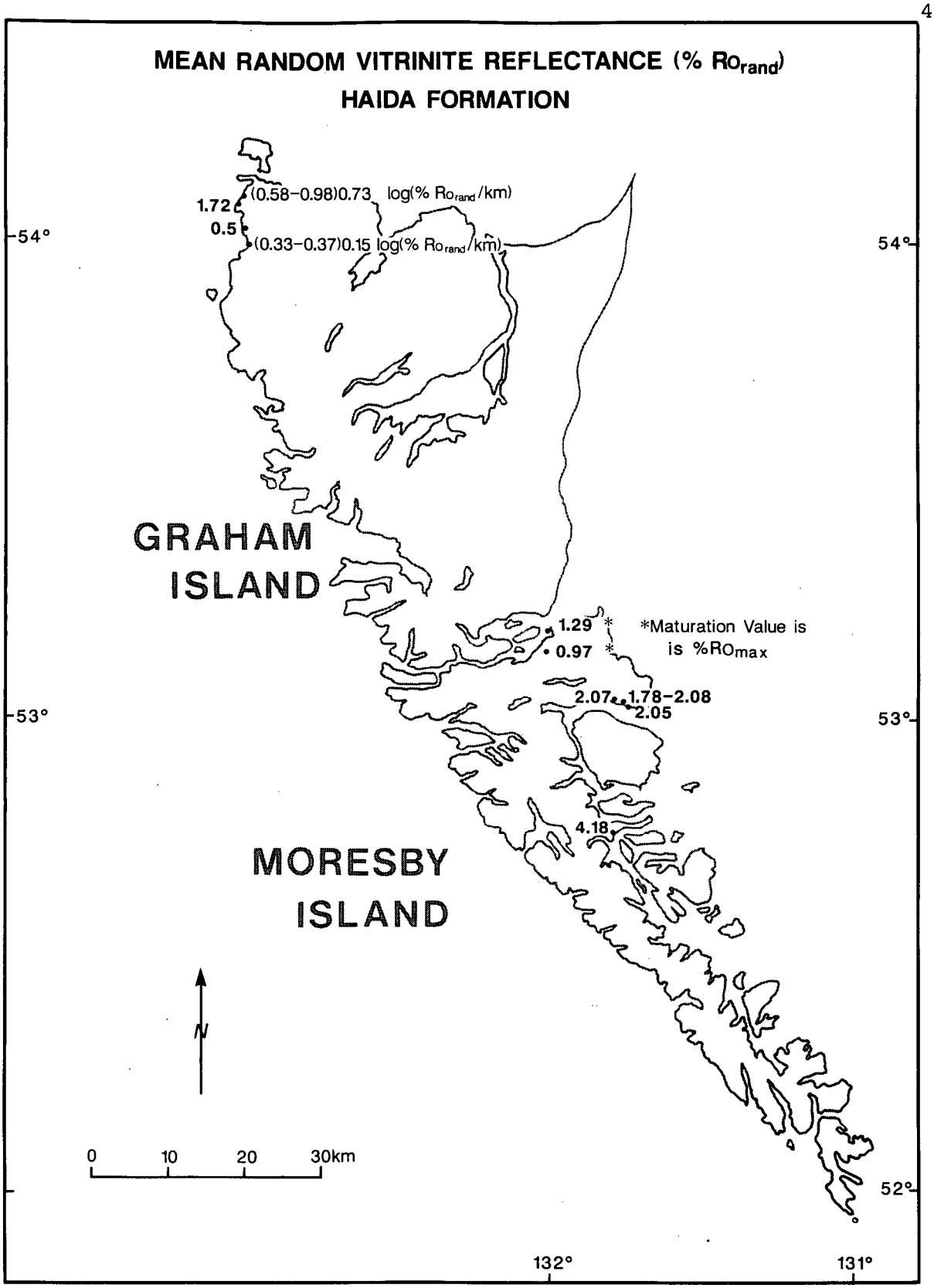

Figure 17. Regional surface maturation patterns (%Ro$_{rand}$) of the Albian Haida Formation. Values in brackets are minimum and maximum vitrinite reflectances. Maturation gradients are 0.73 and 0.15 log (%Ro$_{rand}$)/km

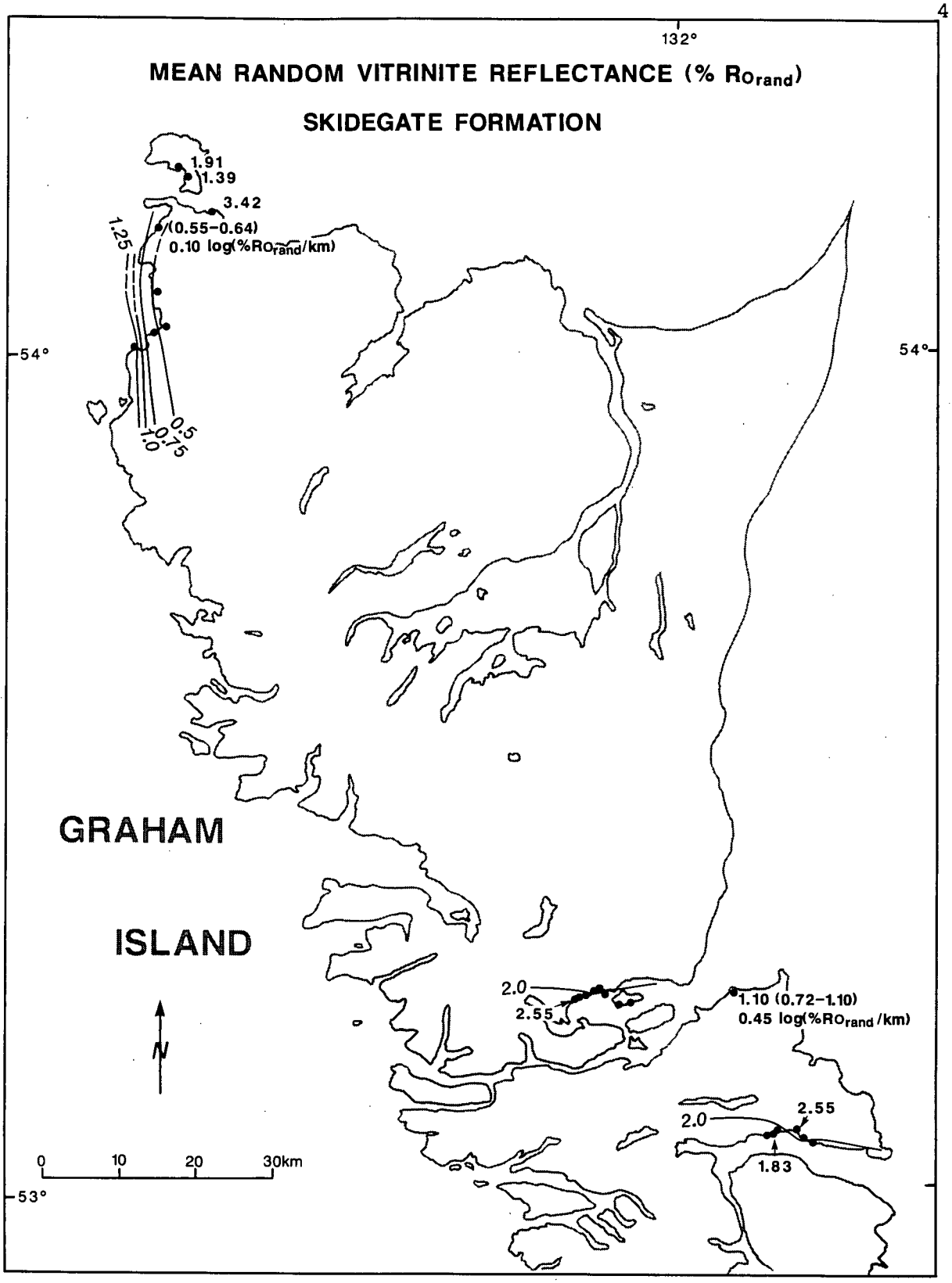

Figure 18. Regional surface maturation patterns (%Ro_{rand}) of the Cenomanian to Turonian Skidegate Formation. Values in brackets are minimum and maximum vitrinite reflectances. Maturation gradients are 0.10 and 0.45 log (%Ro_{rand})/km

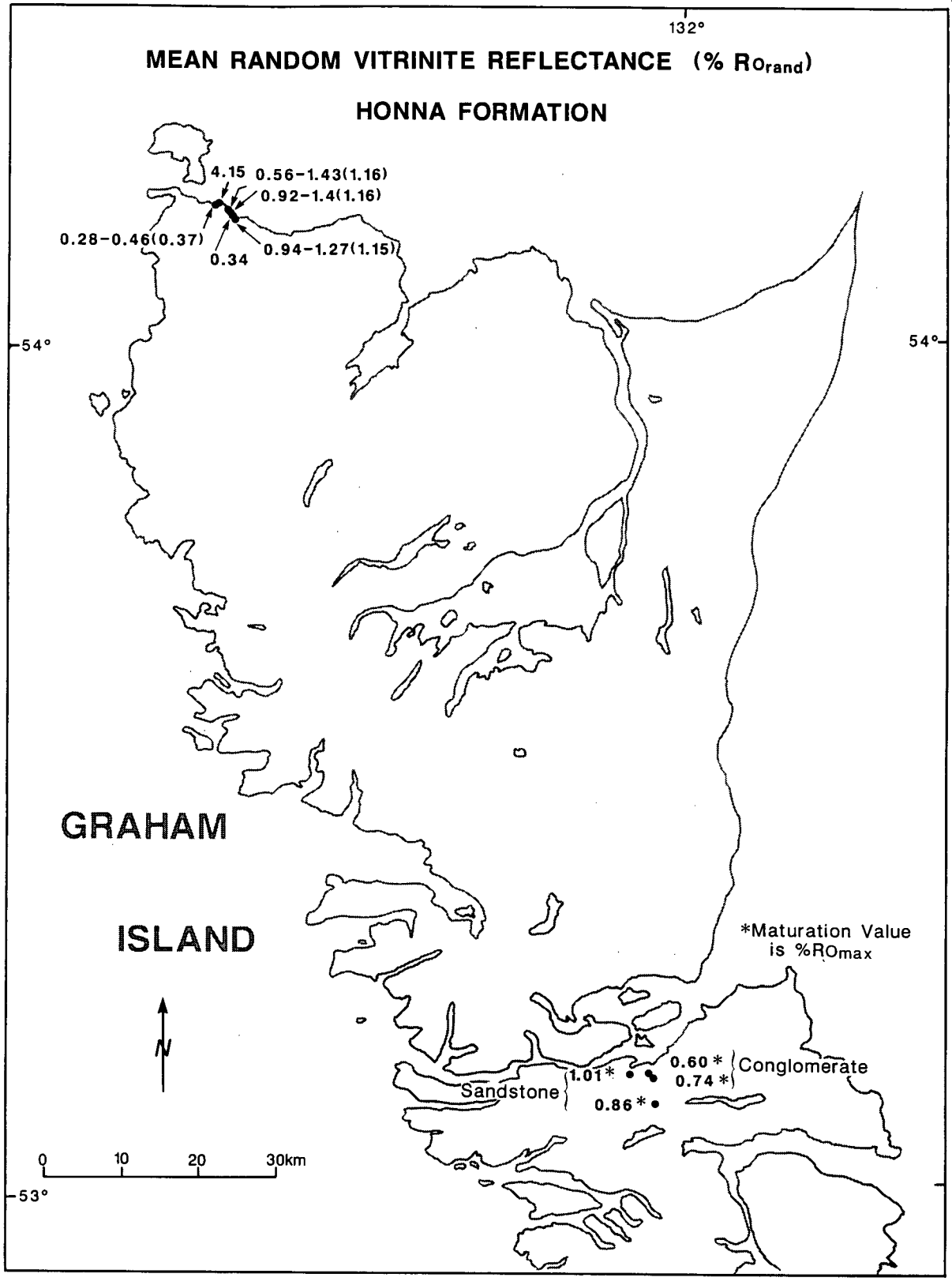

Figure 19. Regional surface maturation patterns (%Ro_{rand}) of the Conacian Honna Formation. Single and numbers in brackets are mean vitrinite reflectance values. Dashed values are minimum and maximum vitrinite reflectance values

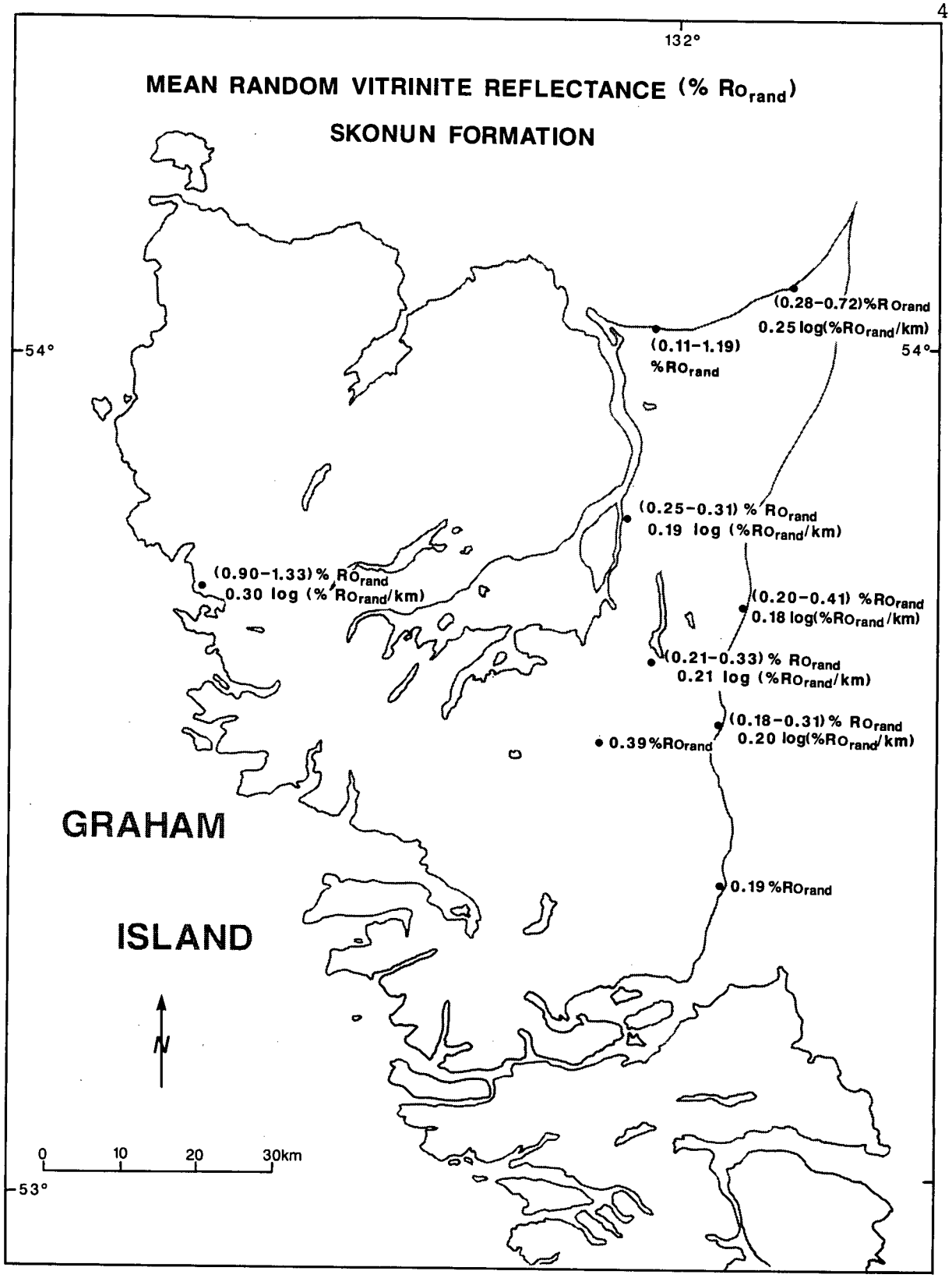

Figure 20. Regional surface maturation patterns (%Ro$_{rand}$) of the Miocene to Pliocene Skonun Formation. Values in brackets are minimum and maximum vitrinite reflectance values. Maturation gradients range from 0.18 to 0.30 log (%Ro$_{rand}$)/km

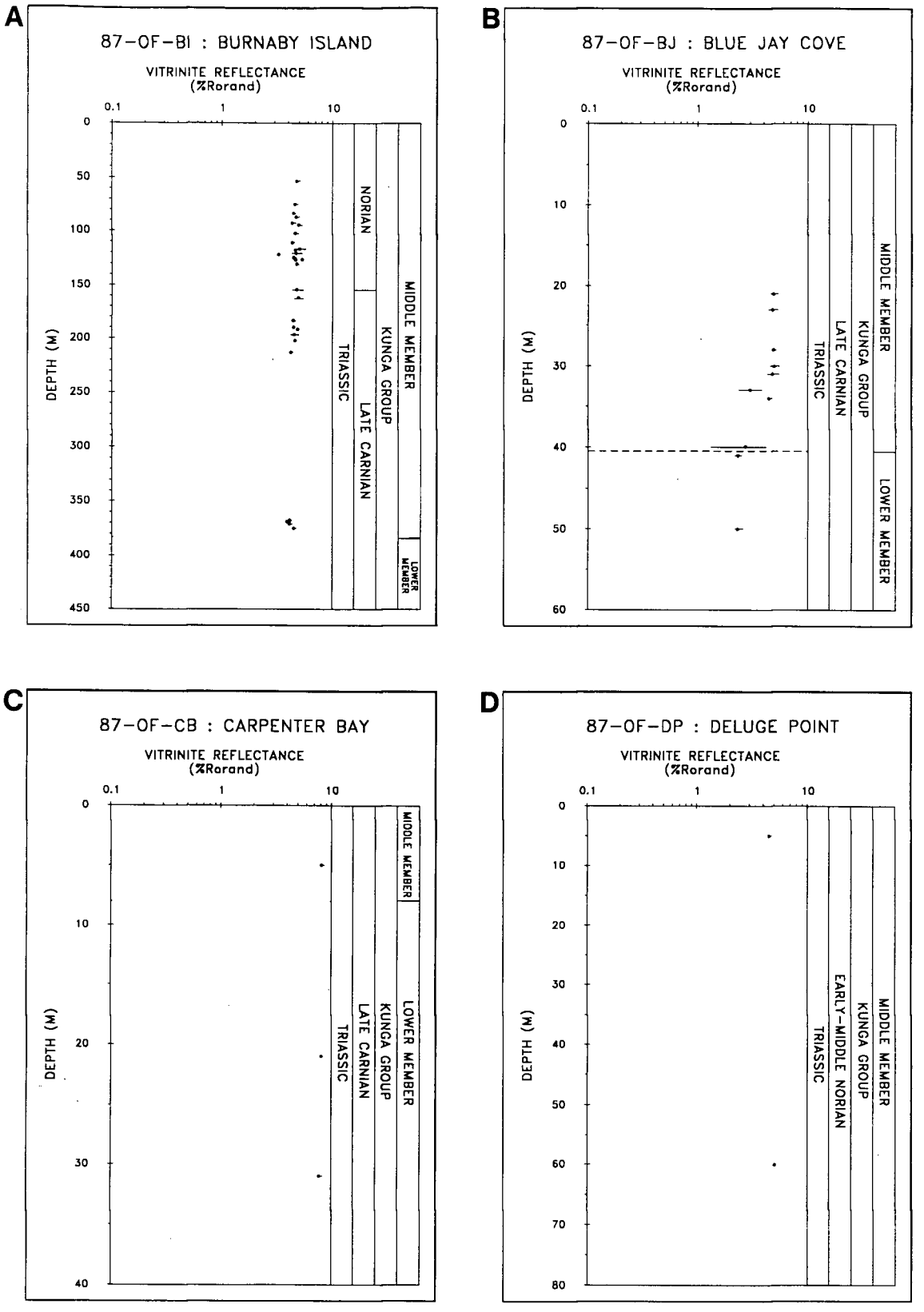

Figure 21. Vertical maturation profiles [vitrinite reflectance (%Ro_{rand})/stratigraphic depth] of the Upper Triassic to Sinemurian Kunga Group; a) near Moresby Island at Burnaby Island; b) on Moresby Island at Blue Jay Cove; c) on Moresby Island at Carpenter Bay; d) on Moresby Island at Deluge Point. Points are mean vitrinite reflectance values. Error bars are calculated as mean values $\pm$ standard deviation

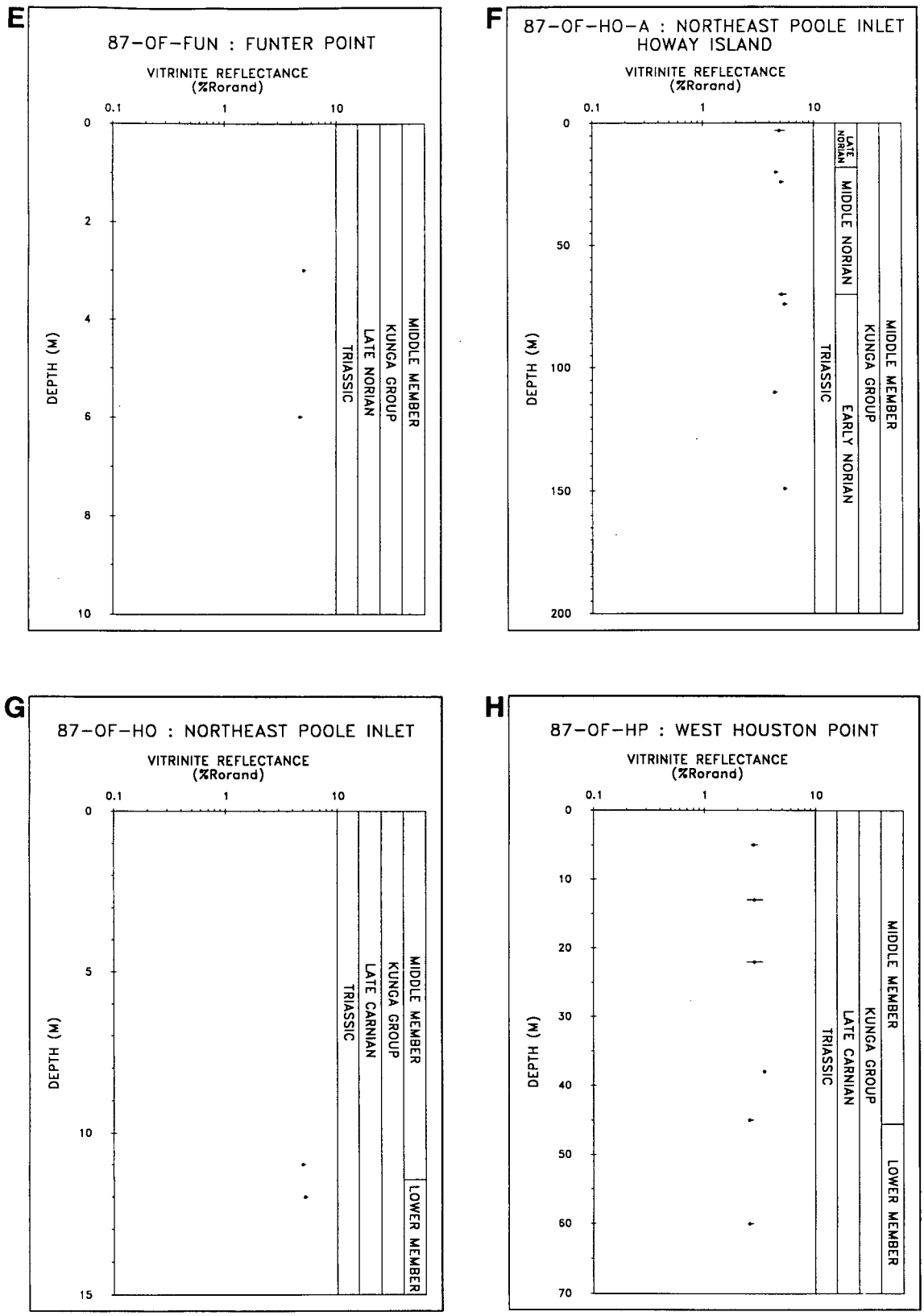

Figure 21. Vertical maturation profiles [vitrinite reflectance ($\%Ro_{rand}$)/stratigraphic depth] of the Upper Triassic to Sinemurian Kunga Group; e) on Moresby Island at Funter Point; f) on Moresby Island in northeast Poole Inlet at Howay Island; g) on Moresby Island in northeast Poole Inlet; h) on Moresby Island at west Huston Inlet. Points are mean vitrinite reflectance values. Error bars are calculated as mean values $\pm$ standard deviation

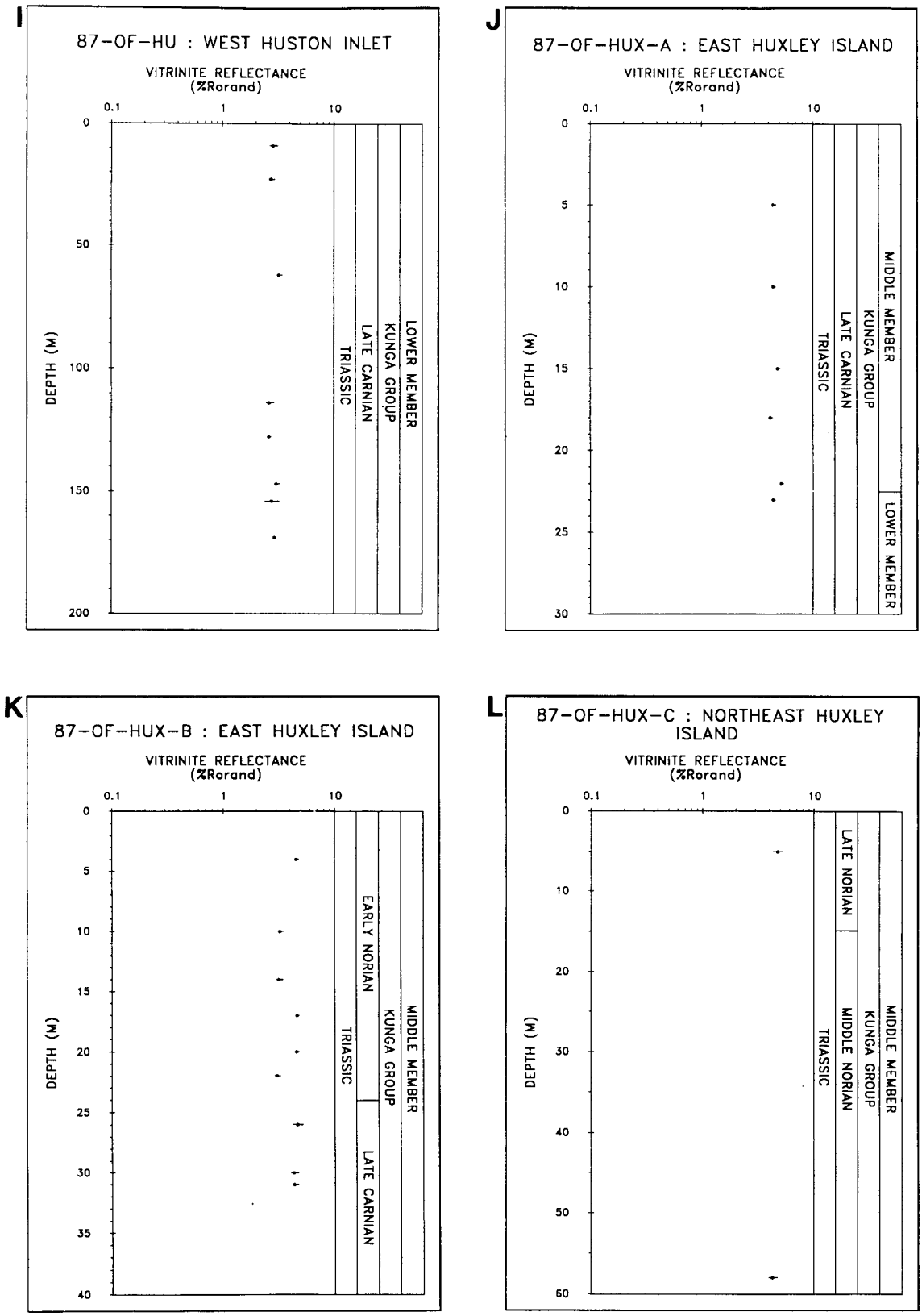

Figure 21. Vertical maturation profiles [vitrinite reflectance ($\%Ro_{rand}$)/stratigraphic depth] of the Upper Triassic to Sinemurian Kunga Group; i) on Moresby Island at west Huston Inlet; j) near Moresby Island on east Huxley Island; k) near Moresby Island on east Huxley Island l) near Moresby Island on northeast Huxley Island. Points are mean vitrinite reflectance values. Error bars are calculated as mean values $\pm$ standard deviation

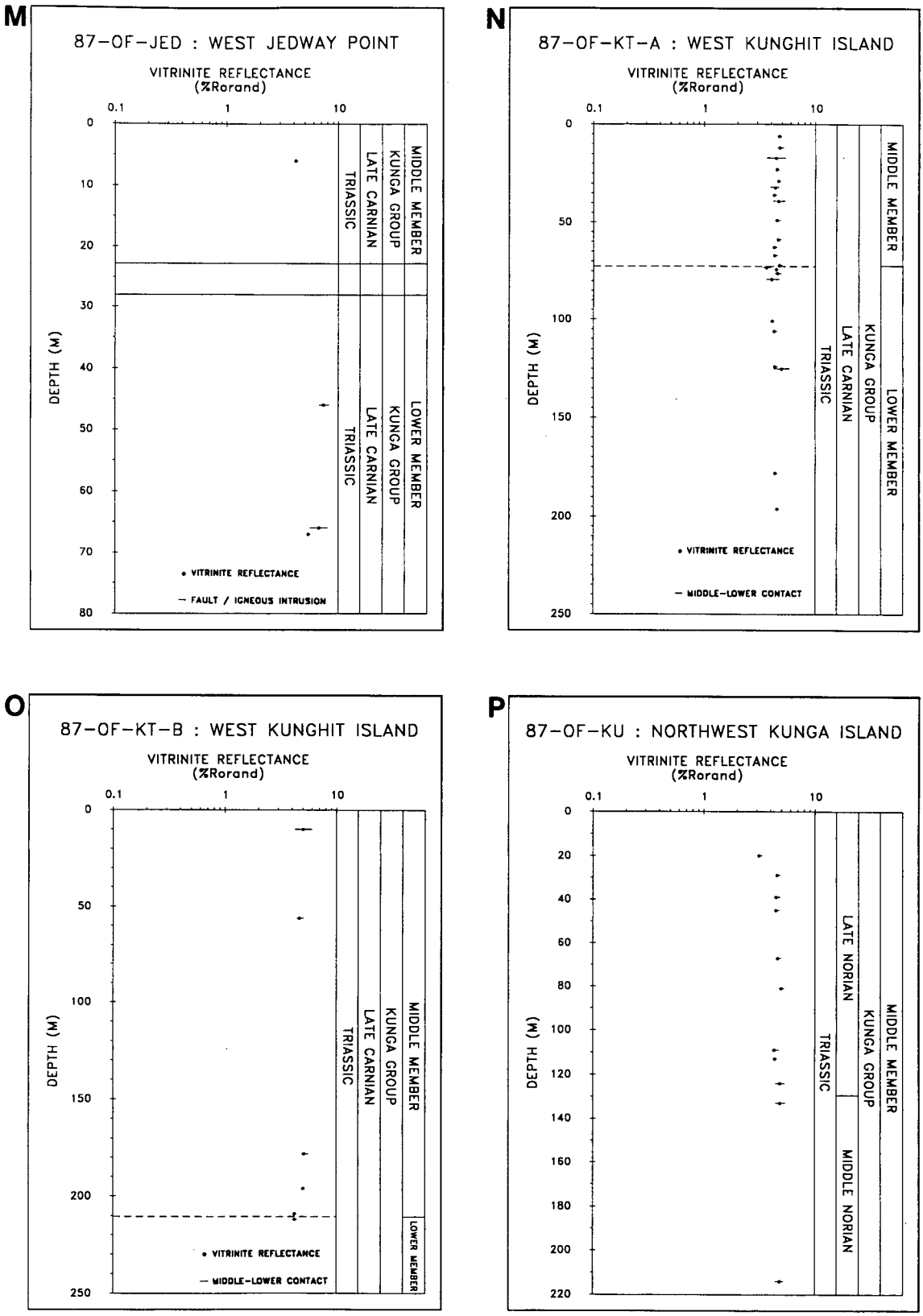

Figure 21. Vertical maturation profiles [vitrinite reflectance (%Ro_{rand})/stratigraphic depth] of the Upper Triassic to Sinemurian Kunga Group; m) on Moresby Island at west Jedway Point; n) near Moresby Island on west Kunghit Island; o) near Moresby Island on west Kunghit Island; p) near Moresby Island at northwest Kunga Island. Points are mean vitrinite reflectance values. Error bars are calculated as mean values $\pm$ standard deviation

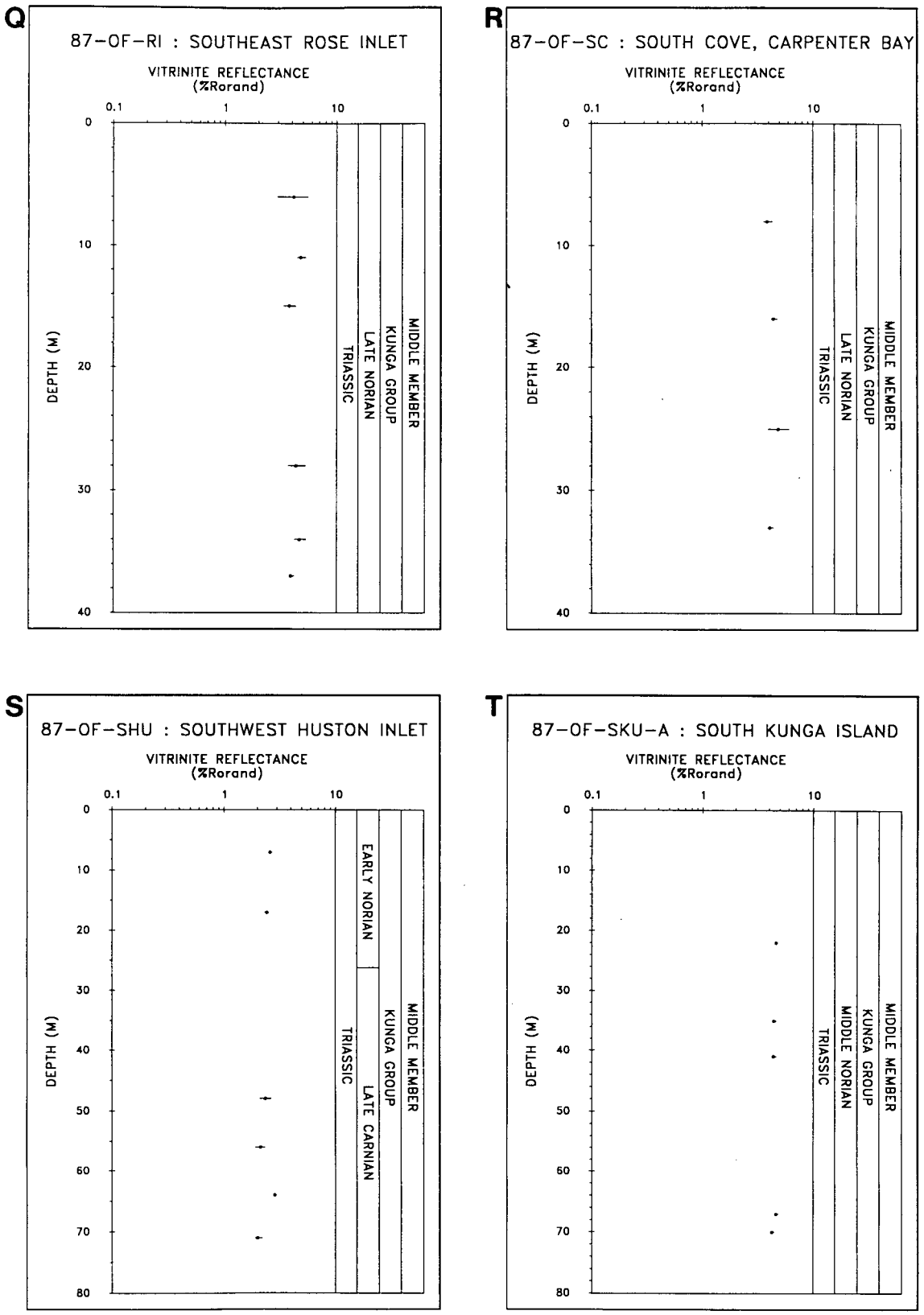

Figure 21. Vertical maturation profiles [vitrinite reflectance ($\%Ro_{rand}$)/stratigraphic depth] of the Upper Triassic to Sinemurian Kunga Group; q) on Moresby Island at southeast Rose Inlet; r) on Moresby Island at South Cove in Carpenter Bay; s) on Moresby Island at southwest Huston Inlet; t) near Moresby Island on south Kunga Island. Points are average vitrinite reflectance values. Error bars are calculated as mean values $\pm$ standard deviation

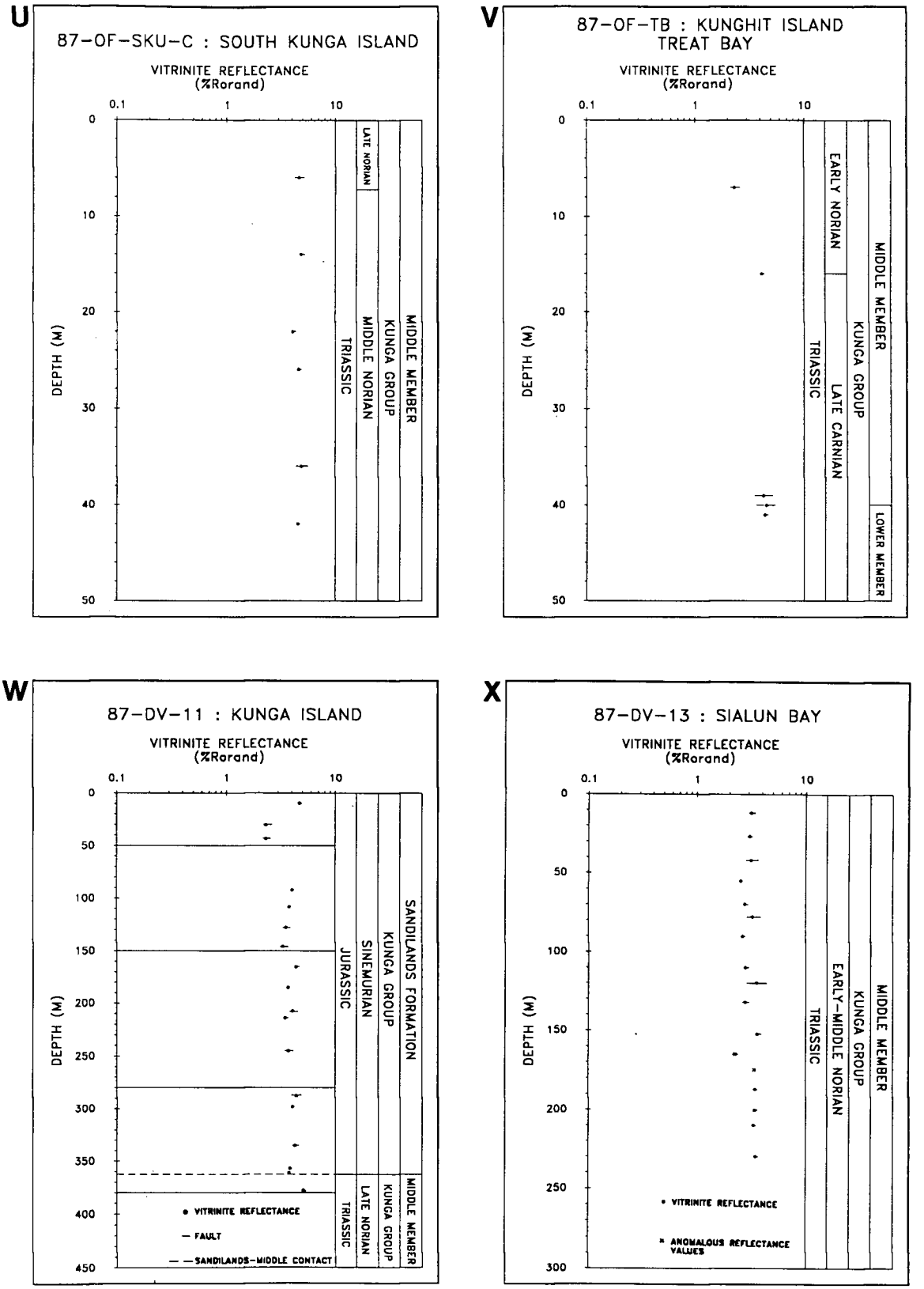

Figure 21. Vertical maturation profiles [vitrinite reflectance (%Ro_{rand})/stratigraphic depth] of the Upper Triassic to Sinemurian Kunga Group; u) near Moresby Island on south Kunga Island; v) near Moresby Island at Treat Bay on Kunghit Island; w) near Moresby Island on Kunga Island; x) on northwest Graham Island at Sialun Bay. Points are mean vitrinite reflectance values. Error bars are calculated as mean values $\pm$ standard deviation

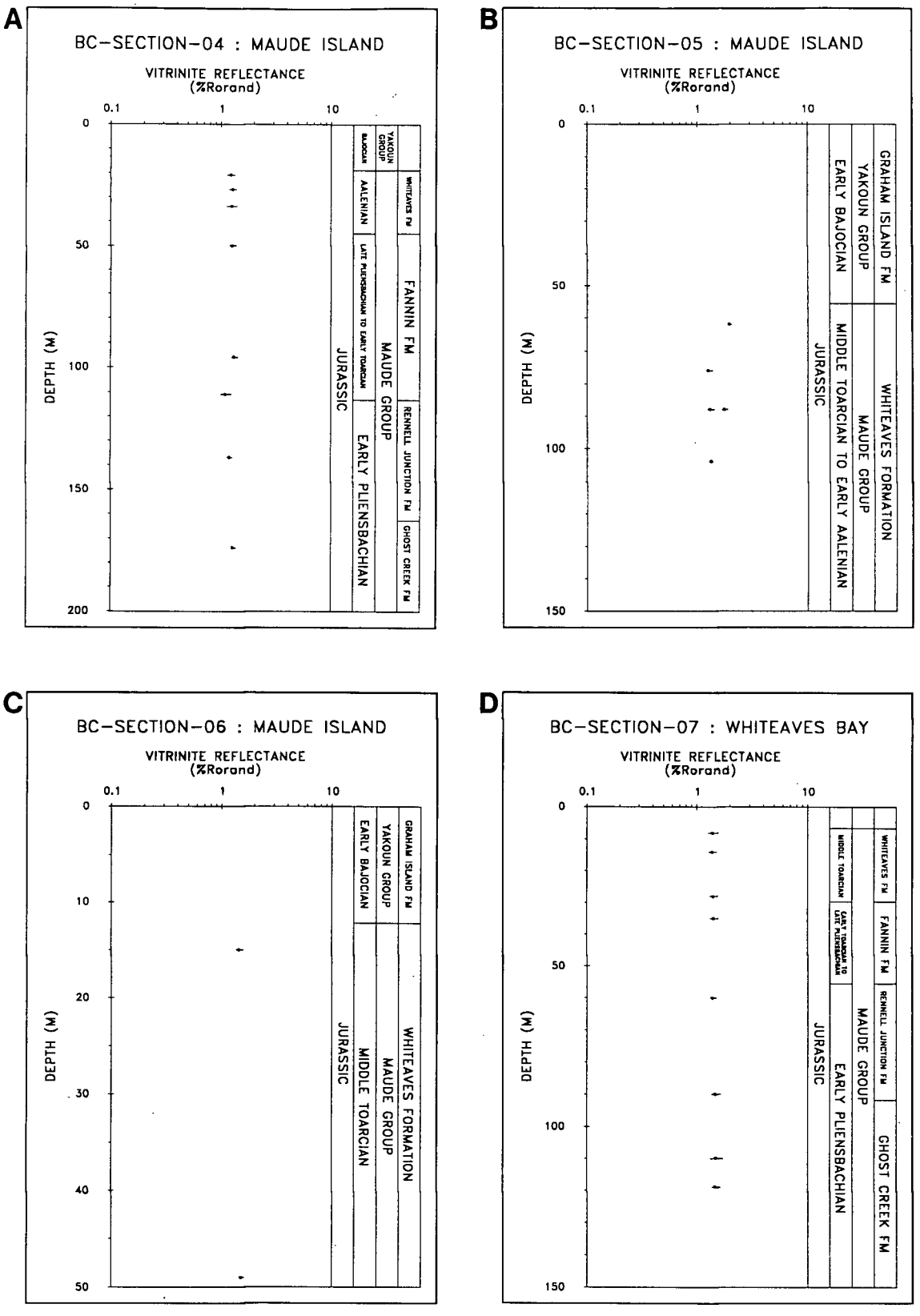

Figure 22. Vertical maturation profiles [vitrinite reflectance (%Ro_{rand})/stratigraphic depth] of the Lower Jurassic Maude Group; a) in Skidegate Inlet on Maude Island; b) in Skidegate Inlet on Maude Island; c) in Skidegate Inlet on Maude Island; d) in Skidegate Inlet at Whiteaves Bay. Points are mean vitrinite reflectance values. Error bars are calculated as mean values $\pm$ standard deviation

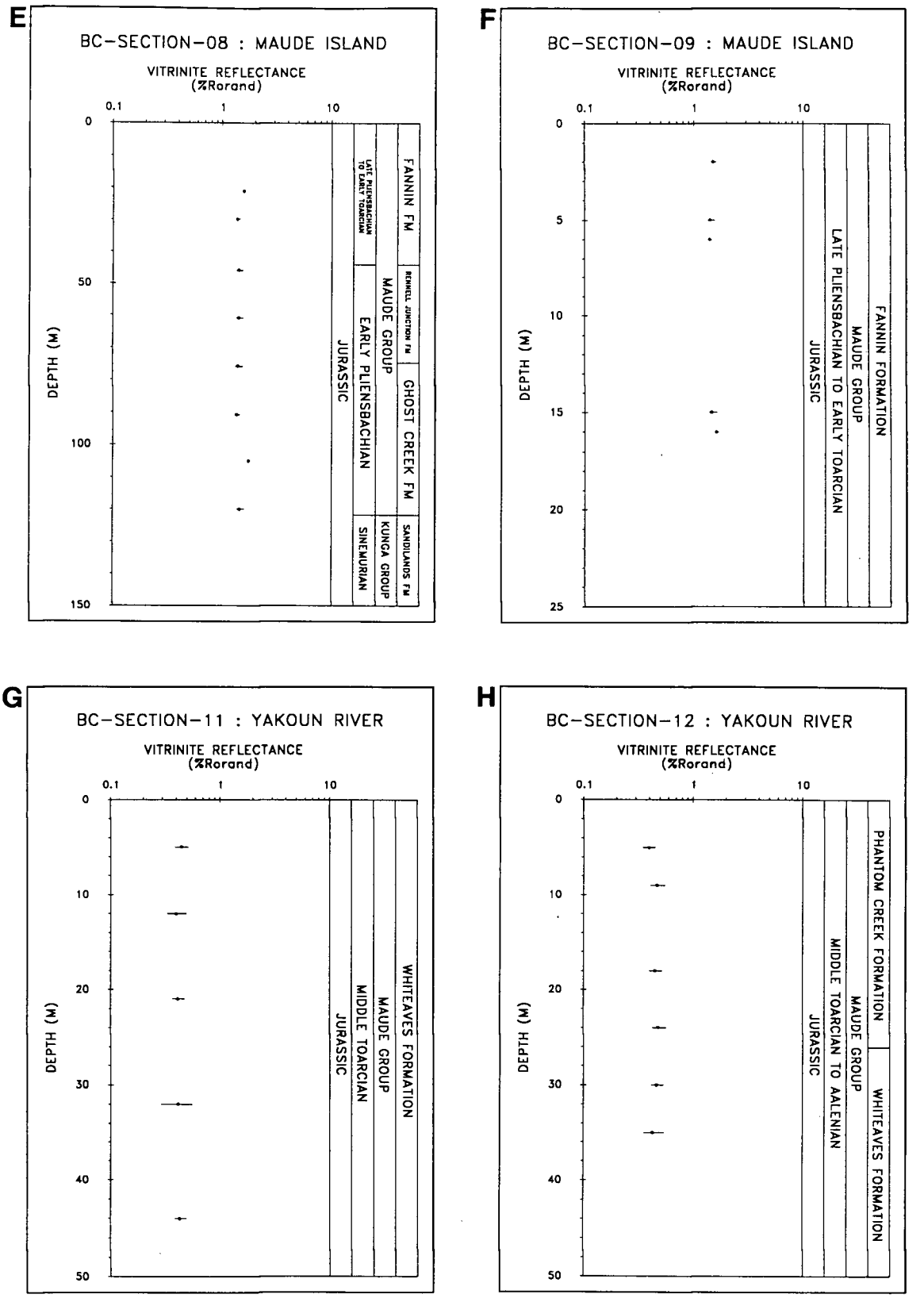

Figure 22. Vertical maturation profiles [vitrinite reflectance (%Ro_{rand})/stratigraphic depth] of the Lower Jurassic Maude Group; e) in Skidegate Inlet on Maude Island; f) in Skidegate Inlet on Maude Island; g) in central Graham Island on the Yakoun River; h) in central Graham Island on the Yakoun River. Points are mean vitrinite reflectance values. Error bars are calculated as mean values $\pm$ standard deviation

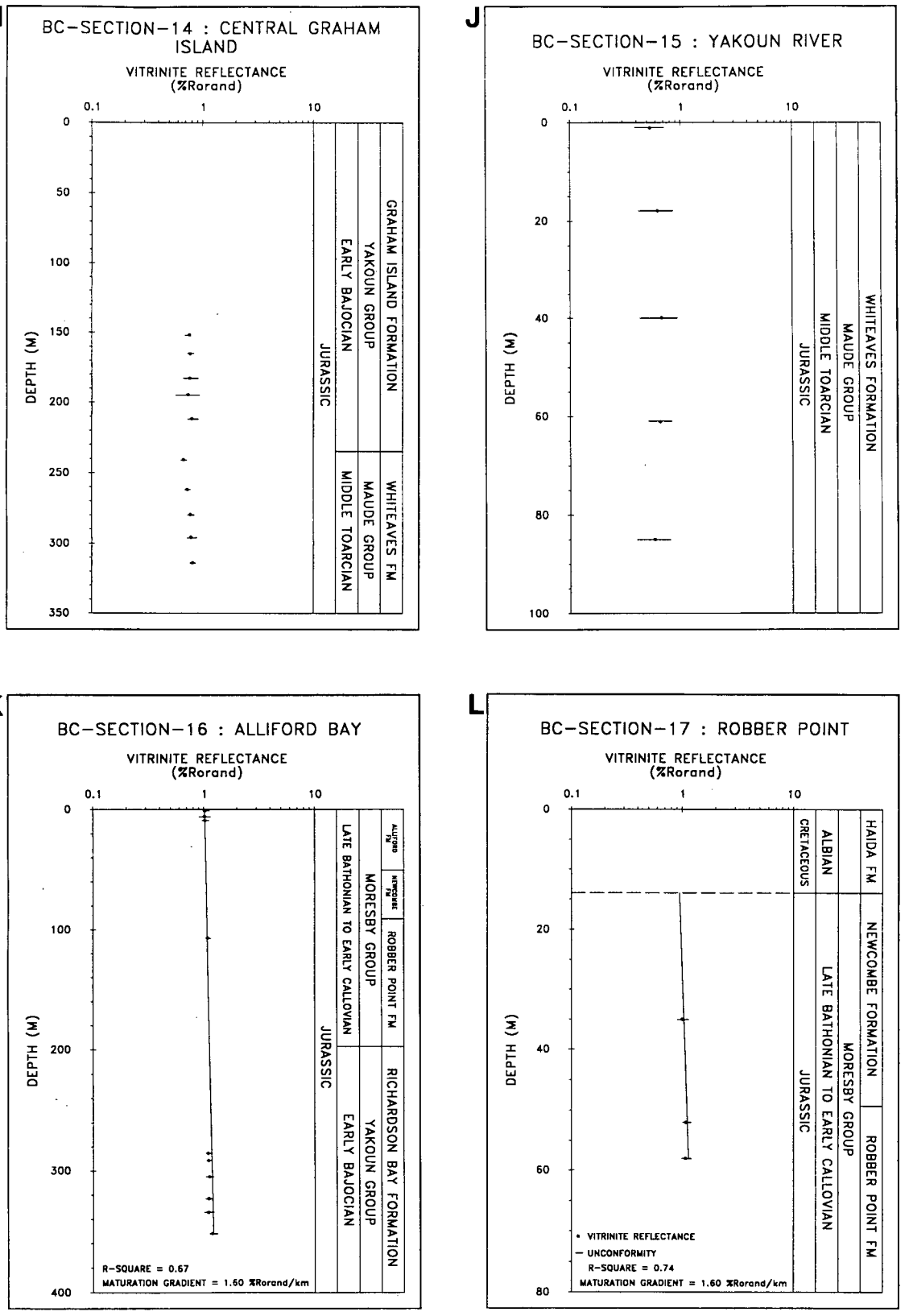

Figure 22. Vertical maturation profiles [vitrinite reflectance ($\%Ro_{rand}$)/stratigraphic depth] of the Lower Jurassic Maude, Yakoun, or Moresby Groups; i) in central Graham Island; j) in central Graham Island on the Yakoun River; k) in Skidegate Inlet at Alliford Bay; l) in Cumshewa Inlet at Robber Point. Points are mean vitrinite reflectance values. Error bars are calculated as mean values $\pm$ standard deviation. Maturation gradient is log ($\%Ro_{rand}$)/km

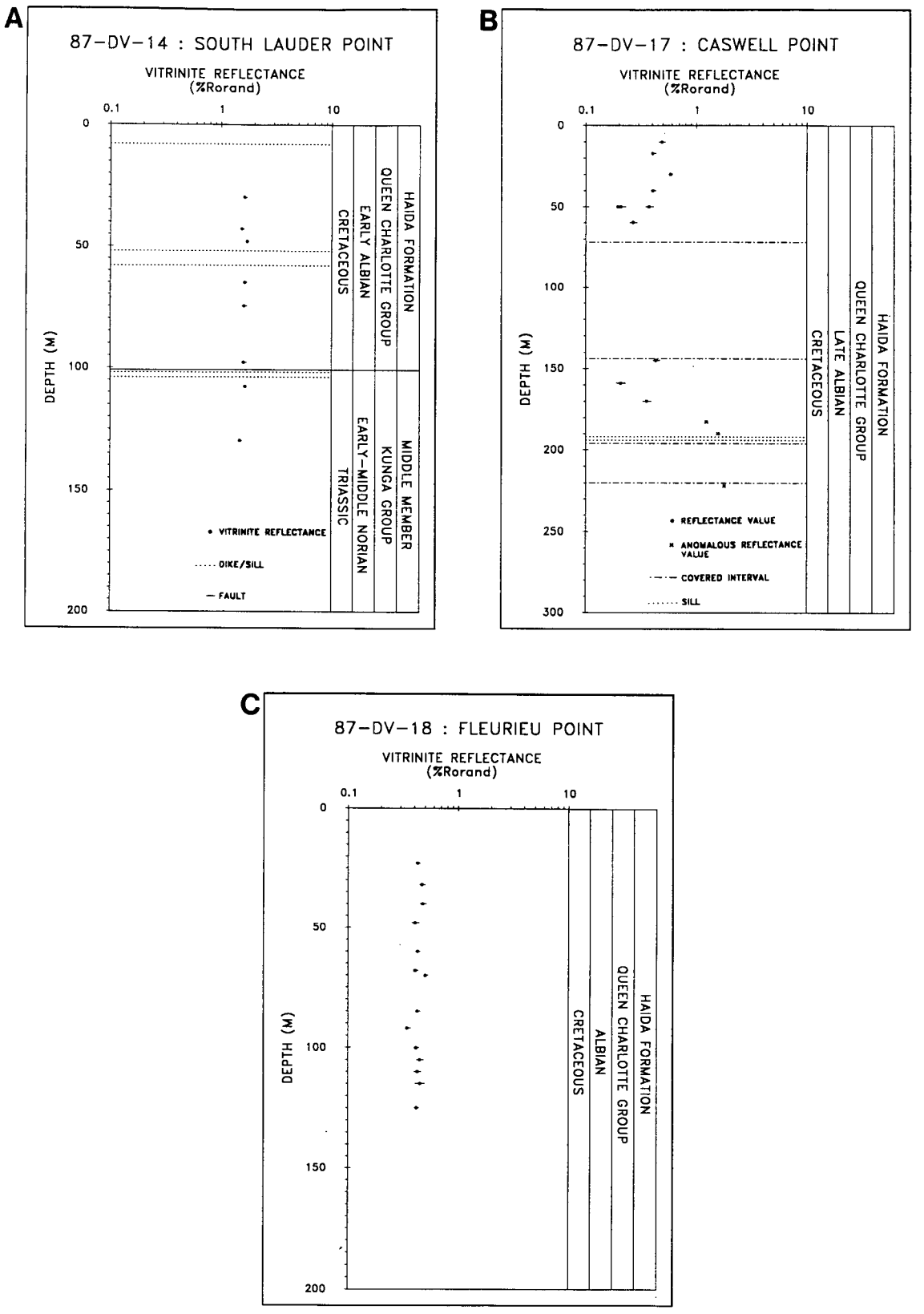

Figure 23. Vertical maturation profiles [vitrinite reflectance ($\%Ro_{rand}$)/stratigraphic depth] of the Cretaceous Haida Formation;a) on northwest Graham Island at south Lauder Point; b) on northwest Graham Island at Caswell Point; c) on northwest Graham Island at Fleurieu Point. Points are mean vitrinite reflectance values. Error bars are calculated as mean values $\pm$ standard deviation

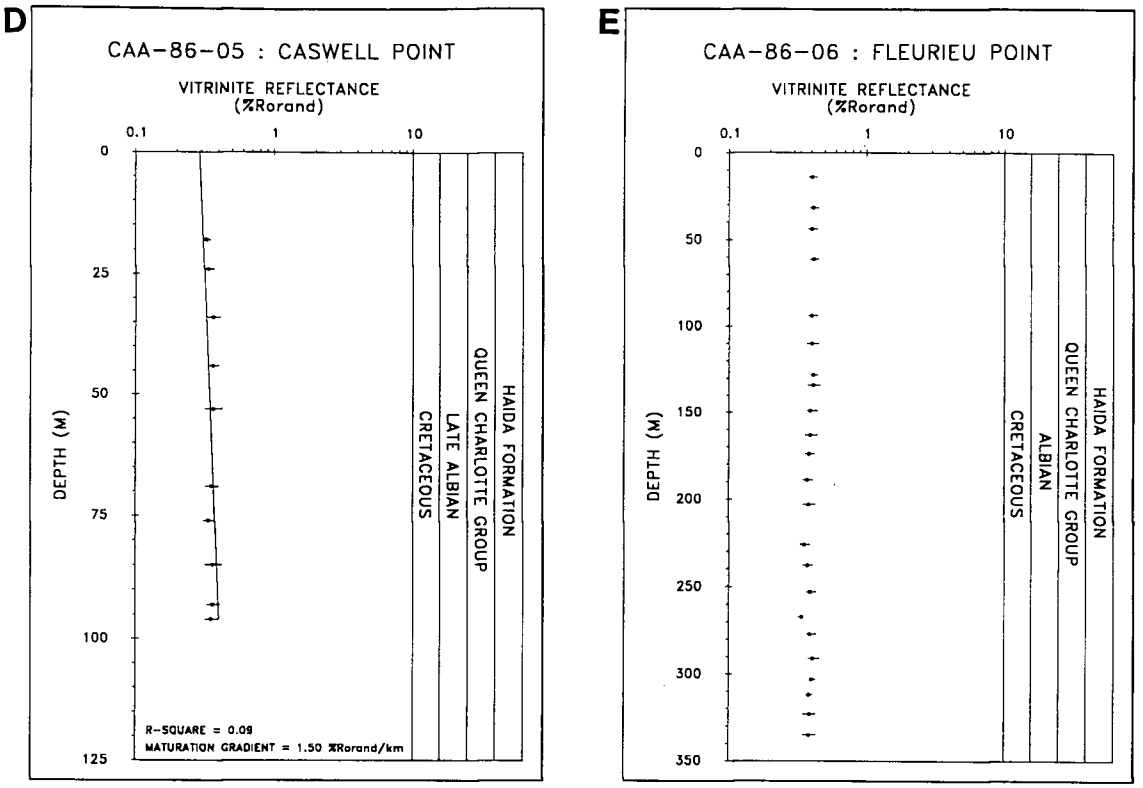

Figure 23. Vertical maturation profiles [vitrinite reflectance (%Ro_{rand})/stratigraphic depth] of the Cretaceous Haida Formation; d) on northwest Graham Island at Caswell Point; e) on northwest Graham Island at Fleurieu Point. Points are mean vitrinite reflectance values. Error bars are calculated as mean values $\pm$ standard deviation. Maturation gradient is log (%Ro_{rand})/km

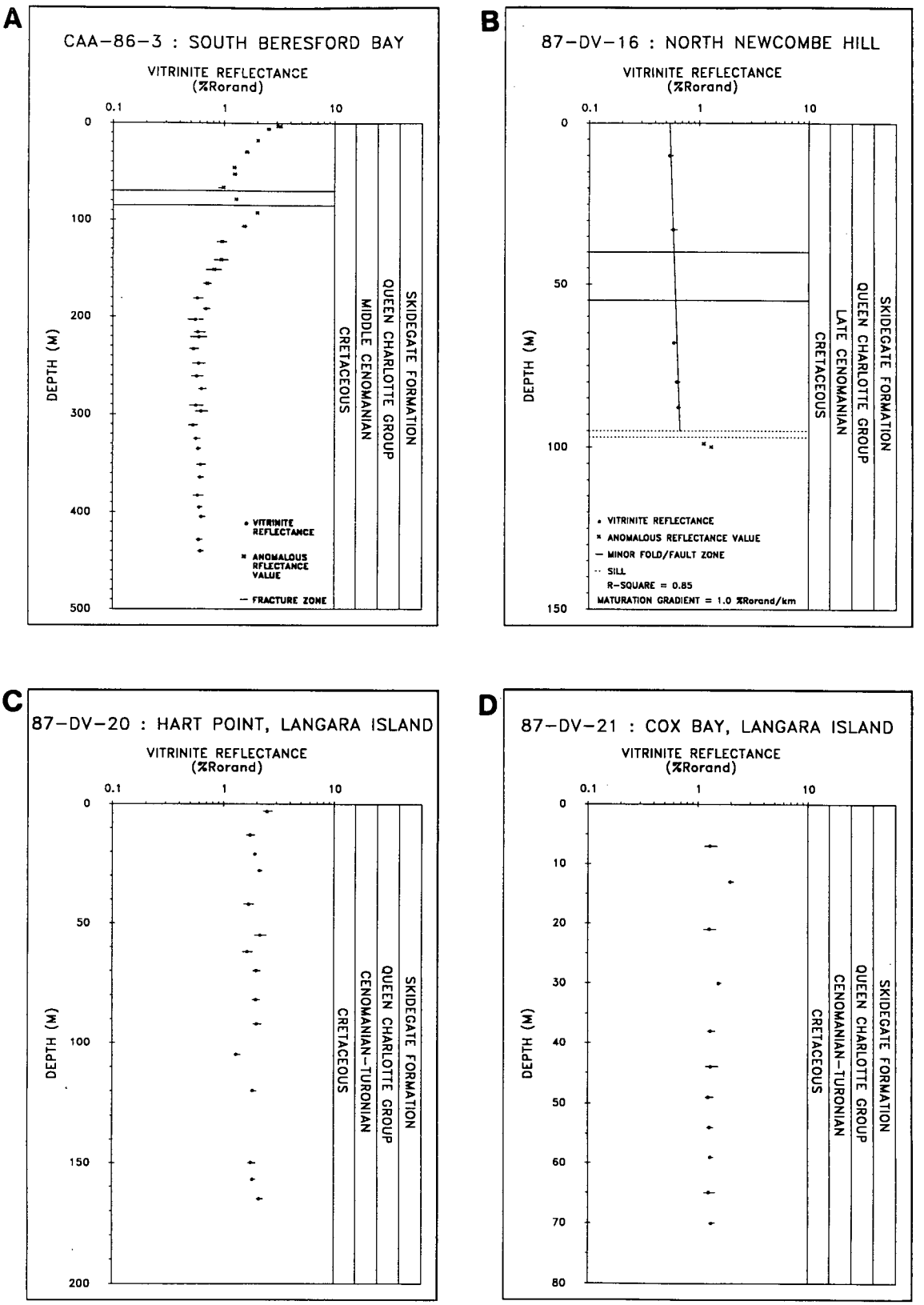

Figure 24. Vertical maturation profiles [vitrinite reflectance ($\%Ro_{rand}$)/stratigraphic depth] of the Cretaceous Skidegate Formation; a) on northwest Graham Island at south Beresford Bay; b) on northwest Graham Island at north Newcombe Hill; c) on Langara Island at Hart Point; d) on Langara Island at Cox Bay. Points are mean vitrinite reflectance values. Error bars are calculated as mean values $\pm$ standard deviation. Maturation gradient is log ($\%Ro_{rand}$)/km

TABLE 1A

GREY LIMESTONE MEMBER (KUNGA GROUP)

SECTION NAME	$\%Ro_{rand}$	TMAX	TOC	S1	S2	PI	QOM	HI	OI
OF SECTION BB									
MEAN	5.8	*	*	*	*	*	*	*	*
# OF SAMPLES	3.	0.	0.	0.	0.	0.	0.	0.	0.
OF SECTION BI									
MEAN	*	*	*	*	*	*	*	*	*
# OF SAMPLES	0.	0.	0.	0.	0.	0.	0.	0.	0.
OF SECTION BJ									
MEAN	2.35	*	*	*	*	*	*	*	*
# OF SAMPLES	1.	0.	0.	0.	0.	0.	0.	0.	0.
OF SECTION BR									
MEAN	2.72	*	*	*	*	*	*	*	*
# OF SAMPLES	4.	0.	0.	0.	0.	0.	0.	0.	0.
OF SECTION CB									
MEAN	8.	*	*	*	*	*	*	*	*
# OF SAMPLES	2.	0.	0.	0.	0.	0.	0.	0.	0.
OF SECTION CRE									
MEAN	4.59	*	*	*	*	*	*	*	*
# OF SAMPLES	1.	0.	0.	0.	0.	0.	0.	0.	0.
OF SECTION HP									
MEAN	2.61	*	*	*	*	*	*	*	*
# OF SAMPLES	1.	0.	0.	0.	0.	0.	0.	0.	0.
OF SECTION HU									
MEAN	2.91	*	*	*	*	*	*	*	*
# OF SAMPLES	8.	0.	0.	0.	0.	0.	0.	0.	0.
OF SECTION JED									
MEAN	6.56	*	*	*	*	*	*	*	*
# OF SAMPLES	3.	0.	0.	0.	0.	0.	0.	0.	0.
OF SECTION KT									
MEAN	4.39	*	*	*	*	*	*	*	*
# OF SAMPLES	10.	0.	0.	0.	0.	0.	0.	0.	0.
OF SECTION TB									
MEAN	4.38	*	*	*	*	*	*	*	*
# OF SAMPLES	4.	0.	0.	0.	0.	0.	0.	0.	0.

TABLE 1A (CONT.)

GREY LIMESTONE MEMBER (KUNGA GROUP)

SECTION NAME	%Ro_{rand}	TMAX	TOC	S1	S2	PI	QOM	HI	OI
OF SECTION TIT									
MEAN	5.28	*	*	*	*	*	*	*	*
# OF SAMPLES	1.	0.	0.	0.	0.	0.	0.	0.	0.
SECTION 1									
MEAN	*	*	1.1	0.01	0.03	0.08	0.02	2.	35.
# OF SAMPLES	0.	0.	3.	3.	3.	3.	3.	3.	3.
SECTION 3									
MEAN	*	*	0.18	0.	0.	0.	0.	0.	33.
# OF SAMPLES	0.	0.	1.	1.	1.	1.	1.	1.	1.
SECTION 6									
MEAN	*	*	0.06	0.	0.	0.	0.	0.	48.
# OF SAMPLES	0.	0.	6.	6.	6.	6.	6.	6.	6.
SECTION 7									
MEAN	*	*	0.28	0.	0.	0.	0.01	0.	26.
# OF SAMPLES	0.	0.	4.	4.	4.	4.	4.	4.	4.
SECTION 8									
MEAN	*	*	0.24	0.	0.02	0.	0.08	8.	24.
# OF SAMPLES	0.	0.	4.	4.	4.	4.	4.	4.	4.
SECTION 9									
MEAN	*	*	0.06	0.	0.	0.	0.	0.	0.
# OF SAMPLES	0.	0.	1.	1.	1.	1.	1.	1.	1.
SECTION 10									
MEAN	*	*	0.06	0.	0.	0.	0.	0.	0.
# OF SAMPLES	0.	0.	1.	1.	1.	1.	1.	1.	1.
SPOT SAMPLE									
MEAN	*	*	0.10	0.	0.	0.	0.	0.	132.
# OF SAMPLES	0.	0.	5.	5.	5.	5.	5.	5.	5.
TF SPOT SAMPLE									
MEAN	2.95	*	0.	0.	0.	0.	*	0.	0.
# OF SAMPLES	3.	0.	3.	3.	3.	3.	0.	3.	3.

TABLE 1B

BLACK LIMESTONE MEMBER (KUNGA GROUP)

SECTION NAME	%Ro_{rand}	TMAX	TOC	S1	S2	PI	QOM	HI	OI
OF SECTION B1									
MEAN	4.56	*	*	*	*	*	*	*	*
# OF SAMPLES	28.	0.	0.	0.	0.	0.	0.	0.	0.
OF SECTION BJ									
MEAN	4.09	*	*	*	*	*	*	*	*
# OF SAMPLES	10.	0.	0.	0.	0.	0.	0.	0.	0.
OF SECTION CB									
MEAN	8.31	*	*	*	*	*	*	*	*
# OF SAMPLES	1.	0.	0.	0.	0.	0.	0.	0.	0.
OF SECTION CRE									
MEAN	4.59	*	*	*	*	*	*	*	*
# OF SAMPLES	1.	0.	0.	0.	0.	0.	0.	0.	0.
OF SECTION DP									
MEAN	4.84	*	*	*	*	*	*	*	*
# OF SAMPLES	2.	0.	0.	0.	0.	0.	0.	0.	0.
OF SECTION EPO									
MEAN	4.81	*	*	*	*	*	*	*	*
# OF SAMPLES	1.	0.	0.	0.	0.	0.	0.	0.	0.
OF SECTION FUN									
MEAN	5.05	*	*	*	*	*	*	*	*
# OF SAMPLES	2.	0.	0.	0.	0.	0.	0.	0.	0.
OF SECTION GB									
MEAN	3.13	*	*	*	*	*	*	*	*
# OF SAMPLES	2.	0.	0.	0.	0.	0.	0.	0.	0.
OF SECTION HO									
MEAN	5.08	*	*	*	*	*	*	*	*
# OF SAMPLES	9.	0.	0.	0.	0.	0.	0.	0.	0.
OF SECTION HP									
MEAN	2.94	*	*	*	*	*	*	*	*
# OF SAMPLES	5.	0.	0.	0.	0.	0.	0.	0.	0.
OF SECTION HUX									
MEAN	4.33	*	*	*	*	*	*	*	*
# OF SAMPLES	19.	0.	0.	0.	0.	0.	0.	0.	0.

TABLE 1B (CONT.)

BLACK LIMESTONE MEMBER (KUNGA GROUP)

SECTION NAME	%Ro_{rand}	TMAX	TOC	S1	S2	PI	QOM	HI	OI
OF SECTION JED									
MEAN	4.23	*	*	*	*	*	*	*	*
# OF SAMPLES	1.	0.	0.	0.	0.	0.	0.	0.	0.
OF SECTION KT									
MEAN	4.66	*	*	*	*	*	*	*	*
# OF SAMPLES	18.	0.	0.	0.	0.	0.	0.	0.	0.
OF SECTION KU									
MEAN	4.56	*	*	*	*	*	*	*	*
# OF SAMPLES	12.	0.	0.	0.	0.	0.	0.	0.	0.
OF SECTION LUX									
MEAN	4.63	*	*	*	*	*	*	*	*
# OF SAMPLES	1.	0.	0.	0.	0.	0.	0.	0.	0.
OF SECTION NPO									
MEAN	4.62	*	*	*	*	*	*	*	*
# OF SAMPLES	3.	0.	0.	0.	0.	0.	0.	0.	0.
OF SECTION POO									
MEAN	3.53	*	*	*	*	*	*	*	*
# OF SAMPLES	5.	0.	0.	0.	0.	0.	0.	0.	0.
OF SECTION RH									
MEAN	5.6	*	*	*	*	*	*	*	*
# OF SAMPLES	2.	0.	0.	0.	0.	0.	0.	0.	0.
OF SECTION RI									
MEAN	4.37	*	*	*	*	*	*	*	*
# OF SAMPLES	6.	0.	0.	0.	0.	0.	0.	0.	0.
OF SECTION ROSS									
MEAN	4.87	*	*	*	*	*	*	*	*
# OF SAMPLES	2.	0.	0.	0.	0.	0.	0.	0.	0.
OF SECTION SC									
MEAN	4.35	*	*	*	*	*	*	*	*
# OF SAMPLES	5.	0.	0.	0.	0.	0.	0.	0.	0.
OF SECTION SHU									
MEAN	2.4	*	*	*	*	*	*	*	*
# OF SAMPLES	6.	0.	0.	0.	0.	0.	0.	0.	0.

TABLE 1B (CONT.)

BLACK LIMESTONE MEMBER (KUNGA GROUP)

SECTION NAME	$\%Ro_{rand}$	TMAX	TOC	S1	S2	PI	QOM	HI	OI
OF SECTION SI									
MEAN	4.1	*	*	*	*	*	*	*	*
# OF SAMPLES	4.	0.	0.	0.	0.	0.	0.	0.	0.
OF SECTION SK									
MEAN	3.78	*	*	*	*	*	*	*	*
# OF SAMPLES	3.	0.	0.	0.	0.	0.	0.	0.	0.
OF SECTION SKU									
MEAN	4.58	*	*	*	*	*	*	*	*
# OF SAMPLES	13.	0.	0.	0.	0.	0.	0.	0.	0.
OF SECTION SPO									
MEAN	3.89	*	*	*	*	*	*	*	*
# OF SAMPLES	1.	0.	0.	0.	0.	0.	0.	0.	0.
OF SECTION TB									
MEAN	2.37	*	*	*	*	*	*	*	*
# OF SAMPLES	1.	0.	0.	0.	0.	0.	0.	0.	0.
OF SECTION VP									
MEAN	3.85	*	*	*	*	*	*	*	*
# OF SAMPLES	1.	0.	0.	0.	0.	0.	0.	0.	0.
SECTION 1									
MEAN	*	*	0.82	0.	0.	0.	0.01	0.	32.
# OF SAMPLES	0.	0.	8.	8.	8.	8.	8.	8.	8.
SECTION 2									
MEAN	*	*	0.9	0.	0.01	0.	0.	0.	231.
# OF SAMPLES	0.	0.	5.	5.	5.	5.	5.	5.	5.
SECTION 3									
MEAN	*	*	1.02	0.	0.	0.	0.01	1.	13.
# OF SAMPLES	0.	0.	8.	8.	8.	8.	8.	8.	8.
SECTION 4									
MEAN	3.64	*	2.21	0.	0.05	0.03	0.05	16.	13.
# OF SAMPLES	3.	0.	4.	4.	4.	4.	4.	4.	4.
SECTION 7									
MEAN	*	*	0.41	0.	0.	0.	0.	0.	3.
# OF SAMPLES	0.	0.	3.	3.	3.	3.	3.	3.	3.

TABLE 1B (CONT.)

BLACK LIMESTONE MEMBER (KUNGA GROUP)

SECTION NAME	$\%Ro_{rand}$	TMAX	TOC	S1	S2	PI	QOM	HI	OI
SECTION 8									
MEAN	*	*	0.25	0.	0.	0.	0.02	0.	50.
# OF SAMPLES	0.	0.	5.	5.	5.	5.	5.	5.	5.
SECTION 9									
MEAN	*	*	0.22	0.	0.	0.	0.01	1.	9.
# OF SAMPLES	0.	0.	9.	9.	9.	9.	9.	9.	9.
SECTION 10									
MEAN	4.29	*	1.16	0.	0.01	0.07	0.01	1.	24.
# OF SAMPLES	14.	0.	15.	15.	15.	15.	15.	15.	15.
SECTION 11									
MEAN	5.11	*	2.56	0.07	0.01	0.87	0.03	0.	11.
# OF SAMPLES	1.	0.	1.	1.	1.	1.	1.	1.	1.
SECTION 12									
MEAN	0.51	440.	3.6	1.21	14.08	0.08	4.19	385.	9.
# OF SAMPLES	6.	6.	6.	6.	6.	6.	6.	6.	6.
SECTION 13									
MEAN	3.19	587.	2.9	0.04	0.08	0.33	0.04	2.	24.
# OF SAMPLES	16.	1.	18.	18.	18.	18.	18.	18.	18.
SECTION 14									
MEAN	1.59	*	*	*	*	*	*	*	*
# OF SAMPLES	2.	0.	0.	0.	0.	0.	0.	0.	0.
SECTION 15									
MEAN	1.47	467.	2.69	0.64	0.83	0.44	0.55	30.	47.
# OF SAMPLES	2.	1.	1.	1.	1.	1.	1.	1.	1.
SECTION 19									
MEAN	1.18	444.	2.17	0.57	4.69	0.12	2.19	192.	14.
# OF SAMPLES	16.	18.	18.	18.	18.	18.	17.	18.	18.
SPOT SAMPLE									
MEAN	4.04	*	1.06	0.	0.01	0.04	0.02	0.	25.
# OF SAMPLES	30.	0.	38.	38.	38.	38.	38.	38.	38.

TABLE 1C

SANDILANDS FORMATION

SECTION NAME	$\%Ro_{rand}$	TMAX	TOC	S1	S2	PI	QOM	HI	OI
SECTION 5									
MEAN	*	*	0.51	0.01	0.03	0.06	0.03	2.	49.
# OF SAMPLES	0.	0.	4.	4.	4.	4.	4.	4.	4.
SECTION 11									
MEAN	3.78	*	1.53	0.04	0.03	0.59	0.05	2.	9.
# OF SAMPLES	18.	0.	21.	21.	21.	21.	21.	21.	21.
SECTION 12									
MEAN	0.45	436.	2.66	0.77	12.9	0.06	4.66	437.	10.
# OF SAMPLES	18.	10.	10.	10.	10.	10.	10.	10.	10.
SPOT SAMPLE									
MEAN	4.	*	0.59	0.	0.	0.	0.01	0.	7.
# OF SAMPLES	5.	0.	8.	8.	8.	8.	8.	8.	8.
CENTRAL GRAHAM ISLAND B-QUARRY									
MEAN	0.40	443.	3.14	1.64	13.85	0.14	4.26	372.	36.
# OF SAMPLES	17.	17.	17.	17.	17.	17.	17.	17.	17.
CENTRAL GRAHAM ISLAND D-QUARRY									
MEAN	0.66	447.	1.32	0.67	3.83	0.16	2.73	229.	525.
# OF SAMPLES	4.	4.	5.	5.	5.	4.	5.	5.	5.
CENTRAL GRAHAM ISLAND BRANCH ROAD 57									
MEAN	0.65	437.	1.25	0.47	3.43	0.16	3.32	264.	42.
# OF SAMPLES	6.	6.	6.	6.	6.	6.	6.	6.	6.
CENTRAL GRAHAM ISLAND MAIN ROAD									
MEAN	0.60	445.	2.08	1.02	4.9	0.15	1.94	159.	68.
# OF SAMPLES	4.	4.	5.	5.	5.	5.	5.	5.	5.
CENTRAL GRAHAM ISLAND WELL I-178									
MEAN	0.60	437.	1.75	1.12	3.86	0.25	2.75	210.	48.
# OF SAMPLES	32.	32.	33.	33.	33.	33.	33.	33.	33.
CENTRAL GRAHAM ISLAND WELL I-179									
MEAN	0.88	447.	9.6	0.50	4.12	0.31	2.71	242.	73.
# OF SAMPLES	40.	37.	40.	40.	40.	38.	39.	39.	39.

TABLE 1C (CONT.)

SANDILANDS FORMATION

SECTION NAME	%Ro_{rand}	TMAX	TOC	S1	S2	PI	QOM	HI	OI
CENTRAL GRAHAM ISLAND WELL I-278									
MEAN	0.65	447.	1.91	0.99	4.60	0.23	2.56	205.	57.
# OF SAMPLES	47.	47.	47.	47.	47.	47.	47.	47.	47.
MAUDE ISLAND									
MEAN	1.35	465.	1.47	0.24	0.52	0.42	0.44	27.	34.
# OF SAMPLES	8.	8.	9.	9.	9.	9.	9.	9.	9.
RENNELL SOUND									
MEAN	1.57	479.	1.47	0.15	0.3	0.40	0.32	17.	18.
# OF SAMPLES	32.	32.	33.	33.	33.	33.	33.	33.	33.
SHIELDS BAY									
MEAN	1.27	*	0.57	0.06	0.0	1.0	0.09	0.0	4.
# OF SAMPLES	7.	0.	7.	7.	7.	7.	7.	7.	7.

TABLE 1D

GHOST CREEK FORMATION

SECTION NAME	%Ro_{rand}	TMAX	TOC	S1	S2	PI	QOM	HI	OI
BC SECTION 10									
MEAN	0.55	448.	1.66	0.39	5.11	0.08	3.19	218.	13.
# OF SAMPLES	3.	4.	4.	4.	4.	4.	4.	4.	4.
BC SECTION 4									
MEAN	1.32	486.	0.68	0.07	0.25	0.22	0.47	36.	29.
# OF SAMPLES	1.	1.	1.	1.	1.	1.	1.	1.	1.
BC SECTION 7									
MEAN	1.51	470.	1.63	0.43	0.63	0.41	0.65	38.	17.
# OF SAMPLES	2.	2.	2.	2.	2.	2.	2.	2.	2.
BC SECTION 8									
MEAN	1.5	480.	1.84	0.44	0.7	0.41	0.66	38.	15.
# OF SAMPLES	4.	4.	4.	4.	4.	4.	4.	4.	4.
BC SECTION CAA-86-2									
MEAN	0.88	454.	1.27	0.43	1.98	0.17	1.73	141.	32.
# OF SAMPLES	6.	4.	5.	5.	5.	5.	5.	5.	5.
CENTRAL GRAHAM ISLAND A-QUARRY									
MEAN	0.50	438.	0.6	1.46	1.76	0.45	5.37	293.	108.
# OF SAMPLES	1.	1.	1.	1.	1.	1.	1.	1.	1.
MAUDE ISLAND									
MEAN	1.38	442.	1.90	0.55	4.66	0.10	2.43	209.	105.
# OF SAMPLES	5.	5.	5.	5.	5.	5.	5.	5.	5.
RENNELL SOUND									
MEAN	1.57	477.	0.79	0.05	0.09	0.48	0.14	9.	106.
# OF SAMPLES	7.	7.	7.	7.	7.	7.	7.	7.	7.
CENTRAL GRAHAM ISLAND WELL I-179									
MEAN	0.88	444.	1.73	0.36	6.64	0.07	3.73	349.	76.
# OF SAMPLES	36.	36.	36.	36.	36.	33.	34.	34.	34.
WHITEAVES BAY									
MEAN	1.35	448.	1.6	0.46	0.60	0.49	0.62	32.	6.
# OF SAMPLES	6.	6.	6.	6.	6.	6.	6.	6.	6.

TABLE 1E

RENNELL JUNCTION FORMATION

SECTION NAME	$\%Ro_{rand}$	TMAX	TOC	S1	S2	PI	QOM	HI	OI
BC SECTION 10									
MEAN	0.52	445.	0.71	0.25	1.27	0.16	2.14	178.	46.
# OF SAMPLES	1.	1.	1.	1.	1.	1.	1.	1.	1.
BC SECTION 4									
MEAN	1.17	467.	0.58	0.05	0.16	0.12	0.33	28.	288.
# OF SAMPLES	2.	1.	2.	2.	2.	2.	2.	2.	2.
BC SECTION 7									
MEAN	1.5	488.	1.57	0.27	0.35	0.44	0.39	22.	8.
# OF SAMPLES	1.	1.	1.	1.	1.	1.	1.	1.	1.
BC SECTION 8									
MEAN	1.45	471.	1.96	0.4	0.59	0.41	0.51	30.	21.
# OF SAMPLES	1.	1.	1.	1.	1.	1.	1.	1.	1.
BC SECTION CAA-86-2									
MEAN	0.88	458.	1.07	0.05	0.3	0.14	0.84	93.	78.
# OF SAMPLES	3.	4.	4.	4.	4.	4.	4.	4.	4.

TABLE 1F

FANNIN FORMATION

SECTION NAME	$\%Ro_{rand}$	TMAX	TOC	S1	S2	PI	QOM	HI	OI
BC SECTION 4									
MEAN	1.31	*	0.18	0.01	0.01	0.25	0.13	8.	74.
# OF SAMPLES	2.	0.	2.	2.	2.	2.	2.	2.	2.
BC SECTION 7									
MEAN	1.45	*	0.23	0.02	0.05	0.22	0.31	25.	27.
# OF SAMPLES	3.	0.	3.	3.	3.	3.	3.	3.	3.
BC SECTION 8									
MEAN	1.47	*	0.26	0.03	0.09	0.24	0.53	42.	88.
# OF SAMPLES	3.	0.	3.	3.	3.	3.	3.	3.	3.
BC SECTION 8									
MEAN	1.51	*	0.28	0.02	0.08	0.2	0.34	28.	136.
# OF SAMPLES	5.	0.	5.	5.	5.	5.	5.	5.	5.
BC SECTION CAA-86-2									
MEAN	0.85	*	*	*	*	*	*	*	*
# OF SAMPLES	2.	0.	0.	0.	0.	0.	0.	0.	0.
NORTH MORESBY									
MEAN	1.42*	*	*	*	*	*	*	*	*
# OF SAMPLES	1.	*	*	*	*	*	*	*	*
($^{*}Ro_{max}$)									

TABLE 1G

WHITEAVES FORMATION

SECTION NAME	%Ro_{rand}	TMAX	TOC	S1	S2	PI	QOM	HI	OI
BC SECTION 10									
MEAN	0.64	448.	0.18	0.01	0.10	0.03	0.62	60.	51.
# OF SAMPLES	5.	1.	5.	5.	5.	5.	5.	5.	5.
BC SECTION 11									
MEAN	0.43	440	0.33	0.01	0.18	0.07	0.62	57.	6.
# OF SAMPLES	5.	1.	5.	5.	5.	5.	5.	5.	5.
BC SECTION 12									
MEAN	0.46	442.	5.27	0.02	0.24	0.09	0.43	88.	14.
# OF SAMPLES	2.	1.	2.	2.	2.	2.	2.	2.	2.
BC SECTION 14									
MEAN	0.78	*	0.26	0.01	0.11	0.11	0.47	42.	10.
# OF SAMPLES	4.	0.	4.	4.	4.	4.	4.	4.	4.
BC SECTION 15									
MEAN	0.63	440.	0.59	0.04	0.36	0.11	0.65	58.	5.
# OF SAMPLES	5.	4.	5.	5.	5.	5.	5.	5.	5.
BC SECTION 4									
MEAN	1.26	*	0.23	0.0	0.01	0.17	0.07	5.	125.
# OF SAMPLES	3.	0.	3.	3.	3.	3.	3.	3.	3.
BC SECTION 5									
MEAN	1.5	*	0.34	0.01	0.05	0.26	0.18	14.	88.
# OF SAMPLES	4.	0.	3.	3.	3.	3.	3.	3.	3.
BC SECTION 6									
MEAN	1.49	*	0.27	0.0	0.02	0.13	0.08	7.	54.
# OF SAMPLES	3.	0.	4.	4.	4.	4.	4.	4.	4.
BC SECTION 7									
MEAN	1.42	*	0.32	0.02	0.08	0.2	0.32	25.	18.
# OF SAMPLES	3.	0.	3.	3.	3.	3.	3.	3.	3.
BC SECTION CAA-86-2									
MEAN	0.82	464.	1.80	0.16	1.13	0.13	0.73	64.	16.
# OF SAMPLES	2.	2.	2.	2.	2.	2.	2.	2.	2.
NORTH MORESBY									
MEAN	1.51*	*	*	*	*	*	*	*	*
# OF SAMPLES	1.	*	*	*	*	*	*	*	*

(* Ro_{max})

TABLE 1H

PHANTOM CREEK FORMATION

SECTION NAME	$\%Ro_{rand}$	TMAX	TOC	S1	S2	PI	QOM	HI	OI
BC SECTION 12									
MEAN	0.46	440.	0.55	0.38	1.85	0.16	3.9	322.	10.
# OF SAMPLES	4.	4.	4.	4.	4.	4.	4.	4.	4.

TABLE 11

GRAHAM ISLAND FORMATION

SECTION NAME	%Ro$_{rand}$	TMAX	TOC	S1	S2	PI	QOM	HI	OI
BC SECTION 10									
MEAN	0.48	446.	0.96	0.08	1.57	0.06	1.17	111.	86.
# OF SAMPLES	8.	5.	8.	8.	8.	8.	8.	8.	8.
BC SECTION 14									
MEAN	0.77	443.	0.88	0.14	2.22	0.23	1.94	127.	14.
# OF SAMPLES	6.	4.	7.	7.	7.	7.	7.	7.	7.
BC SECTION 6									
MEAN	1.5	*	0.34	0.01	0.08	0.08	0.26	24.	43.
# OF SAMPLES	3.	0.	3.	3.	3.	3.	3.	3.	3.

TABLE 1J

RICHARDSON BAY FORMATION

SECTION NAME	$\%Ro_{rand}$	TMAX	TOC	S1	S2	PI	QOM	HI	OI
BC SECTION 16									
MEAN	1.13	396.	1.13	0.20	0.52	0.28	0.63	45.	11.
# OF SAMPLES	6.	6.	6.	6.	6.	6.	6.	6.	6.

TABLE 1K

ROBBER POINT FORMATION

SECTION NAME	$\%Ro_{rand}$	TMAX	TOC	S1	S2	PI	QOM	HI	OI
BC SECTION 16									
MEAN	1.10	468.	0.78	0.14	0.35	0.29	0.63	44.	15.
# OF SAMPLES	1.	1.	1.	1.	1.	1.	1.	1.	1.

TABLE 1L

NEWCOMBE FORMATION

SECTION NAME	$\%Ro_{rand}$	TMAX	TOC	S1	S2	PI	QOM	HI	OI
BC SECTION 17									
MEAN	1.08	*	0.51	0.02	0.15	0.12	0.34	30.	14.
# OF SAMPLES	3.	0.	3.	3.	3.	3.	3.	3.	3.

TABLE 1M

ALLIFORD FORMATION

SECTION NAME	%Ro_{rand}	TMAX	TOC	S1	S2	PI	QOM	HI	OI
BC SECTION 16									
MEAN	1.04	320.	1.10	0.22	0.89	0.20	1.01	80.	13.
# OF SAMPLES	3.	3.	3.	3.	3.	3.	3.	3.	3.

TABLE 1N

LONGARM FORMATION

SECTION NAME	%Ro_{rand}	TMAX	TOC	S1	S2	PI	QOM	HI	OI
SPOT SAMPLE									
MEAN	3.18	*	0.26	0.	0.	0.03	0.03	5.	44.
# OF SAMPLES	20.	0.	33.	33.	33.	33.	33.	33.	33.
NORTH MORESBY									
MEAN	2.07*	*	*	*	*	*	*	*	*
# OF SAMPLES	5.	*	*	*	*	*	*	*	*

(*Ro_{max})

TABLE 1O

HAIDA FORMATION

SECTION NAME	%Ro_{rand}	TMAX	TOC	S1	S2	PI	QOM	HI	OI
BC SECTION CAA-86-1									
MEAN	0.98	701.	0.68	0.05	0.36	0.1	0.56	49.	5.
# OF SAMPLES	26.	17.	26.	26.	26.	26.	26.	26.	26.
BC SECTION CAA-86-5									
MEAN	0.36	439.	0.73	0.01	0.48	0.02	0.67	65.	29.
# OF SAMPLES	10.	10.	11.	11.	11.	11.	11.	11.	11.
SECTION 14									
MEAN	1.51	504.	2.23	0.35	0.74	0.27	0.48	34.	36.
# OF SAMPLES	8.	2.	3.	3.	3.	3.	3.	3.	3.
SECTION 15									
MEAN	0.77	449.	2.49	0.07	0.9	0.08	0.43	39.	50.
# OF SAMPLES	40.	2.	2.	2.	2.	2.	2.	2.	2.
SECTION 17									
MEAN	0.68	*	*	*	*	*	*	*	*
# OF SAMPLES	11.	0.	0.	0.	0.	0.	0.	0.	0.
SECTION 18									
MEAN	0.43	*	*	*	*	*	*	*	*
# OF SAMPLES	14.	0.	0.	0.	0.	0.	0.	0.	0.
SPOT SAMPLE									
MEAN	4.04	*	0.13	0.	0.	0.14	0.02	0.	33.
# OF SAMPLES	3.	0.	7.	7.	7.	7.	7.	7.	7.
NORTH MORESBY									
MEAN	1.13*	*	*	*	*	*	*	*	*
# OF SAMPLES	2.	*	*	*	*	*	*	*	*

(* Ro_{max})

TABLE 1P

SKIDEGATE FORMATION

SECTION NAME	%Ro$_{rand}$	TMAX	TOC	S1	S2	PI	QOM	HI	OI
SECTION 20									
MEAN	1.91	497.	0.6	0.01	0.08	0.16	0.24	33.	74.
# OF SAMPLES	14.	1.	11.	11.	11.	11.	11.	11.	11.
BC SECTION CAA-86-3									
MEAN	0.96	433.	0.26	0.03	0.18	0.15	0.95	79.	68.
# OF SAMPLES	35.	11.	32.	32.	32.	32.	32.	32.	32.
BC SECTION CAA-86-4									
MEAN	*	*	*	*	*	*	*	*	*
# OF SAMPLES	0.	0.	0.	0.	0.	0.	0.	0.	0.
BC SECTION CAA-86-6									
MEAN	0.4	439.	0.73	0.02	0.54	0.03	0.73	70.	26.
# OF SAMPLES	23.	25.	25.	25.	25.	25.	25.	25.	25.
BC SECTION CAA-86-T-3									
MEAN	1.09	464.	0.17	0.01	0.10	0.07	0.85	65.	146.
# OF SAMPLES	7.	2.	7.	7.	7.	7.	6.	7.	7.
BC SECTION CAA-86-T-4									
MEAN	0.47	437.	0.43	0.	0.19	0.	0.32	31.	70.
# OF SAMPLES	8.	2.	5.	5.	5.	5.	5.	5.	5.
BC SPOT SAMPLE									
MEAN	1.8	470.	0.51	0.02	0.18	0.06	0.4	37.	28.
# OF SAMPLES	66.	10.	53.	53.	53.	53.	53.	53.	53.
SECTION 16									
MEAN	0.71	442.	0.3	0.01	0.19	0.04	0.71	67.	81.
# OF SAMPLES	10.	2.	8.	8.	8.	8.	8.	8.	8.
SECTION 21									
MEAN	1.39	456.	0.32	0.02	0.12	0.11	0.44	36.	14.
# OF SAMPLES	11.	1.	10.	10.	10.	10.	10.	10.	10.
SECTION 22									
MEAN	0.87	436.	0.63	0.	0.17	0.	0.25	24.	76.
# OF SAMPLES	3.	1.	2.	2.	2.	2.	2.	2.	2.
SPOT SAMPLE									
MEAN	2.94	*	0.13	0.	0.02	0.04	0.31	20.	95.
# OF SAMPLES	3.	0.	4.	4.	4.	4.	3.	4.	4.

TABLE 1Q

HONNA FORMATION

SECTION NAME	%Ro_{rand}	TMAX	TOC	S1	S2	PI	QOM	HI	OI
SECTION 22									
MEAN	1.14	436.	0.43	0.03	0.24	0.09	0.7	60.	125.
# OF SAMPLES	16.	7.	12.	12.	12.	12.	12.	12.	12.
SPOT SAMPLE									
MEAN	*	*	0.08	0.	0.	0.	0.	0.	87.
# OF SAMPLES	0.	0.	1.	1.	1.	1.	1.	1.	1.
NORTH MORESBY									
MEAN	0.80*	*	*	*	*	*	*	*	*
# OF SAMPLES	4.	*	*	*	*	*	*	*	*

(*Ro_{max})

TABLE 1R

SKONUN FORMATION

SECTION NAME	$\%Ro_{rand}$	TMAX	TOC	S1	S2	PI	QOM	HI	OI
CAPE BALL WELL									
MEAN	0.32	403.	41.68	16.3	81.42	0.15	2.2	179.	38.
# OF SAMPLES	22.	16.	16.	16.	16.	16.	16.	16.	16.
GOLD CREEK WELL									
MEAN	0.27	418.	24.44	0.97	14.42	0.08	0.70	64.	68.
# OF SAMPLES	7.	4.	4.	4.	4.	4.	4.	4.	4.
LOG CREEK									
MEAN	0.39	420.	2.47	1.32	5.2	0.2	2.64	210.	14.
# OF SAMPLES	1.	1.	1.	1.	1.	1.	1.	1.	1.
MILLER CREEK									
MEAN	0.19	*	*	*	*	*	*	*	*
# OF SAMPLES	1.	0.	0.	0.	0.	0.	0.	0.	0.
NADU RIVER WELL									
MEAN	0.29	400.	6.67	1.36	7.72	0.46	0.9	64.	199
# OF SAMPLES	10.	4.	8.	8.	8.	8.	8.	8.	8.
PORT LOUIS WELL									
MEAN	1.05	486.	10.45	0.73	10.3	0.07	0.87	79.	9.
# OF SAMPLES	24.	13.	14.	14.	14.	14.	14.	14.	14.
TLELL WELL									
MEAN	0.27	417.	22.88	7.27	39.12	0.15	1.91	161.	74.
# OF SAMPLES	17.	14.	15.	15.	15.	15.	15.	15.	15.
TOW HILL WELL									
MEAN	0.48	430.	36.18	7.17	31.76	0.17	1.19	93.	28.
# OF SAMPLES	45.	36.	40.	40.	40.	40.	40.	40.	39.

Honna Formation

The Conacian Honna Formation is exposed locally between central Graham Island and Langara Island. Maturation values obtained from northwest Graham (1.14 $\%Ro_{rand}$) and northern Moresby (0.60 $\%Ro_{max}$ to 1.01 $\%Ro_{max}$) Islands indicate that the strata are generally mature (Fig. 19). On northwest Graham Island, vitrinite reflectance values were measured on samples taken from in-situ coal stringers wherever possible. If no coal stringers were found, measurements were taken on shale or sandstone samples which included dispersed organic matter. Maturation values from coal particles averaged less than 0.60 $\%Ro_{rand}$ whereas maturation values from samples with dispersed organic matter at or near the same locality ranged from 0.56 $\%Ro_{rand}$ to 1.43 $\%Ro_{rand}$. The high maturation values associated with dispersed organic matter is considered the result of reworking of more mature organic matter in older strata.

SKONUN FORMATION

The Miocene-Pliocene Skonun Formation is exposed locally on eastern Graham Island and underlies most of Graham Island and Hecate Strait. The DOM for the Skonun Formation is generally immature with the exception of the mature succession in the Port Louis well (west central Graham Island) and the basal strata in the Tow Hill Well (northeast Graham Island). Regional organic maturation values for the basal strata of the Skonun Formation increase from east to west with vitrinite reflectance values ranging from 0.31 $\%Ro_{rand}$ at Cape Ball to 1.33 $\%Ro_{rand}$ at Port Louis (Fig. 20).

Maturation Gradients

Maturation gradients determined from outcrop and well sections are important for calculating the thickness of eroded strata, the thickness of strata within the oil window, and for estimating the paleogeothermal gradient. In this study, the vertical variation in DOM was determined from a total of 12 vitrinite reflectance/depth plots derived from six onshore petroleum exploration wells and six measured

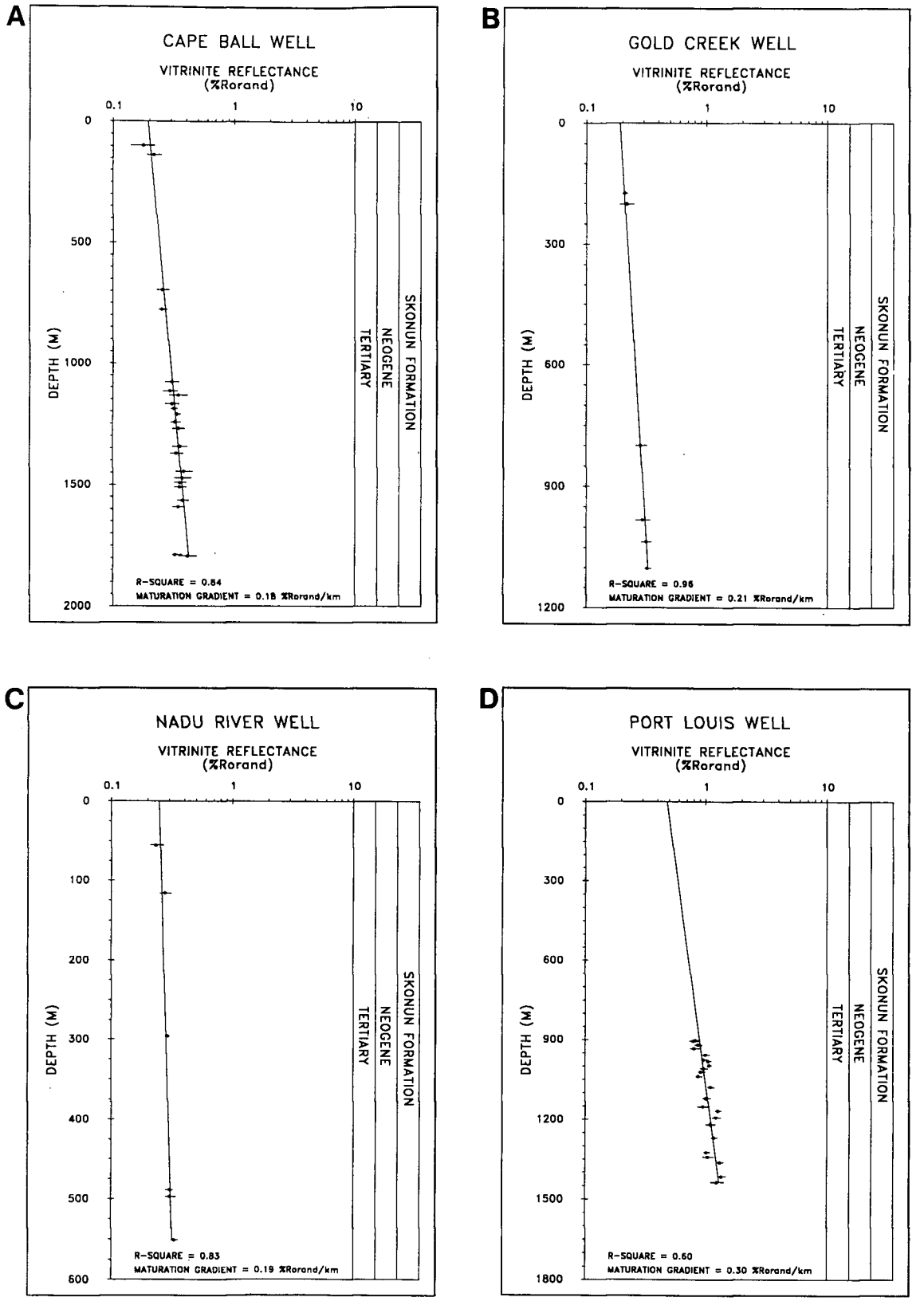

Figure 25. Maturation gradients for the Tertiary Skonun Formation. Points are mean vitrinite reflectance values. Error bars are calculated as mean values $\pm$ standard deviation. Regression lines are calculated with a least square fit algorithm. R-square value represents the goodness of fit. Maturation gradient [log(%Ro_{rand})/km] is derived from the regression line; a) at the Cape Ball well; b) at the Gold Creek well; c) at the Nadu River well; d) at the Port Louis well

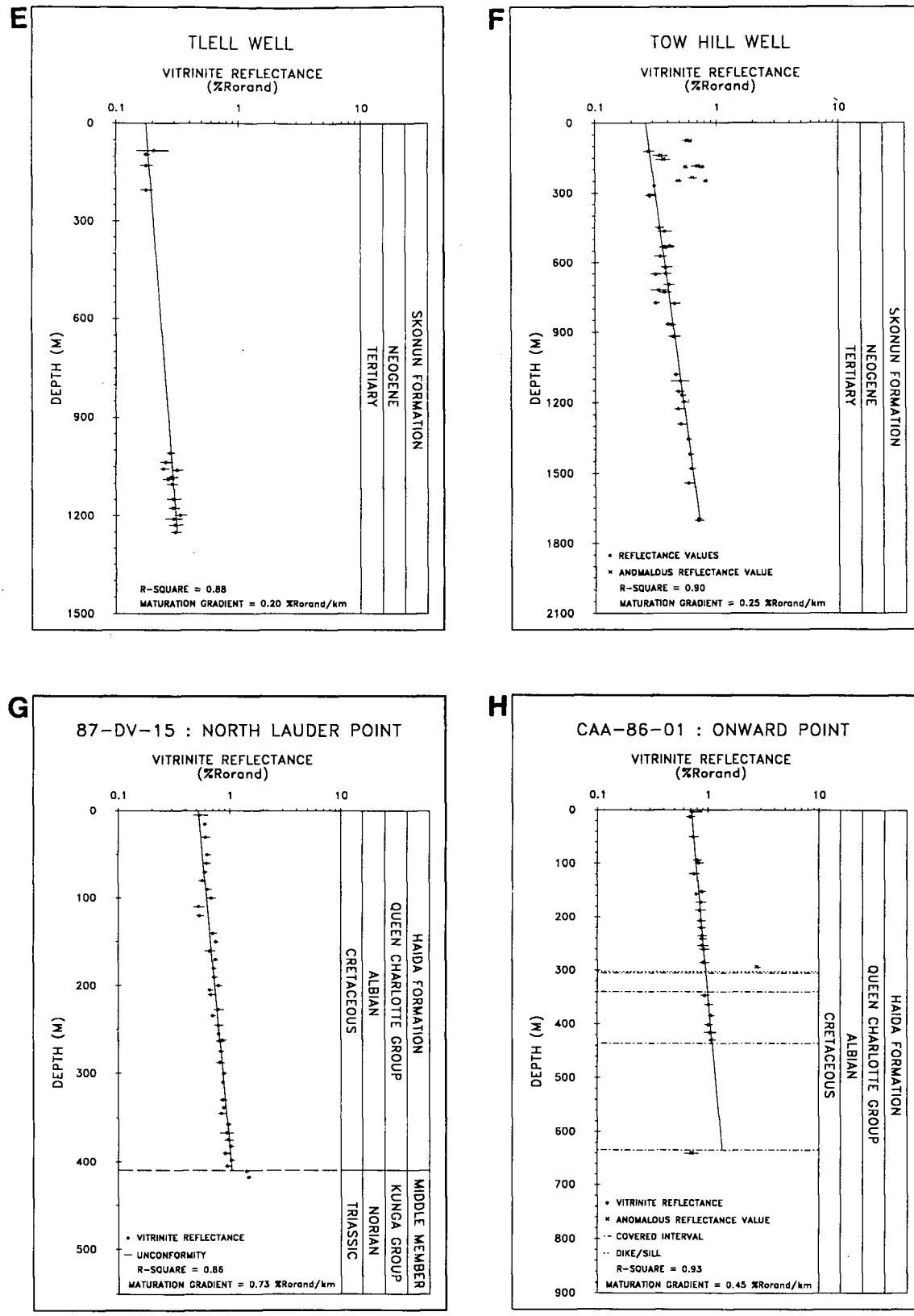

Figure 25. Maturation gradients for the Tertiary Skonun Formation. Points are mean vitrinite reflectance values. Error bars are calculated as mean values ± standard deviation. Regression lines are calculated with a least square fit algorithm. R-square value represents the goodness of fit. Maturation gradient [log(%Ro_{rand})/km] is derived from the regression line; e) at the Tlell well; f) at the Tow Hill well. Maturation gradients for the Cretaceous Haida Formation; g) at north Lauder Point; h) at Onward Point

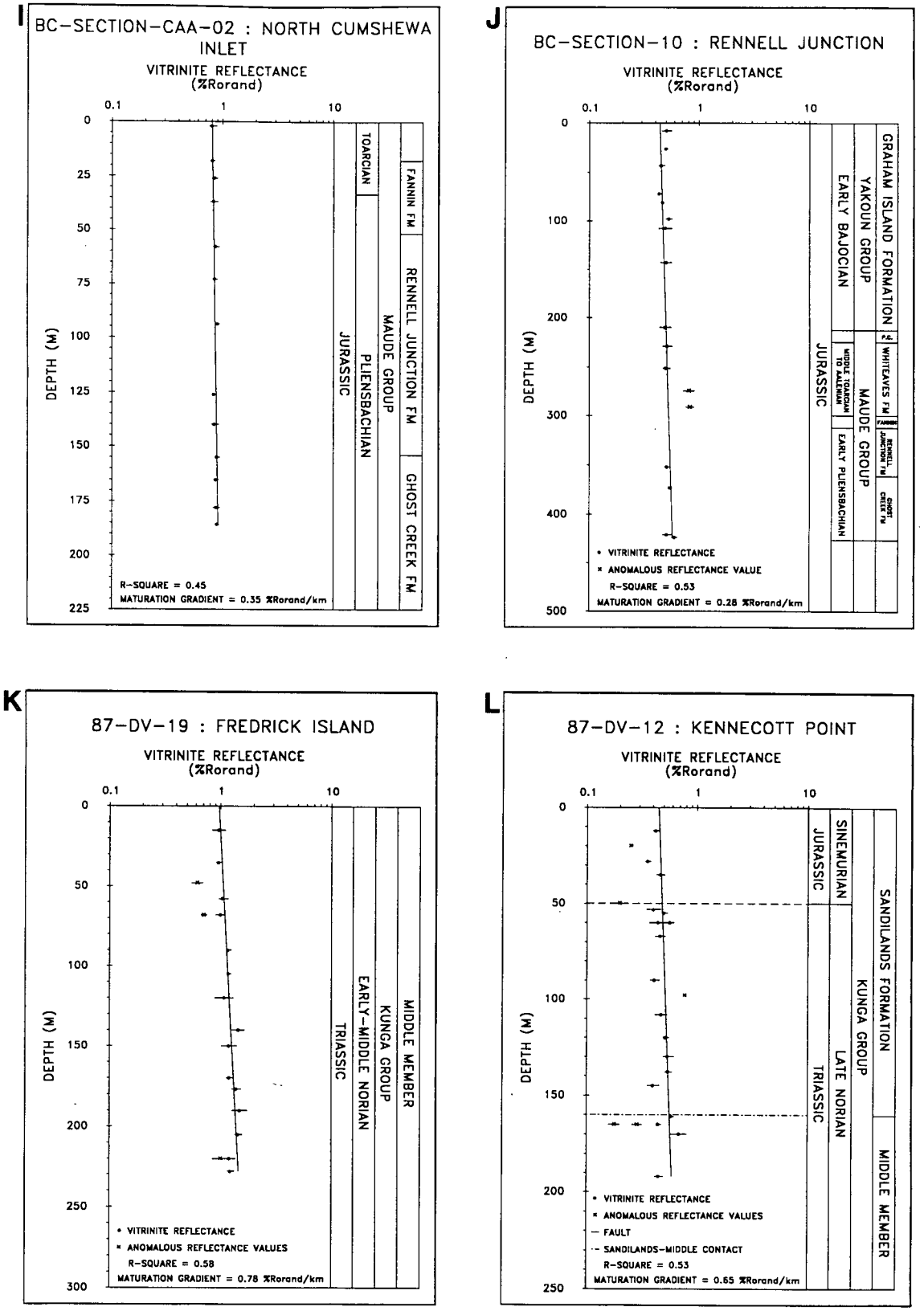

Figure 25. Maturation gradients for the Jurassic Maude and Yakoun Groups. Points are mean vitrinite reflectance values. Error bars are calculated as mean values ± standard deviation. Regression lines are calculated with a least square fit algorithm. R-square value represents the goodness of fit. Maturation gradient [$\log(\%Ro_{rand})$/km] is derived from the regression line; i) at Cumshewa Inlet; j) at Rennell Junction. Maturation gradients for the Triassic Kunga Group; k) at Fredrick Island; l) at Kennecott Point

outcrop sections (Fig. 25). Numerous other outcrop sections were measured but were not of sufficient length to obtain accurate maturation gradients. The maturation data best fit a log (vitrinite reflectance) linear depth relationship and the maturation gradients were derived with a first order regression algorithm.

Maturation gradients for the Skonun Formation range from 0.18 log ($\%Ro_{rand}$)/km to 0.25 log ($\%Ro_{rand}$)/km on eastern Graham Island and 0.30 log ($\%Ro_{rand}$)/km on western Graham Island (Figs. 25A-F).

Haida Formation maturation gradients (Figs. 25G and 25H) range from 0.45 log ($\%Ro_{rand}$)/km at Onward Point (Skidegate Inlet) to 0.73 log ($\%Ro_{rand}$)/km at Lauder Point (northwest Graham Island).

Maturation gradients for the Maude Group (Figs. 25I and 25J) vary from 0.28 log ($\%Ro_{rand}$)/km at Rennell Junction (central Graham Island) to 0.35 log ($\%Ro_{rand}$)/km at Cumshewa Inlet (northern Moresby Island).

Two maturation gradients were derived for the Kunga Group on northwest Graham Island; 0.78 log ($\%Ro_{rand}$)/km at Fredrick Island and 0.65 log ($\%Ro_{rand}$)/km at nearby Kennecott Point (Figs. 25K and 25L).

Thickness of Eroded Strata

The thickness of eroded strata can be calculated by extrapolating the measured maturation gradient to the zero maturation level of 0.15 $\%Ro_{rand}$ assuming a constant paleogeothermal gradient (Bustin, 1986; England and Bustin, 1986). If the paleogeothermal gradient is not constant, the predicted thickness of eroded strata can be over- or under- estimated. In the study area, high heat flow associated with Mesozoic or Tertiary volcanism (Sutherland Brown, 1966; Cameron and Tipper, 1985) is considered to have increased the paleogeothermal gradients for 5-25 million years in the Middle-Late Jurassic or Tertiary (as discussed later) resulting in elevated maturation gradients. Hence, the erosional thickness values may be

underestimated for strata which were affected by high heat flow. The calculated values, therefore, represent a minimum estimate.

The calculated thickness of eroded strata for the Skonun Formation ranges from 375 m at the Tlell well to 1685 m at the Port Louis well (Table 2). The amount of eroded strata increases towards the north except at the Nadu River well (1160 m) which lies proximal to a structural high in the underlying Masset Formation (Sutherland Brown, 1968) suggesting the area was differentially uplifted following deposition of the Skonun Formation.

Predicted thickness of eroded strata (Table 2) for Cretaceous outcrop sections increases from north Lauder Point (745 m) to Onward Point (1500 m). The predicted thickness of eroded strata increases from Rennell Junction (1725 m) to Cumshewa Inlet (1985 m) for Jurassic outcrop sections. Predicted values for Triassic outcrop sections range from 735 m at Kennecott Point to 1040 m at Fredrick Island.

The maturation gradients are too variable in the study area (as a result of local thermal effects associated with volcanism or plutonism) to be confidently extrapolated to adjacent areas in order to calculate thicknesses of eroded strata such as done by Bustin (1986).

Depth to the Oil Window

The stratigraphic depth to the top of the oil window (Table 2) was calculated by extrapolation of the maturation gradient to 0.50 $\%Ro_{rand}$ which corresponds to the onset of oil generation for Types II and III organic matter (Dow, 1977). Similarly, the stratigraphic depth to the base of the oil window (Table 2) has been established by extrapolation of the maturation gradient to 1.35 $\%Ro_{rand}$ which corresponds to the base of the oil window for Types II and III organic matter (Dow, 1977).

TABLE 2

WELL NAME (LOCATION)	MINIMUM VITRINITE REFLECTANCE ($\%Ro_{rand}$)	MAXIMUM VITRINITE REFLECTANCE ($\%Ro_{rand}$)	CALCULATED DEPTH TO THE TOP AND BASE OF THE OIL WINDOW (M)	CALCULATED THICKNESS OF ERODED SECTION (M)
TERTIARY STRATA				
SKONUN FORMATION (EXPLORATION WELLS)				
CAPE BALL	0.18	0.42	2283-4685	615
GOLD CREEK	0.22	0.36	2010-4104	530
NADU RIVER	0.24	0.33	1622-3917	1160
PORT LOUIS	0.81	1.38	0053-1486	1685
TLELL	0.18	0.34	2291-4491	375
TOW HILL	0.28	0.72	1125-2864	985
NORTH LAUDER POINT	0.53	1.05	**-563	745
ONWARD POINT	0.7	1.1	**-624	1500
CUMSHEWA INLET	0.82	0.91	**-554	1985
RENNELL JUNCTION	0.44	0.57	178-1747	1725
FREDRICK ISLAND	0.97	1.51	**-183	1040
KENNECOTT POINT	0.36	0.70	69-733	735

Depth to the oil window values cannot be calculated for areas from which measured maturation gradients were not obtained. The maturation gradients are too variable to extrapolate to adjacent areas as discussed in the previous section.

Calculated depths to the top of the oil window for the Skonun Formation strata in the six onshore wells on Graham Island generally increase from north to south and range from a minimum of 53 m on west Graham Island (Port Louis well) to a maximum of 2291 m on east Graham Island (Tlell well). Similarly, the calculated depths to the base of the oil window range increase from west (1486 m at the Port Louis well) to east (4685 m at the Cape Ball well) Graham Island (Table 2). Thicknesses of strata within the oil window range from 1433 m on west Graham Island (Port Louis well) to 2402 m on east Graham Island (Cape Ball well).

Exposed Cretaceous strata at north Lauder Point and Onward Point are within the oil window and the calculated stratigraphic depth to the base of the oil window ranges from 563 m at north Lauder Point to 624 m at Onward Point (Table 2). Thicknesses of strata within the oil window range from 563 m at north Lauder Point to 624 m at Onward Point.

Exposed Jurassic strata at Cumshewa Inlet are within the oil window and the calculated stratigraphic depth to the base of the oil window is 554 m. The calculated stratigraphic depth to the top and base of the oil window is 178 m and 1747 m respectively at Rennell Junction (Table 2). Thicknesses of strata within the oil window range from 554 m at Cumshewa Inlet to 1569 m at Rennell Junction.

The calculated stratigraphic depth to the top and base of the oil window for exposed Triassic strata at Kennecott Point range from 69 m to 733 m. Strata at Fredrick Island are within the oil window and the calculated stratigraphic depth to the base of the oil window is 183 m (Table 2). Thicknesses of strata within the oil window range from 183 m at Fredrick Island to 664 m at Kennecott Point.

THERMAL MODELLING

Numerous researchers have demonstrated that the DOM depends upon the thermal history of the strata (Karweil, 1955; Lopatin, 1971; Bostick, 1973; Waples, 1980). Numerical models have been developed by petroleum and coal geologists to help predict organic maturation based on knowledge of the thermal history, or conversely, to interpret the thermal history where the levels of organic maturation are known. Most models are based on some form of the Arrhenius equation (including the Arrhenius model used in this study) as described by Karweil (1955) and Tissot and Espitalie (1975):

$$K = Ae^{(-E/RT)}$$

where E = activation energy

T = absolute temperature

A = frequency factor

K = reaction constant

R = universal gas constant

Lopatin (1971) suggested that the level of organic maturation could be represented as an integration of the time-temperature history of the strata where maturation increases exponentially with temperature and linearly with time (see Waples, 1980). In the Lopatin model, the total level of organic maturation (TTI) is the sum of interval maturations calculated for 10 ^{o}C heating increments:

$$TTI = \sum_{nmin}^{nmax} \Delta T_n (r^n)$$

where nmin = lowest temperature interval

nmax = highest temperature interval

n = number of temperature intervals

r = 2 (assuming the DOM doubles for every 10 ^{o}C increment of heating)

Both the modified Arrhenius and Lopatin models are utilized in this study to predict paleogeothermal gradients, fractional kerogen conversion to liquid hydrocarbons, and timing of hydrocarbon generation for six onshore wells and six measured outcrop sections in the study area. In order to estimate paleogeothermal gradients, the measured maturation gradients were modelled using integral forms of the Arrhenius and Lopatin equations. The models iteratively solve for maturation gradients assuming a constant burial history but varying geothermal gradient. The base of each well or outcrop section was modelled with varying input geothermal gradients until the predicted DOM was similar to the measured level of organic maturation. Attempts to model maturation gradients (rather than single points) were unsuccessful possibly due to poor age constraints on the strata, or nonlinearities in sedimentation rates and non-constant paleogeothermal gradients throughout the depositional histories of the strata.

In this study, the Arrhenius model utilizes a constant activation energy ($E = 218$ kJ/mol) and frequency factor [$A = (5.45)^{26}$] based on average values for Type II and Type III organic matter within the maturation ranges measured in this study (Wood, 1988). The Lopatin model, on the other hand, assumes that the reaction rate doubles with every 10 ^{o}C increase in temperature. Thermal conductivity, and surface temperature (5 ^{o}C) are held constant and compacted rock thickness are assumed for both the Arrhenius and Lopatin models. Variations in thermal conductivity with depth, and changes in rock thickness resulting from compaction are not considered here because they are beyond the precision of the geology constraints.

Burial Histories

The following section outlines the burial histories which form the basis for the maturation models presented later (ages based on Geological Society of America time scale, 1983). Burial histories were reconstructed for the base of the modelled stratigraphic horizon using data acquired from published and unpublished sources. Maximum burial depth is estimated as the sum of the current thickness and the predicted eroded thickness of strata. Due to the paucity of data constraining the ages and thicknesses of strata as well as the timing of tectonic elements, the burial histories presented here are preliminary and, at best, considered a first approximation. Accordingly, conservative estimates based upon the available

geologic data have been utilized to quantify parameters used in modelling. Due to the relative insensitivity of both the Arrhenius and Lopatin models to time for all temperature ranges, the timing of uplift has little effect on the DOM. Therefore, the timing of erosional events does not require a great deal of accuracy for the models to yield useful results.

TERTIARY BURIAL HISTORIES

Burial histories for Skonun Formation strata in the six onshore well sections are described together due to their similarity (Figs. 26A, 27A, 28A, 29A, 30A, 31A). The age of the Tertiary Skonun Formation is poorly known and has been estimated to be Late Miocene to Early Pliocene by Martin and Rouse, 1966; Sutherland Brown, 1968 whereas Cameron and Hamilton (1988) consider the Skonun Formation to be as old as Early Miocene (18 Ma).

On Graham Island, deposition of the Skonun Formation followed the culmination of Masset volcanism between 20 Ma and 25 Ma (Hickson, 1988). There are, however, intercalations of sediments similar to Skonun Formation strata within flows of the Masset Formation. For this study, the Skonun Formation is assumed to have been deposited between 18 Ma and 2 Ma followed by uplift in the Quaternary (1.6 Ma to the present). Maximum burial depths are presumed to have been attained at 2 Ma and range from 1625 m at the Tlell well to 3150 m at the Port Louis well.

CRETACEOUS BURIAL HISTORIES

At north Lauder Point (Fig. 32A) and Onward Point Fig. 33A), Cretaceous strata were deposited beginning with the Albian Haida Formation (113-97.5 Ma). It is presumed that the Cenomanian-Turonian Skidegate Formation (97.5-88.5 Ma) and the Conacian Honna Formation (88.5-87.5 Ma) were deposited following Haida Formation deposition in order to account for the calculated thickness of eroded strata values at north Lauder Point (745 m) and at Onward Point (1500 m). A period of erosion removing the Skidegate and Honna Formations occurred between 87.5 Ma (Conacian) and 45 Ma (estimated initial

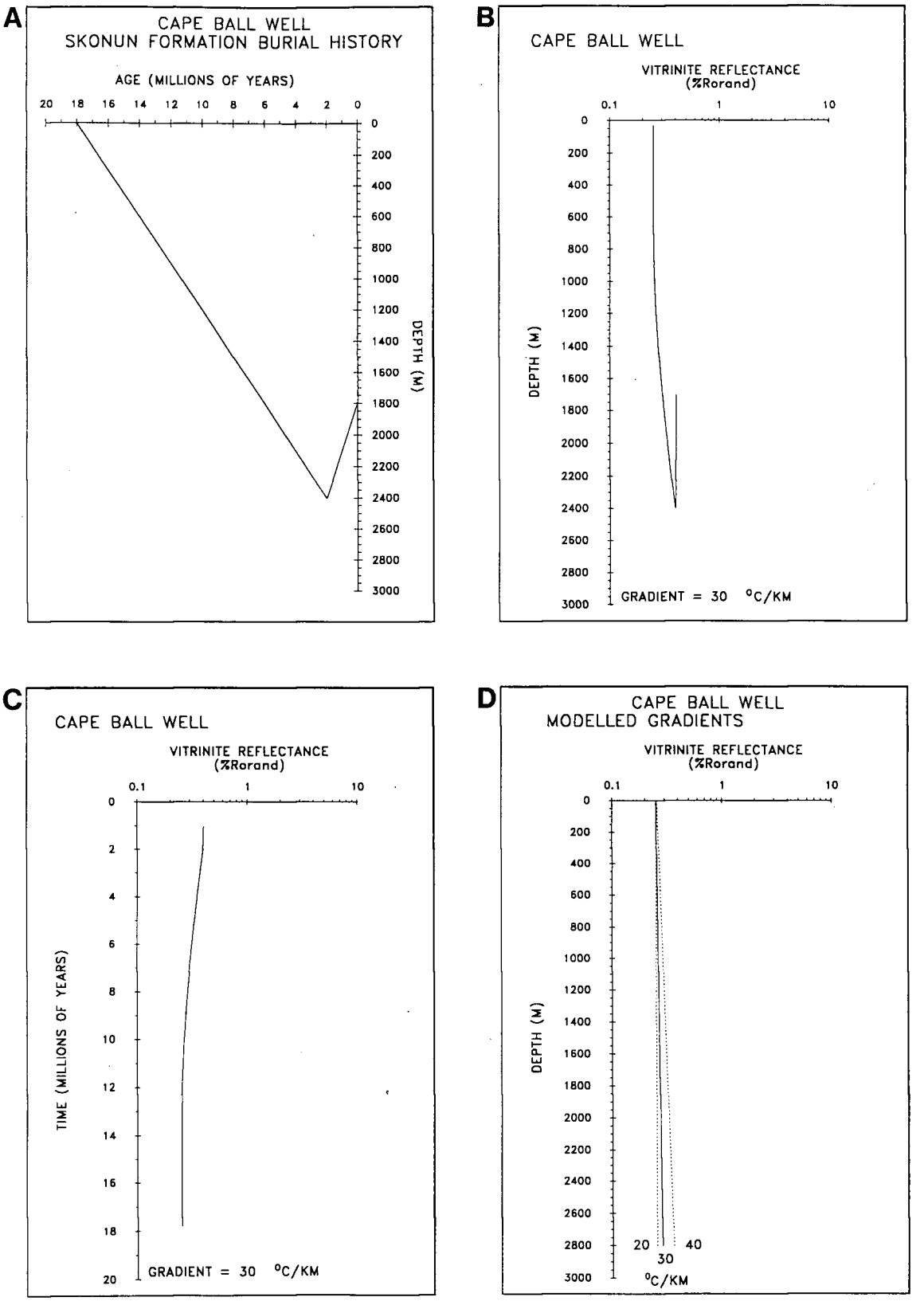

Figure 26. Tertiary Skonun Formation strata at the Cape Ball well (see text): a) interpreted burial history for the base of the Skonun Formation assuming uniform subsidence and uplift rates derived from published and unpublished data; b) maturation history (relative to depth) for the basal strata utilizing a modified Arrhenius model (constant geothermal gradient = 30 ^{o}C/km); c) maturation history (relative to time) for the basal strata utilizing a modified Arrhenius model (constant geothermal gradient = 30 ^{o}C/km); d) calculated geothermal gradients and measured maturation gradients are plotted through the origin (0.15 %Ro_{rand}) to facilitate comparison of slopes

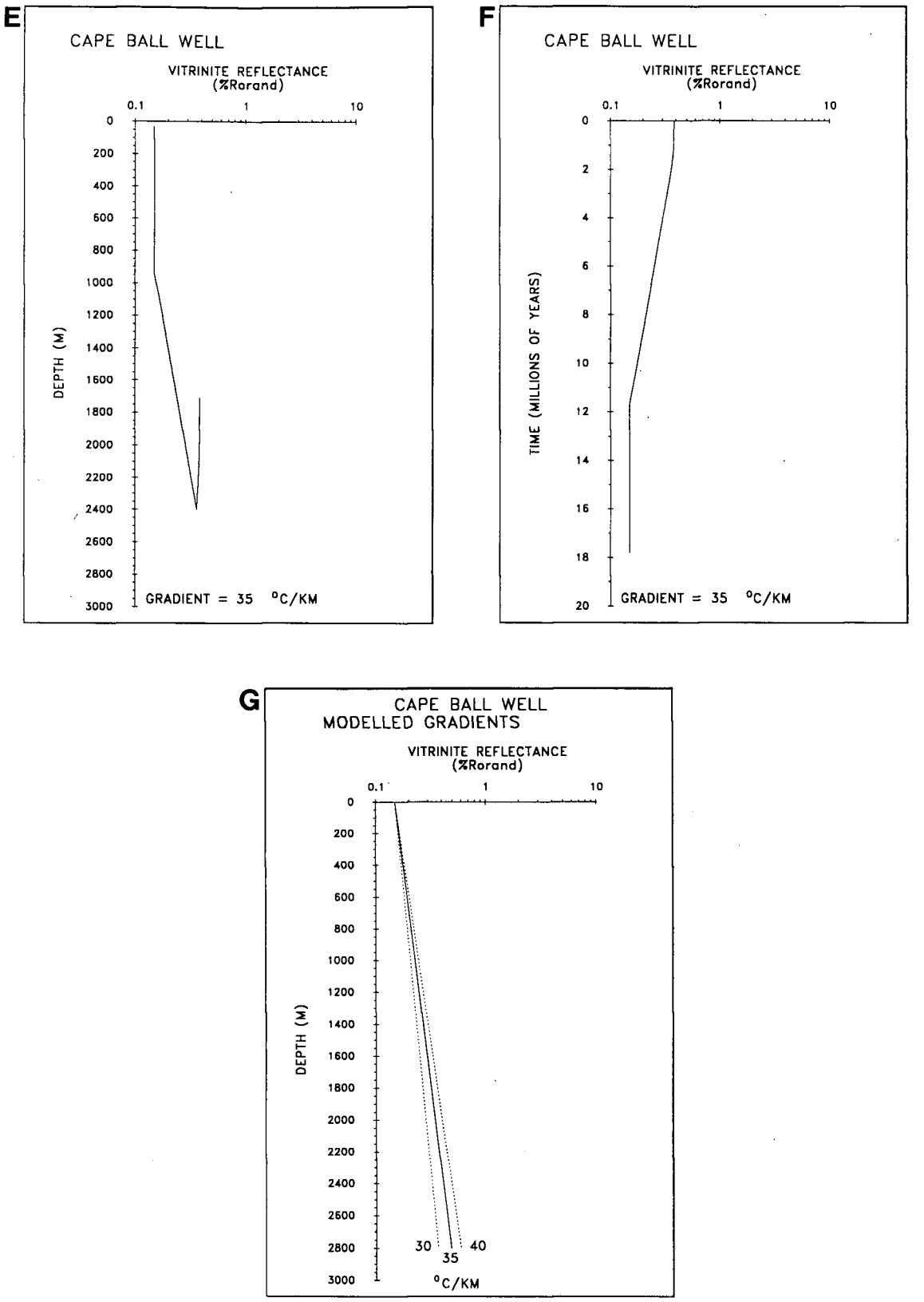

Figure 26. Tertiary Skonun Formation strata at the Cape Ball well (see text): e) maturation history (relative to depth) for the basal strata utilizing a modified Lopatin model (constant geothermal gradient = 35 ^{o}C/km); f) maturation history (relative to time) for the basal strata utilizing a modified Lopatin model (constant geothermal gradient = 35 ^{o}C/km); g) calculated geothermal gradients and measured maturation gradients are plotted through the origin (0.15 $\%Ro_{rand}$) to facilitate comparison of slopes

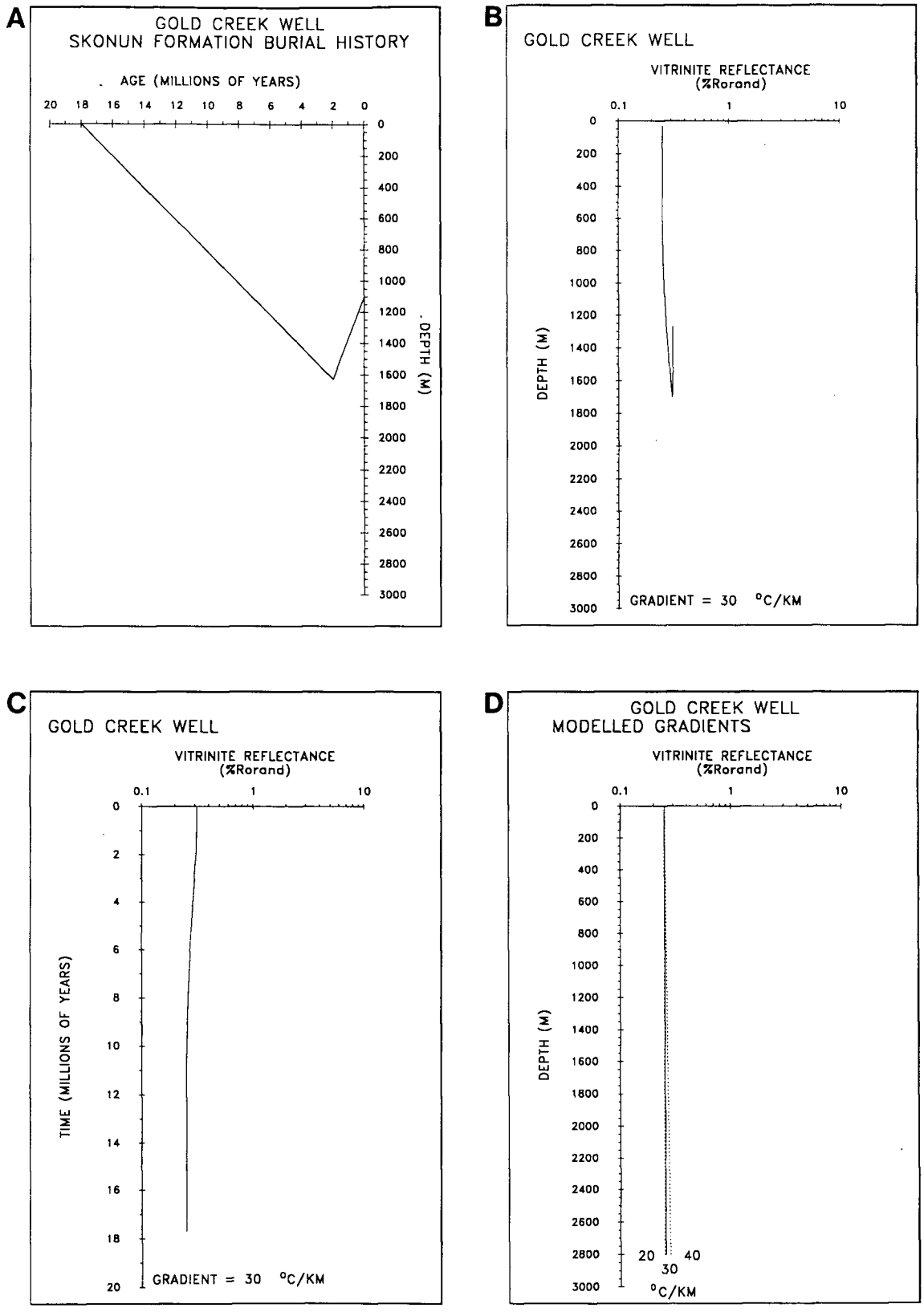

Figure 27. Tertiary Skonun Formation strata at the Gold Creek well (see text): a) interpreted burial history for the base of the Skonun Formation assuming uniform subsidence and uplift rates derived from published and unpublished data; b) maturation history (relative to depth) for the basal strata utilizing a modified Arrhenius model (constant geothermal gradient = 30 ^{o}C/km); c) maturation history (relative to time) for the basal strata utilizing a modified Arrhenius model (constant geothermal gradient = 30 ^{o}C/km); d) calculated geothermal gradients and measured maturation gradients are plotted through the origin (0.15 %Ro_{rand}) to facilitate comparison of slopes

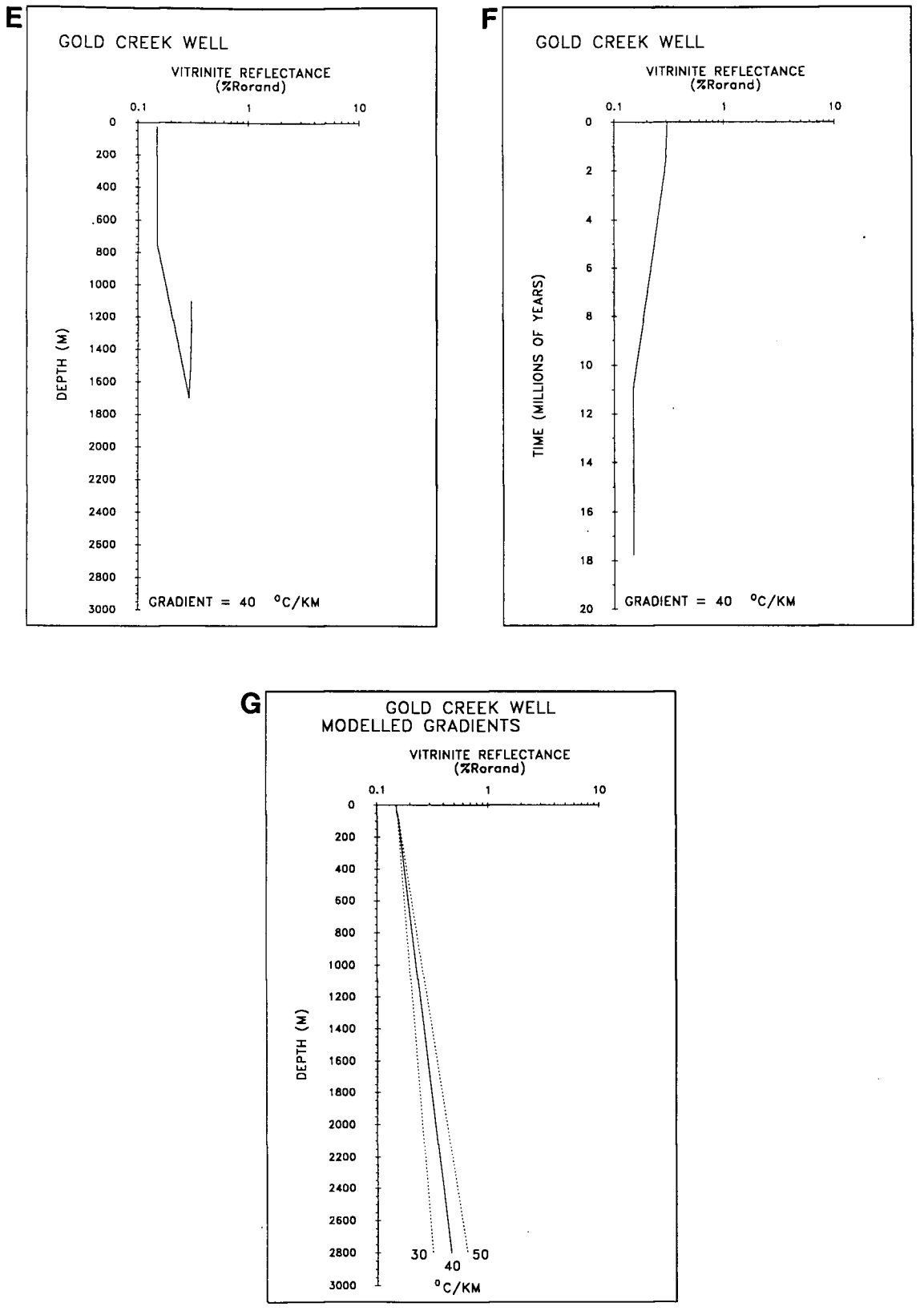

Figure 27. Tertiary Skonun Formation strata at the Gold Creek well (see text): e) maturation history (relative to depth) for the basal strata utilizing a modified Lopatin model (constant geothermal gradient = 40 ^{o}C/km); f) maturation history (relative to time) for the basal strata utilizing a modified Lopatin model (constant geothermal gradient = 40 ^{o}C/km); g) calculated geothermal gradients and measured maturation gradients are plotted through the origin (0.15 $\%Ro_{rand}$) to facilitate comparison of slopes

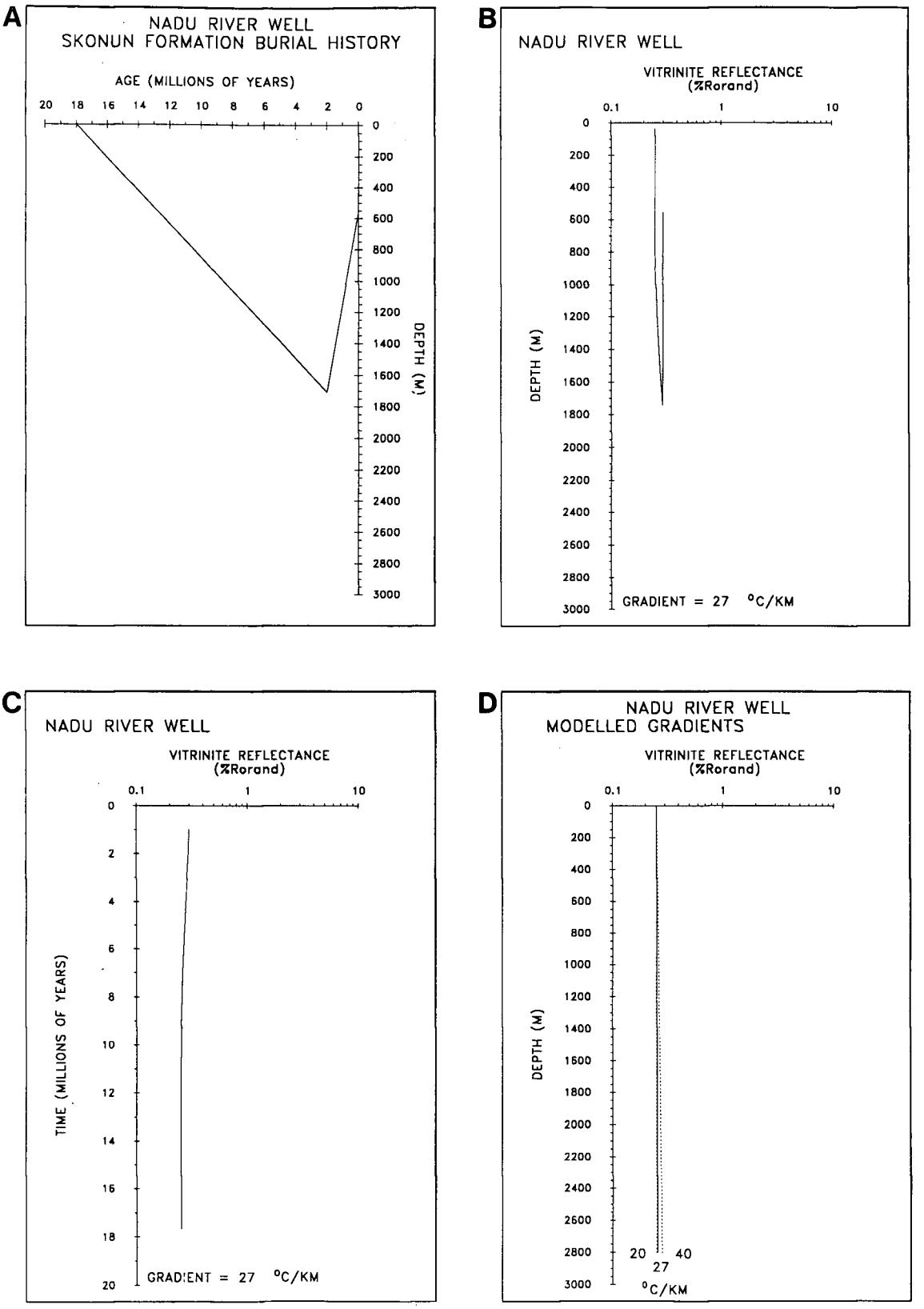

Figure 28. Tertiary Skonun Formation strata at the Nadu River well (see text): a) interpreted burial history for the base of the Skonun Formation assuming uniform subsidence and uplift rates derived from published and unpublished data; b) maturation history (relative to depth) for the basal strata utilizing a modified Arrhenius model (constant geothermal gradient = 27 ^{o}C/km); c) maturation history (relative to time) for the basal strata utilizing a modified Arrhenius model (constant geothermal gradient = 27 ^{o}C/km); d) calculated geothermal gradients and measured maturation gradients are plotted through the origin (0.15 %Ro_{rand}) to facilitate comparison of slopes

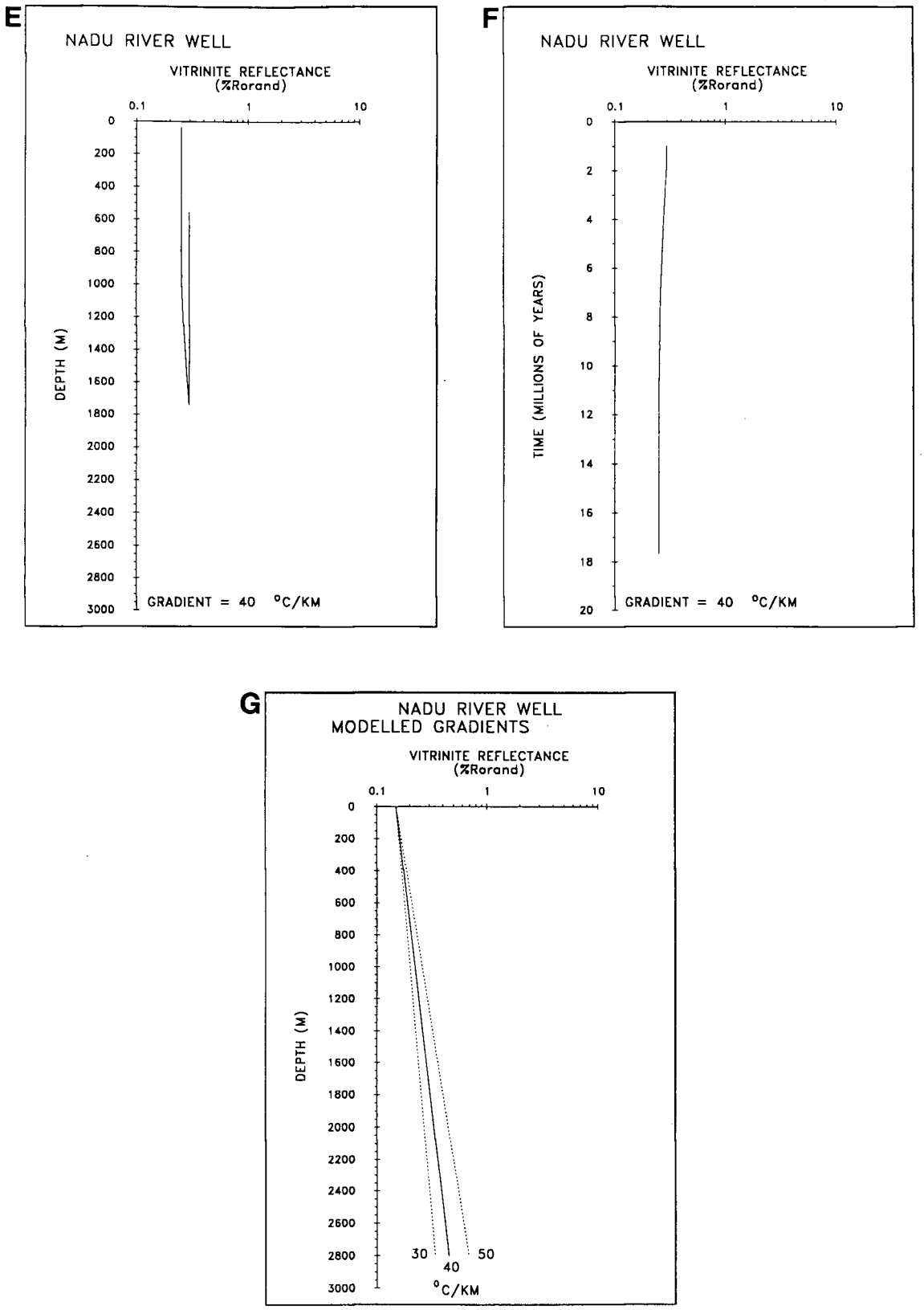

Figure 28. Tertiary Skonun Formation strata at the Nadu River well (see text): e) maturation history (relative to depth) for the basal strata utilizing a modified Lopatin model (constant geothermal gradient=40 ^{o}C/km); f) maturation history (relative to time) for the basal strata utilizing a modified Lopatin model (constant geothermal gradient=40 ^{o}C/km); g) calculated geothermal gradients and measured maturation gradients are plotted through the origin (0.15 $\%Ro_{rand}$) to facilitate comparison of slopes

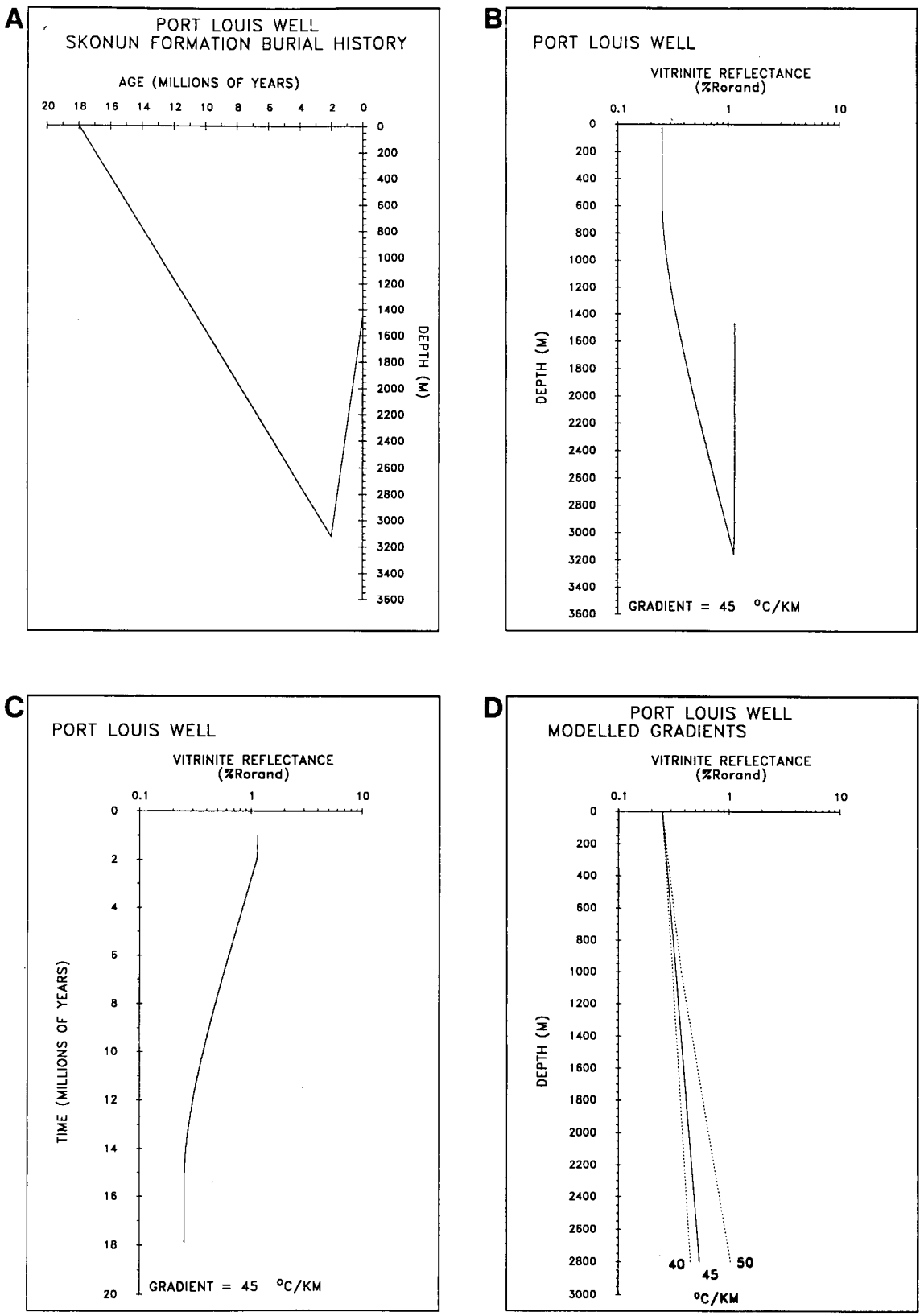

Figure 29. Tertiary Skonun Formation strata at the Port Louis well (see text): a) interpreted burial history for the base of the Skonun Formation assuming uniform subsidence and uplift rates derived from published and unpublished data; b) maturation history (relative to depth) for the basal strata utilizing a modified Arrhenius model (constant geothermal gradient = 30 ^{o}C/km); c) maturation history (relative to time) for the basal strata utilizing a modified Arrhenius model (constant geothermal gradient = 30 ^{o}C/km); d) calculated geothermal gradients and measured maturation gradients are plotted through the origin (0.15 %Ro_{rand}) to facilitate comparison of slopes

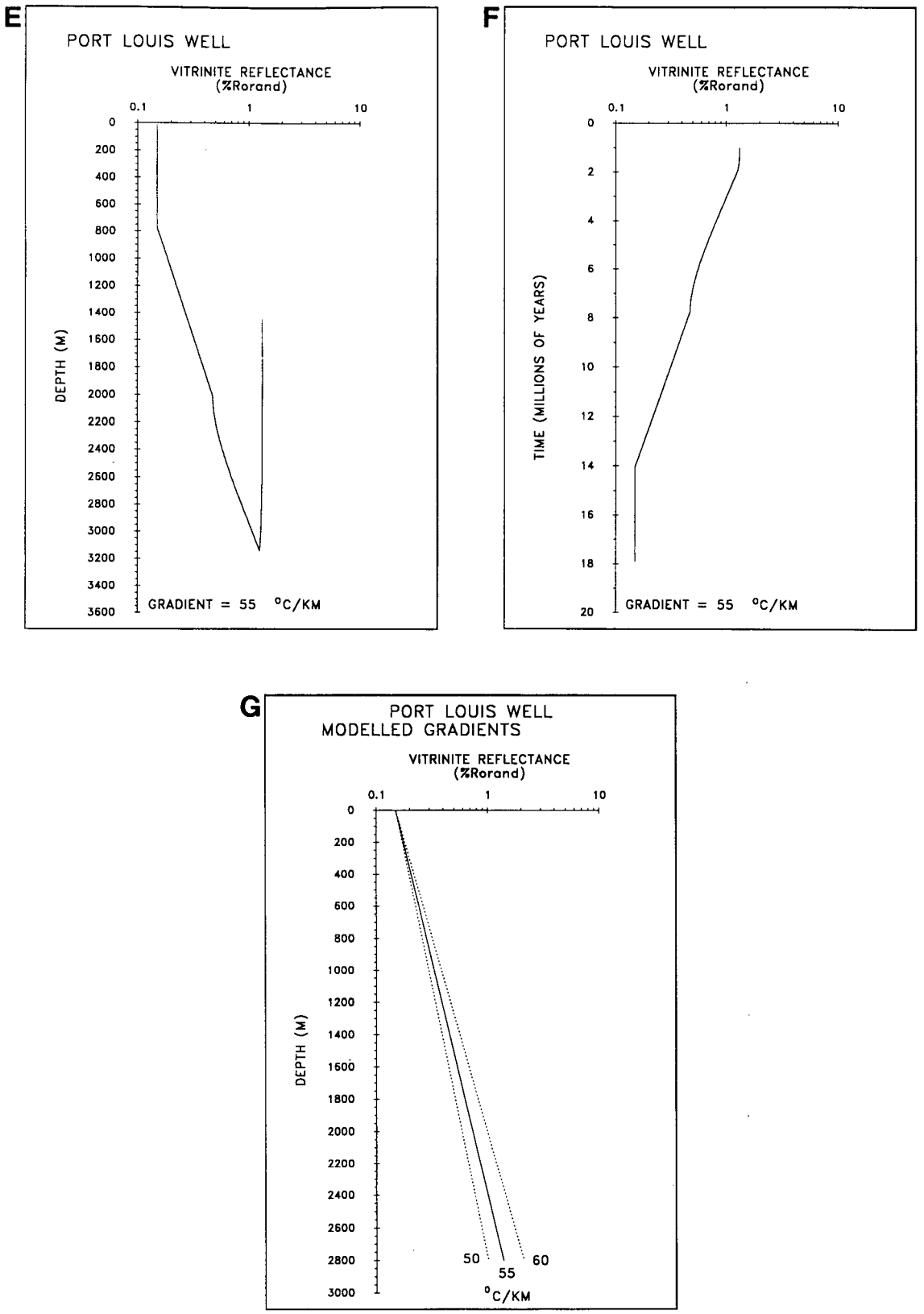

Figure 29. Tertiary Skonun Formation strata at the Port Louis well (see text): e) maturation history (relative to depth) for the basal strata utilizing a modified Lopatin model (constant geothermal gradient = 55 °C/km); f) maturation history (relative to time) for the basal strata utilizing a modified Lopatin model (constant geothermal gradient = 55 °C/km); g) calculated geothermal gradients and measured maturation gradients are plotted through the origin (0.15 $\%Ro_{rand}$) to facilitate comparison of slopes

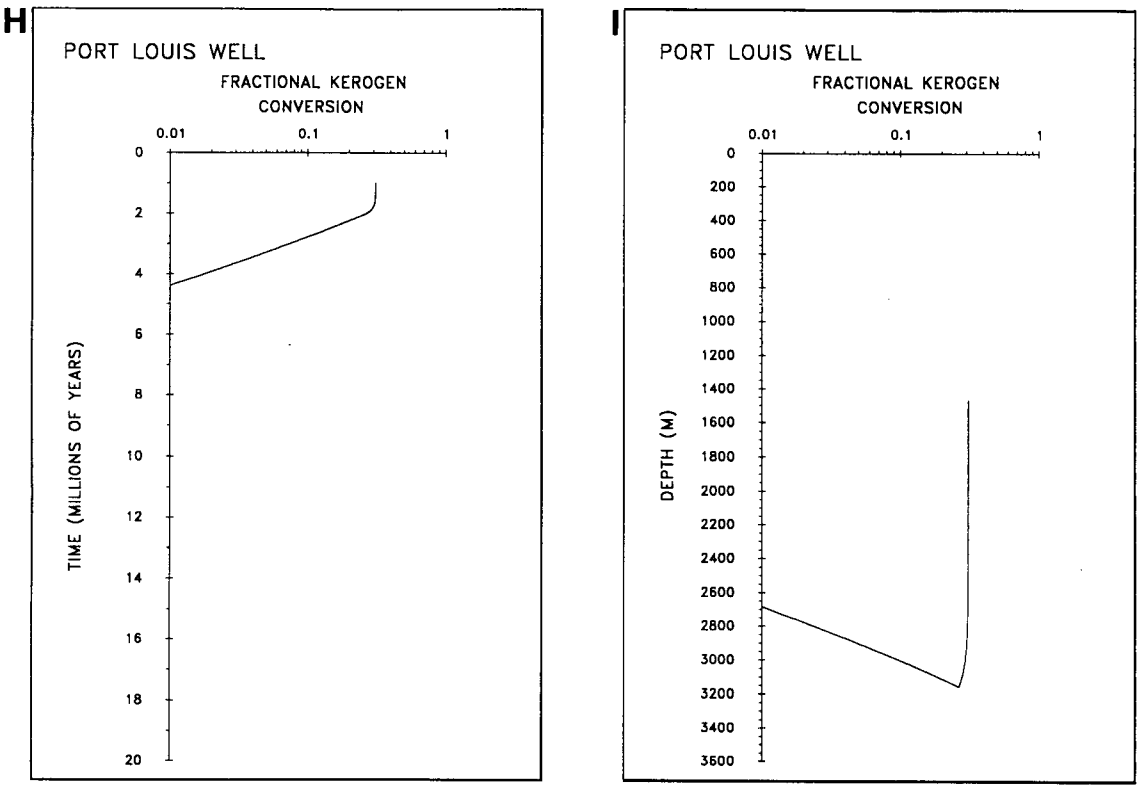

Figure 29. Tertiary Skonun Formation strata at the Port Louis well (see text): h) fractional kerogen conversion (relative to time) utilizing a modified Arrhenius model (constant geothermal gradient = 30 ^{o}C/km); i) fractional kerogen conversion (relative to depth) utilizing a modified Arrhenius model (constant geothermal gradient = 30 ^{o}C/km)

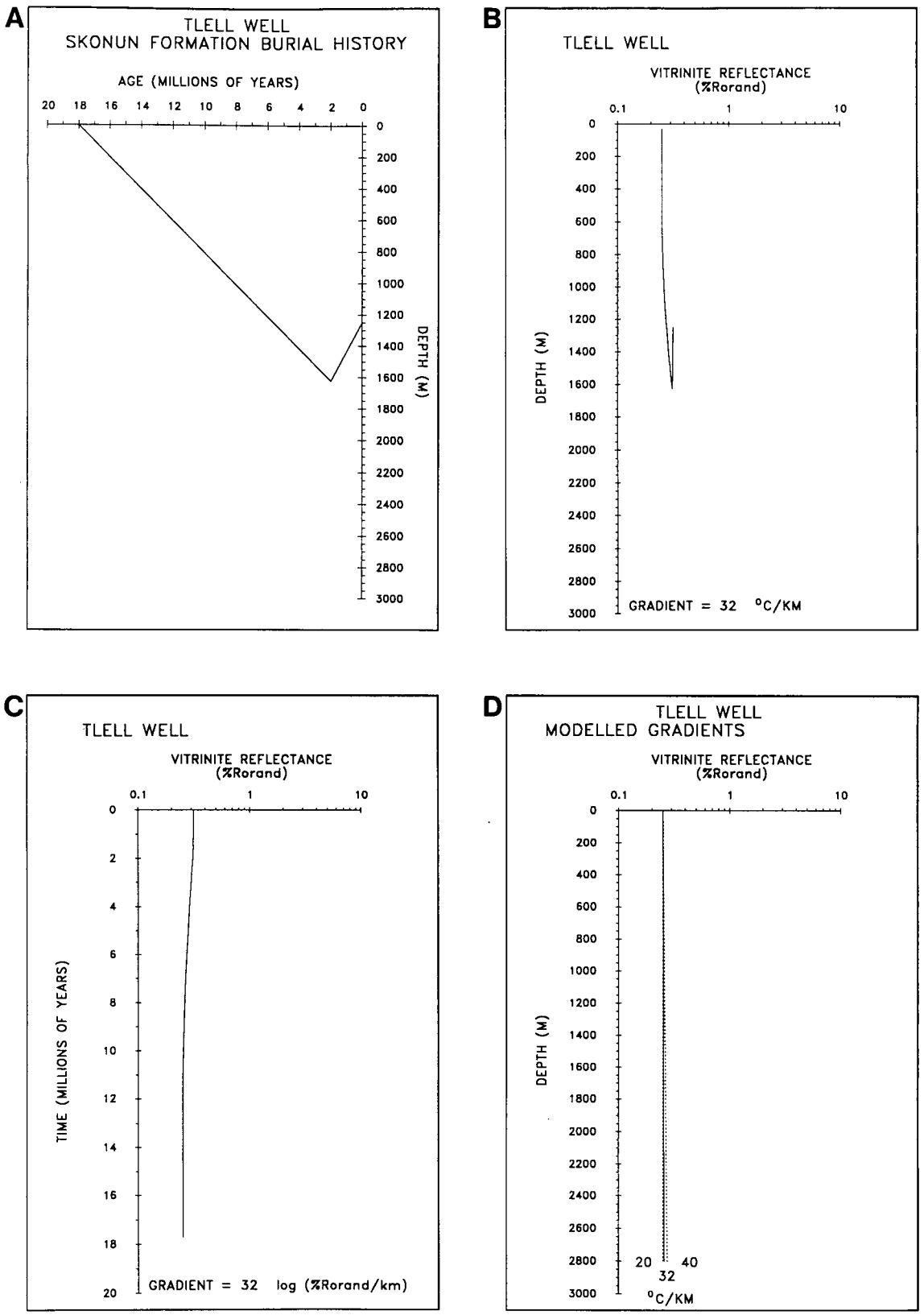

Figure 30. Tertiary Skonun Formation strata at the Tlell well (see text): a) interpreted burial history for the base of the Skonun Formation assuming uniform subsidence and uplift rates derived from published and unpublished data; b) maturation history (relative to depth) for the basal strata utilizing a modified Arrhenius model (constant geothermal gradient = 32 ^{o}C/km); c) maturation history (relative to time) for the basal strata utilizing a modified Arrhenius model (constant geothermal gradient = 32 ^{o}C/km); d) calculated geothermal gradients and measured maturation gradients are plotted through the origin (0.15 %Ro_{rand}) to facilitate comparison of slopes

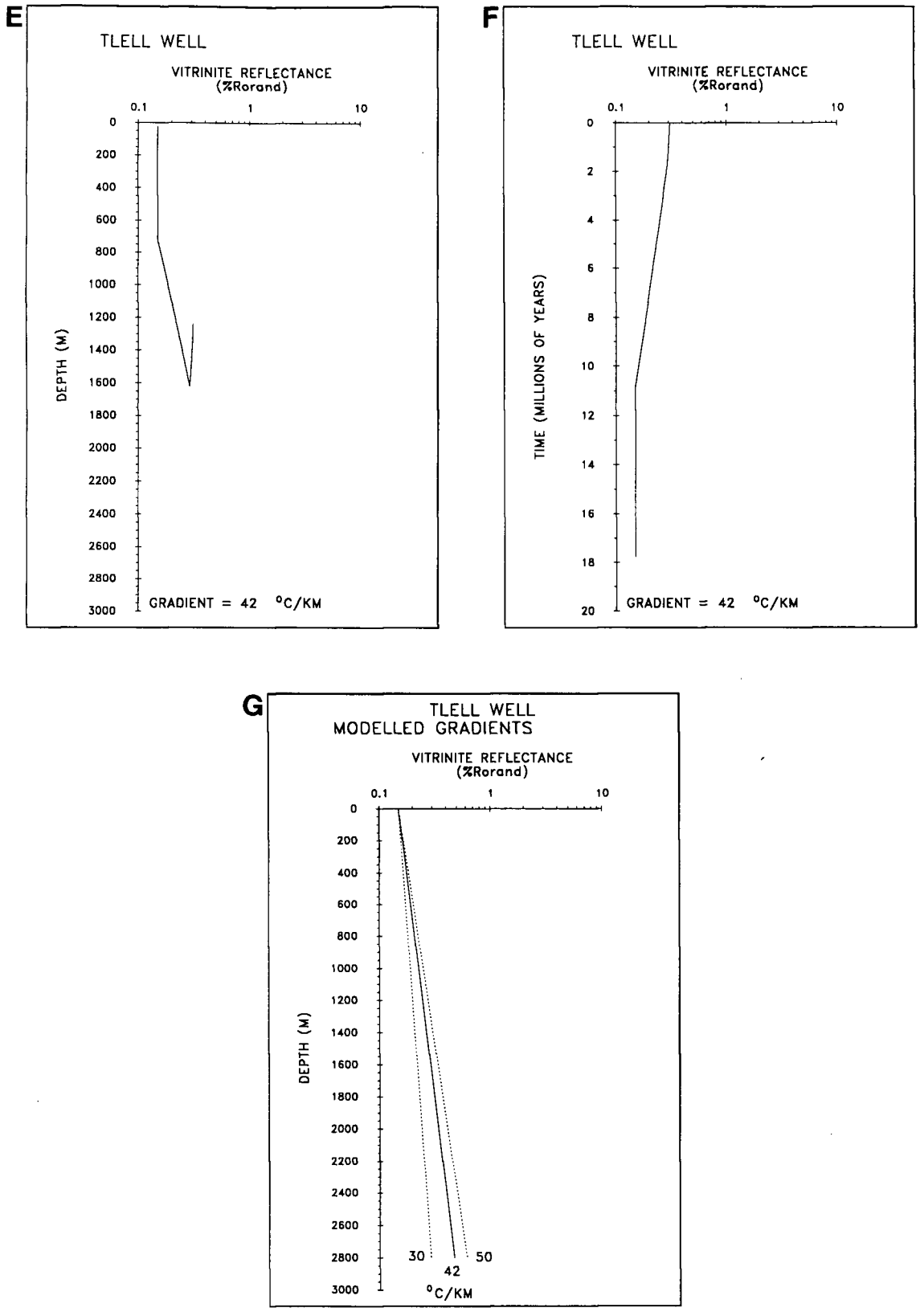

Figure 30. Tertiary Skonun Formation strata at the Tlell well (see text): e) maturation history (relative to depth) for the basal strata utilizing a modified Lopatin model (constant geothermal gradient = 42 °C/km); f) maturation history (relative to time) for the basal strata utilizing a modified Lopatin model (constant geothermal gradient = 42 °C/km); g) calculated geothermal gradients and measured maturation gradients are plotted through the origin (0.15 $\%Ro_{rand}$) to facilitate comparison of slopes

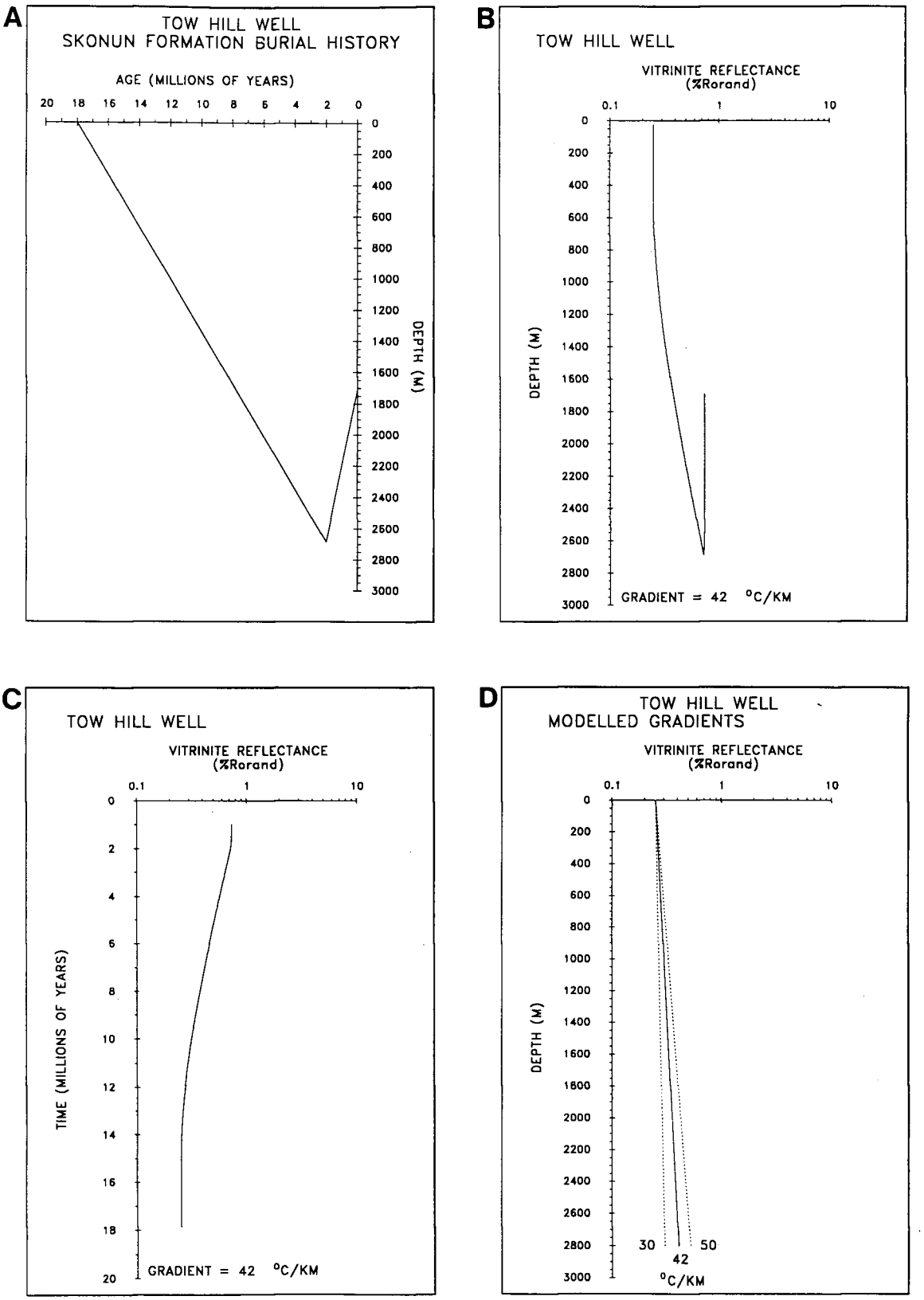

Figure 31. Tertiary Skonun Formation strata at the Tow Hill well (see text): a) interpreted burial history for the base of the Skonun Formation assuming uniform subsidence and uplift rates derived from published and unpublished data; b) maturation history (relative to depth) for the basal strata utilizing a modified Arrhenius model (constant geothermal gradient = 42 ^{o}C/km); c) maturation history (relative to time) for the basal strata utilizing a modified Arrhenius model (constant geothermal gradient = 42 ^{o}C/km); d) calculated geothermal gradients and measured maturation gradients are plotted through the origin (0.15 %Ro_{rand}) to facilitate comparison of slopes

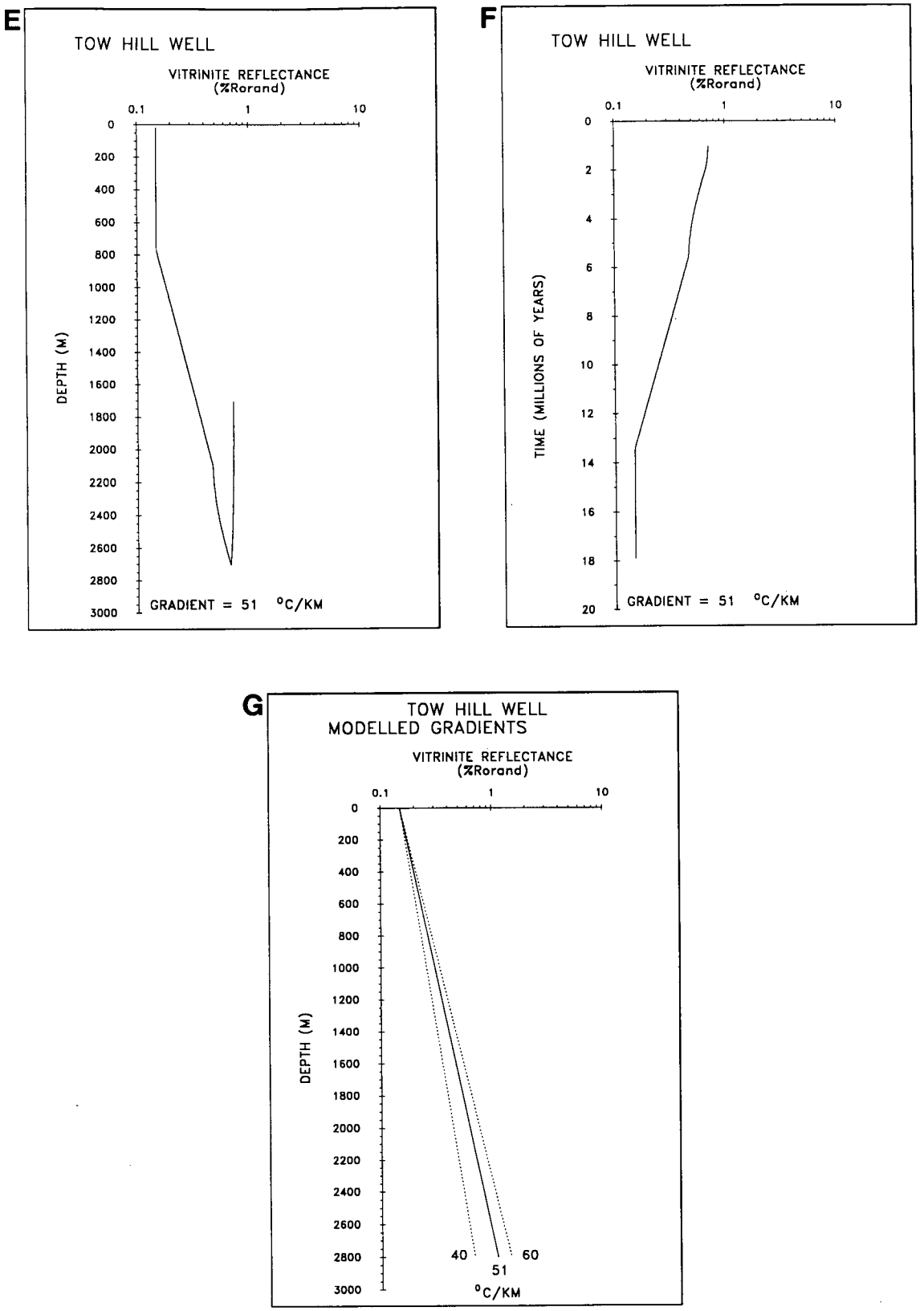

Figure 31. Tertiary Skonun Formation strata at the Tow Hill well (see text): e) maturation history (relative to depth) for the basal strata utilizing a modified Lopatin model (constant geothermal gradient = 51 ^{o}C/km); f) maturation history (relative to time) for the basal strata utilizing a modified Lopatin model (constant geothermal gradient = 51 ^{o}C/km); g) calculated geothermal gradients and measured maturation gradients are plotted through the origin (0.15 %Ro_{rand}) to facilitate comparison of slopes

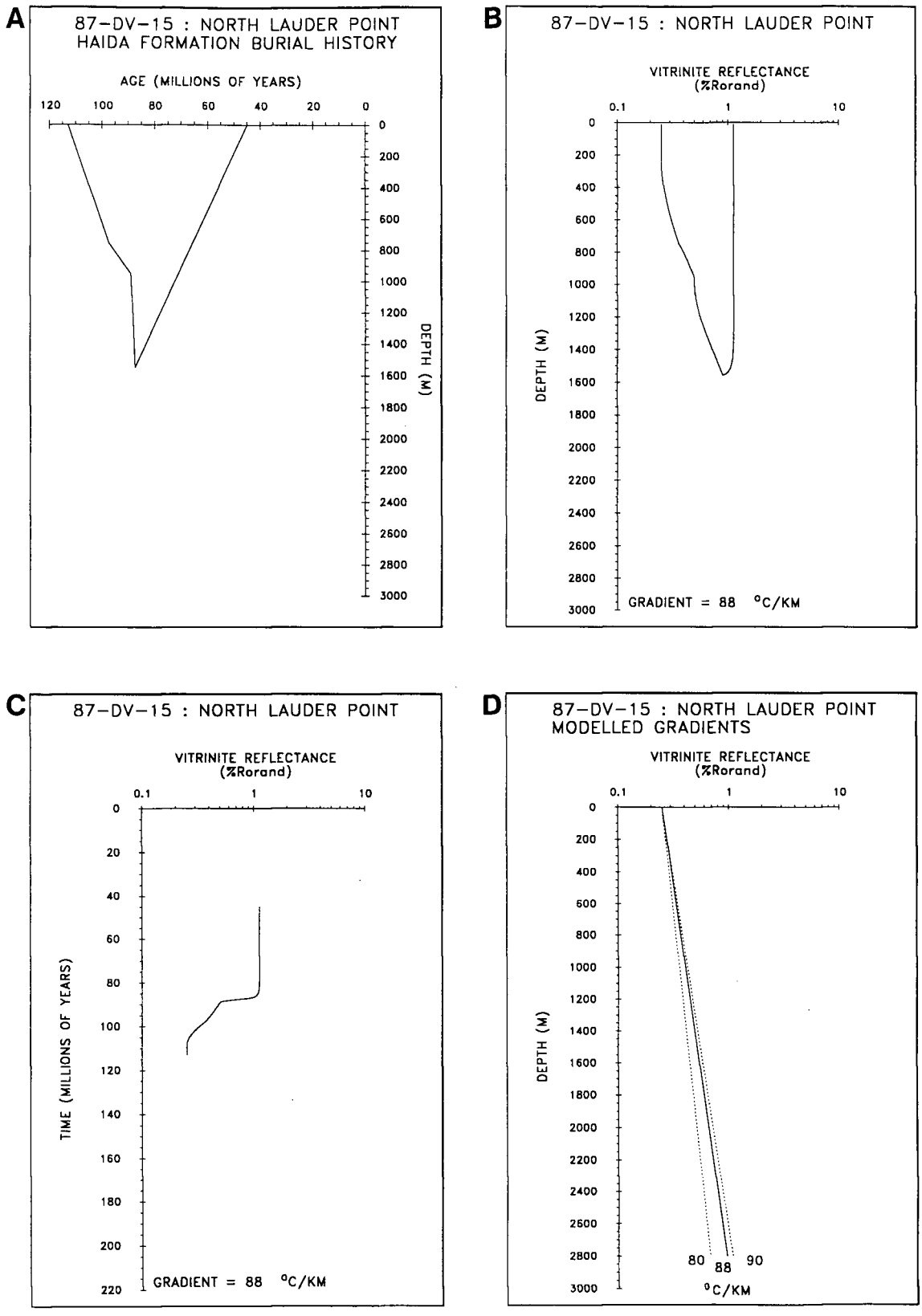

Figure 32. Cretaceous Haida Formation strata at north Lauder Point (see text): a) interpreted burial history for the base of the Skonun Formation assuming uniform subsidence and uplift rates derived from published and unpublished data; b) maturation history (relative to depth) for the basal strata utilizing a modified Arrhenius model (constant geothermal gradient = 88 ^{o}C/km); c) maturation history (relative to time) for the basal strata utilizing a modified Arrhenius model (constant geothermal gradient = 88 ^{o}C/km); d) calculated geothermal gradients and measured maturation gradients are plotted through the origin (0.15 %Ro_{rand}) to facilitate comparison of slopes

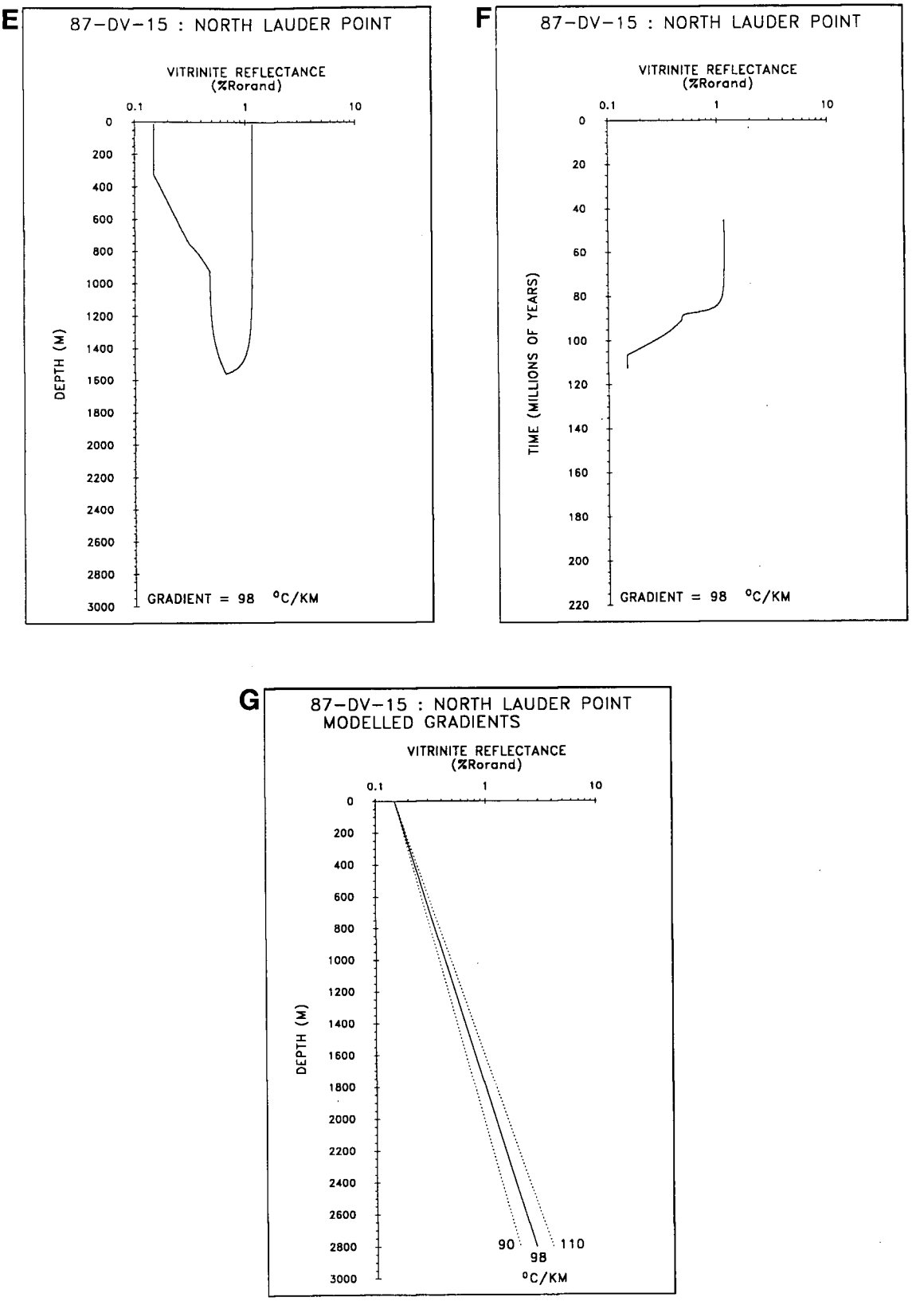

Figure 32. Cretaceous Haida Formation strata at north Lauder Point (see text): e) maturation history (relative to depth) for the basal strata utilizing a modified Lopatin model (constant geothermal gradient = 98 °C/km); f) maturation history (relative to time) for the basal strata utilizing a modified Lopatin model (constant geothermal gradient = 98 °C/km); g) calculated geothermal gradients and measured maturation gradients are plotted through the origin (0.15 $\%Ro_{rand}$) to facilitate comparison of slopes

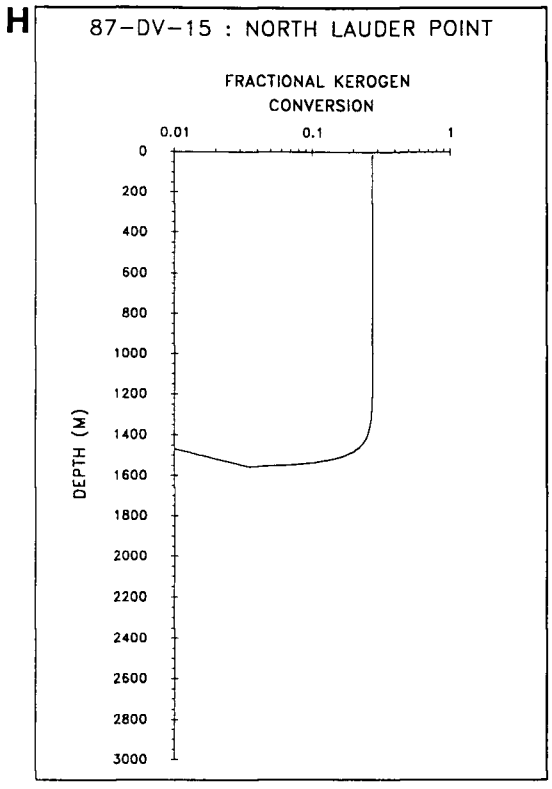

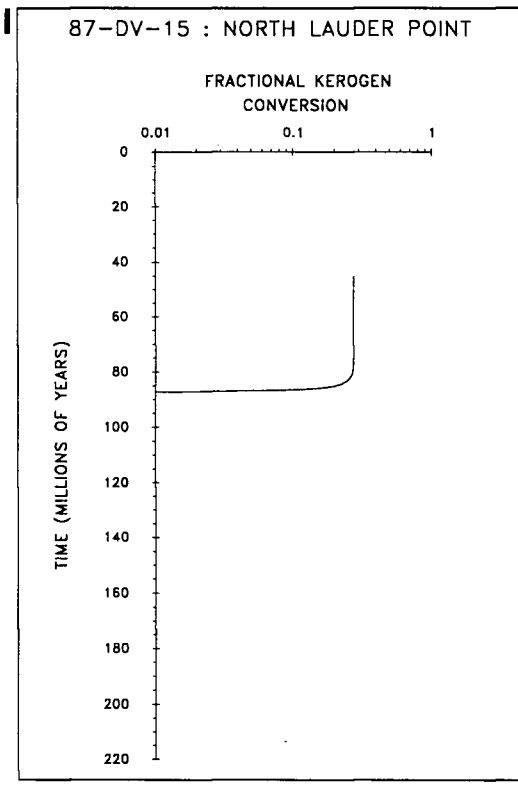

Figure 32. Cretaceous Haida Formation strata at north Lauder Point (see text): h) fractional kerogen conversion (relative to time) utilizing a modified Arrhenius model (constant geothermal gradient = 88 ^{o}C/km); i) fractional kerogen conversion (relative to depth) utilizing a modified Arrhenius model (constant geothermal gradient = 88 ^{o}C/km)

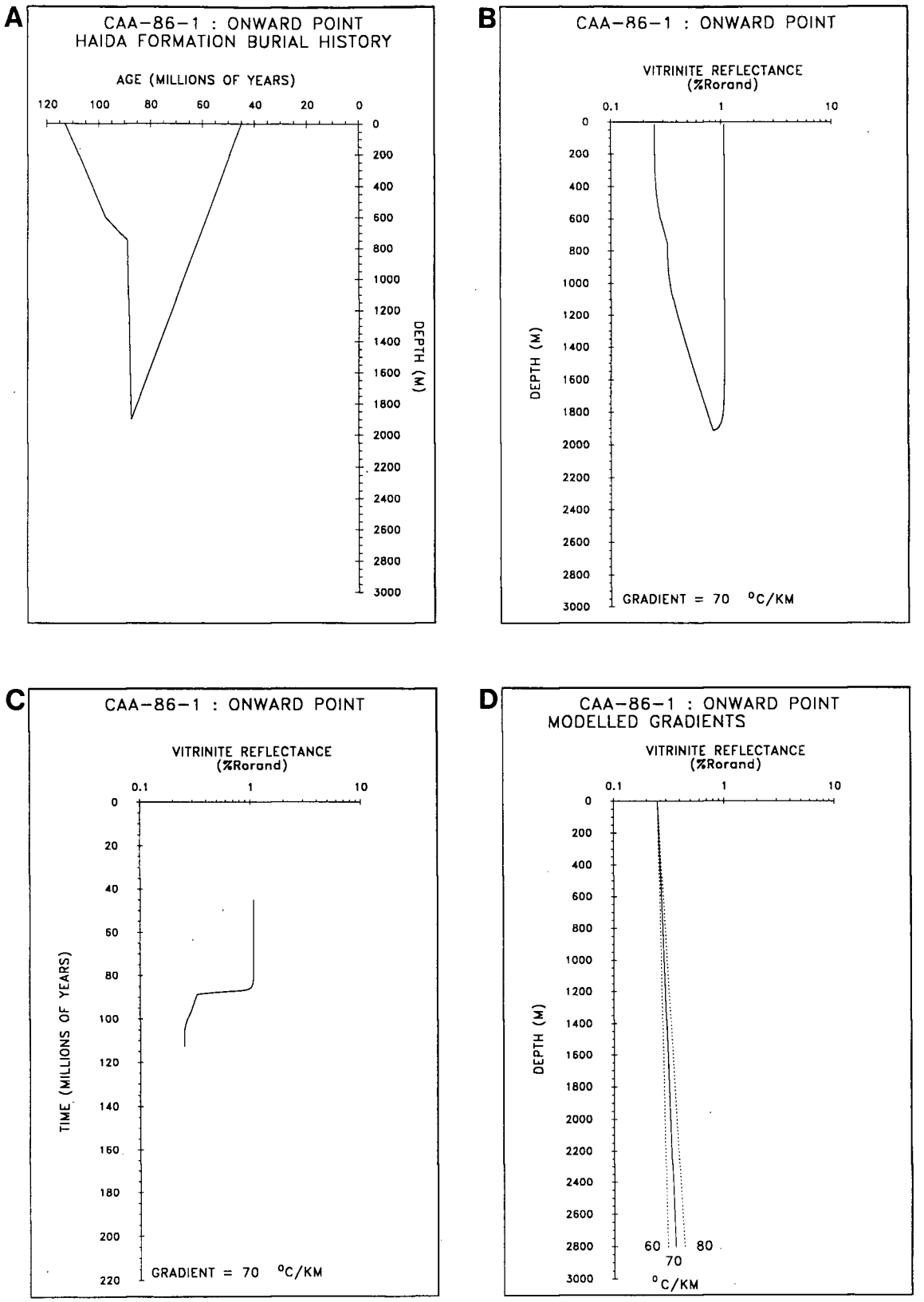

Figure 33. Cretaceous Haida Formation strata at Onward Point (see text): a) interpreted burial history for the base of the Skonun Formation assuming uniform subsidence and uplift rates derived from published and unpublished data; b) maturation history (relative to depth) for the basal strata utilizing a modified Arrhenius model (constant geothermal gradient = 70 ^{o}C/km); c) maturation history (relative to time) for the basal strata utilizing a modified Arrhenius model (constant geothermal gradient = 70 ^{o}C/km); d) calculated geothermal gradients and measured maturation gradients are plotted through the origin (0.15 %Ro_{rand}) to facilitate comparison of slopes

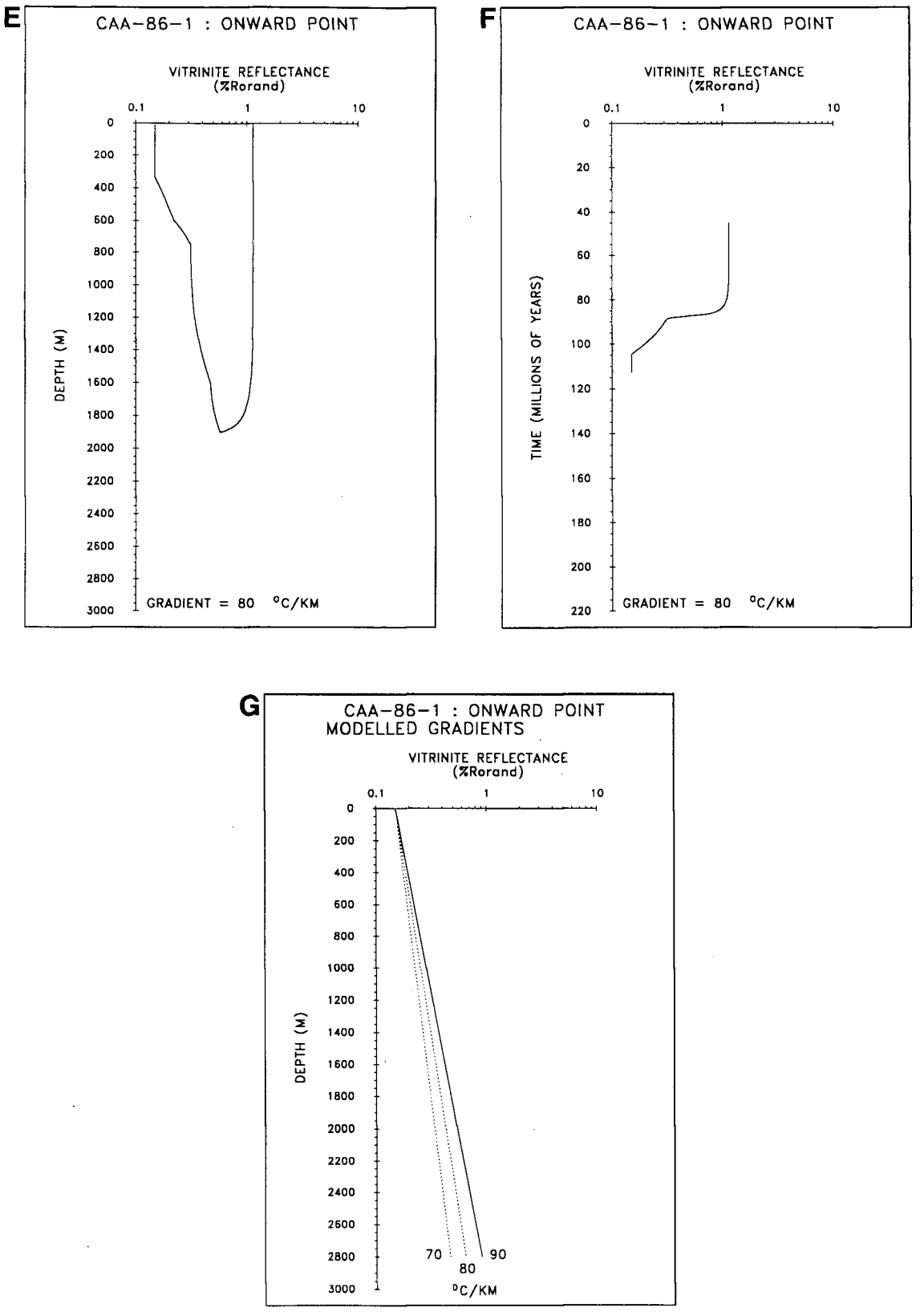

Figure 33. Cretaceous Haida Formation strata at Onward Point (see text): e) maturation history (relative to depth) for the basal strata utilizing a modified Lopatin model (constant geothermal gradient = 80 ^{o}C/km); f) maturation history (relative to time) for the basal strata utilizing a modified Lopatin model (constant geothermal gradient = 80 ^{o}C/km); g) calculated geothermal gradients and measured maturation gradients are plotted through the origin (0.15 $\%Ro_{rand}$) to facilitate comparison of slopes

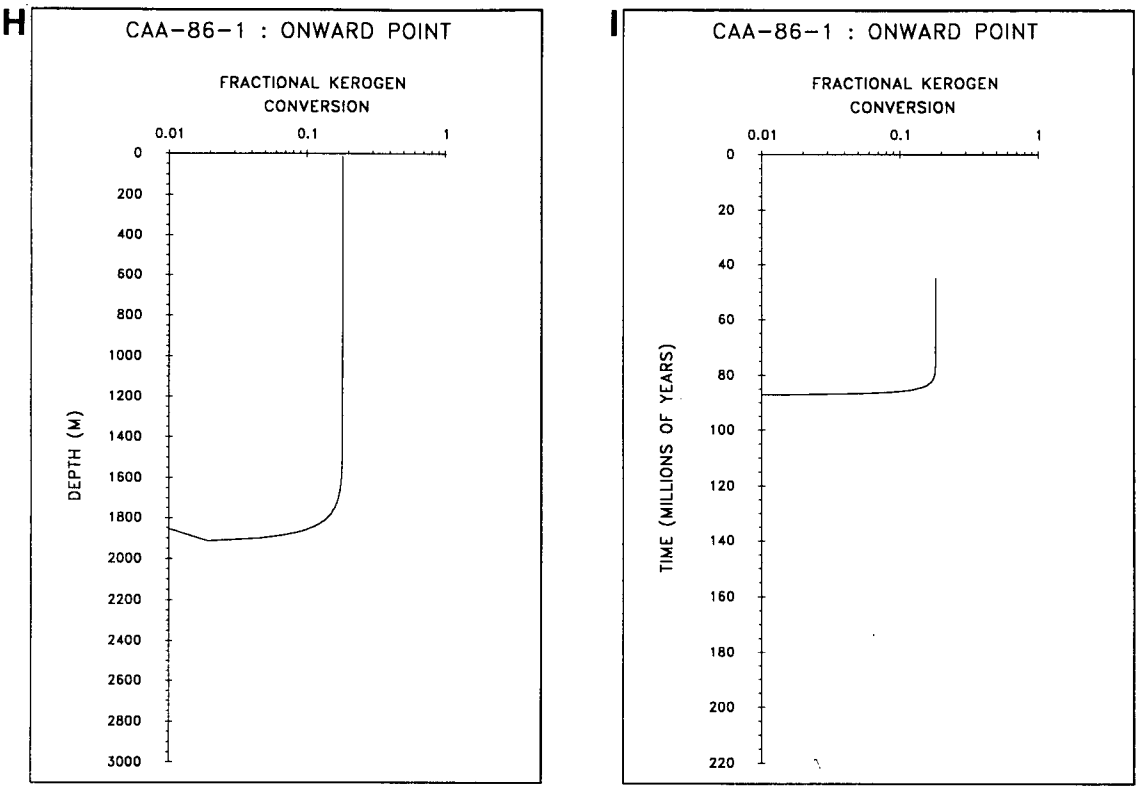

Figure 33. Cretaceous Haida Formation strata at Onward Point (see text): h) fractional kerogen conversion (relative to time) utilizing a modified Arrhenius model (constant geothermal gradient = 70 ^{o}C/km); i) fractional kerogen conversion (relative to depth) utilizing a modified Arrhenius model (constant geothermal gradient = 70 ^{o}C/km)

deposition of the subaerial erupted Masset Formation) (Cameron and Tipper, 1985; Cameron and Hamilton, 1988; Hickson, 1988).

There is insufficient data to conclude if the Masset Formation was deposited at north Lauder Point or Onward Point. However, even if the Masset Formation was deposited in these areas, it is unlikely that the burial depth of the Skonun Formation exceeded the maximum depth of burial attained in the Cretaceous and thus the Masset Formation would have little effect on the modelled DOM except near dikes or sills. The Skonun Formation is assumed to have never been deposited in these areas because both north Lauder Point and Onward Point are west of the presumed depositional edge of the Skonun Formation.

JURASSIC BURIAL HISTORIES

At Cumshewa Inlet (Fig. 34A) and Rennell Junction (Fig. 35A), Lower Jurassic strata of the Maude Group were deposited from the Early Pliensbachian to the Aalenian (198-183 Ma) to a total estimated depth of 300 m (Cameron and Tipper, 1985). Minor erosion or non-deposition within the Maude Group are documented by Cameron and Tipper (1985). Following Maude deposition, sediments of the Lower Bajocian Yakoun Group (Graham Island and Richardson Bay Formations) were deposited at the Rennell Junction section while partially contemporaneous volcanic facies of the Yakoun Group were erupted at Cumshewa Inlet (Cameron and Tipper, 1985).

In order to account for the predicted thickness of eroded strata at Rennell Junction (1725 m) and Cumshewa Inlet (1985 m), the Upper Bathonian to Lower Callovian Moresby Group (Robber Point, Newcombe, and Alliford Formations) are assumed to have been deposited following Yakoun deposition and then uplifted and eroded during the Late Jurassic and Early Cretaceous. The Longarm Formation (Upper Valanginian-Lower Barremian) is inferred to have been deposited, and partially or totally eroded before the Albian (113 Ma). The Cretaceous Haida, Skidegate, and Honna Formations appear to have been deposited during Albian to Conacian time (113 Ma to 87.5 Ma) followed by uplift and erosion until the initiation of Masset volcanism (45 Ma).

There is no evidence for deposition of the Masset Formation or the Skonun Formation at Rennell Junction or Cumshewa Inlet. Even if Masset Formation or Skonun Formation strata were deposited, the burial depths of Lower Jurassic sediments are assumed to be less than the maximum burial depths previously attained, thereby having little effect on maturation levels.

TRIASSIC BURIAL HISTORIES

At Fredrick Island (Fig. 36A) and Kennecott Point (Fig. 37A), the Early to Late Norian middle limestone member and the Sinemurian Sandilands Formation of the Kunga Group were buried until the Lower Pliensbachian. There is no evidence for post-Sinemurian Jurassic deposition north of Rennell Sound on western Graham Island (Tipper, pers. comm., 1988); therefore, a period of non-deposition or uplift is assumed during Early Pliensbachian to Early Callovian time (Maude, Yakoun, and Moresby Groups). The Longarm Formation was deposited during the Late Valanginian-Early Barremian followed by uplift and partial erosion as is evident from exposures of the Longarm Formation north of Fredrick Island (Tipper, pers. comm., 1988). Cretaceous Haida, Skidegate, and Honna Formations are exposed north of Fredrick Island and are assumed to have been deposited in the Fredrick Island-Kennecott Point area.

Deposition of the Masset Formation is estimated to not have been sufficient to bury the Triassic strata to exceed maximum burial depths attained during the Cretaceous. The Skonun Formation is assumed to never have been deposited in the area; both Fredrick Island and Kennecott Point are west of the inferred depositional edge of the Skonun Formation.

Maturation Histories

Maturation histories derived from both Arrhenius (Figs. 26B-37B, and 26C-37C) and Lopatin (Figs. 26E-37E, and 26F-37F) numerical methods incorporate the burial histories reviewed above for the modelled sections. Measured maturation gradients are compared with calculated paleogeothermal gradients in

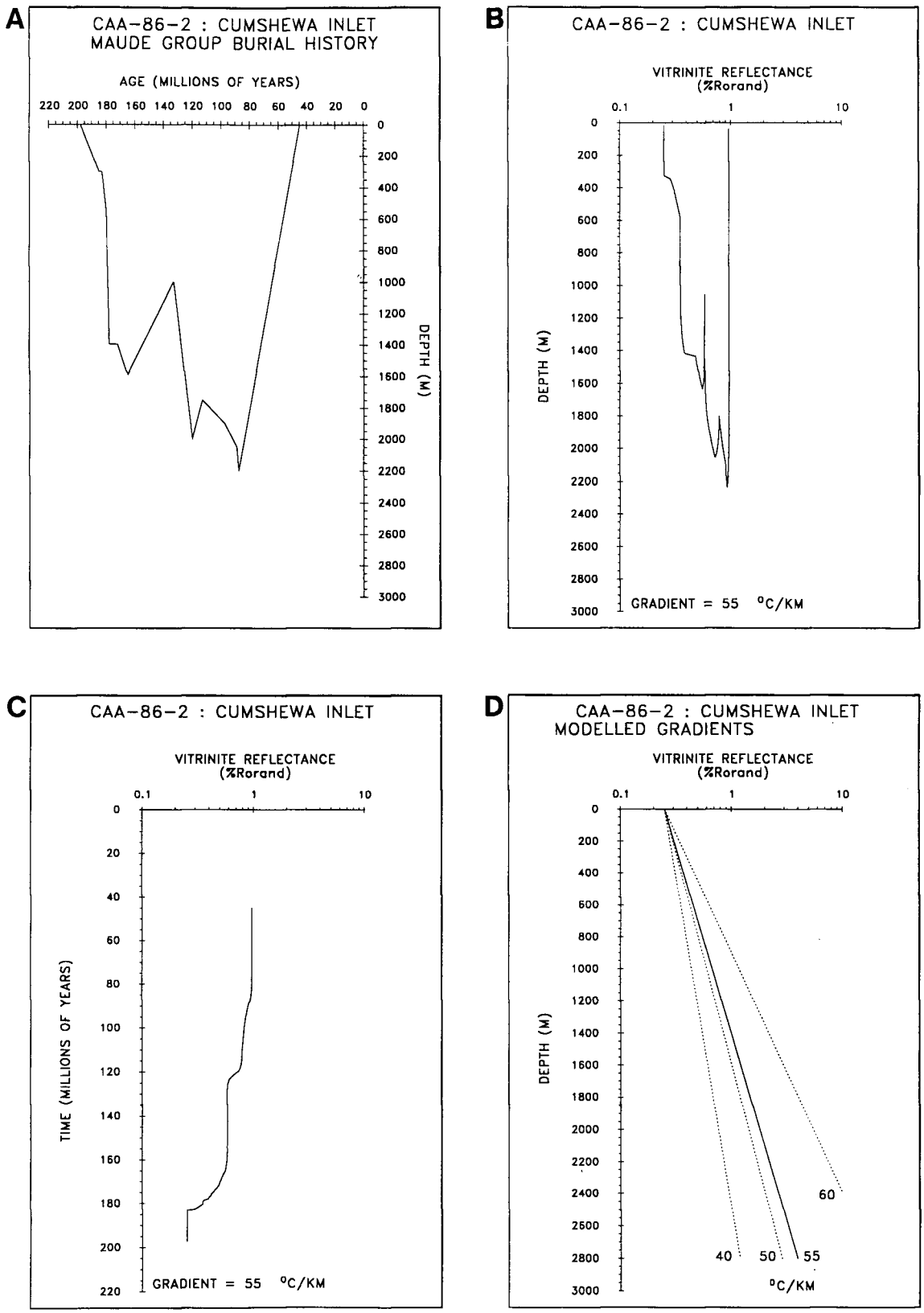

Figure 34. Jurassic Maude Formation strata at Cumshewa Inlet (see text): a) interpreted burial history for the base of the Skonun Formation assuming uniform subsidence and uplift rates derived from published and unpublished data; b) maturation history (relative to depth) for the basal strata utilizing a modified Arrhenius model (constant geothermal gradient = 55 ^{o}C/km); c) maturation history (relative to time) for the basal strata utilizing a modified Arrhenius model (constant geothermal gradient = 55 ^{o}C/km); d) calculated geothermal gradients and measured maturation gradients are plotted through the origin (0.15 %Ro_{rand}) to facilitate comparison of slopes

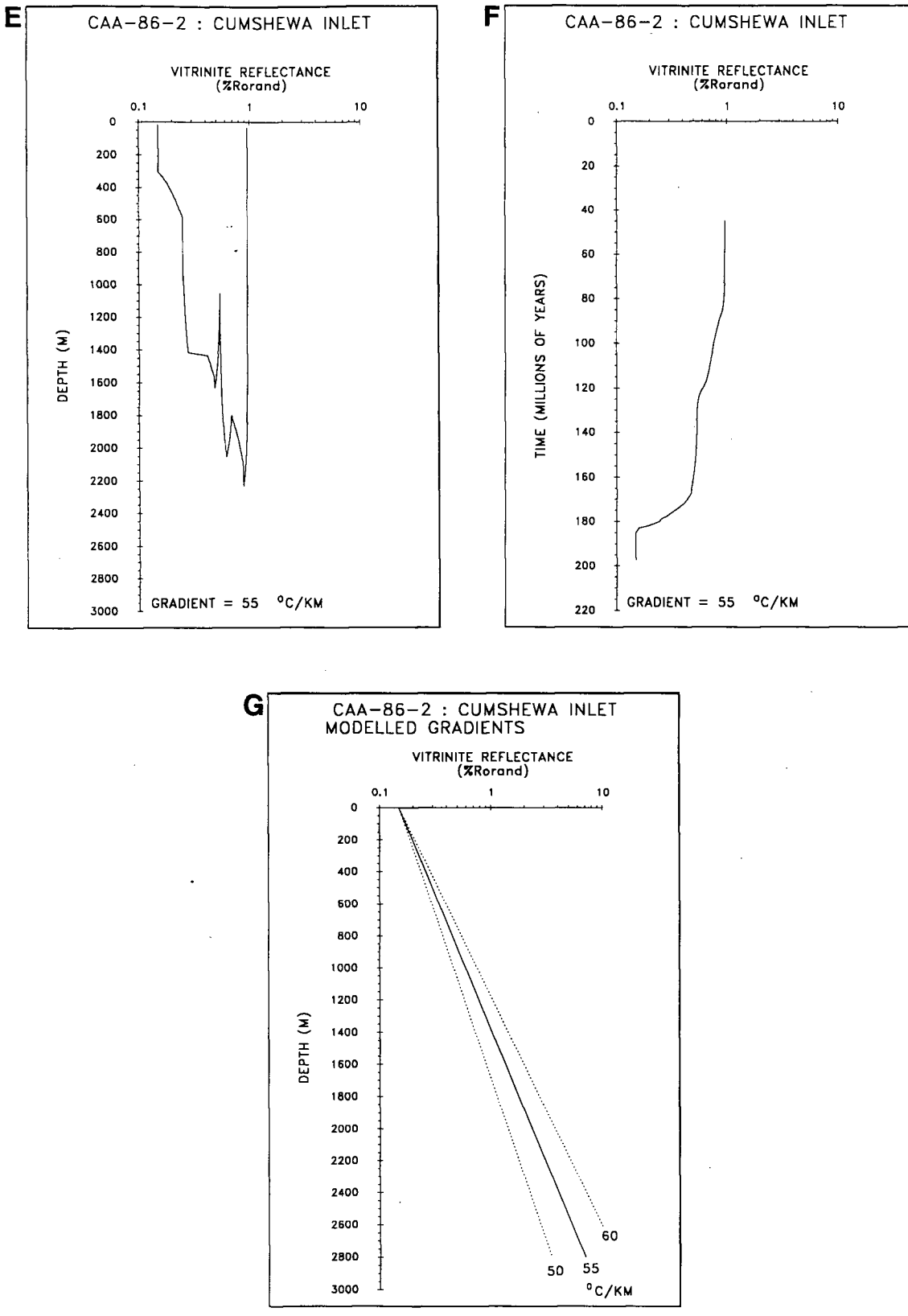

Figure 34. Jurassic Maude Formation strata at Cumshewa Inlet (see text): e) maturation history (relative to depth) for the basal strata utilizing a modified Lopatin model (constant geothermal gradient = 55 °C/km); f) maturation history (relative to time) for the basal strata utilizing a modified Lopatin model (constant geothermal gradient = 55 °C/km); g) calculated geothermal gradients and measured maturation gradients are plotted through the origin (0.15 $\%Ro_{rand}$) to facilitate comparison of slopes

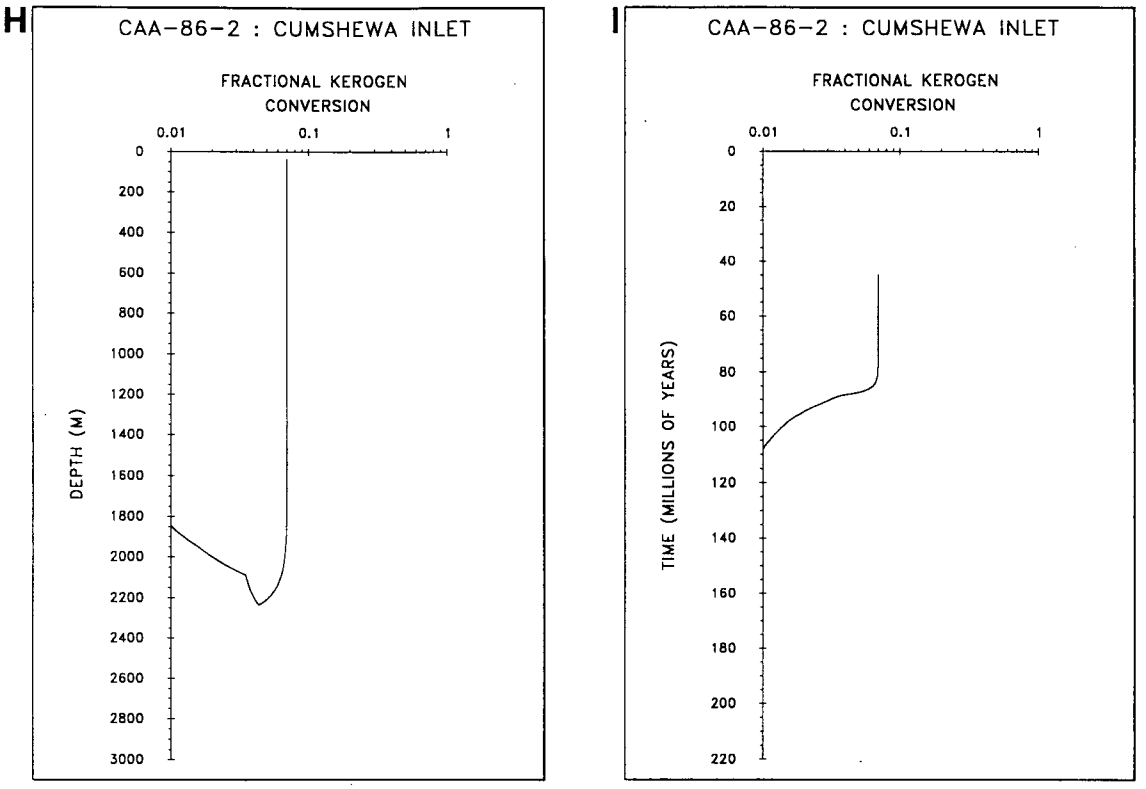

Figure 34. Jurassic Maude Formation strata at Cumshewa Inlet (see text): h) fractional kerogen conversion (relative to time) utilizing a modified Arrhenius model (constant geothermal gradient = 55 ^{o}C/km); i) fractional kerogen conversion (relative to depth) utilizing a modified Arrhenius model (constant geothermal gradient = 55 ^{o}C/km)

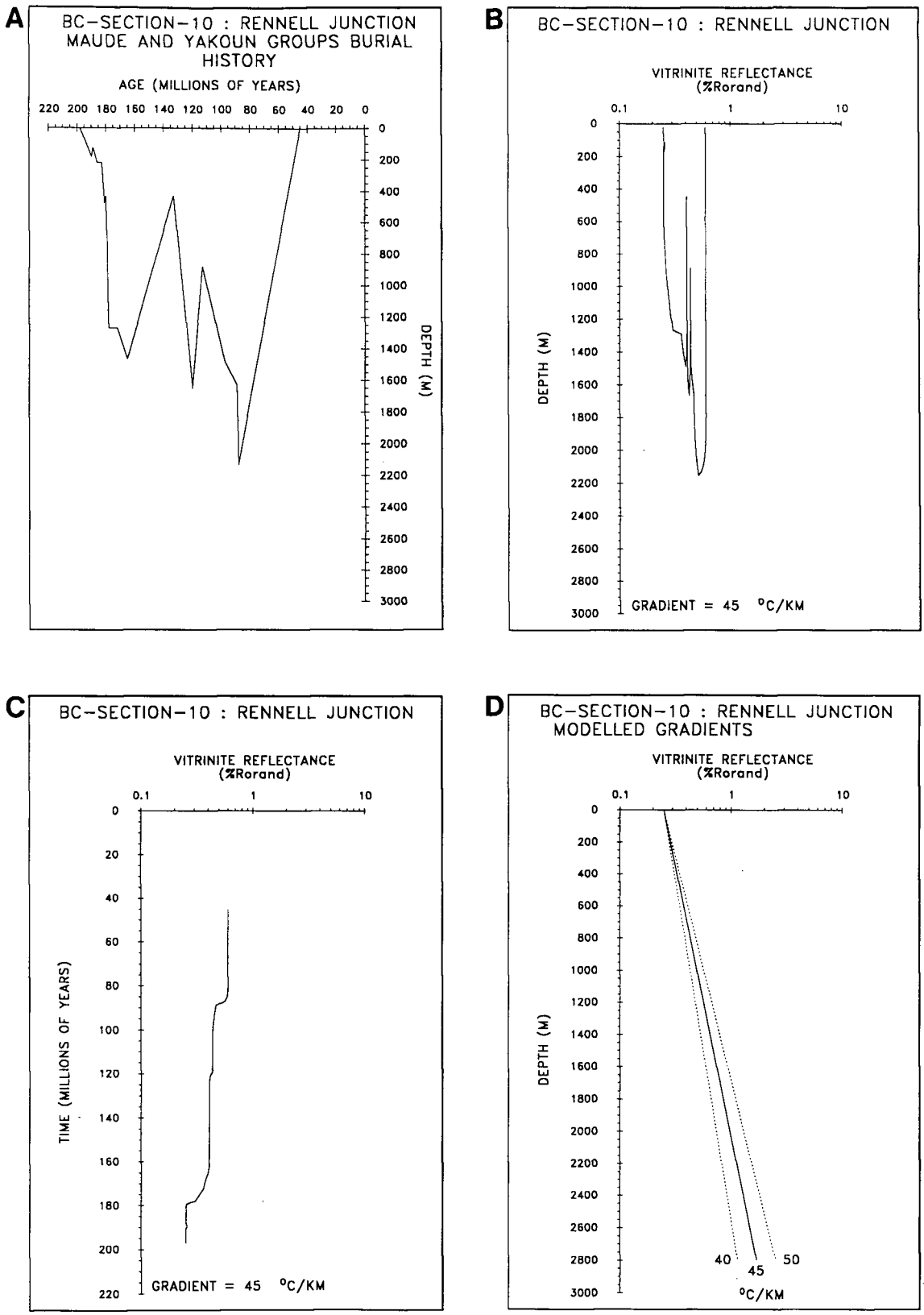

Figure 35. Jurassic Maude Formation strata at Rennell Junction (see text): a) interpreted burial history for the base of the Skonun Formation assuming uniform subsidence and uplift rates derived from published and unpublished data; b) maturation history (relative to depth) for the basal strata utilizing a modified Arrhenius model (constant geothermal gradient = 45 ^{o}C/km); c) maturation history (relative to time) for the basal strata utilizing a modified Arrhenius model (constant geothermal gradient = 45 ^{o}C/km); d) calculated geothermal gradients and measured maturation gradients are plotted through the origin (0.15 %Ro_{rand}) to facilitate comparison of slopes

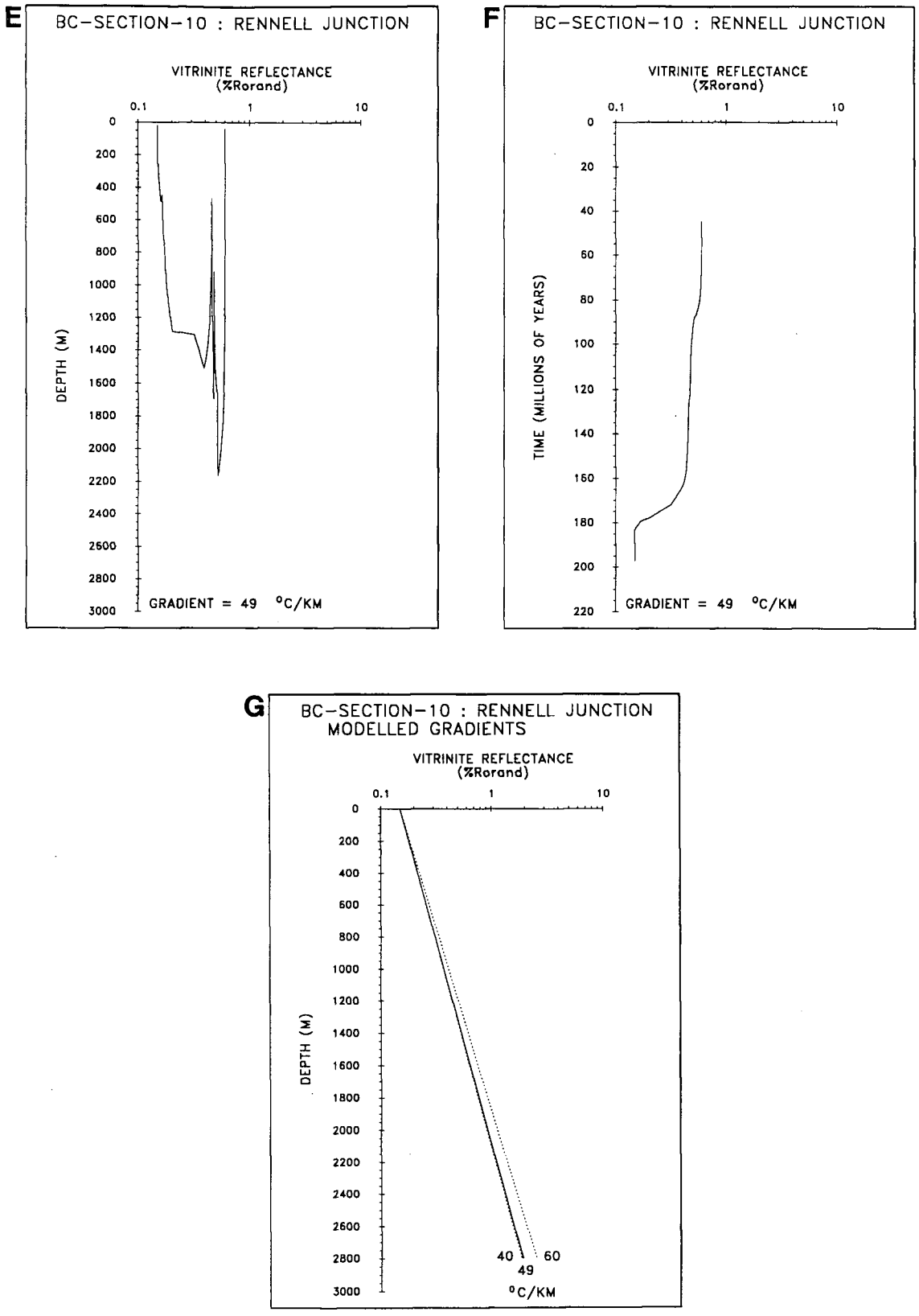

Figure 35. Jurassic Maude Formation strata at Rennell Junction (see text): e) maturation history (relative to depth) for the basal strata utilizing a modified Lopatin model (constant geothermal gradient = 49 °C/km); f) maturation history (relative to time) for the basal strata utilizing a modified Lopatin model (constant geothermal gradient = 49 °C/km); g) calculated geothermal gradients and measured maturation gradients are plotted through the origin (0.15 $\%Ro_{rand}$) to facilitate comparison of slopes

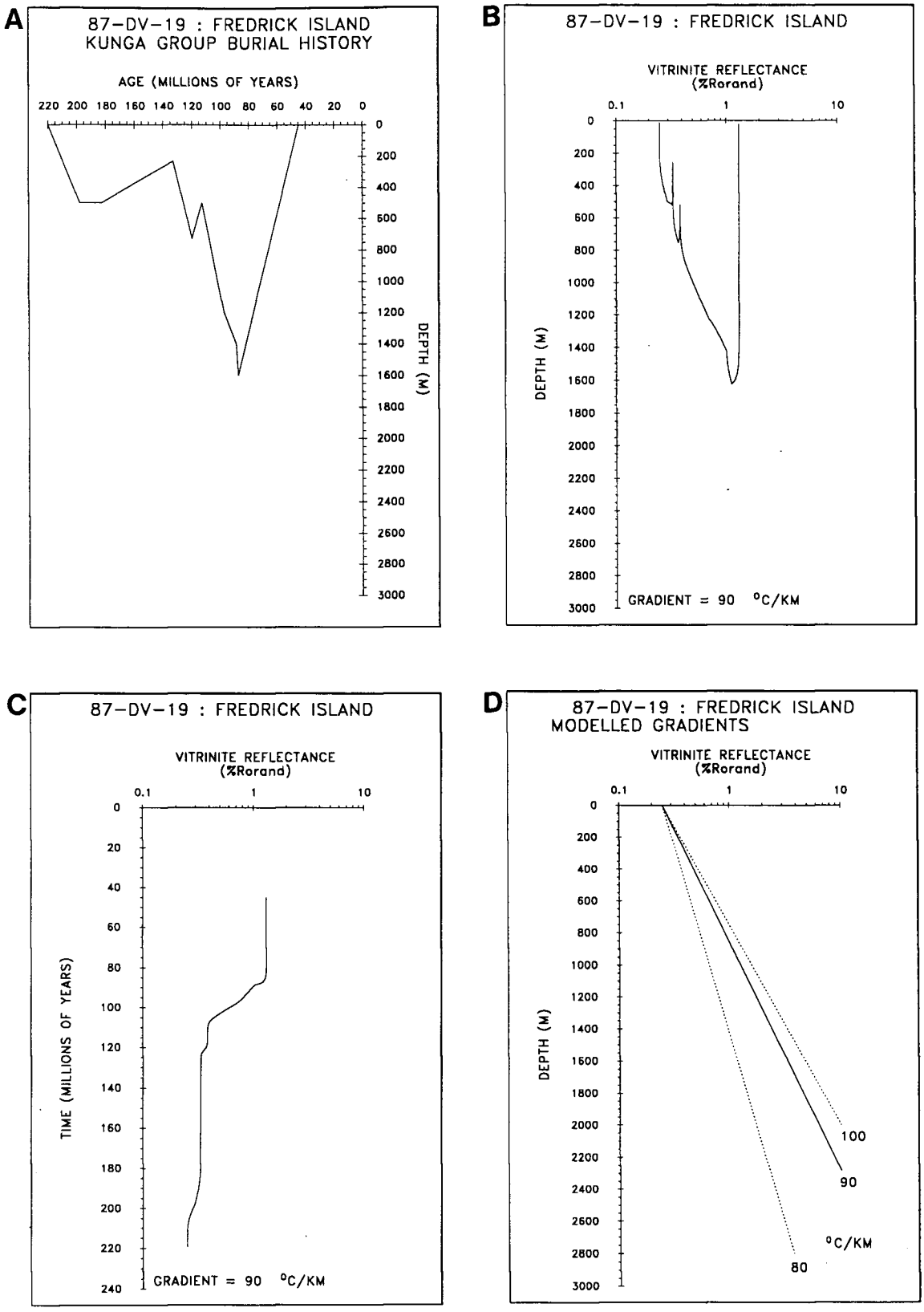

Figure 36. Triassic Sandilands Formation strata at Fredrick Island (see text): a) interpreted burial history for the base of the Skonun Formation assuming uniform subsidence and uplift rates derived from published and unpublished data; b) maturation history (relative to depth) for the basal strata utilizing a modified Arrhenius model (constant geothermal gradient = 90 ^{o}C/km); c) maturation history (relative to time) for the basal strata utilizing a modified Arrhenius model (constant geothermal gradient = 90 ^{o}C/km); d) calculated geothermal gradients and measured maturation gradients are plotted through the origin (0.15 %Ro_{rand}) to facilitate comparison of slopes

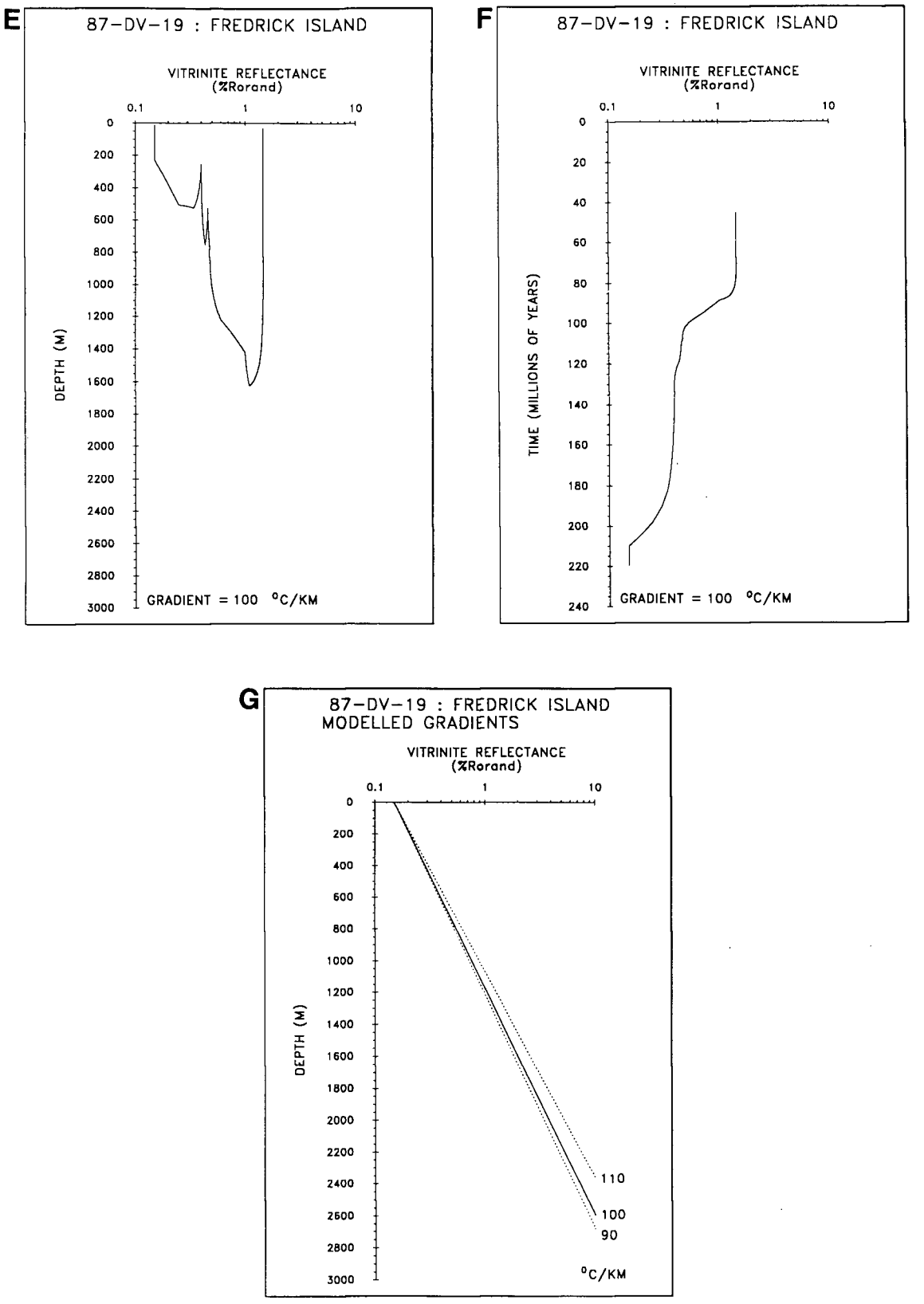

Figure 36. Triassic Sandilands Formation strata at Fredrick Island (see text): e) maturation history (relative to depth) for the basal strata utilizing a modified Lopatin model (constant geothermal gradient = 100 °C/km); f) maturation history (relative to time) for the basal strata utilizing a modified Lopatin model (constant geothermal gradient = 100 °C/km); g) calculated geothermal gradients and measured maturation gradients are plotted through the origin (0.15 $\%Ro_{rand}$) to facilitate comparison of slopes

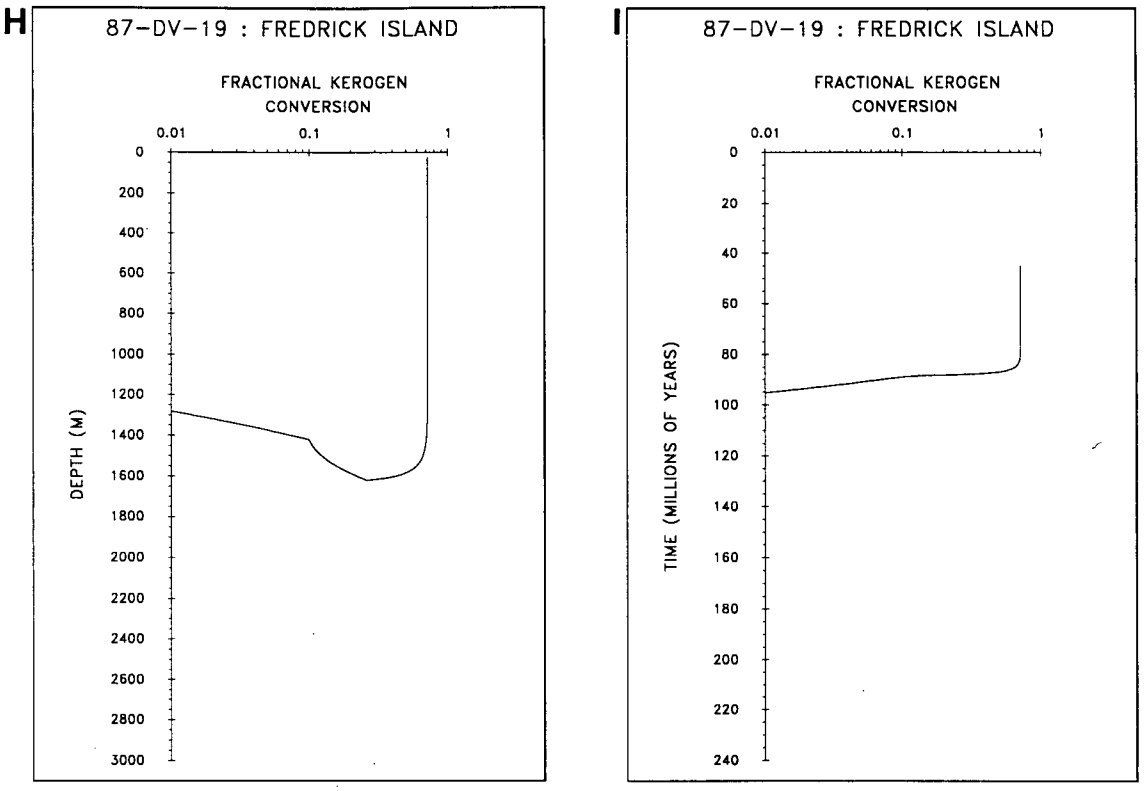

Figure 36. Triassic Sandilands Formation strata at Fredrick Island (see text): h) fractional kerogen conversion (relative to time) utilizing a modified Arrhenius model (constant geothermal gradient = 90 ^{o}C/km); i) fractional kerogen conversion (relative to depth) utilizing a modified Arrhenius model (constant geothermal gradient = 90 ^{o}C/km)

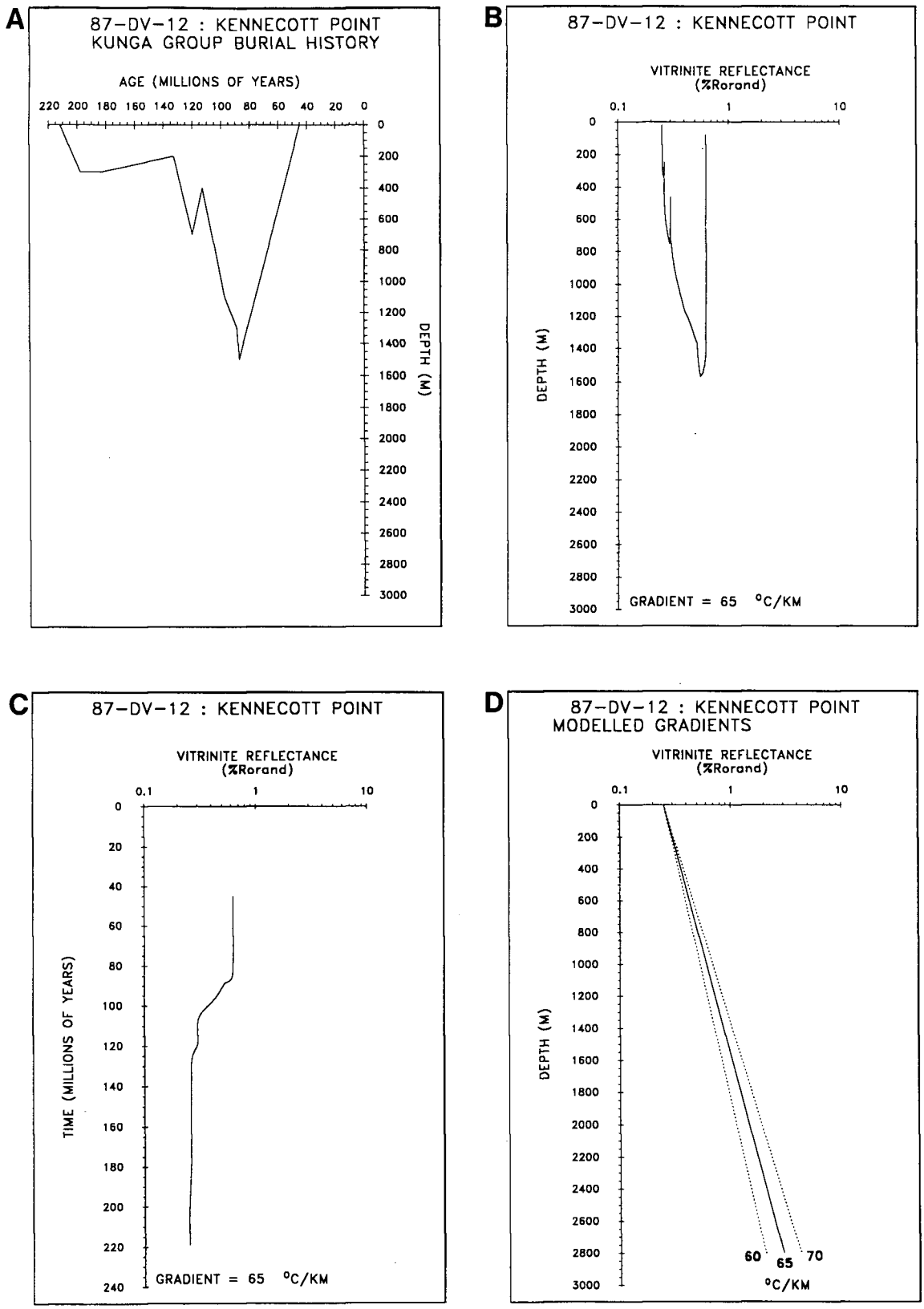

Figure 37. Triassic Sandilands Formation strata at Kennecott Point (see text): a) interpreted burial history for the base of the Skonun Formation assuming uniform subsidence and uplift rates derived from published and unpublished data; b) maturation history (relative to depth) for the basal strata utilizing a modified Arrhenius model (constant geothermal gradient = 65 ^{o}C/km); c) maturation history (relative to time) for the basal strata utilizing a modified Arrhenius model (constant geothermal gradient = 65 ^{o}C/km); d) calculated geothermal gradients and measured maturation gradients are plotted through the origin (0.15 %Ro_{rand}) to facilitate comparison of slopes

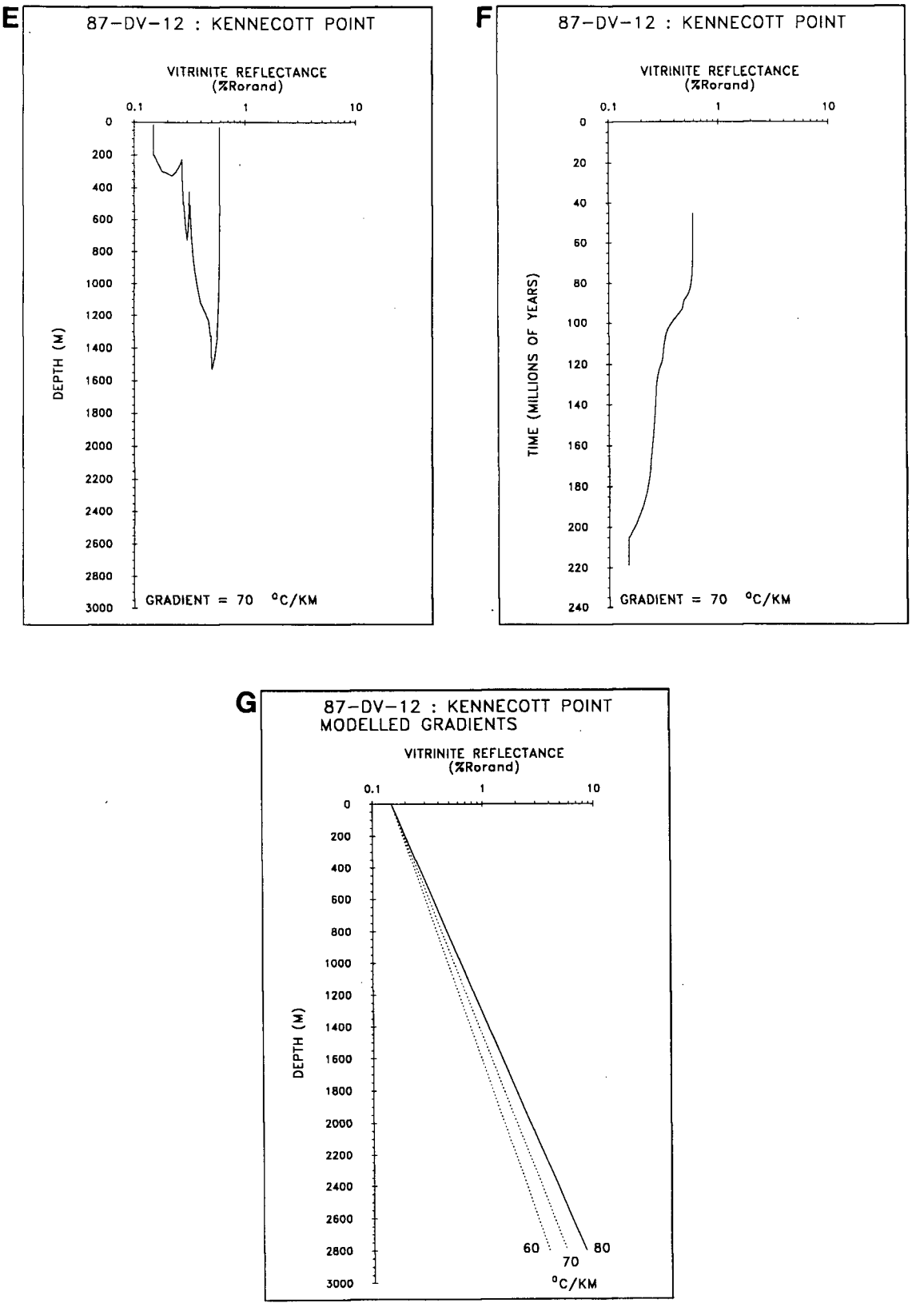

Figure 37. Triassic Sandilands Formation strata at Kennecott Point (see text): e) maturation history (relative to depth) for the basal strata utilizing a modified Lopatin model (constant geothermal gradient = 70 ^{o}C/km); f) maturation history (relative to time) for the basal strata utilizing a modified Lopatin model (constant geothermal gradient = 70 ^{o}C/km); g) calculated geothermal gradients and measured maturation gradients are plotted through the origin (0.15 $\%Ro_{rand}$) to facilitate comparison of slopes

Figures 26D-37D for the Arrhenius model and Figures 26G-37G for the Lopatin model. The base of the oldest modelled stratigraphic horizon is shown for each section. The fractional kerogen conversion to petroleum relative to depth and time (based on the Arrhenius model) is illustrated for some well or outcrop sections in Figures 29H, 32H, 33H, 34H, 36H, and 29I, 32I, 33I, 34I, 36I)

Wood (1988) has shown that at high heating rates, the Lopatin model underestimates the DOM (relative to the Arrhenius model) and overestimates the DOM at low heating rates (relative to the Arrhenius model). A comparison of the paleogeothermal gradients derived from both the Arrhenius and Lopatin type models (Table 3) illustrates that in all cases but one, the Lopatin model required a higher paleogeothermal gradient than the Arrhenius model suggesting that these strata have undergone high heating rates sometime during their history (Wood, 1988). Alternatively, the assumption in the Lopatin model that the reaction rate (and hence DOM) doubles every 10 ^{o}C (for temperatures between 50 ^{o}C and 150 ^{o}C and activation energies between 42 kJ/mol and 105 kJ/mol; Tissot and Welte, 1984) may not apply for Mesozoic and Tertiary strata in the Queen Charlotte Islands due to high temperatures (> 150 ^{o}C) attained during Yakoun and Masset volcanism. The Lopatin model, therefore, underestimates the DOM for strata which have been heated beyond 150 ^{o}C.

Results and Interpretations

The Queen Charlotte Islands are in an island arc tectonic setting; therefore, it is likely that heat flow (and thus paleogeothermal gradients) were influenced by volcanism and subduction and varied laterally between adjacent areas and with time (Watanabe et al., 1977; Cameron and Tipper, 1985). The following section discusses two possible thermal regimes for Mesozoic and Tertiary strata; constant, and variable paleogeothermal gradients. In order to account for the measured level of organic maturation (Figs. 26-37), the models predict paleogeothermal gradients in excess of 40 ^{o}C/km. Geologic evidence, however, suggests that heat flow (and paleogeothermal gradients) increased during volcanic/plutonic episodes in the Middle-Late Jurassic (Yakoun volcanism) and Eocene-Miocene (Masset volcanism). In this study, models which

TABLE 3

CONSTANT GEOTHERMAL GRADIENT MODEL

WELL (SECTION) NAME (LOCALITIES)	PREDICTED PALEOGEOTHERMAL GRADIENT (^{0}C/KM) (ARRHENIUS MODEL)	PREDICTED PALEOGEOTHERMAL GRADIENT (^{0}C/KM) (LOPATIN MODEL)
TERTIARY STRATA		
SKONUN FORMATION (EXPLORATION WELLS)		
CAPE BALL	30	35
GOLD CREEK	30	40
NADU RIVER	27	40
PORT LOUIS	45	55
TLELL	32	42
TOW HILL	42	51
CRETACEOUS STRATA		
HAIDA FORMATION (OUTCROP)		
NORTH LAUDER POINT	88	98
ONWARD POINT	70	80
JURASSIC STRATA		
MAUDE AND YAKOUN GROUPS (OUTCROP)		
CUMSHEWA INLET	55	55
RENNELL JUNCTION	45	49
TRIASSIC STRATA		
KUNGA GROUP (OUTCROP)		
FREDRICK ISLAND	90	100
KENNECOTT POINT	65	70

VARIABLE GEOTHERMAL GRADIENT MODEL (30 ^{0}C/KM BACKGROUND PALEOGEOTHERMAL GRADIENT)

WELL (SECTION) NAME	PREDICTED PEAK PALEOGEOTHERMAL GRADIENT (^{0}C/KM) (ARRHENIUS MODEL)	PREDICTED PEAK PALEOGEOTHERMAL GRADIENT (^{0}C/KM) (LOPATIN MODEL)
CRETACEOUS STRATA		
HAIDA FORMATION (OUTCROP)		
NORTH LAUDER POINT	130	145
ONWARD POINT	130	145
JURASSIC STRATA		
MAUDE AND YAKOUN GROUPS (OUTCROP)		
CUMSHEWA INLET	97	118
RENNELL JUNCTION	83	105
TRIASSIC STRATA		
KUNGA GROUP (OUTCROP)		
FREDRICK ISLAND	150	160
KENNECOTT POINT	100	115

allow for variable geothermal gradients are utilized to incorporate the assumed high heat flow during volcanic episodes. The modelled geothermal gradients were increased (up to 150 ^{o}C/km) above the ambient background geothermal gradient (assumed to be 30 ^{o}C/km) for short intervals of time consistent with geological evidence (assumed to be between 183-178 Ma for Yakoun volcanism, and between 35-10 Ma for Masset volcanism). The background geothermal gradient was chosen to be similar to average paleogeothermal gradients (30 ^{o}C/km) modelled for the Skonun Formation. Paleogeothermal gradients for Tertiary strata are considered to be the least effected by high heat flow associated with volcanism because the Skonun Formation was deposited after the cessation of Yakoun and Masset volcanism. However, if Mesozoic background paleogeothermal gradients were higher than the modelled 30 ^{o}C/km geothermal gradients, little effect in the levels of organic maturation are predicted in that the maximum temperatures (which were attained during volcanic episodes when heat flow was substantially elevated above the background levels) have the most pronounced effect on maturation (Figs. 38-43).

The paleogeothermal gradients predicted for each section are documented in the following section. The predicted paleogeothermal gradients were derived from geothermal gradients which were modelled to attain the measured DOM. Both the Arrhenius and Lopatin models generally yielded similar results, therefore only the Arrhenius model is described in the following discussion. Results from the Lopatin model are presented for comparative purposes in Table 3.

TERTIARY PALEOGEOTHERMAL GRADIENTS

Paleogeothermal gradients predicted by the Arrhenius model (assuming a constant thermal regime) range from 27 ^{o}C/km to 45 ^{o}C/km (Nadu River and Port Louis wells respectively) and average 30 ^{o}C/km.

CRETACEOUS PALEOGEOTHERMAL GRADIENTS

Predicted paleogeothermal gradients for Cretaceous strata (assuming a constant thermal regime) range from 70 ^{o}C/km at Onward Point to 88 ^{o}C/km to north Lauder Point.

Variable thermal regime modelling with 30 ^{o}C/km background paleogeothermal gradients predicts peak paleogeothermal gradients up to 130 ^{o}C/km during the culmination of Masset Formation volcanism (between 35 Ma and 10 Ma) for Cretaceous strata at both Onward and north Lauder Points (see burial histories). Significant lateral variation in heat flow during Masset time between northwest and southeast Graham Island is not predicted by the Arrhenius model.

JURASSIC PALEOGEOTHERMAL GRADIENTS

Predicted paleogeothermal gradients for a constant thermal regime for Jurassic strata range from 45 ^{o}C/km at Rennell Junction to 55 ^{o}C/km at Cumshewa Inlet.

Predicted peak paleogeothermal gradients (assuming a variable thermal regime with 30 ^{o}C/km background paleogeothermal gradients) range up to 83 ^{o}C/km at Rennell Junction and 97 ^{o}C/km at Cumshewa Inlet during the culmination of Yakoun volcanism between 183 Ma and 178 Ma. The increased paleogeothermal gradients in Cumshewa Inlet suggest that the Jurassic strata at that locality were more proximal to a source of high heat flow than at Rennell Junction.

TRIASSIC PALEOGEOTHERMAL GRADIENTS

Although Fredrick Island and Kennecott Point are proximally located, higher paleogeothermal gradients are predicted at Fredrick Island (90 ^{o}C/km) than at Kennecott Point (65 ^{o}C/km) assuming a constant thermal regime.

Peak paleogeothermal gradients (assuming a variable thermal regime with 30 ^{o}C/km background paleogeothermal gradients) range up to 100 ^{o}C/km at Kennecott Point and 150 ^{o}C/km at Fredrick Island during the culmination of Masset volcanism between 35 Ma and 10 Ma. A higher geothermal gradient predicted for Fredrick Island (relative to Kennecott Point) is probably due to increased heat flow from Masset feeder dikes/sills located closer to Fredrick Island than to Kennecott Point.

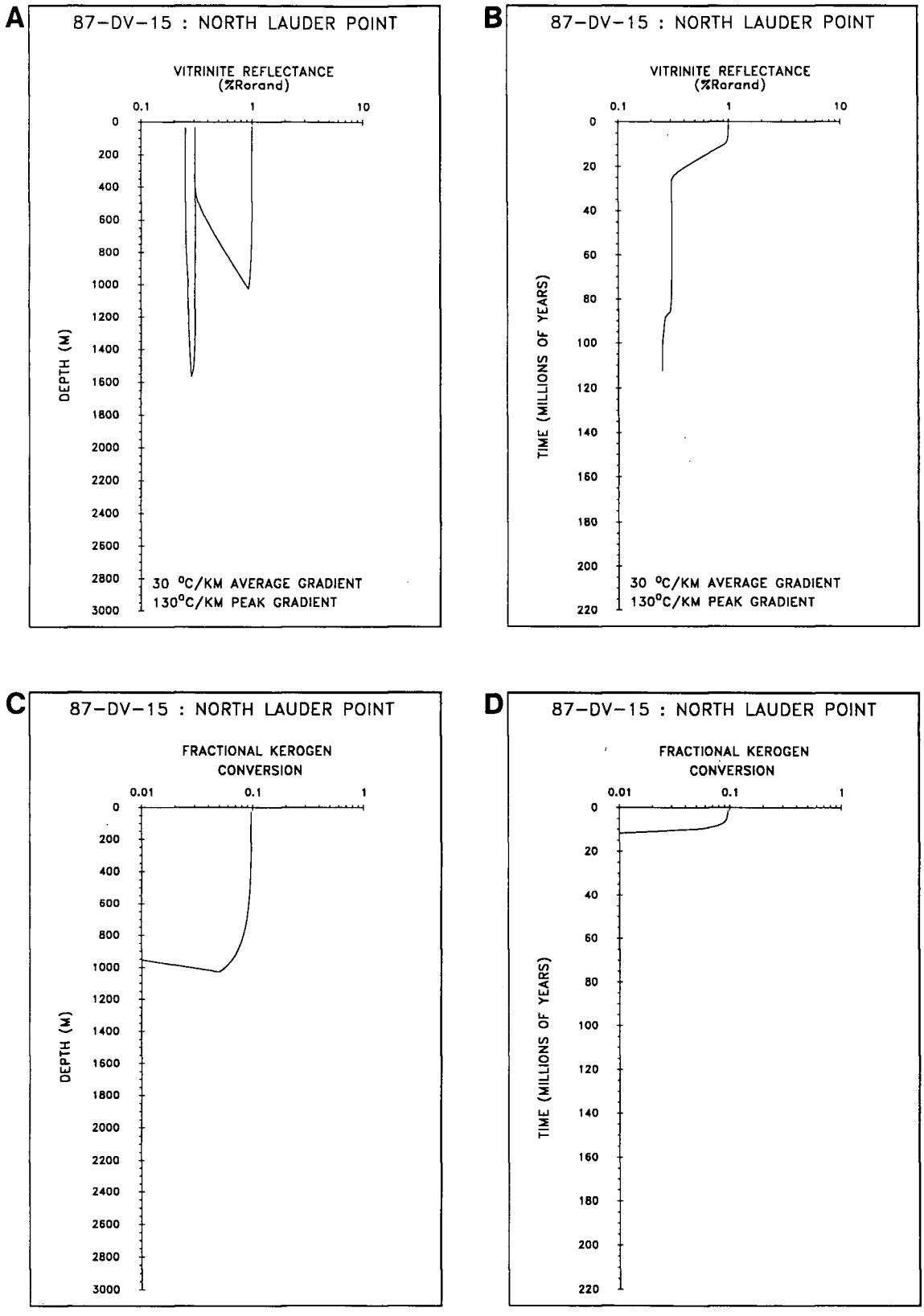

Figure 38. Cretaceous Haida Formation strata at north Lauder Point (variable geothermal gradient model with 30 ^{o}C/km average gradient): a) maturation history (relative to depth) for the basal strata utilizing a modified Arrhenius model (130 ^{o}C/km peak geothermal gradient); b) maturation history (relative to time) for the basal strata utilizing a modified Arrhenius model (130 ^{o}C/km peak geothermal gradient); c) fractional kerogen conversion (relative to depth) utilizing a modified Arrhenius model (130 ^{o}C/km peak geothermal gradient); d) fractional kerogen conversion (relative to time) utilizing a modified Arrhenius model (130 ^{o}C/km peak geothermal gradient)

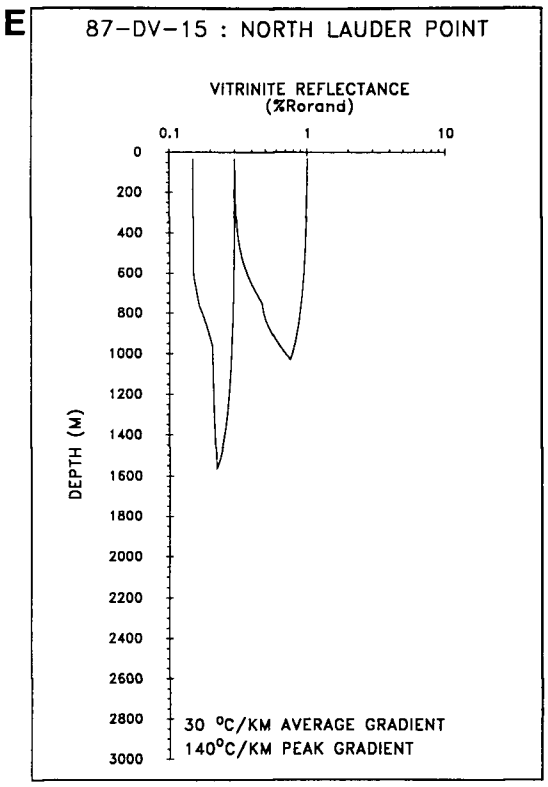

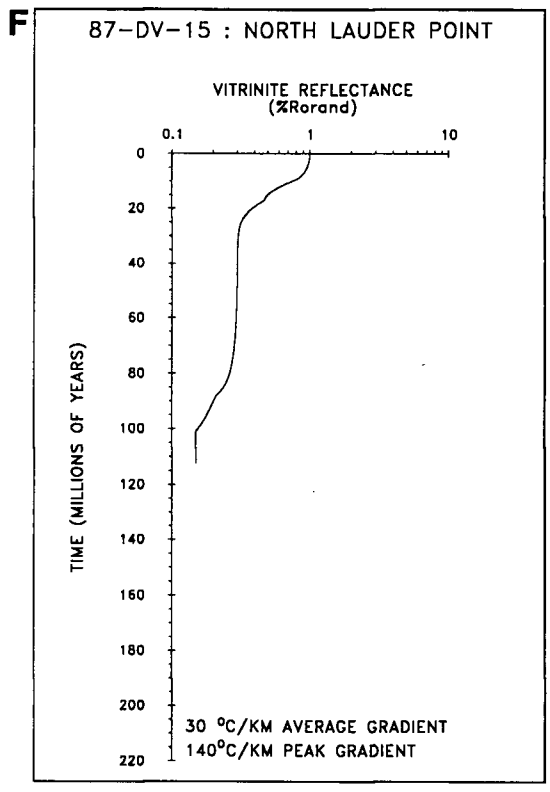

Figure 38. Cretaceous Haida Formation strata at north Lauder Point (variable geothermal gradient model with 30 ^{o}C/km average gradient): e) maturation history (relative to depth) for the basal strata utilizing a modified Lopatin model (140 ^{o}C/km peak geothermal gradient); f) maturation history (relative to time) for the basal strata utilizing a modified Lopatin model (140 ^{o}C/km peak geothermal gradient)

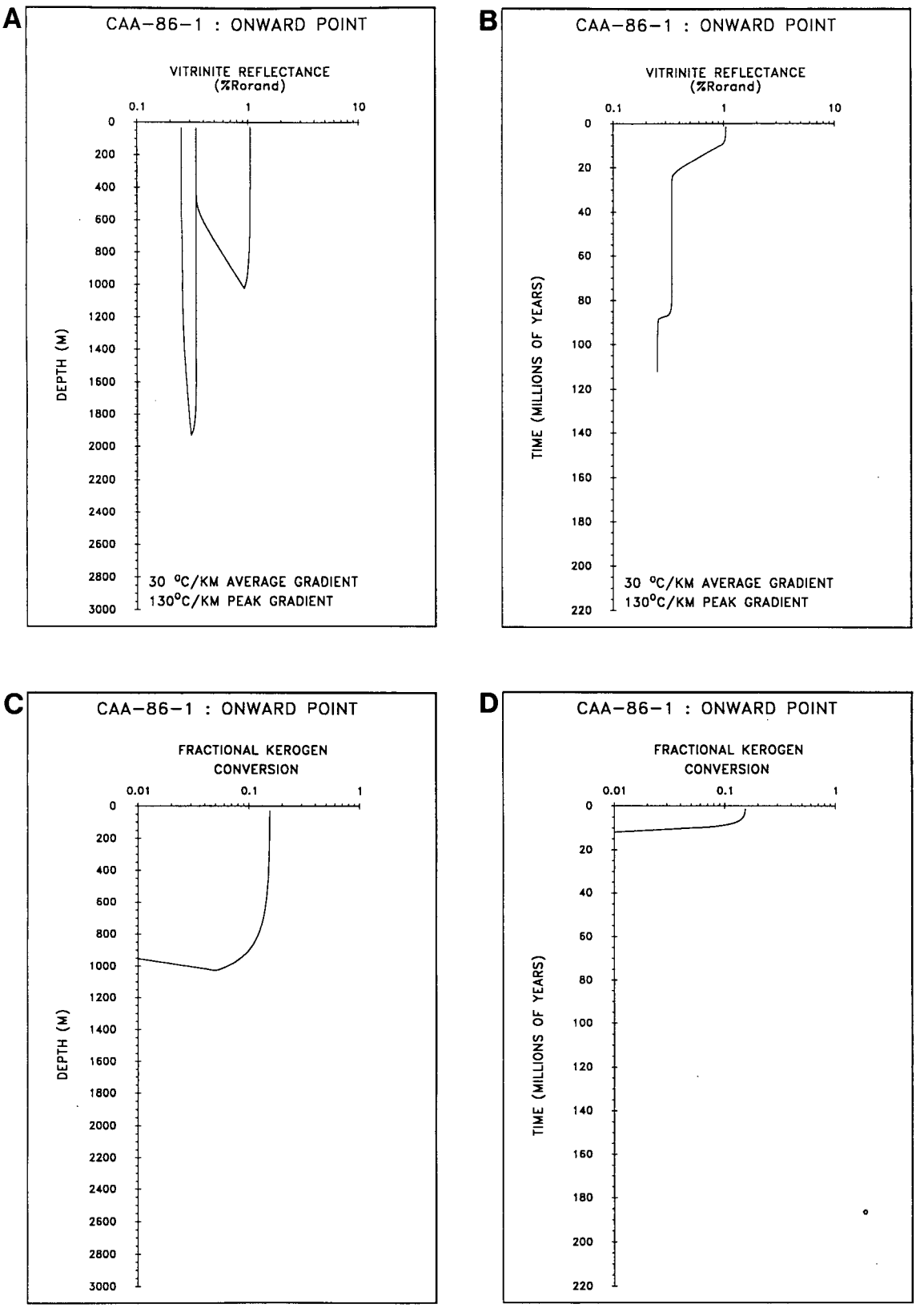

Figure 39. Cretaceous Haida Formation strata at Onward Point (variable geothermal gradient model with 30 ^{o}C/km average gradient): a) maturation history (relative to depth) for the basal strata utilizing a modified Arrhenius model (130 ^{o}C/km peak geothermal gradient); b) maturation history (relative to time) for the basal strata utilizing a modified Arrhenius model (130 ^{o}C/km peak geothermal gradient); c) fractional kerogen conversion (relative to depth) utilizing a modified Arrhenius model (130 ^{o}C/km peak geothermal gradient); d) fractional kerogen conversion (relative to time) utilizing a modified Arrhenius model (130 ^{o}C/km peak geothermal gradient)

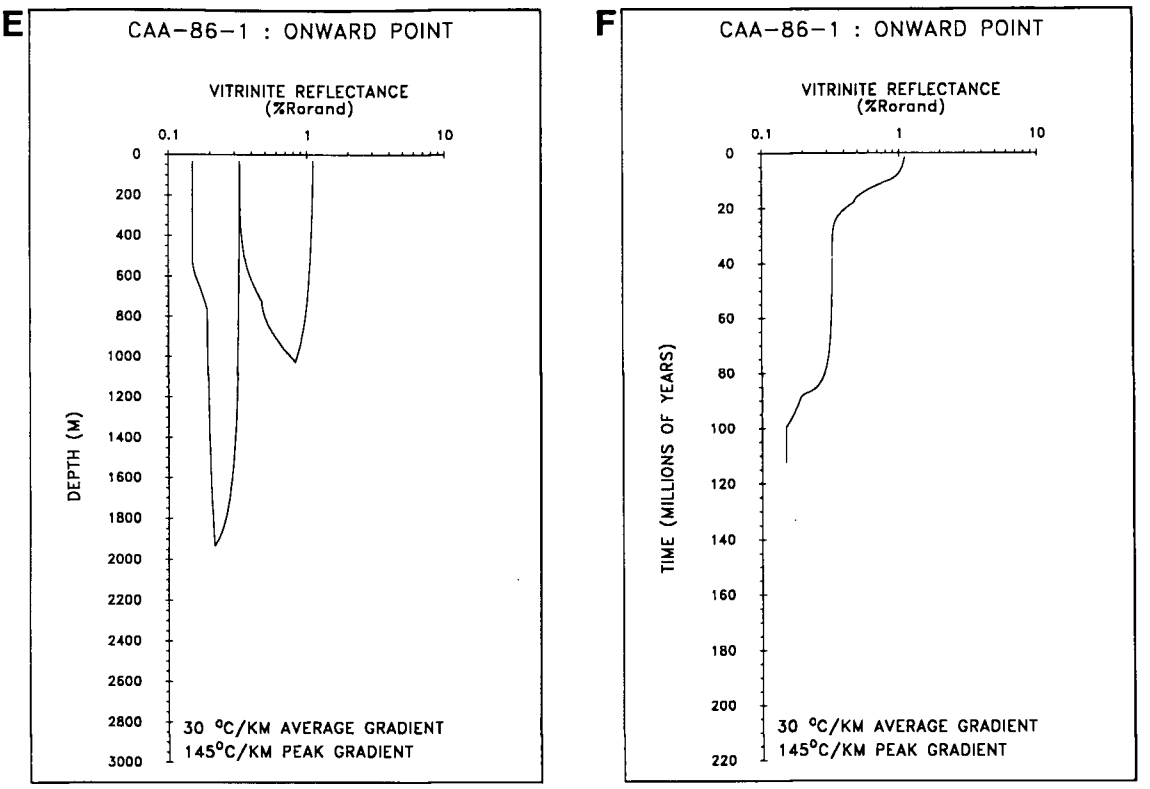

Figure 39. Cretaceous Haida Formation strata at Onward Point (variable geothermal gradient model with 30 ^{o}C/km average gradient): e) maturation history (relative to depth) for the basal strata utilizing a modified Lopatin model (145 ^{o}C/km peak geothermal gradient); f) maturation history (relative to time) for the basal strata utilizing a modified Lopatin model (145 ^{o}C/km peak geothermal gradient)

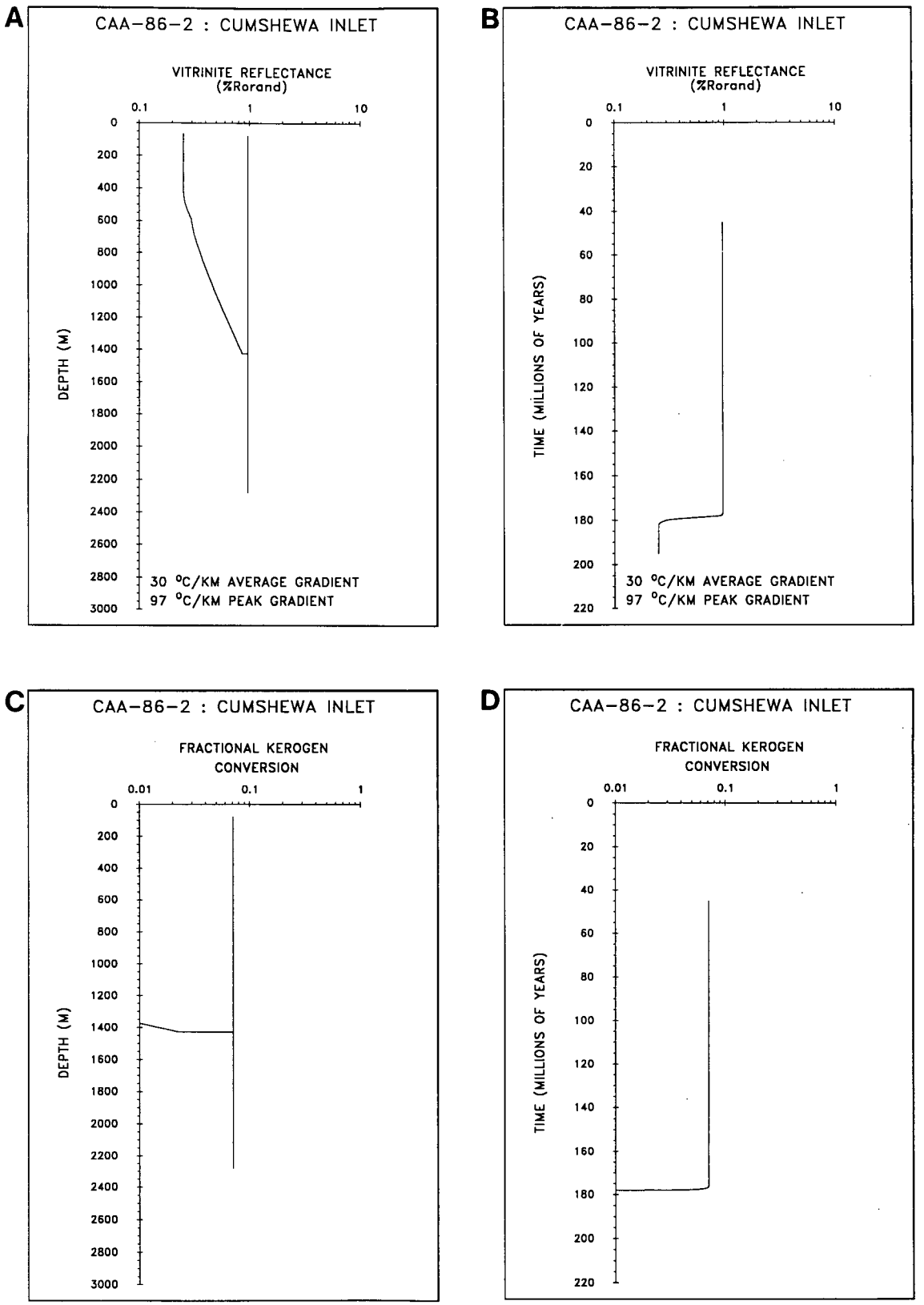

Figure 40. Jurassic Maude Group strata at Cumshewa Inlet (variable geothermal gradient model with 30 °C/km average gradient): a) maturation history (relative to depth) for the basal strata utilizing a modified Arrhenius model (97 °C/km peak geothermal gradient); b) maturation history (relative to time) for the basal strata utilizing a modified Arrhenius model (97 °C/km peak geothermal gradient); c) fractional kerogen conversion (relative to depth) utilizing a modified Arrhenius model (97 °C/km peak geothermal gradient); d) fractional kerogen conversion (relative to time) utilizing a modified Arrhenius model (97 °C/km peak geothermal gradient)

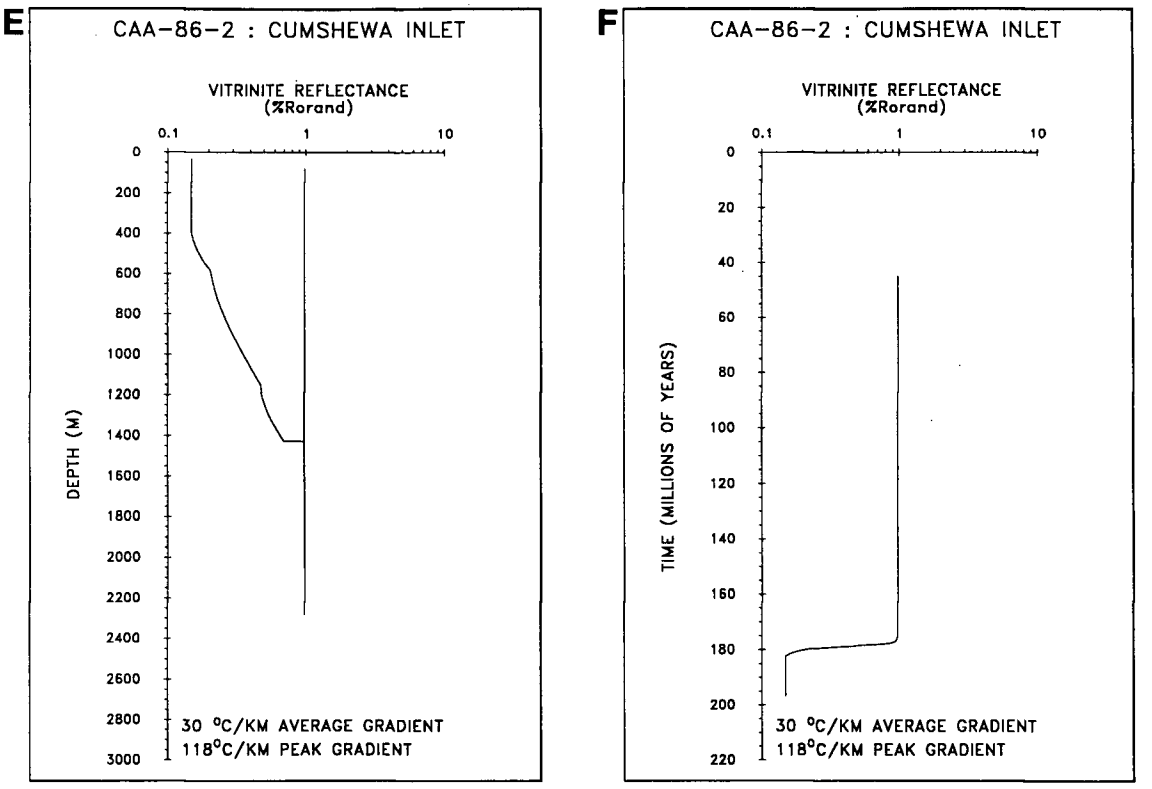

Figure 40. Jurassic Maude Group strata at Cumshewa Inlet (variable geothermal gradient model with 30 °C/km average gradient): e) maturation history (relative to depth) for the basal strata utilizing a modified Lopatin model (118 °C/km peak geothermal gradient); f) maturation history (relative to time) for the basal strata utilizing a modified Lopatin model (118 °C/km peak geothermal gradient)

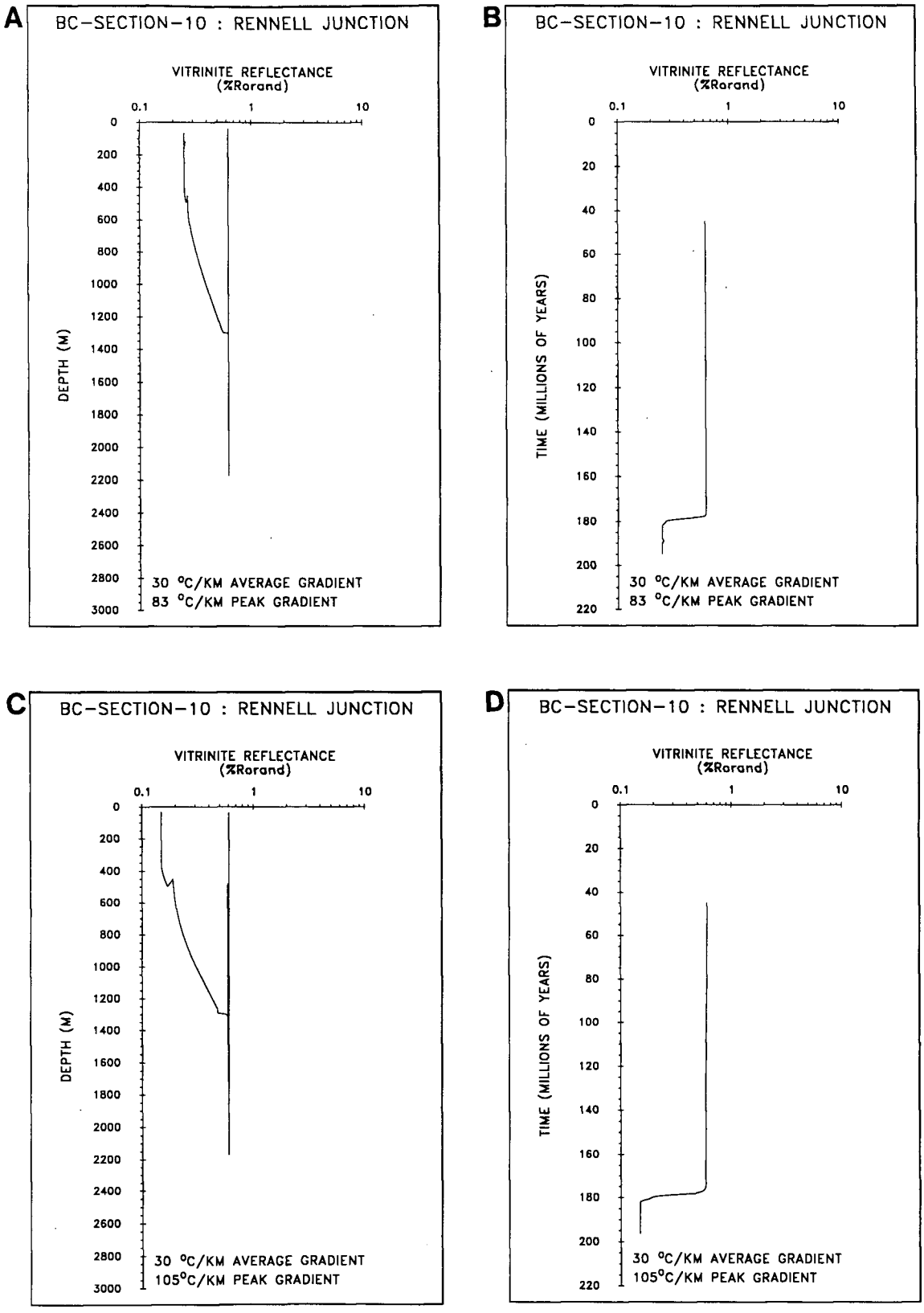

Figure 41. Jurassic Maude Group strata at Rennell Junction (variable geothermal gradient model with 30 ^{o}C/km average gradient): a) maturation history (relative to depth) for the basal strata utilizing a modified Arrhenius model (83 ^{o}C/km peak geothermal gradient); b) maturation history (relative to time) for the basal strata utilizing a modified Arrhenius model (83 ^{o}C/km peak geothermal gradient); c) maturation history (relative to depth) for the basal strata utilizing a modified Lopatin model (105 ^{o}C/km peak geothermal gradient); d) maturation history (relative to time) for the basal strata utilizing a modified Lopatin model (105 ^{o}C/km peak geothermal gradient)

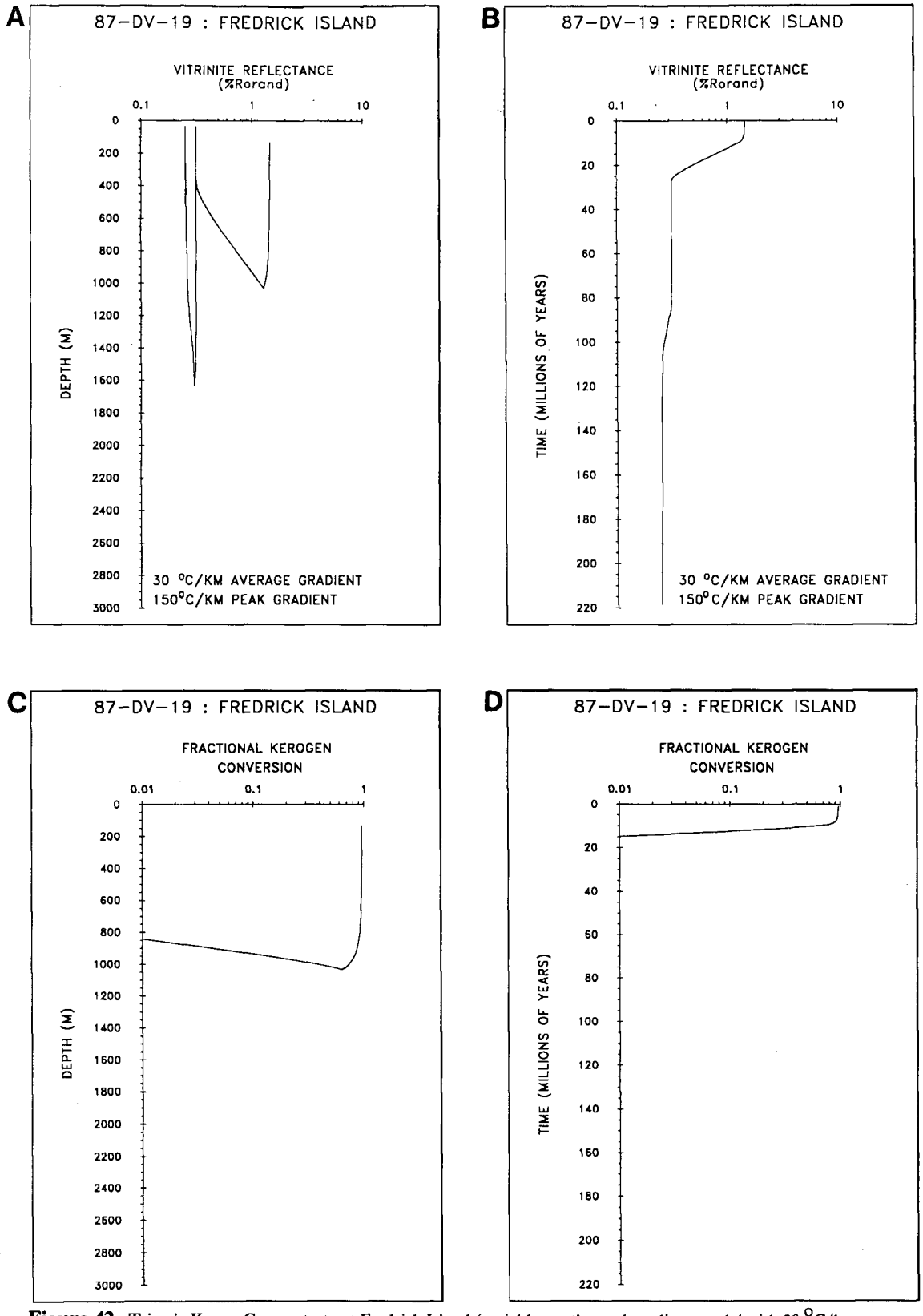

Figure 42. Triassic Kunga Group strata at Fredrick Island (variable geothermal gradient model with 30 ^{o}C/km average gradient): a) maturation history (relative to depth) for the basal strata utilizing a modified Arrhenius model (150 ^{o}C/km peak geothermal gradient); b) maturation history (relative to time) for the basal strata utilizing a modified Arrhenius model (150 ^{o}C/km peak geothermal gradient); c) fractional kerogen conversion (relative to depth) utilizing a modified Arrhenius model (150 ^{o}C/km peak geothermal gradient); d) fractional kerogen conversion (relative to time) utilizing a modified Arrhenius model (150 ^{o}C/km peak geothermal gradient)

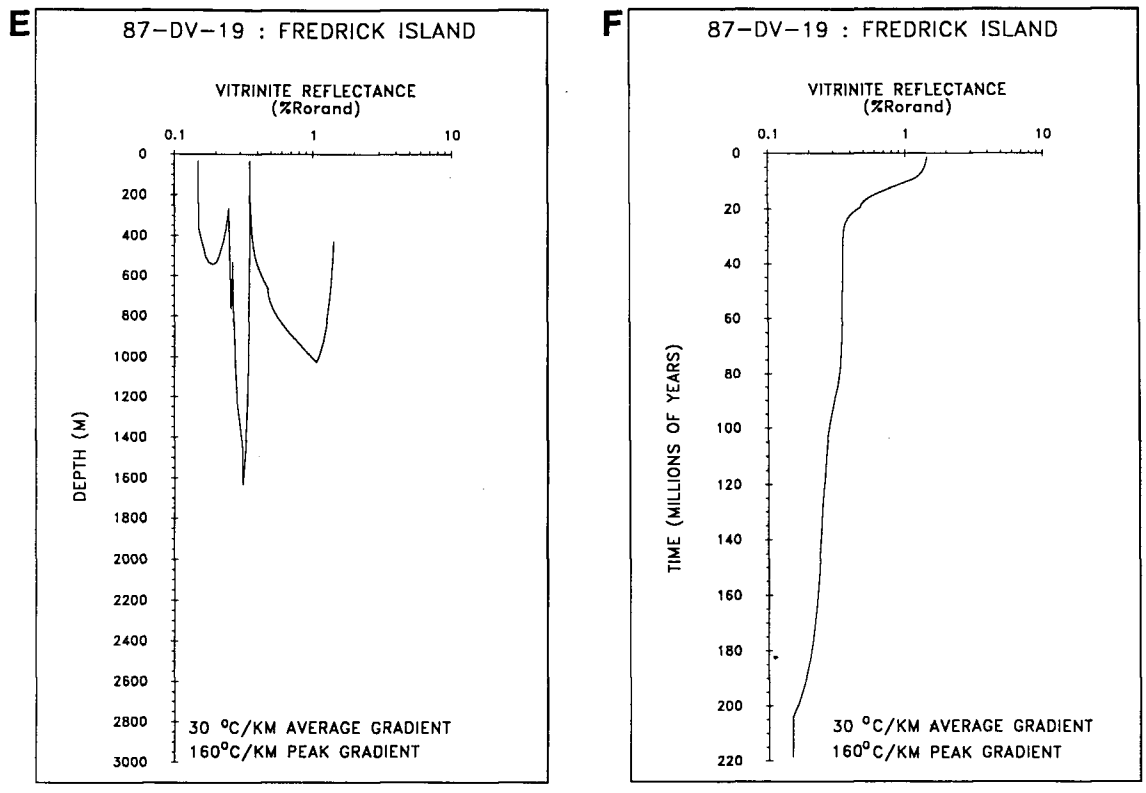

Figure 42. Triassic Kunga Group strata at Fredrick Island (variable geothermal gradient model with 30 ^{o}C/km average gradient): e) maturation history (relative to depth) for the basal strata utilizing a modified Lopatin model (160 ^{o}C/km peak geothermal gradient); f) maturation history (relative to time) for the basal strata utilizing a modified Lopatin model (160 ^{o}C/km peak geothermal gradient)

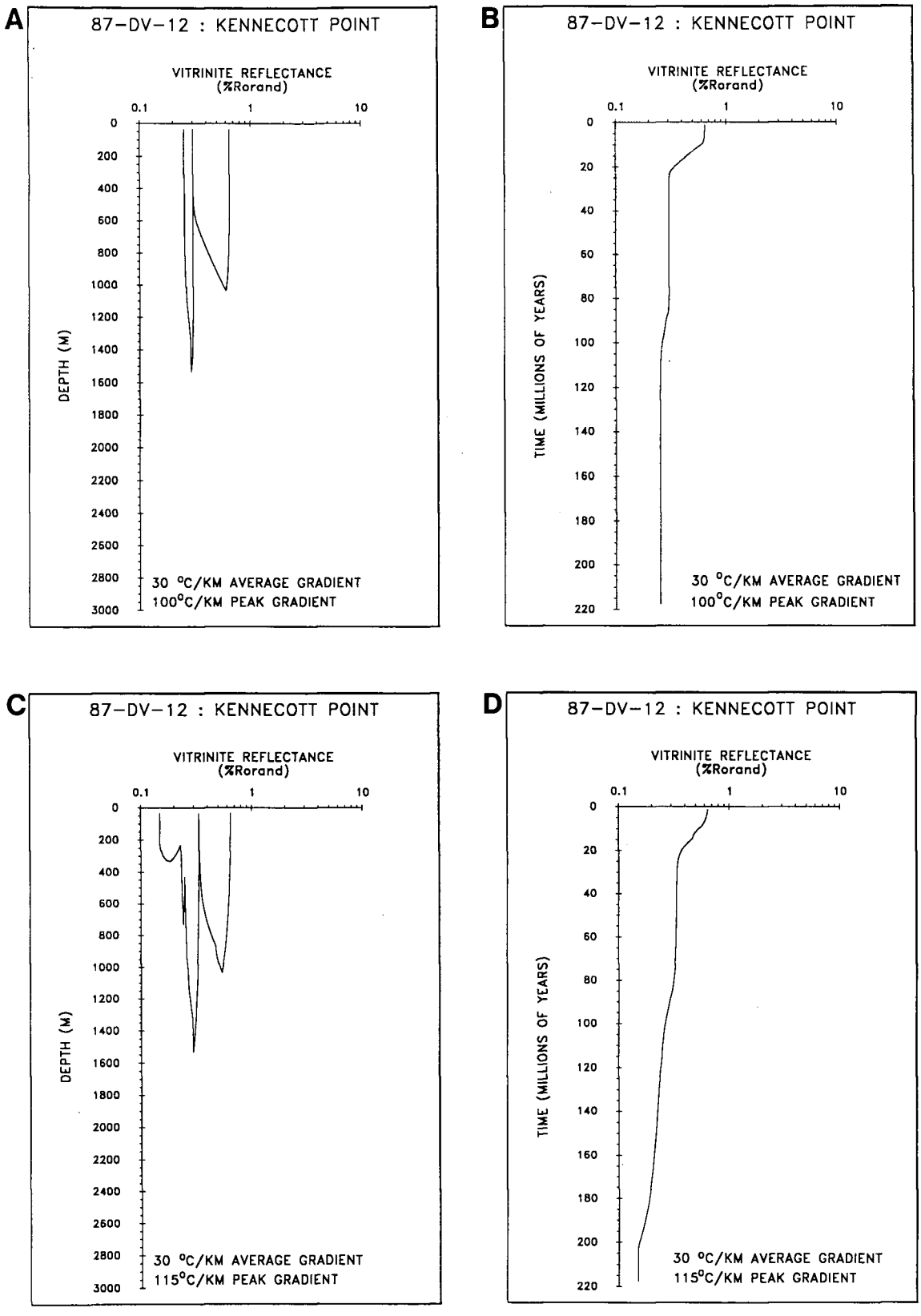

Figure 43. Triassic Kunga Group strata at Kennecott Point (variable geothermal gradient model with 30 ^{o}C/km average gradient): a) maturation history (relative to depth) for the basal strata utilizing a modified Arrhenius model (100 ^{o}C/km peak geothermal gradient); b) maturation history (relative to time) for the basal strata utilizing a modified Arrhenius model (100 ^{o}C/km peak geothermal gradient); c) maturation history (relative to depth) for the basal strata utilizing a modified Lopatin model (115 ^{o}C/km peak geothermal gradient); d) maturation history (relative to time) for the basal strata utilizing a modified Lopatin model (115 ^{o}C/km peak geothermal gradient)

INTERPRETATION OF AREAL MATURATION TRENDS

The paleogeothermal gradients predicted for the Tertiary Skonun Formation are within the average ranges for geothermal gradients (15 ^{o}C/km to 64 ^{o}C/km) reported from back arc basins found in other parts of the world (Watanabe et al., 1977; and Blackwell et al., 1982). Present day heat flow values for the west coast of North America average 60-80 mW/m^2 (Chapman and Rybach, 1985) and recent heat flow measurements from Moresby Island average 50-60 mW/m^2 (geothermal gradients of approximately 18-20 ^{o}C/km; Lewis, pers. comm., 1988) suggesting that onshore heat flow has decreased since Skonun Formation deposition.

If constant paleogeothermal gradients are assumed for Mesozoic strata in the Queen Charlotte Islands, geothermal gradients ranging from 45 ^{o}C/km to 90 ^{o}C/km are required for up to 180 Ma from the Upper Triassic to Middle Eocene (which was predominantly volcanically quiescent). In particular, the Arrhenius model predicts paleogeothermal gradients of 90 ^{o}C/km for Triassic strata at Fredrick Island for 180 Ma between the Norian and the Middle Eocene. However, there is no evidence of igneous activity to generate the predicted high heat flow near Fredrick Island until the Tertiary. Similarly, unusually high paleogeothermal gradients are required during periods of volcanic quiescence to produce the maturation levels measured from Jurassic and Cretaceous strata. Similar results are achieved with constant paleogeothermal gradients for other Triassic strata. Thus, a variable thermal regime with a moderate background geothermal gradients and high peak geothermal gradients more reasonably describes Mesozoic maturation than does a constant thermal regime. If the heat flow was higher during volcanic episodes than assumed in the models used here, less time would be required to achieve the same measured DOM.

The DOM of Lower Jurassic Maude and Yakoun Group strata increases from Rennell Junction to Cumshewa Inlet. Although burial depths are similar at both localities, variable thermal regime modelling predicts higher peak heat flow during the Lower Bajocian at Cumshewa Inlet (97 oC/km) than at Rennell Junction (83 oC/km). The higher paleogeothermal gradient at Cumshewa Inlet is most likely the result of

elevated heat flow from Yakoun Group volcanism or from coeval plutonism on Moresby Island. Furthermore, at Rennell Junction, Yakoun Group sediments (Graham Island and Richardson Bay Formations) were deposited rather than Yakoun andesites (Cameron and Tipper, 1985) suggesting that diminished volcanic activity near Rennell Junction may account for the lower heat flow predicted in central Graham Island.

Jurassic strata younger than the Sinemurian Sandilands Formation were probably not deposited in the Fredrick Island-Kennecott Point area, therefore, Yakoun volcanism was most likely not significant to the thermal maturation of Kunga strata. Heat flow associated with Masset feeder dikes and sills near Fredrick Island and Kennecott Point were the most likely cause of the elevated paleogeothermal gradients predicted by maturation modelling. A higher geothermal gradient predicted for Fredrick Island (relative to Kennecott Point) is probably due to increased heat flow from Masset feeder dikes/sills more proximally located to Fredrick Island.

Timing of Hydrocarbon Generation

The timing of hydrocarbon generation was estimated from numerical modelling (Table 4) using the vitrinite reflectance/time diagrams assuming the oil window is between 0.50 $\%Ro_{rand}$ and 1.35 $\%Ro_{rand}$ (see Part II). Figures 38C, 39C, 40C, 42C, and 38D, 39D, 40D, 42D illustrate the degree of converted kerogen to petroleum with respect to depth and time for each section (Espitalie et al., 1975) plotted with respect to time and depth. Diagrams for immature strata which have not generated significant amounts of hydrocarbons are not presented.

The Tertiary Skonun Formation is everywhere immature with respect to oil generation except at west (Port Louis well) and northeast Graham Island (basal strata of the Tow Hill well). Strata from west Graham Island (Port Louis well) are predicted to have entered the oil window in the Late Miocene (7.6 Ma) and are currently in the oil window (Table 4). The models predicts that strata from northeast Graham Island (basal strata of the Tow Hill well) entered the oil window in the Late Miocene (5.1

TABLE 4

CONSTANT GEOTHERMAL GRADIENT MODEL

WELL (SECTION) NAME (LOCALITIES)	TIMING OF ENTERING AND EXITING OIL WINDOW (MA) (ARRHENIUS MODEL)	TIMING OF ENTERING AND EXITING OIL WINDOW (MA) (LOPATIN MODEL)
TERTIARY STRATA		
SKONUN FORMATION (EXPLORATION WELLS)		
CAPE BALL	*,*	*,*
GOLD CREEK	*,*	*,*
NADU RIVER	*,*	*,*
PORT LOUIS	7.6 Ma,*	6.8 Ma, 1.7 Ma
TLELL	*,*	*,*
TOW HILL	5.1 Ma,*	4.3 Ma,*
CRETACEOUS STRATA		
HAIDA FORMATION (OUTCROP)		
NORTH LAUDER POINT	88 Ma,*	88 Ma,*
ONWARD POINT	87 Ma,*	87 Ma,*
JURASSIC STRATA		
MAUDE AND YAKOUN GROUPS (OUTCROP)		
CUMSHEWA INLET	169 Ma,*	159 Ma,*
RENNELL JUNCTION	88 Ma,*	92 Ma,*
TRIASSIC STRATA		
KUNGA GROUP (OUTCROP)		
FREDRICK ISLAND	102 Ma, 83 Ma	102 Ma, 85 Ma
KENNECOTT POINT	90 Ma,*	87 Ma,*

VARIABLE GEOTHERMAL GRADIENT MODEL (30 ^{o}C/KM BACKGROUND PALEOGEOTHERMAL GRADIENT)

WELL (SECTION) NAME	TIMING OF ENTERING AND EXITING OIL WINDOW (MA) (ARRHENIUS MODEL)	TIMING OF ENTERING AND EXITING OIL WINDOW (MA) (LOPATIN MODEL)
CRETACEOUS STRATA		
HAIDA FORMATION (OUTCROP)		
NORTH LAUDER POINT	18 Ma,*	15 Ma,*
ONWARD POINT	18 Ma,*	16 Ma,*
JURASSIC STRATA		
MAUDE AND YAKOUN GROUPS (OUTCROP)		
CUMSHEWA INLET	178 Ma,*	178 Ma,*
RENNELL JUNCTION	178 Ma,*	178 Ma,*
TRIASSIC STRATA		
KUNGA GROUP (OUTCROP)		
FREDRICK ISLAND	20 Ma, 10 Ma	17 Ma, 7 Ma
KENNECOTT POINT	13 Ma,*	12 Ma,*

Ma) and never exited the oil window. The generation of hydrocarbons at west and northeast Graham Island (Port Louis and Tow Hill wells) is probably the result of higher paleogeothermal gradients and deeper burial than adjacent strata. Strata from west Graham Island (Port Louis well) are intercalated with Masset volcanics and may be of limited lateral extent suggesting that the area has questionable potential to generate exploitable amounts of liquid hydrocarbons. Oil staining occurs in a thin interval of strata at northeast Graham Island in the Tow Hill well suggesting hydrocarbons may have been generated from Tertiary Skonun Formation.

Cretaceous strata at north Lauder Point and Onward Point are presently within the oil window. The Arrhenius model predicts that strata at north Lauder Point and Onward Point entered the oil window during the Early Miocene (18 Ma).

Lower Jurassic strata at Cumshewa Inlet and Rennell Junction are mature with respect to hydrocarbon generation and are presently within the oil window. The strata entered the oil window during the Lower Bajocian (178 Ma).

Triassic strata from Fredrick Island entered and exited the oil window during the Early and Late Miocene (20 Ma and 10 Ma respectively). The strata at Kennecott Point are mature and are presently within the oil window. Lower predicted paleogeothermal gradients suggest that the strata entered the oil window during the Middle Miocene (13 Ma).

Hydrocarbon Generation Relative to Tectonic Elements

Major structural deformation in the Queen Charlotte Islands occurred primarily in two episodes: syn- and post- Yakoun volcanism in the Middle and Late Jurassic; and between deposition of the Honna and the Masset Formations in the Late Cretaceous and Early Tertiary. Any hydrocarbons generated from the Skonun Formation postdates the formation of Mesozoic reservoir structures. Given the correct basin

geometry and migration paths, Tertiary oil may be trapped in Mesozoic structures. Skonun sourced hydrocarbons may also be pooled in stratigraphic or growth fault traps onshore or in Hecate Strait.

Variable paleogeothermal gradient modelling suggests that Cretaceous strata from Graham Island and Triassic strata from northwest Graham Island generated hydrocarbons from the Early Miocene to the present and were available for migration to potential Jurassic and Cretaceous-Tertiary aged structural traps. Jurassic sourced hydrocarbons from central Graham Island and northern Moresby Island were generated from the Bajocian to the present and were available for migration to potential Jurassic and Cretaceous-Tertiary aged structural traps.

DISCUSSION

Organic maturation of strata on the Queen Charlotte Islands is primarily controlled by high heat flow adjacent plutons and dike/sill swarms on Moresby Island and by 'normal' subsidence on Graham Island. In particular, Mesozoic strata on Moresby Island are overmature as a result of pluton emplacement during the Middle-Late Jurassic and possibly the Oligocene whereas strata on Graham Island which have not been effected by plutonism are immature to mature (Fig. 44). Large scale plutonic activity in Hecate Strait and Dixon Entrance, however, is not apparent suggesting that Mesozoic and Tertiary aged potential source strata in the offshore are possibly mature and may have sourced and pooled or reservoired hydrocarbons. Commercial hydrocarbon accumulations, therefore, more likely occur offshore in Hecate Strait and Dixon Entrance.

The Queen Charlotte Islands have been part of an island arc system since the Sinemurian (Sutherland Brown, 1968; Cameron and Tipper, 1985). During the geologic history of volcanic arcs, average heat flow (and geothermal gradient) can vary significantly from below average up to four times average heat flow depending upon the proximity to the subduction zone (Hasabe et al., 1970; Watanabe et al., 1977; Blackwell et al., 1982). It is therefore likely that the Queen Charlotte Islands have experienced substantial fluctuations in heat flow and thus geothermal gradient in the Mesozoic and Tertiary. Lateral variations in

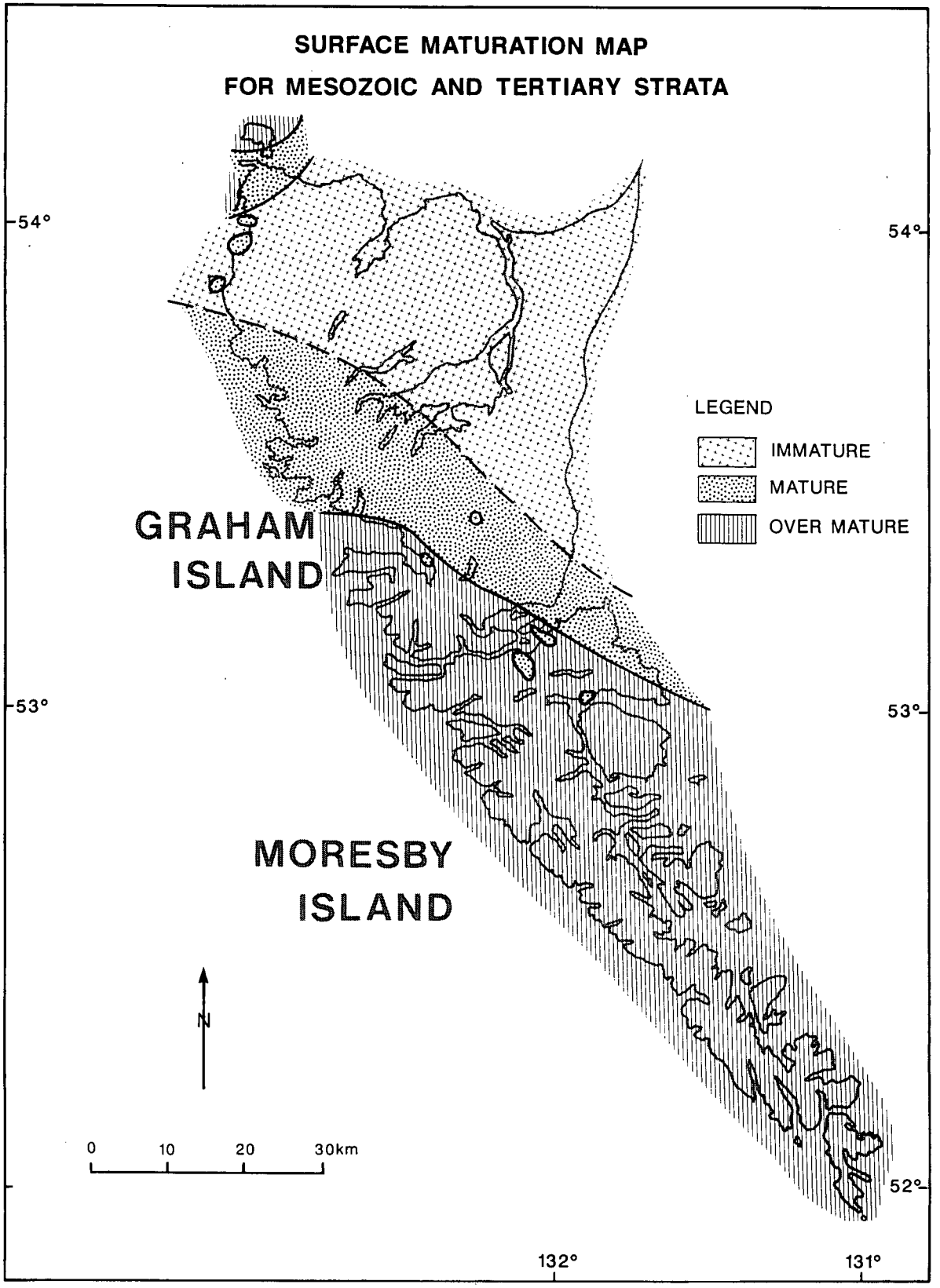

Figure 44. Surface maturation trends for Mesozoic and Tertiary strata derived from vitrinite reflectance data (%Ro_{rand}). Oil window is between 0.50 %Ro_{rand} and 1.35 %Ro_{rand}

the DOM of various strata on the Queen Charlotte Islands attest to the variable heat flow associated with arc volcanism and plutonism. The Triassic Kunga Group strata on Moresby Island have been subjected to high heat flow are evident from DOM values up to 5.80 $\%Ro_{rand}$. The Sinemurian Sandilands Formation and the Albian Haida Formation best illustrate the north/south regional variations in organic maturity where the DOM increases substantially from north (0.45 $\%Ro_{rand}$) to south (4.73 $\%Ro_{rand}$).

All strata south of Cumshewa Inlet are overmature as a result of high heat flow associated with pluton emplacement on Moresby Island during the Jurassic and Tertiary. The heat flow was not uniform across Moresby Island. In particular, The DOM for the grey limestone and black limestone members of the Kunga Group increases from west to east with decreasing distance from the Late Jurassic Burnaby Island Plutonic Suite (BIPS; ages range from 156 $\pm$ 5 Ma to 142 $\pm$ 19 Ma) suggesting that the emplacement of the BIPS was the dominant thermal event on Moresby Island. Hydrothermal activity associated with the BIPS has resulted in sericite and endoskarn alteration (with associated mineralization) and higher levels of organic maturation occur proximal to the Burnaby Island Plutonic Suite than to the adjacent San Christoval Plutonic Suite (SCPS). The highest levels of organic maturation, however, are observed in Carpenter Bay near dike/sill swarms associated with the Carpenter Bay Plutonic Suite (CBPS). Anderson (pers. comm., 1988) suggests that the CBPS is Oligocene in age and possibly related to Masset volcanism. Although the lateral extent of the CBPS is limited, organic maturation resulting from Tertiary plutonism and related igneous intrusives appears to overprint earlier maturation events associated with Middle-Late Jurassic plutonism. More detailed sample collection and analysis is required to determine if high heat flow coeval with Masset volcanism is a contributing factor to the regional organic maturation of Moresby Island and Hecate Strait.

Mesozoic strata in the Cumshewa Inlet and Skidegate Inlet areas are mature to overmature with Jurassic and Cretaceous strata generally having similar DOM values. The high DOM values may have resulted from hydrothermal activity related to heat flow from distant Jurassic-Tertiary plutonism on Moresby Island or Rennell Sound-Shields Bay.

Most of the measured strata (Jurassic Maude, Yakoun, and Moresby Groups) from central Graham Island are mature with some local marginally immature strata. Included in this area are the potential source rocks of the Sandilands and Ghost Creek Formations (see Part II). The lowest measured maturation gradients and modelled paleogeothermal gradients from the Queen Charlotte Islands occur in central Graham Island where maturation tends to increase from east to west (opposite that of Moresby Island) suggesting that thermal effects from Jurassic and Tertiary volcanism on Moresby Island were not pronounced in central Graham Island. Instead, heat flow associated with plutonism near Rennell Sound-Shields Bay may have been the dominant thermal event effected organic maturation in central Graham Island. Deposition of Yakoun and Moresby Group sediments and the lack of equivalent volcanic strata in central Graham Island suggests that Jurassic volcanism may never have been extensive in the area (Cameron and Tipper, 1985). The source potential for central Graham Island is uncertain in that the thermal regime in this area and the lateral extent of the source rocks are poorly known due to the limited outcrop distribution.

Organic maturation in northwest Graham Island ranges from immature to overmature with most of the strata ranging from marginally mature to mature. Overmature strata are most likely the result of high heat flow from plutonic activity on Langara Island. High heat flow from Masset igneous intrusives near Fredrick Island has resulted in the local overmaturation of potential Triassic source strata of the Kunga Group.

SUMMARY AND CONCLUSIONS

1. Upper Triassic to Sinemurian Kunga Group strata on northwest Graham Island are generally marginally mature (0.45 $\%Ro_{rand}$) and the major component of the maturation is predicted to have occurred during the Tertiary whereas the major component of the maturation of the Sandilands Formation on central Graham Island and Moresby Island is considered to be generally syn- or post- tectonic (Late Jurassic-Cretaceous). Sandilands Formation strata are marginally mature (0.48 $\%Ro_{rand}$) on central Graham Island and overmature in Skidegate Inlet (1.35 to 1.75 $\%Ro_{rand}$). All Kunga Group strata on

Moresby Island are overmature (2.40 to 5.80 $\%Ro_{rand}$) as a result of high heat flow associated with Middle-Late Jurassic plutonism and the DOM increases from west to east with increasing proximity to the Burnaby Island Plutonic Suite. The DOM near Carpenter Bay increases to 8.31 $\%Ro_{rand}$ as a result of Oligocene plutonism which has overprinted maturation events associated with Middle-Late Jurassic plutonism (San Christoval and Burnaby Island Plutonic Suites).

2. Jurassic strata (Maude, Yakoun, and Moresby Groups) from central Graham Island are marginally mature to mature and the DOM increase from east to west with decreasing distance from plutonic complexes near Rennell Sound-Shields Bay. The level of organic maturation increase from central Graham Island (0.43 $\%Ro_{rand}$) to northern Moresby Island (1.58 $\%Ro_{rand}$). The major component of the maturation is considered to be generally syn- or post- tectonic (Late Jurassic-Cretaceous).

3. The DOM of Cretaceous strata on Moresby Island increases from north (1.53-2.43 $\%Ro_{max}$) to central (2.31-4.78 $\%Ro_{rand}$) Moresby Island. Maturation values for Cretaceous strata on Graham Island increase from 0.33 $\%Ro_{rand}$ in the northwest to 2.21 $\%Ro_{rand}$ in Skidegate Inlet. The major component of the maturation is generally considered to be Cretaceous and Tertiary.

4. Tertiary strata are generally immature with the exception of the mature succession on west Graham Island (Port Louis well) and northeast Graham Island (basal strata of the Tow Hill well). Regional organic maturation values for the basal strata of the Skonun Formation increase from east (0.31 $\%Ro_{rand}$ at Cape Ball) to west (1.33 $\%Ro_{rand}$ at Port Louis). The major component of the maturation is considered to have occurred during the Late Tertiary.

5. Time-temperature modelling suggests that the measured maturation gradients would require constant paleogeothermal gradients ranging from 45 to 90 $^{o}C/km$ (Arrhenius model) for up to 180 million years. Variable geothermal gradient modelling (assuming a background paleogeothermal gradient of 30 $^{o}C/km$), on the other hand, predicts high heat flow with peak geothermal gradients ranging from 83 $^{o}C/km$ on central Graham Island to 150 $^{o}C/km$ on Fredrick Island during Yakoun (183-178 Ma) and Masset

volcanism (35-10 Ma). Higher peak temperatures than those predicted in modelling require shorter heating times to attain the measured level of organic maturation.

6. The thickness of eroded strata has been calculated from maturation gradients (assuming 0.15 $\%Ro_{rand}$ as zero maturation level and constant maturation gradients). The calculated thickness of eroded strata for the Tertiary Skonun Formation ranges from 375 m at east Graham Island (Tlell well) to 1685 m at west Graham Island (Port Louis well). Twice as much strata has been eroded from Onward Point (1500 m) than north Lauder Point (745 m). Similar amounts of strata have been removed from Jurassic sections at Cumshewa Inlet (1985 m) and Rennell Junction (1725 m). 1040 m of strata have been eroded from Fredrick Island and 735 m of strata have been eroded from Kennecott Point.

7. Similar results are predicted for modified Arrhenius and Lopatin time-temperature modelling. Generally, the Arrhenius model predicts lower paleogeothermal gradients than the Lopatin model as a result of rapid heating of the strata or too high an activation energy (E=218 kJ/mol) utilized here by the Arrhenius model (relative to the Lopatin model). Variable geothermal time-temperature modelling suggests that Tertiary strata at west Graham Island (Port Louis) and northeast Graham Island (Tow Hill well) entered the oil window during the Late Miocene and are still within the oil window. Tertiary strata on east Graham Island are immature and never entered the oil window as a result of shallow burial depths and low paleogeothermal gradients ($<32\ ^{o}C/km$) than west Graham Island. Cretaceous strata on northwest Graham Island and Skidegate Inlet entered the oil window during the Early Miocene and are still within the oil window. Jurassic strata on central Graham Island and north Moresby Island entered the oil window during the Bajocian and are still within the oil window as a result of shallow burial depths. Triassic strata at Fredrick Island entered the oil window during the Early Miocene and exited during the Late Miocene whereas strata at Kennecott Point entered the oil window later during the Middle Miocene and are still within the oil window as a result of lower paleogeothermal gradients.

REFERENCES

Anderson, R.G. 1988
Jurassic and Cretaceous-Tertiary plutonic rocks on the Queen Charlotte Islands, British Columbia; in Current Research, Part E, Geological Survey of Canada, Paper 88-1E, p. 213-216.

Armstrong, R.L. 1988
Mesozoic and Early Cenozoic magmatic evolution of the Canadian Cordillera: Special Paper 218, Geological Society of America, p. 55-91

Blackwell, D.D., Bowen, R.G., Hull, D.A., Riccio, J., and Steele, J.L. 1982
Heat flow, arc volcanism, and subduction in northern Oregon; Journal of Geophysical Research, v. 87, no. B10, p. 8735-8754

Bustin, R.M. 1986
Organic maturity of Late Cretaceous and Tertiary coal measures, Canadian Arctic Archipelago; International Journal of Coal Geology, v. 6, p. 71-106.

Bustin, R.M., Cameron, A.R., Grieve, D.A., and Kalkreuth, W.D. 1983
Coal Petrology, its principle, methods, and applications; Geological Association of Canada, Short Course Notes, v. 3., pp. 273

Bostick, N.H. 1973
Time as a factor in thermal metamorphism of phytoclasts; Congres International de Stratigraphie et de Geologie du Carboniferie Septieme, Krefeld. August 23-28, 1971. Compte Readu, 2, Illinois State Geologic Survey reprint series 1974-H, p. 183-193.

Cameron, B.E.B. 1987
Significance of Lower Jurassic hydrocarbon source rocks in the Cumshewa Inlet area, Queen Charlotte Islands, British Columbia; in Current Research, Part A, Geological Survey of Canada, Paper 87-1A, p. 925-928.

Cameron, B.E.B. and Tipper, H.W. 1985
Jurassic stratigraphy of the Queen Charlotte Islands, British Columbia; Geological Survey of Canada, Bulletin, v. 365, 49 p.

Cameron, B.E.B. and Hamilton, T.S. 1988
Contributions to the stratigraphy and tectonics of the Queen Charlotte Basin, British Columbia; in Current Research, Part E, Geological Survey of Canada, Paper 88-1E, p. 221-227.

Chapman, D.S., and Rybach, L. 1985
Heat flow anomalies and their interpretation; Journal of Geodynamics, v. 4, p. 3-37.

Coney, P.J., Jones, D.L., and Monger, J.W.H. 1980
Cordilleran suspect terranes; Nature, v. 288, p. 329-333.

Davis, A. 1978
The reflectance of coal; in Analytical Methods for Coal and Coal Particles, C. Karr, ed., London, Academic Press, 1, p. 27-28.

Dow, W.G. 1977
Kerogen studies and geologic interpretations; Journal of Geochemical Exploration, 7, p. 79-99.

England, T.D.J. and Bustin, R.M. 1986
Thermal maturation of the western Canadian sedimentary basin south of the Red Deer River: 1) Alberta Plains; Bulletin of Canadian Petroleum Geology, v. 34, p. 71-90.

Espitalie, J., Deroo, G., Marquis, F. 1985
Rock-Eval pyrolysis and its applications; Institut Francais du Petrole, reprint 27299, 132 pp.

Fogarassy, J.A.S. and Barnes, W.C. 1988
Stratigraphy, diagenesis and petroleum reservoir potential of the mid- to Upper Cretaceous Haida and Honna formations of the Queen Charlotte Islands, British Columbia; in Current Research, Part E, Geological Survey of Canada, Paper 88-1E, p. 265-268.

Galloway, W.E. 1974
Deposition and diagenetic alteration of sandstone in northeast Pacific arc-related basins: implications for greywacke genesis; Geological Society of America Bulletin, v. 85, p. 379-390.

Hasabe, K., Fujii, N., and Uyeda, S. 1970
Thermal processes under island arcs; Tectonophysics, 10, p. 335-355.

Haggart, J.W. 1987
On the age of the Queen Charlotte Group of British Columbia; Canadian Journal of Earth Sciences, v. 24, p. 2470-2476.

Hamilton, T. 1985
Volcanics of the Cenozoic Masset Formation: implications for geological and tectonic evolution of the Queen Charlotte Islands, British Columbia, Canada; Geological Society of America, Cordilleran Section Annual Meeting, Program with Abstracts, Vancouver, British Columbia, May 8-10, p. 359

Hickson, C.J. 1988
Structure and stratigraphy of the Masset Formation, Queen Charlotte Islands, British Columbia; *in* Current Research, Part E, Geological Survey of Canada, Paper 88-1E, p. 269-274.

Hillhouse, J.W. 1977
Paleomagnetism of the Triassic Nicolai Greenstone, McCarthy Quadrangle, Alaska; Canadian Journal of Earth Sciences, 14, p. 2578-2592.

Irving, E., Woodsworth,G.J., Wynne, P.J., and Morrison, A. 1985
Paleomagnetic evidence for displacement from the south of the Coast Plutonic Complex, British Columbia; Canadian Journal of Earth Sciences, 22, p. 584-598.

Jones, D.L., Silberling, N.J., and Hillhouse, J. 1977
Wrangellia-A displaced terrane in northwestern North America; Canadian Journal of Earth Sciences, 14, p. 2565-2577.

Karweil, J. 1955
The metamorphism of coals from the standpoint of physical chemistry; Zeitschrift der Geologischen gesellschaft, 107, p. 132-139.

Lopatin, N.V. 1971
Temperature and geologic time as factors in coalification; Izvestiya Akademii Nauk USSR, Seriya Geologicheskaya, 3, p. 95-106.

Martin, H.A. and Rouse, G.E. 1966
palynology of Late Tertiary sediments from the Queen Charlotte Islands, British Columbia; Canadian Journal of Botony, 44, p. 171-208.

Monger, J.W.H., Souther, J.G., and Gabrielse, H. 1972
Evolution of the Canadian Cordillera: a plate tectonic model; American Journal of Sciences, 272, p. 577-602.

Muller, J.E., Northcote, K.E., and Carlisle, D. 1974
Geology and mineral deposits of Alert Bay-Cape Scott map-area, Vancouver Island, British Columbia. Geological Survey of Canada, Paper 74-8. 77 pp.

Muller, J.E. 1977
Evolution of the Pacific Margin, Vancouver Island and adjacent areas; Canadian Journal of Earth Sciences, 14, p. 2062-2085.

Souther, J.G. 1977
Volcanism and tectonic environments in the Canadian Cordillera-a second look. *in* Volcanic regimes in Canada. *ed.* W.R.A. Baragar, L.C. Coleman, and M.Hall. Geological Association of Canada, Special Paper 16, p. 3-24.

Souther, J.G. 1988
Implications for hydrocarbon exploration of dyke emplacement in the Queen Charlotte Islands, British Columbia; *in* Current Research, Part E, Geological Survey of Canada, Paper 88-1E, p. 241-245.

Sutherland Brown, A. 1968
Geology of the Queen Charlotte Islands; British Columbia Department of Mines and Petroleum Resources Bulletin 54, 226 pp.

Tissot, B.P. and Espitalie. J. 1975
L'evolution thermique de la matiere organique des sediments: Applications d'une simulation mathematique. Rev. Inst. Fr. Pet. 30, p. 743-777.

Tissot, B.P. and Welte, D.H. 1984
Petroleum Formation and Occurrence. Springer-Verlag, Berlin, 699 pp.

Watanabe, T., Langseth, M.G., and Anderson, R.N. 1977
Heat flow in back-arc basins of the western Pacific; *in* Island Arcs, Deep Sea Trenches, and Back-Arc Basins, Maurice Ewing Ser., vol. 1, *ed.* M. Talwani and W.C. Pitman III, p. 137-161, AGU, Washington, D.C., 1977.

Waples, D.W. 1980
Time and temperature in petroleum formation with application of Lopatin's method to petroleum exploration; American Association of Petroleum Geologists, Bulletin 64, p. 916-926.

Wood, D.A. 1988
Relationships between thermal maturity indices calculated using Arrhenius equation and Lopatin method: implications for petroleum exploration; American Association of Petroleum Geologists, vol. 72, #2, p. 115-134.

Woodsworth, G.J. 1988
Karmutsen Formation and the east boundary of Wrangellia, Queen Charlotte Basin, British Columbia; *in* Current Research, Part E, Geological Survey of Canada, Paper 88-1E, p. 209-212.

Yole and Irving, 1980
Displacement of Vancouver Island: paleomagnetic evidence from the Karmutsen Formation; Canadian Journal of Earth Sciences, 17 p. 1210-1228.

PART II

SOURCE ROCK POTENTIAL OF MESOZOIC AND TERTIARY STRATA OF THE QUEEN CHARLOTTE ISLANDS

ABSTRACT

The hydrocarbon source potential for Mesozoic and Tertiary strata in the Queen Charlotte Islands has been determined by Rock-Eval pyrolysis. Mean total organic carbon (TOC) contents are generally low to moderate (0.1 to 3.6 %) and some organic-rich intervals occur throughout the succession. Horizons with high TOC values up to 10.3 % occur in the Upper Triassic black limestone member of the Kunga Group and 11.2 % in the Lower Jurassic Whiteaves Formation. Generally, Mesozoic and Tertiary strata contain Type III organic matter except for the Upper Triassic-Lower Jurassic Kunga Group and the Lower Jurassic Ghost Creek Formation which contain oil and gas prone Type II and significant amounts of oil prone Type I organic matter.

Lateral variations in TOC and the quality of organic matter (QOM) for Mesozoic strata on Moresby Island are primarily related to the level of organic maturation. High heat flow associated with plutonism on Moresby Island has resulted in generally poor hydrocarbon source potential due to high levels of maturation of the strata. Equivalent Triassic and Jurassic strata on Graham Island are generally immature to mature and have fair to good hydrocarbon source potential.

Hydrocarbon source potential of Cretaceous and Tertiary strata on Graham Island is controlled primarily by the level of organic maturation and to a lesser extent depositional patterns. Cretaceous strata from Moresby Island are generally overmature and have poor source potential whereas equivalent strata from Graham Island are immature to overmature and have fair to moderate gas source potential. The Cretaceous Haida and Honna Formations generally contain terrestrially derived Type III organic matter with poor to fair gas source potential. The Skidegate Formation contains a mixture of Types II and III organic matter and has fair gas generative potential. The Haida Formation contains only terrestrially derived Type III organic matter whereas the Skidegate contains less Type III organic matter and more Type II organic matter. The Tertiary Skonun Formation contains abundant, generally immature coal and lignite with some gas source potential. Mature resinite horizons containing hydrogen-rich organic matter have fair

to good oil and gas source potential. Siltstone and shale facies of the Skonun Formation contain moderate amounts of Type II organic matter and have good hydrocarbon source potential.

INTRODUCTION

The Queen Charlotte Islands contain a thick sedimentary sequence which includes potential source and reservoir strata. The documented occurrence of numerous oil seeps, oil shales, and carbonaceous black shales suggest that hydrocarbons have been generated in the past and may have accumulated in commercial quantities (Cameron and Tipper, 1985; Cameron, 1987; Bustin and Macauley, 1988; Snowdon et al., 1988). To date, the lateral and vertical variations in source rock quality for Mesozoic and Tertiary strata in the Queen Charlotte Islands have not been documented. The purpose of this study is to establish the source rock potential of sedimentary strata on the Queen Charlotte Islands. Bustin and Macauley (1988) have previously documented the DOM and source rock quality for Lower Jurassic oil shales found in central Graham Island and Skidegate Inlet and Snowdon et al. (1988) have performed preliminary organic geochemical analysis on oil seeps from Tertiary strata. The present study has been expanded from the initial work of Bustin and Macauley (1988) to include the entire stratigraphic sequence (Mesozoic to Tertiary) for all of the Queen Charlotte Islands region. Rock-Eval pyrolysis in conjunction with petrologic and organic maturation data are used here to identify and asses potential source strata and delineate their stratigraphic and areal extent.

Microscopic and geochemical analysis of organic matter are an important part of petroleum exploration in assessing the hydrocarbon source potential of sedimentary strata. Geochemical data from Rock-Eval pyrolysis (Espitalie et al., 1977) can be used to establish the quantity, type, and thermal maturity of organic matter in sedimentary rocks (Tissot and Welte, 1984). Combined with organic facies and thermal maturity data, Rock-Eval analysis can be used to identify the lateral and vertical extent of potential source strata.

METHODS

Sample Preparation

One thousand four hundred and sixty outcrop and well samples were analyzed by Rock-Eval pyrolysis (Espitalie et al., 1977; Peters, 1986) and organic petrographic techniques (Bustin et al., 1985). Whole rock samples were crushed with ring and centrifugal grinders to approximately -60 mesh particle size. Coal and lignite samples were crushed and sieved to between -50 and -200 mesh particle size to eliminate ultra-fine particles which adversely effect pyrolysis results. The crushed whole rock samples were split for both Rock-Eval pyrolysis (80 to 100 mg) and vitrinite reflectance analyses. Coal and lignite samples weighing between 5 and 30 mg were layered in crushed, pure quartz prior to Rock-Eval pyrolysis to prevent carbon caking of the Rock-Eval pyrolysis instrument.

Measured Parameters

Rock-Eval pyrolysis provides several measurements to characterize potential source rocks. The S1 peak (mg HC/g rock) represents hydrocarbons distilled from the whole rock (2 minutes at 300 ^{O}C). The S2 peak (mg HC/g rock) represents hydrocarbons pyrolyzed from kerogen at temperatures between 300 ^{O}C and 600 ^{O}C (Espitalie et al., 1977). The S3 peak is a measure of the volatilized carbon dioxide between temperatures of 300 ^{O}C and 390 ^{O}C (mg HC/g rock). The total organic carbon content (TOC) is determined by oxidizing the residual organic matter in air at 600 ^{O}C and summed with S1, S2, and S3 peaks (Espitalie et al., 1977). Outcrop samples are commonly depleted in S1 and S2 values as a result of oxidation of the organic matter. Similarly, oxidation from erosional events near unconformities can result in S1 and S2 depletion.

The temperature of maximum S2 hydrocarbon generation (T_{max}) reflects the degree of organic maturation (Espitalie et al., 1977). The oil birth line occurs at a T_{max} value between 430-435 ^{O}C for Types II and III organic matter. The oil death line occurs at a T_{max} value of 450 ^{O}C for Type II organic matter

and at 465 ^{o}C for Type III organic matter (Espitalie et al., 1977). Type I organic matter has T_{max} values ranging from 460 ^{o}C to 470 ^{o}C and generally displays a poor correlation between organic maturity and T_{max} (Link, 1988).

Calculated Parameters

In addition to the aforementioned measured Rock-Eval parameters, additional parameters calculated from the S1, S2, S3, and TOC values can be used to determine the nature and quality of potential source rocks. The production index (PI) is calculated as the ratio S1/(S1+S2) which is a measure of thermal maturity. PI values between 0.1 and 0.4 define the oil window (Peters, 1986). With increasing hydrocarbon generation, PI values increase to 1.0 marking the exhaustion of the hydrocarbon generative potential of the source kerogen. Anomalously high PI values indicate hydrocarbon accumulation and anomalously low PI values indicate hydrocarbon depletion (Espitalie et al., 1985; Peters, 1986). The hydrogen index (HI), defined as S2/TOC, and the oxygen index (OI), defined as S3/TOC, are used to classify organic matter with a hydrogen index/oxygen index (HI/OI) diagram as described by Espitalie et al. (1977). HI values > 600 mg HC/g C_{org} suggests oil prone Type I organic matter, HI values between 300 and 600 mg HC/g C_{org} suggests oil and gas prone Type II organic matter, and HI values < 300 mg HC/g C_{org} suggests gas prone Type III organic matter, assuming a DOM equivalent to 0.6 %Ro (Espitalie et al., 1977).

The quality of organic matter (QOM), defined as the ratio (S1+S2)/TOC, is used to determine the type of organic matter and to measure thermal maturity. QOM values vary with the degree of thermal maturation, the type of organic matter, and migration effects of hydrocarbons (Espitalie et al., 1985). High QOM ratios suggest immature to mature hydrogen-rich organic matter. Variations in QOM values which cannot be attributed to differences in the level of thermal maturity are considered to be the result of hydrocarbon migration.

RESULTS

In this study, lateral and vertical trends in the degree of organic maturation (DOM) and organic matter richness and type were examined to assess the regional hydrocarbon source potential for individual units. Here, average values are reported for interval horizons (group, formation, or informal member) rather than for discreet samples.

Source rock data from Rock-Eval pyrolysis is summarized in Table 1 (see Part I). Rock-Eval data are also presented for some formations as TOC histograms (Figure 45), hydrogen index versus T_{max} diagrams (Figure 46), hydrogen index versus oxygen index diagrams (Figure 47), and Rock-Eval logs for the onshore Tertiary wells (Figures 48-53). Lateral variations in TOC (Figures 54-69) and QOM (Figures 70-85) are plotted by group, formation, or member. T_{max} versus vitrinite reflectance diagrams are in Appendix B.

Source rocks are strata which are capable of generating migratable hydrocarbons (Conford, 1984). The hydrocarbon generative potential is primarily controlled by the volume, richness, and thermal maturity of the organic matter within the strata (Dow, 1977; Espitalie et al., 1977; Durand, 1980; Conford, 1984; Tissot and Welte, 1984; Espitalie et al., 1985). The level of organic maturity was determined in this study from vitrinite reflectance (see part I) and Rock-Eval pyrolysis (T_{max} and PI). Interpretation of lateral trends in organic maturation and source rock potential of Mesozoic and Tertiary strata on the Queen Charlotte Islands is difficult due to limited lateral continuity of stratigraphic units and limited outcrop distribution. Hence, the interpretations presented in the following sections are based on limited data and are preliminary.

Organic Maturation

High heat flow associated with volcanism and plutonism is an important control on source rock quality in the Queen Charlotte Islands. Figure 86 illustrates surface maturation trends with respect to

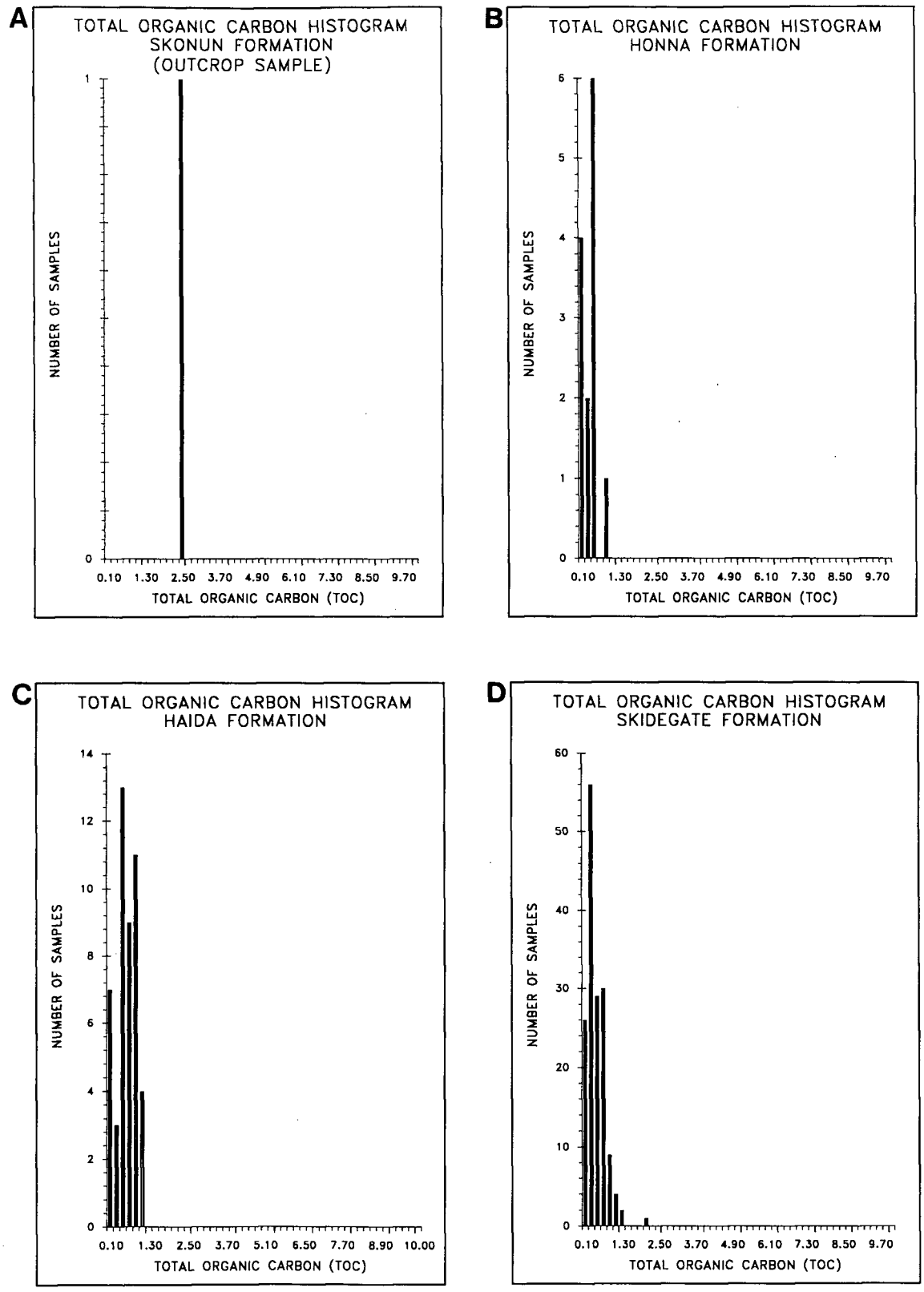

Figure 45. Histograms of total organic carbon (TOC) content. Class interval is 0.2 % TOC. Data includes outcrop and well cuttings samples. TOC is expressed as a weight percent. a) Skonun Formation; b) Honna Formation; c) Haida Formation; d) Skidegate Formation

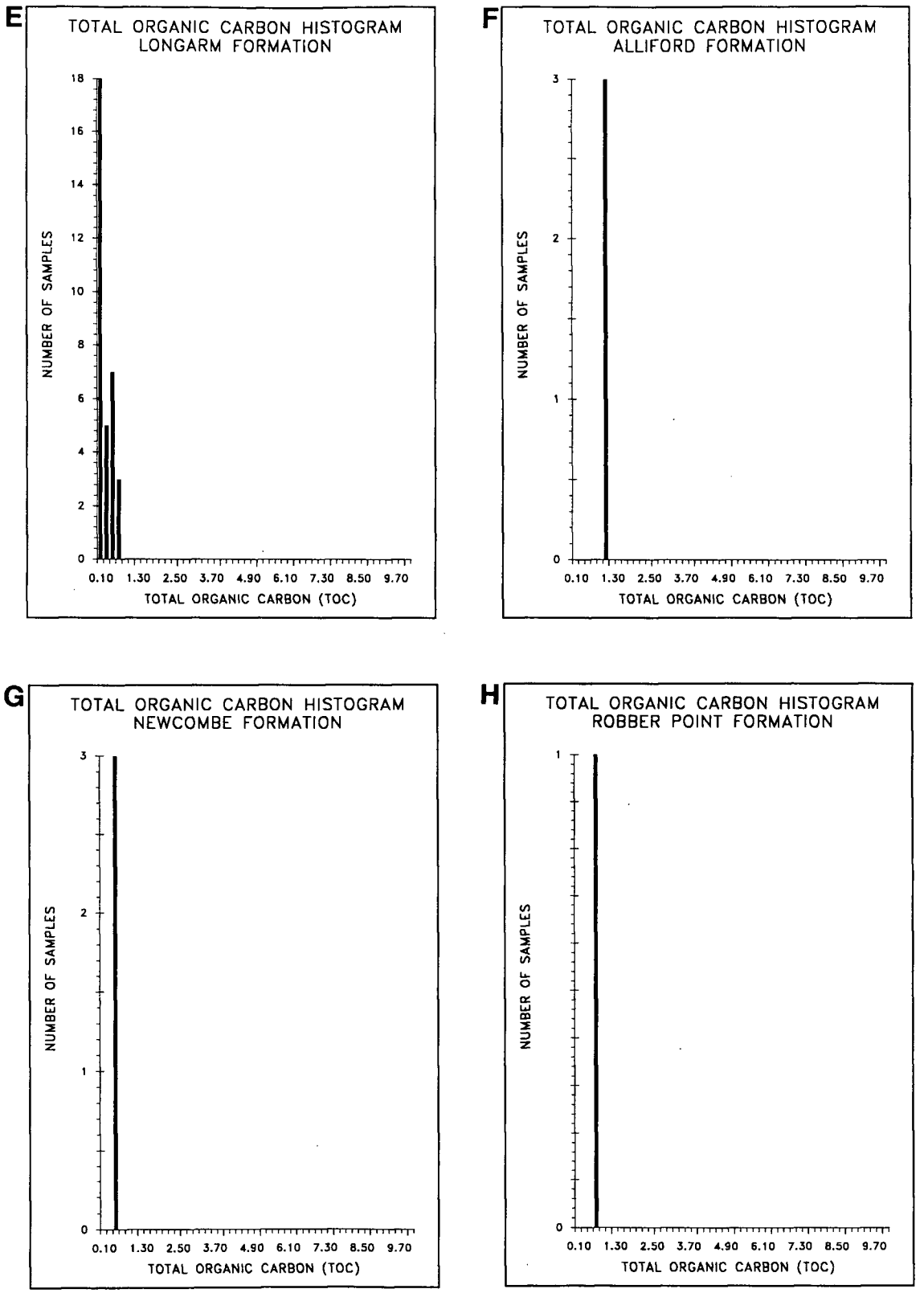

Figure 45. Histograms of total organic carbon (TOC) content. Class interval is 0.2 % TOC. Data includes outcrop and well cuttings samples. TOC is expressed as a weight percent. e) Longarm Formation; f) Alliford Formation; g) Newcombe Formation; h) Robber Point Formation

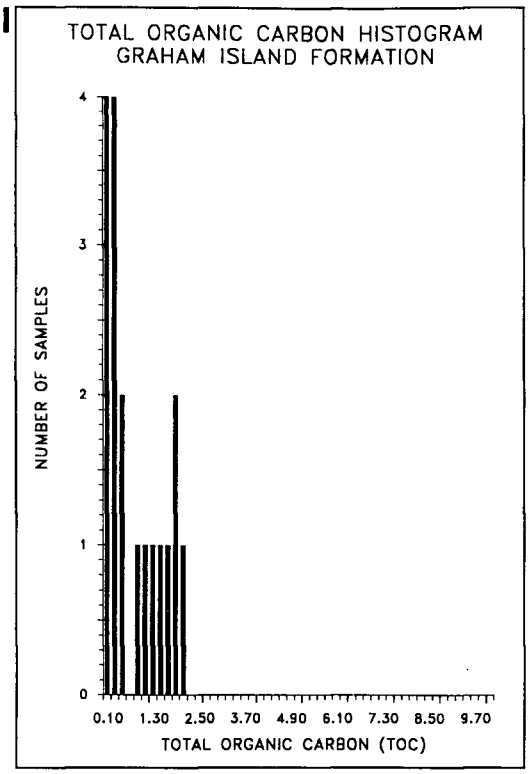

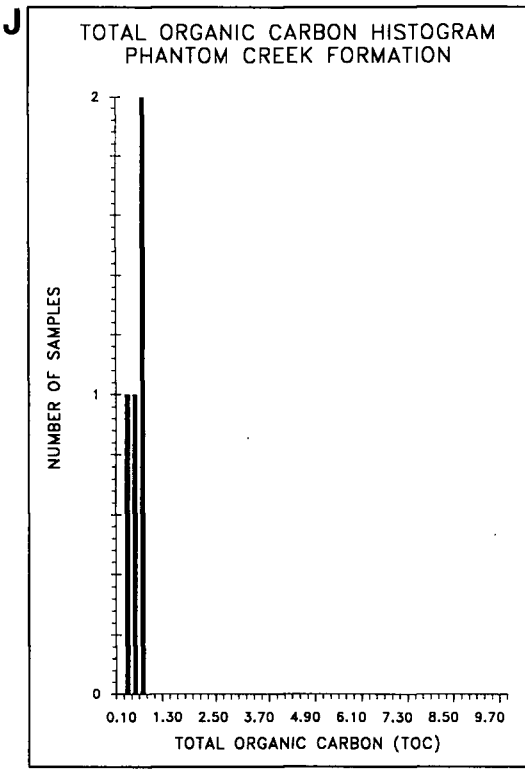

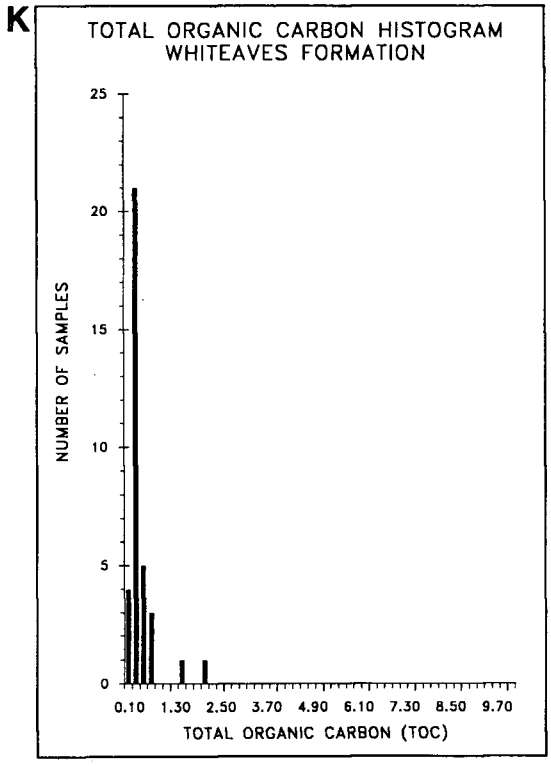

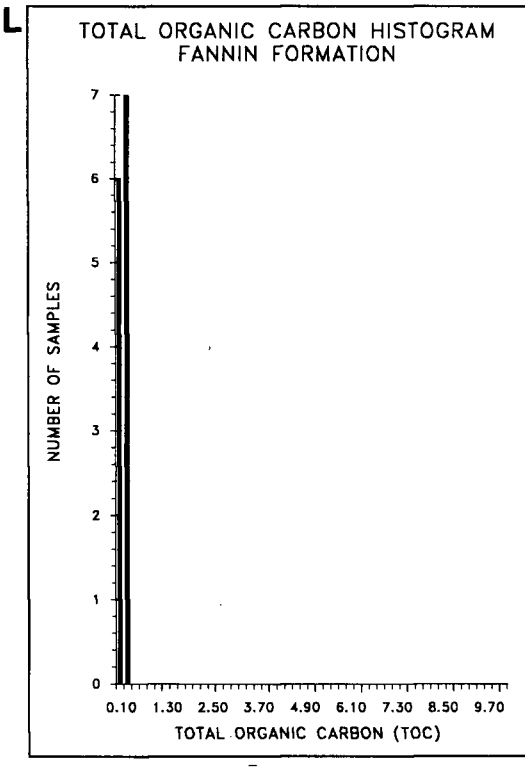

Figure 45. Histograms of total organic carbon (TOC) content. Class interval is 0.2 % TOC. Data includes outcrop and well cuttings samples. TOC is expressed as a weight percent. i) Graham Island Formation; j) Phantom Creek Formation; k) Whiteaves Formation; l) Fannin Formation

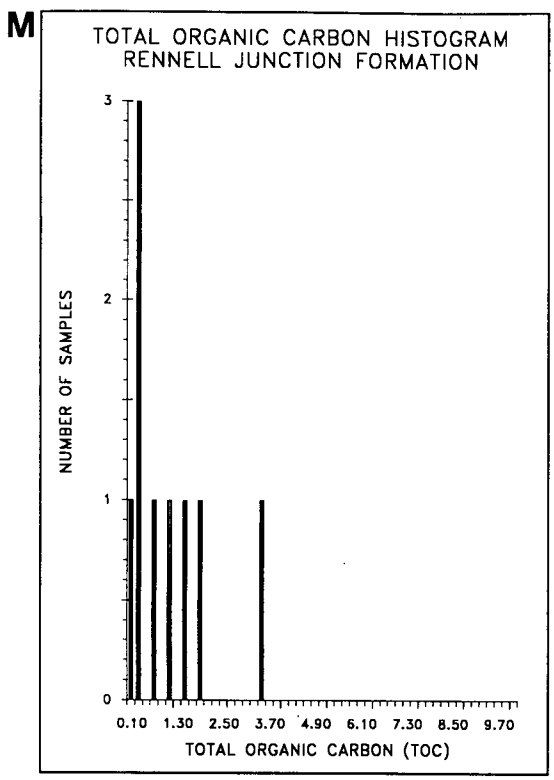

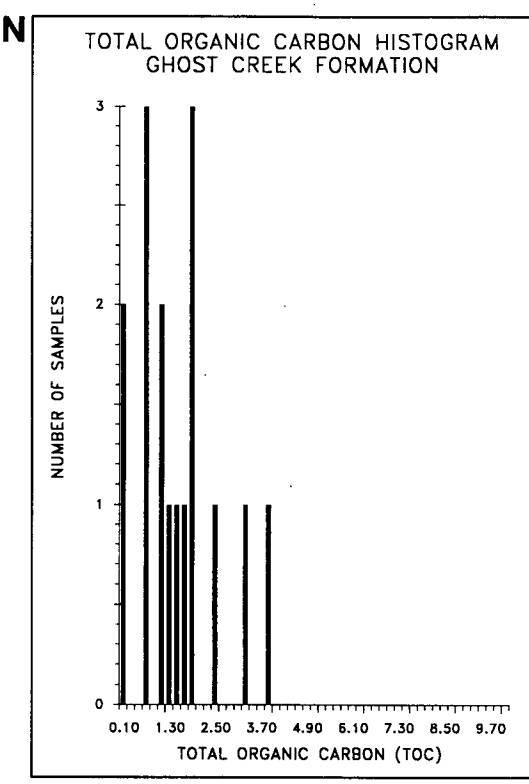

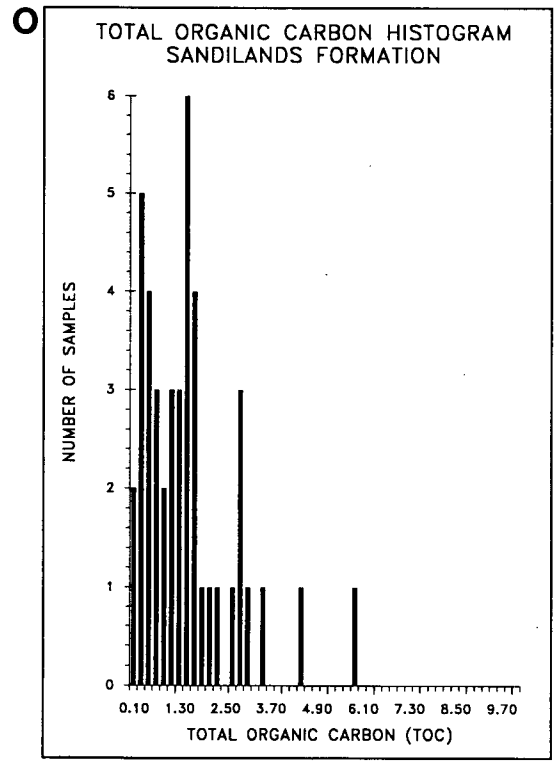

Figure 45. Histograms of total organic carbon (TOC) content. Class interval is 0.2 % TOC. Data includes outcrop and well cuttings samples. TOC is expressed as a weight percent. m) Rennell Junction Formation; n) Ghost Creek Formation; o) Sandilands Formation

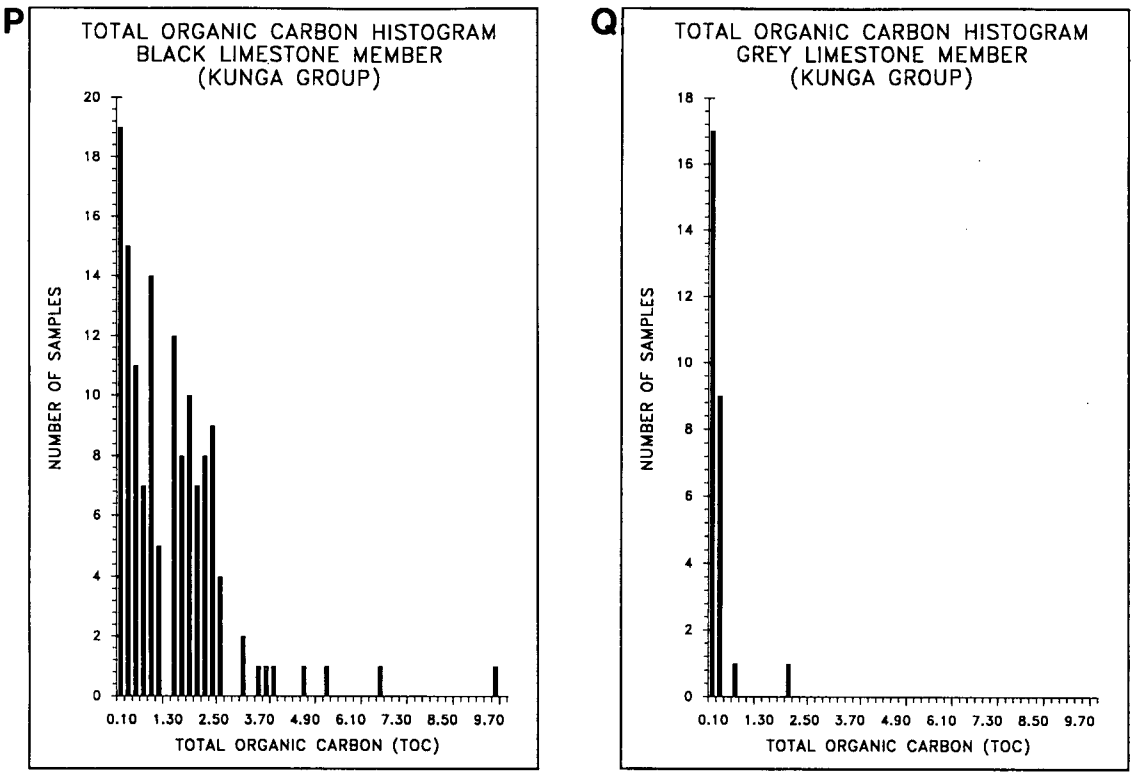

Figure 45. Histograms of total organic carbon (TOC) content. Class interval is 0.2 % TOC. Data includes outcrop and well cuttings samples. TOC is expressed as a weight percent. p) black limestone member (Kunga Group); q) grey limestone member (Kunga Group)

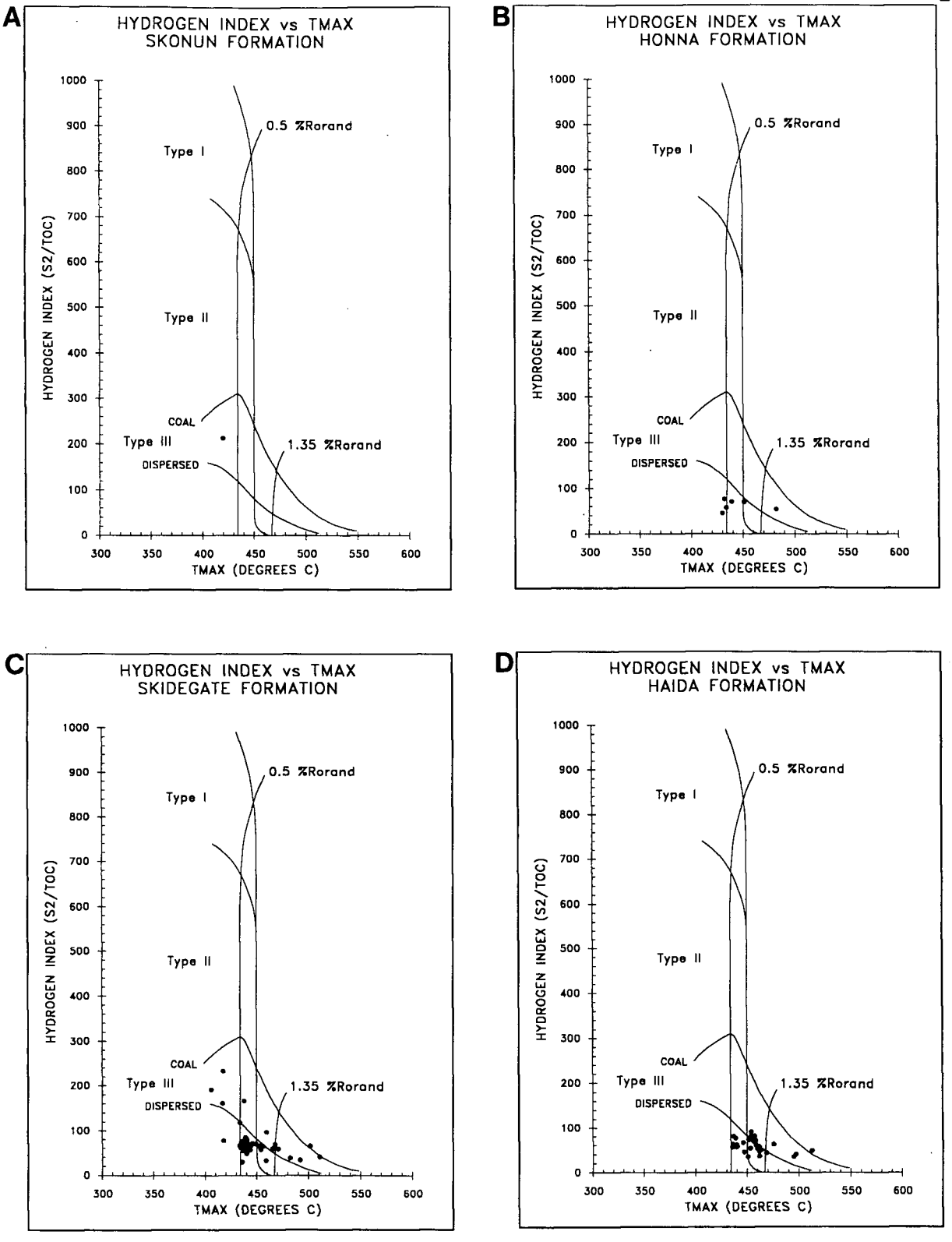

Figure 46. Hydrogen index/Tmax (HI/Tmax) diagrams. Organic matter types and oil window limits based on Espitalie et al. (1985). [HI=S2/TOC (mg HC/gm C_{org}); Tmax ^{o}C]. Data includes outcrop and well cuttings samples. 0.50 $\%Ro_{rand}$ (430-435 ^{o}C Tmax) to 1.35 $\%Ro_{rand}$ (465 ^{o}C Tmax) define the oil window for Types II and III organic matter. a) Skonun Formation; b) Honna Formation; c) Skidegate Formation; d) Haida Formation

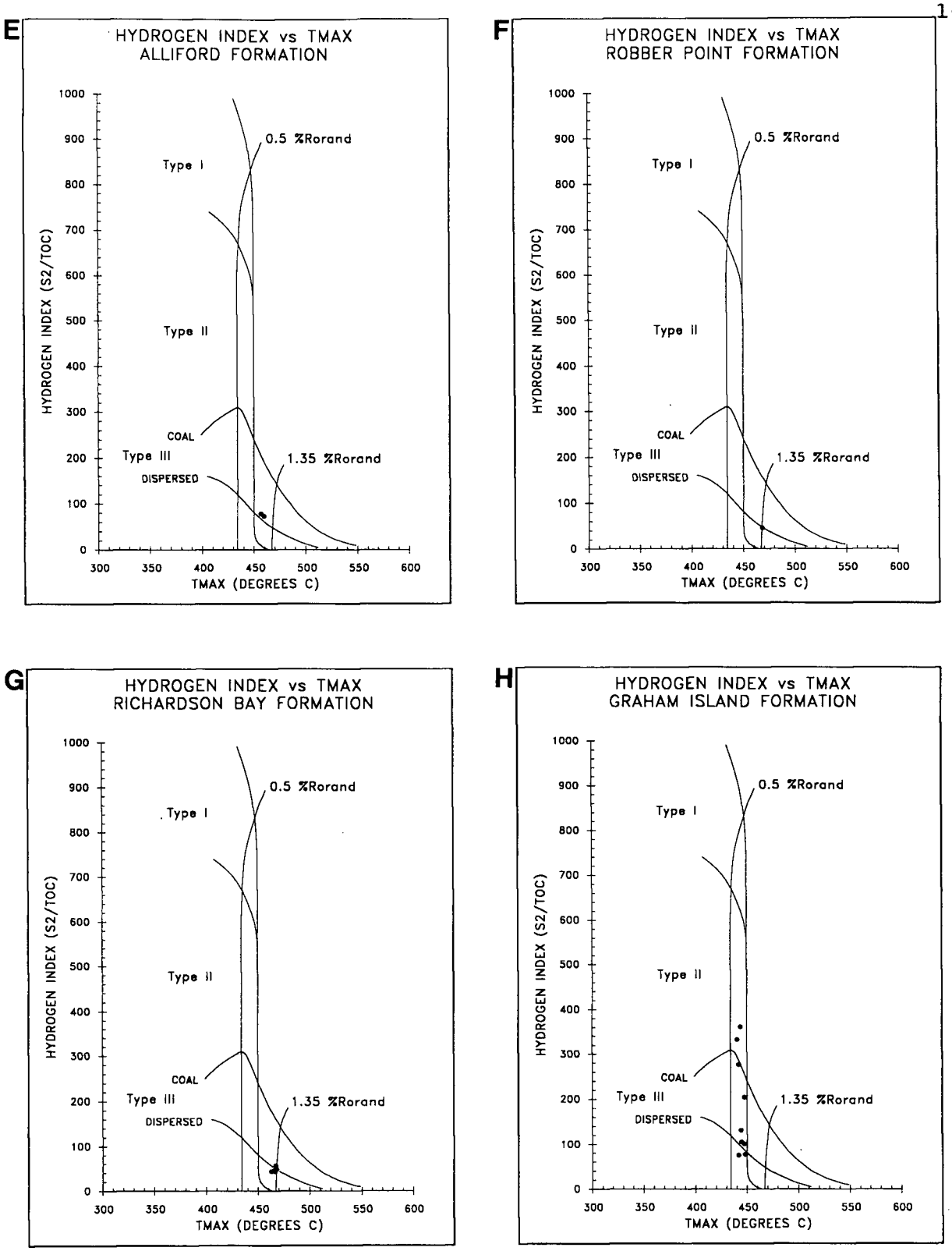

Figure 46. Hydrogen index/Tmax (HI/Tmax) diagrams. Organic matter types and oil window limits based on Espitalie et al. (1985). [HI = S2/TOC (mg HC/gm C_{org}); Tmax ^{o}C]. Data includes outcrop and well cuttings samples. 0.50 %Ro_{rand} (430-435 ^{o}C Tmax) to 1.35 %Ro_{rand} (465 ^{o}C Tmax) define the oil window for Types II and III organic matter. e) Alliford Formation; f) Robber Point Formation; g) Richardson Bay Formation; h) Graham Island Formation

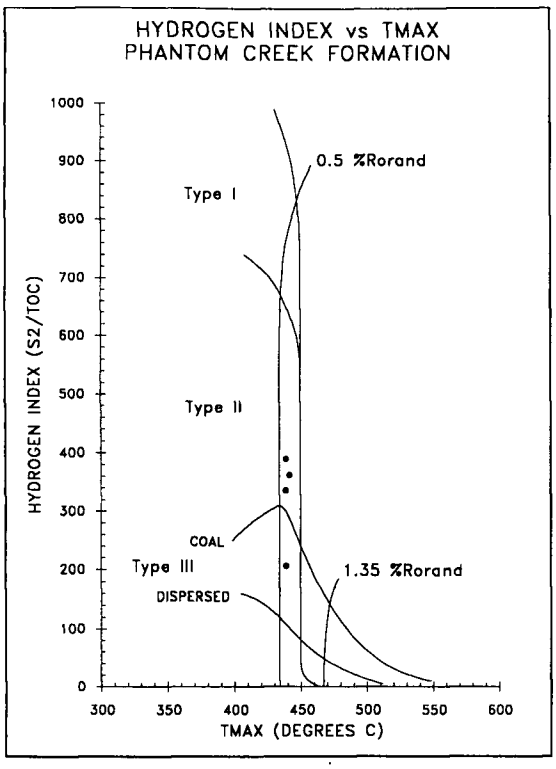

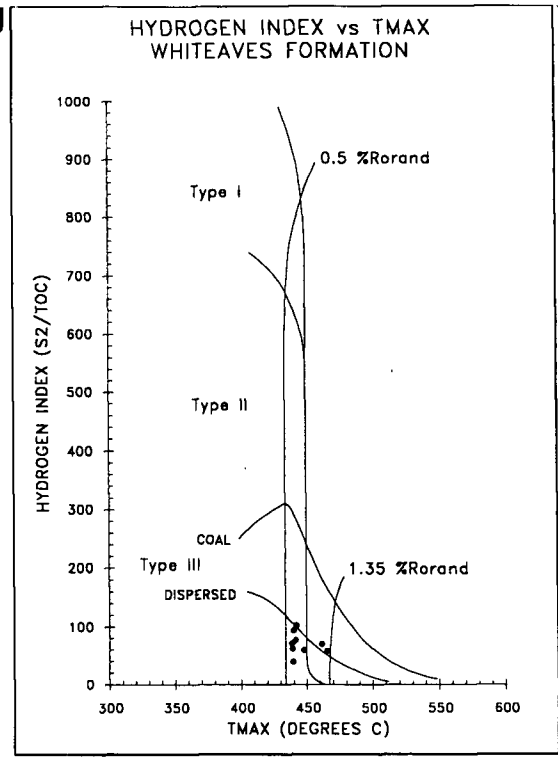

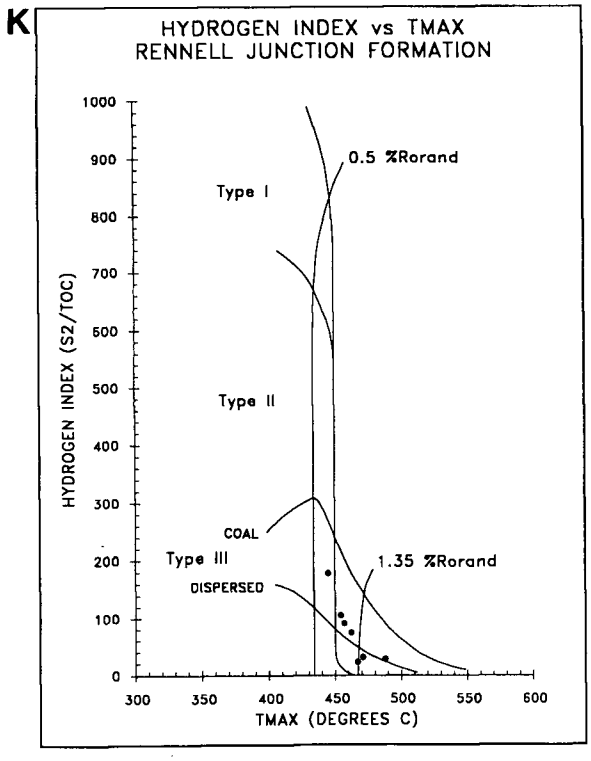

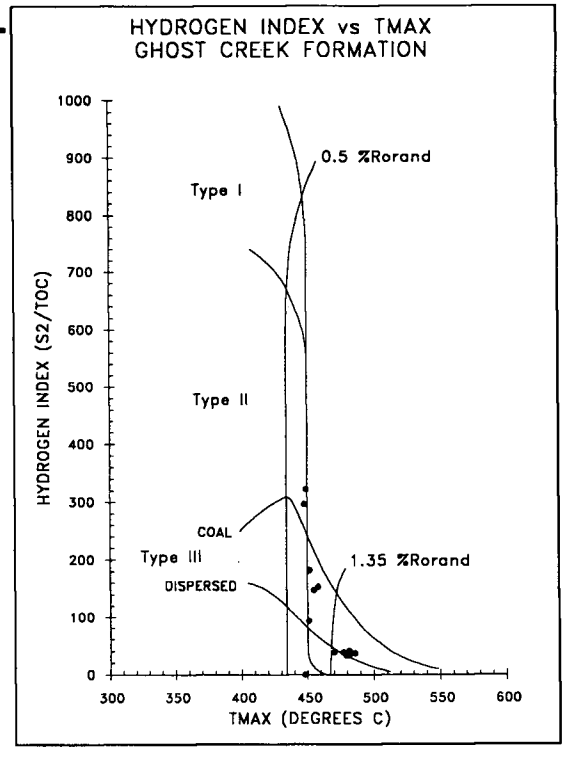

Figure 46. Hydrogen index/Tmax (HI/Tmax) diagrams. Organic matter types and oil window limits based on Espitalie et al. (1985). [HI=S2/TOC (mg HC/gm C_{org}); Tmax ^{o}C]. Data includes outcrop and well cuttings samples. 0.50 $\%Ro_{rand}$ (430-435 ^{o}C Tmax) to 1.35 $\%Ro_{rand}$ (465 ^{o}C Tmax) define the oil window for Types II and III organic matter. i) Phantom Creek Formation; j) Whiteaves Formation; k) Rennell Junction Formation; l) Ghost Creek formation

M

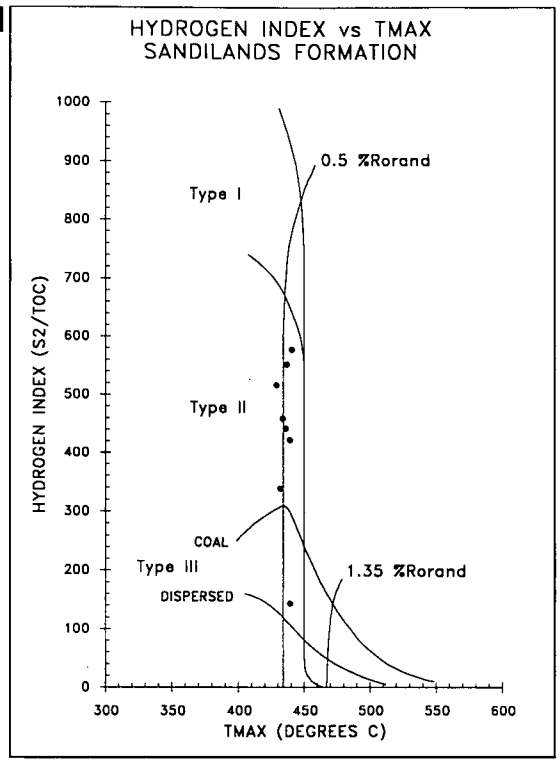

N

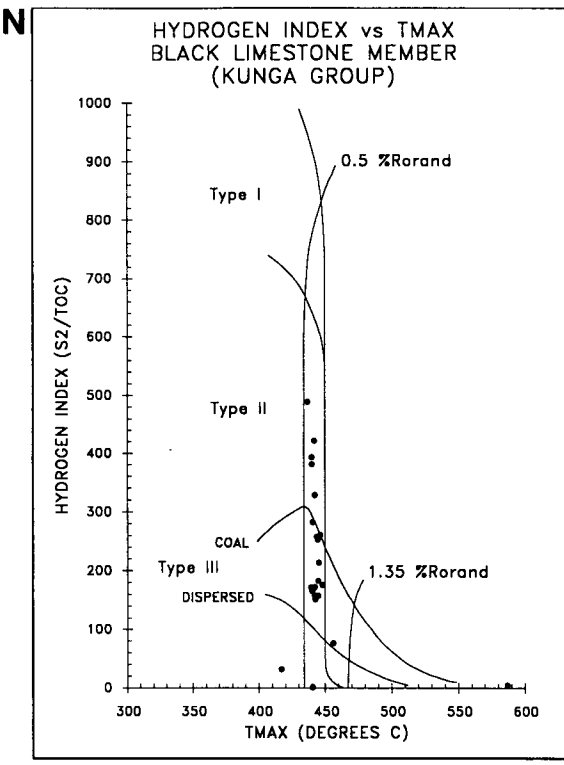

Figure 46. Hydrogen index/Tmax (HI/Tmax) diagrams. Organic matter types and oil window limits based on Espitalie et al. (1985). [HI = S2/TOC (mg HC/gm C_{org}); Tmax ^{o}C]. Data includes outcrop and well cuttings samples. 0.50 $\%Ro_{rand}$ (430-435 ^{o}C Tmax) to 1.35 $\%Ro_{rand}$ (465 ^{o}C Tmax) define the oil window for Types II and III organic matter. m) Sandilands Formation; n) black limestone member (Kunga Group)

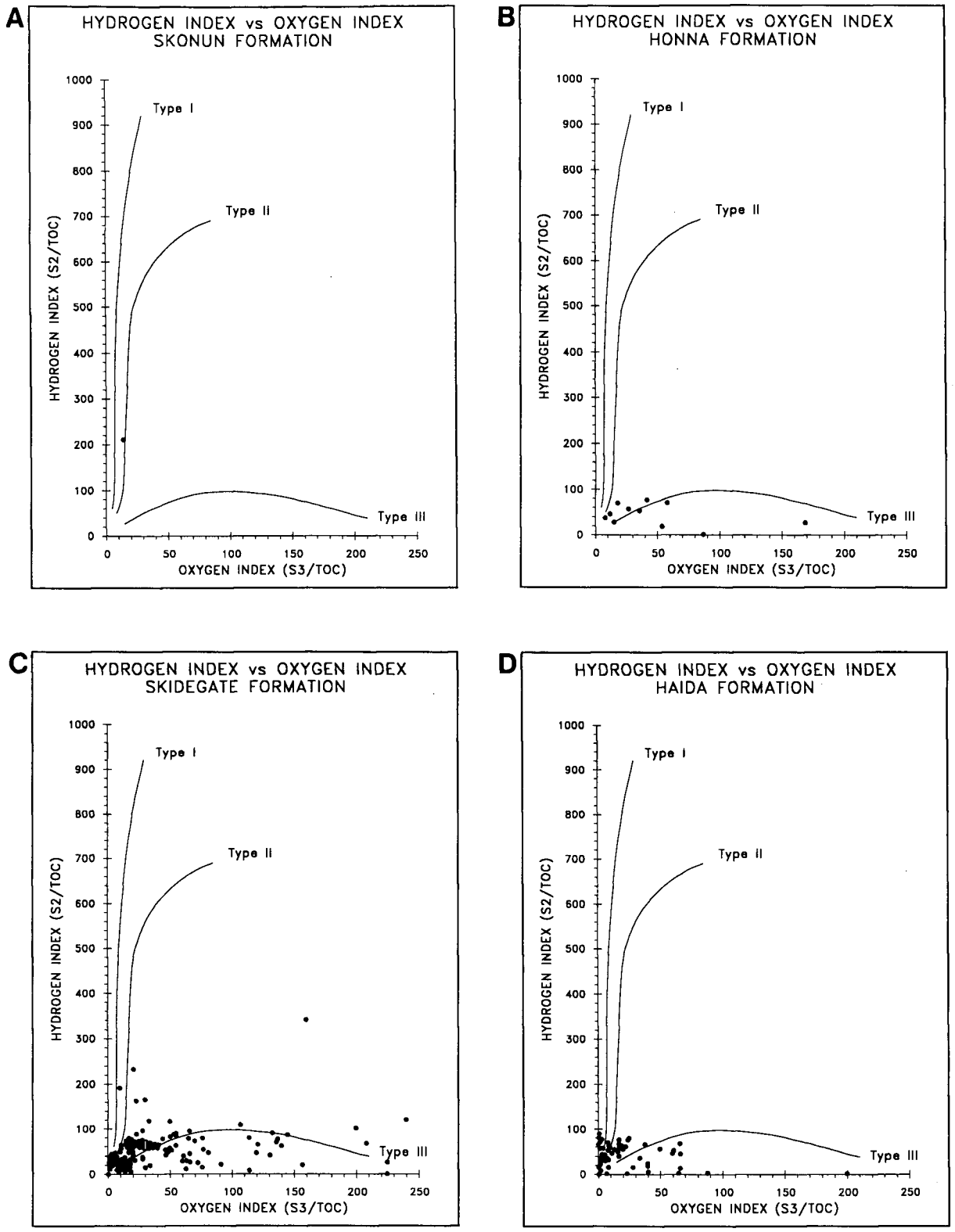

Figure 47. Hydrogen index/Oxygen index (HI/OI) diagrams. Maturation pathways modified from Espitalie et al. (1985). [HI = S2/TOC (mg HC/gm C_{org}); OI = S3/TOC (mg HC/gm C_{org})]. Data includes outcrop and well cuttings samples. a) Skonun Formation; b) Honna Formation; c) Skidegate Formation; d) Haida Formation

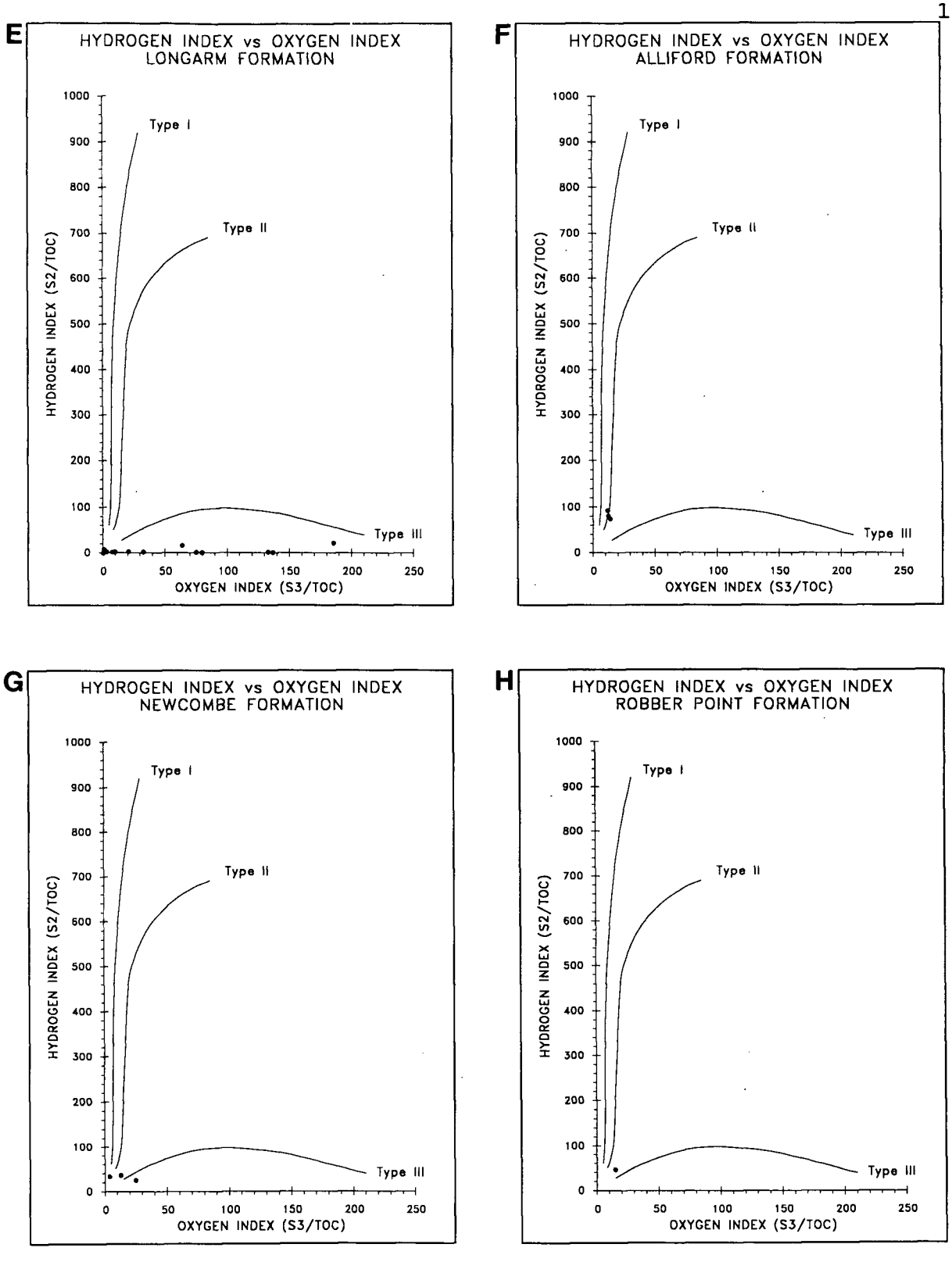

Figure 47. Hydrogen index/Oxygen index (HI/OI) diagrams. Maturation pathways modified from Espitalie et al. (1985). [HI = S2/TOC (mg HC/gm C_{org}); OI = S3/TOC (mg HC/gm C_{org})]. Data includes outcrop and well cuttings samples. e) Longarm Formation; f) Alliford Formation; g) Newcombe Formation; h) Robber Point Formation

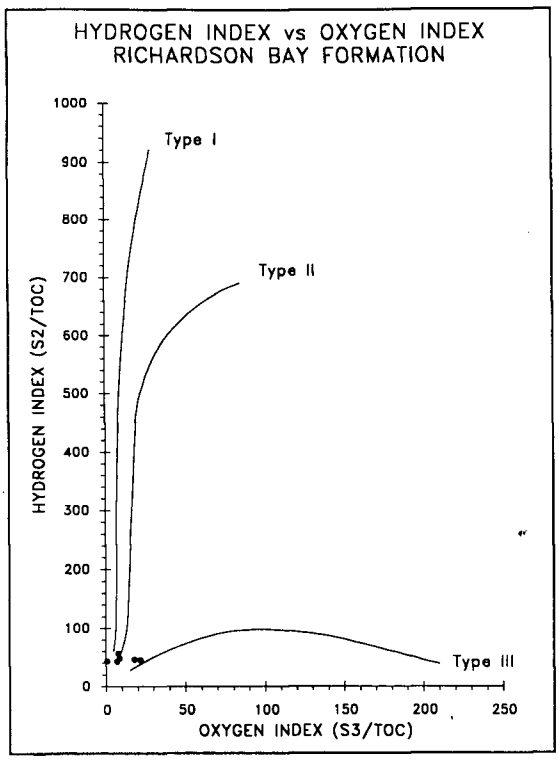

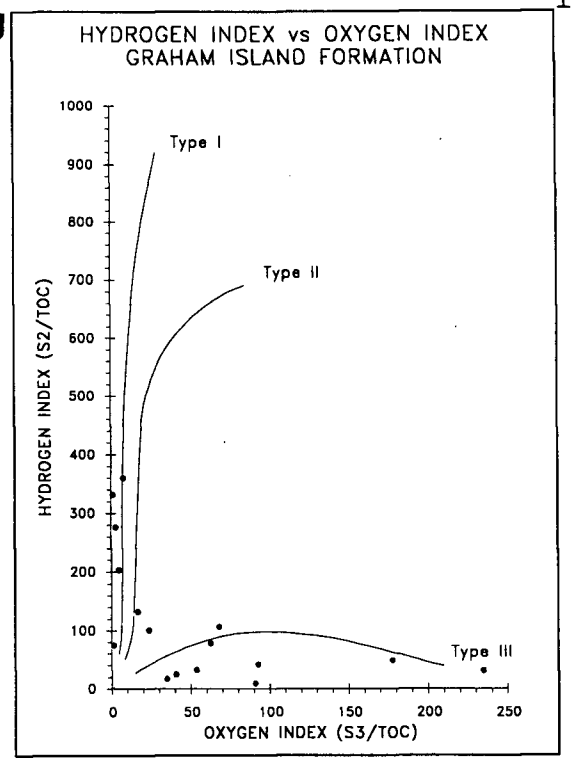

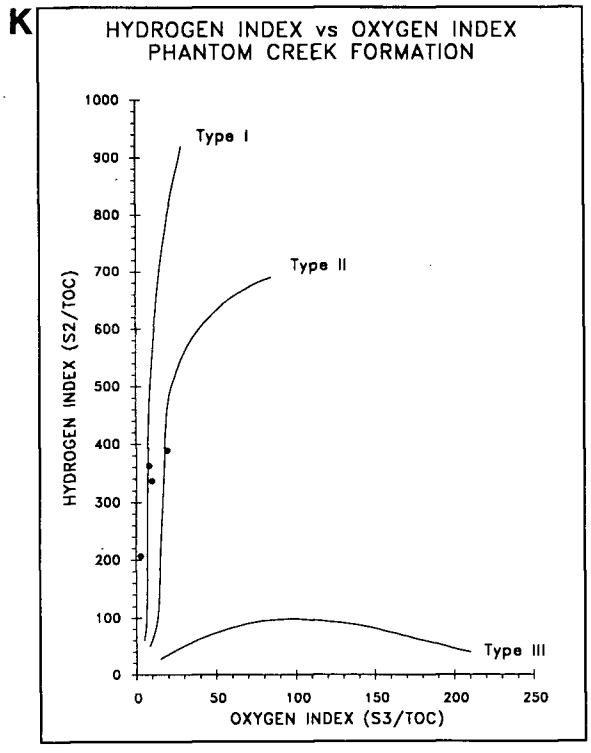

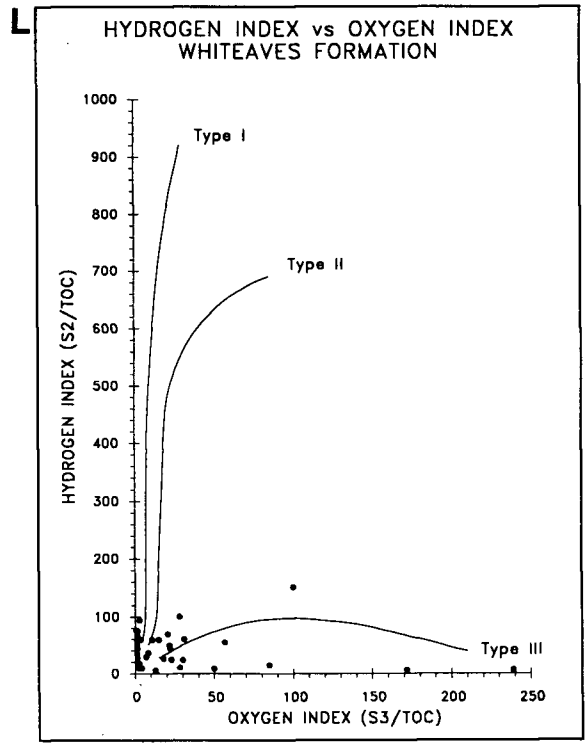

Figure 47. Hydrogen index/Oxygen index (HI/OI) diagrams. Maturation pathways modified from Espitalie et al. (1985). [HI=S2/TOC (mg HC/gm C_{org}); OI=S3/TOC (mg HC/gm C_{org})]. Data includes outcrop and well cuttings samples. i) Richardson Bay Formation; j) Graham Island Formation; k) Phantom Creek Formation; l) Whiteaves Formation

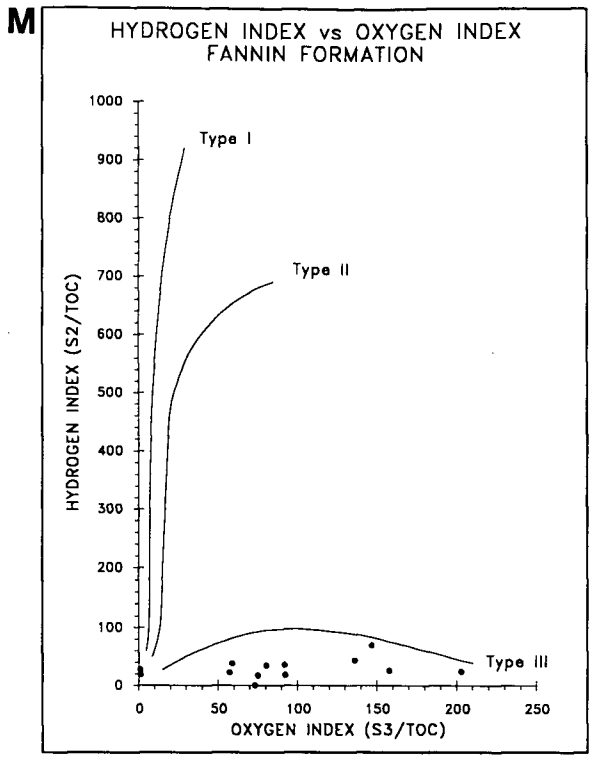

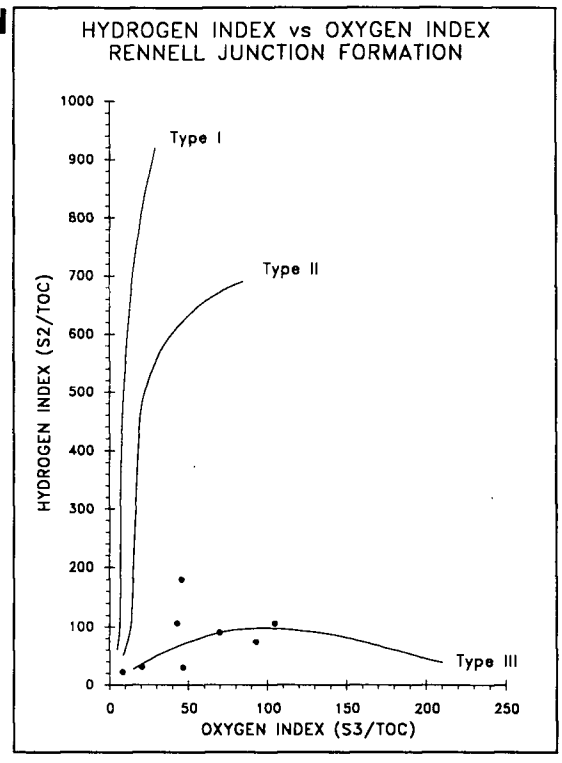

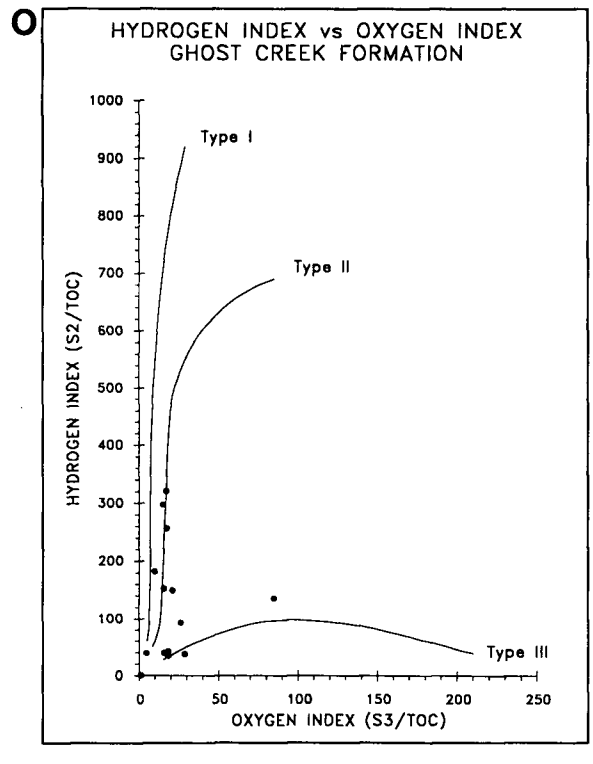

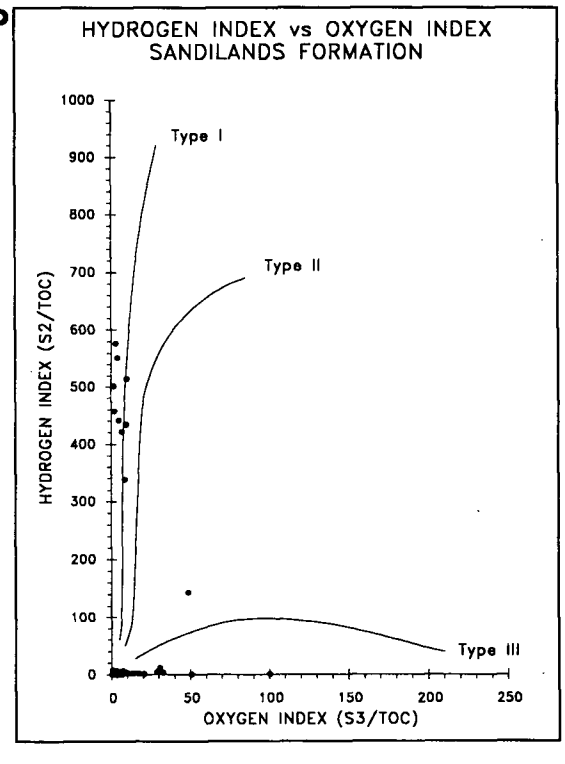

Figure 47. Hydrogen index/Oxygen index (HI/OI) diagrams. Maturation pathways modified from Espitalie et al. (1985). [HI = S2/TOC (mg HC/gm C_{org}); OI = S3/TOC (mg HC/gm C_{org})]. Data includes outcrop and well cuttings samples. m) Fannin Formation; n) Rennell Junction Formation; o) Ghost Creek Formation; p) Sandilands Formation

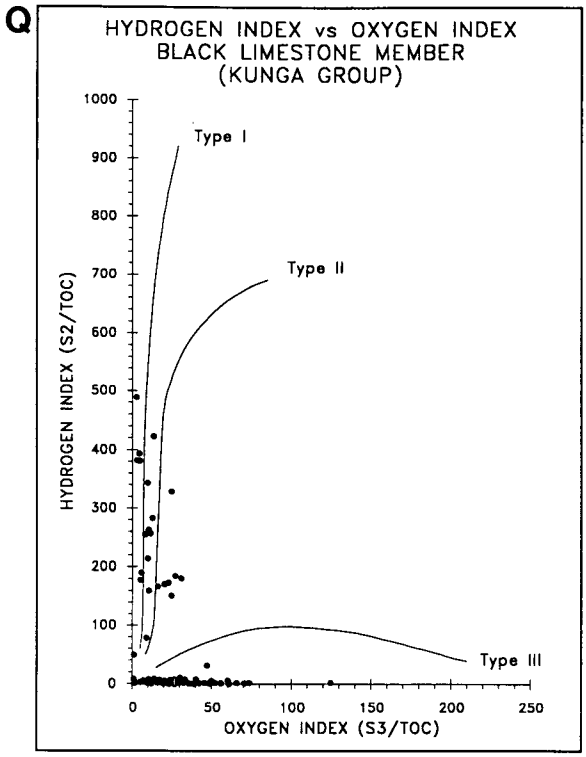

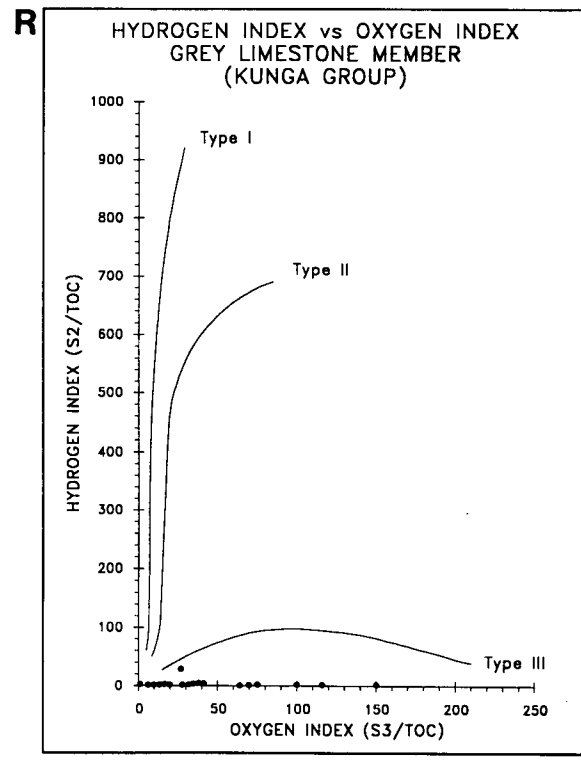

Figure 47. Hydrogen index/Oxygen index (HI/OI) diagrams. Maturation pathways modified from Espitalie et al. (1985). [HI = S2/TOC (mg HC/gm C_{org}); OI = S3/TOC (mg HC/gm C_{org})]. Data includes outcrop and well cuttings samples. q) black limestone member (Kunga Group); r) grey limestone member (Kunga Group)

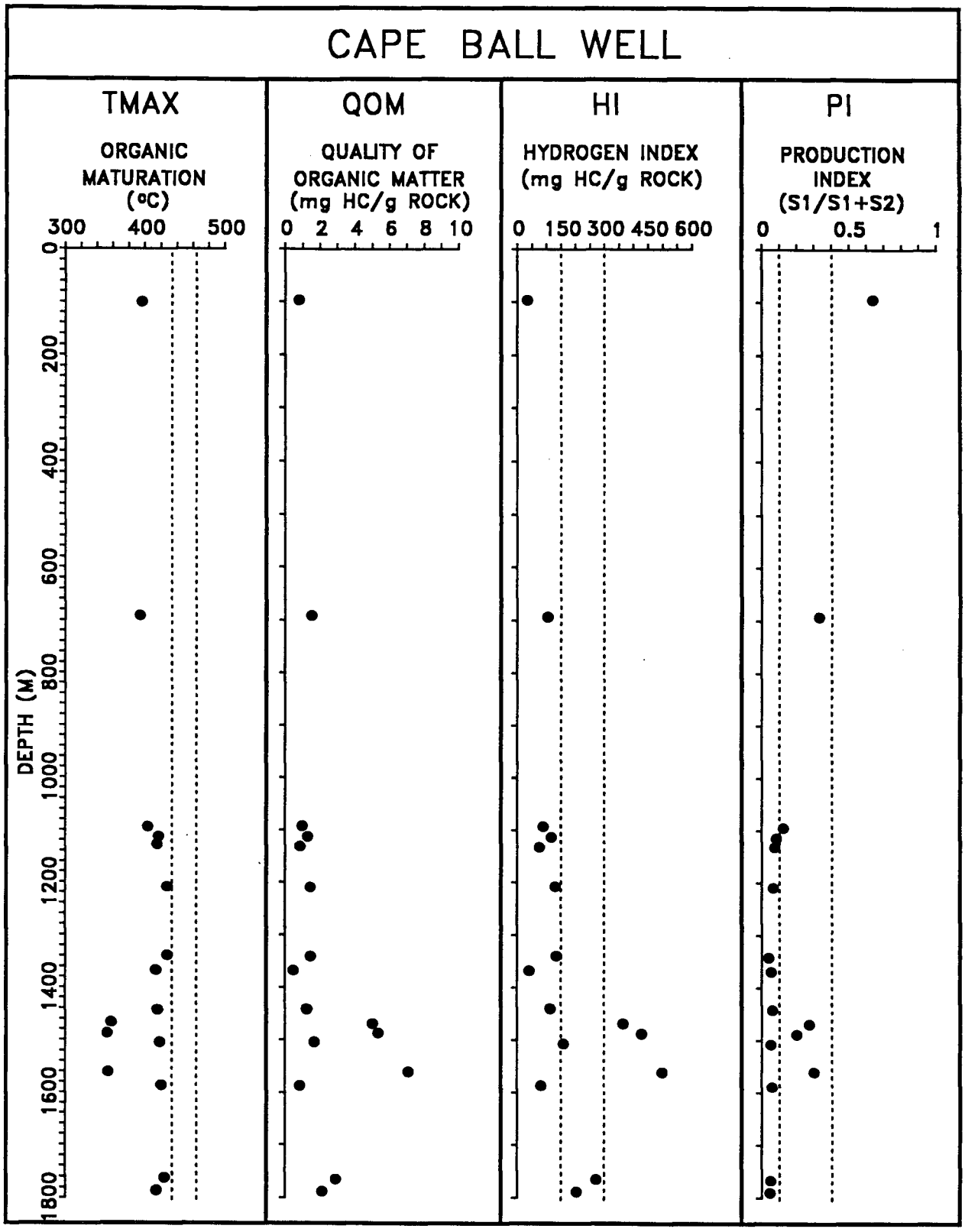

Figure 48. Rock-Eval logs for the Cape Ball well which penetrates Tertiary Skonun Formation strata on Graham Island. Tmax, HI, and PI are standard Rock-Eval parameters (Espitalie et al., 1977), QOM = (S1+S2)/TOC. 430 (435) ^{o}C to 465 ^{o}C T_{max} defines the oil window. HI from 0-150 mg HC/gm C_{org} defines a gas source, HI from 150-300 mg HC/gm C_{org} defines a oil and gas source, HI from 300+ defines an oil source. PI values between 0.1 and 0.4 define the oil window. Samples are predominantly coal and lignite with minor siltstone/sandstone from cuttings and core.

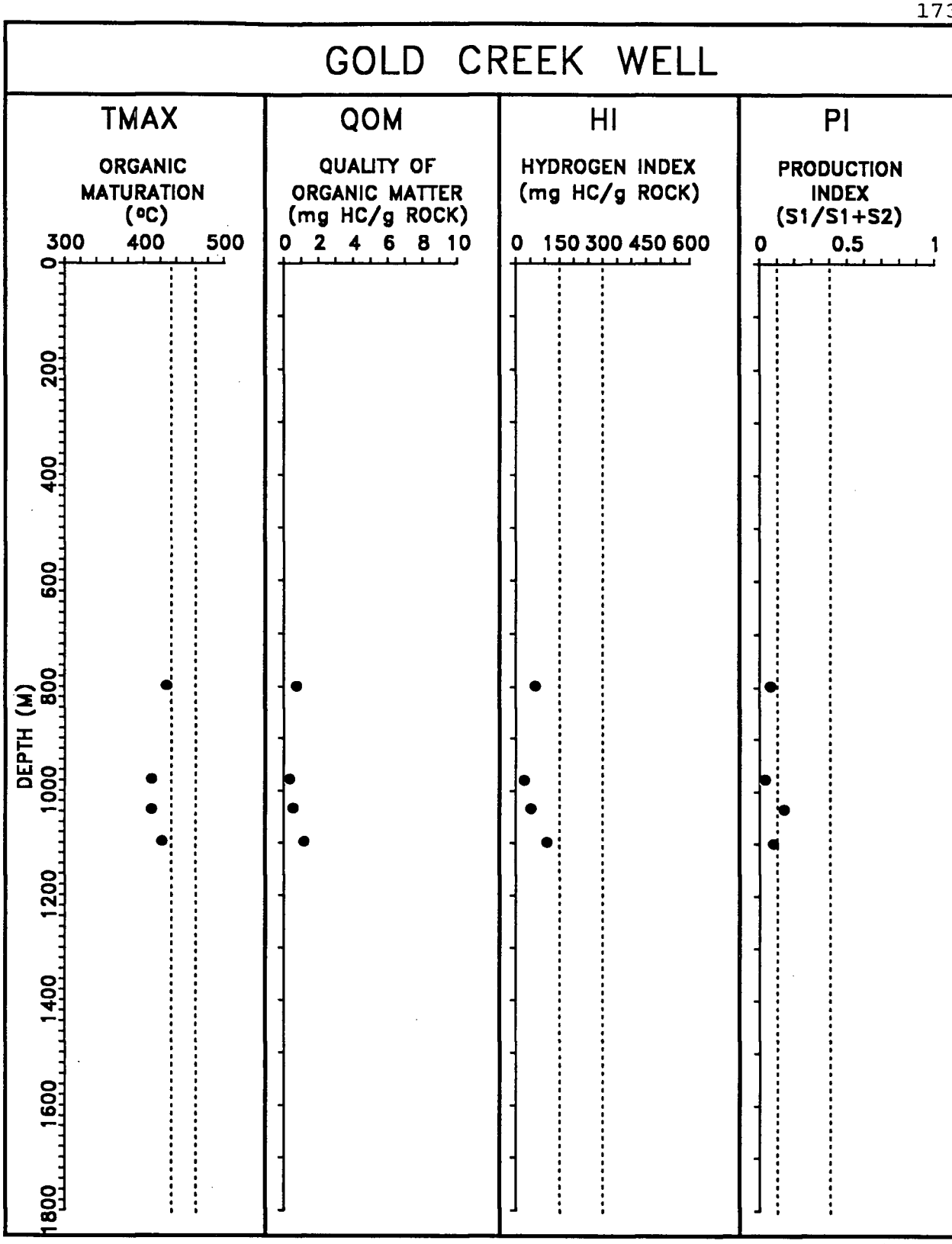

Figure 49. Rock-Eval logs for the Gold Creek well which penetrates Tertiary Skonun Formation strata on Graham Island. Tmax, HI, and PI are standard Rock-Eval parameters (Espitalie et al., 1977), QOM = (S1 + S2)/TOC. 430 (435) ^{o}C to 465 ^{o}C T_{max} defines the oil window. HI from 0-150 mg HC/gm C_{org} defines a gas source, HI from 150-300 mg HC/gm C_{org} defines a oil and gas source, HI from 300+ defines an oil source. PI values between 0.1 and 0.4 define the oil window. Samples are predominantly coal and lignite with minor siltstone/sandstone from cuttings and core.

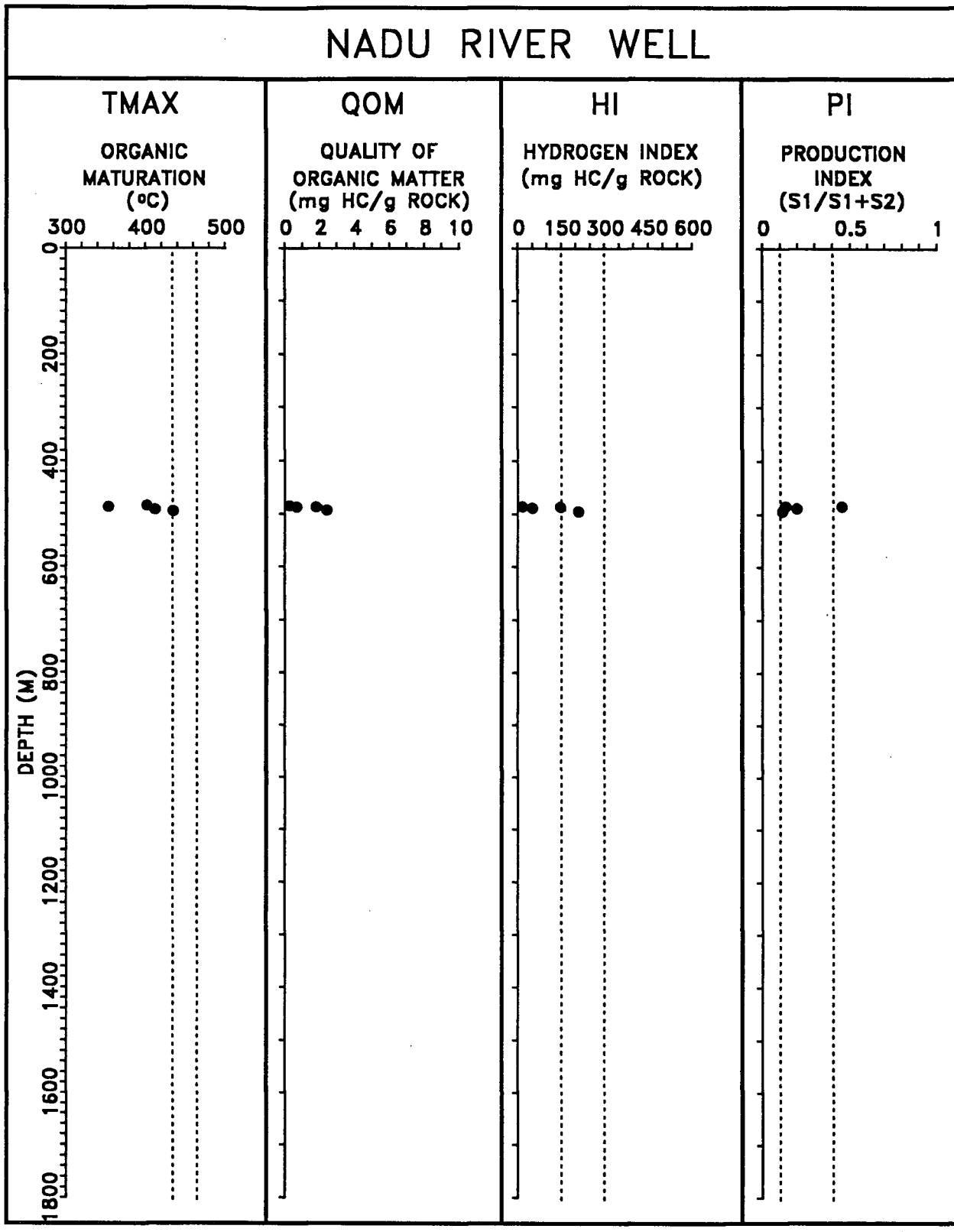

Figure 50. Rock-Eval logs for the Nadu River well which penetrates Tertiary Skonun Formation strata on Graham Island. Tmax, HI, and PI are standard Rock-Eval parameters (Espitalie et al., 1977), QOM = (S1 + S2)/TOC. 430 (435) ^{o}C to 465 ^{o}C T_{max} defines the oil window. HI from 0-150 mg HC/gm C_{org} defines a gas source, HI from 150-300 mg HC/gm C_{org} defines a oil and gas source, HI from 300+ defines an oil source. PI values between 0.1 and 0.4 define the oil window. Samples are predominantly coal and lignite with minor siltstone/sandstone from cuttings and core.

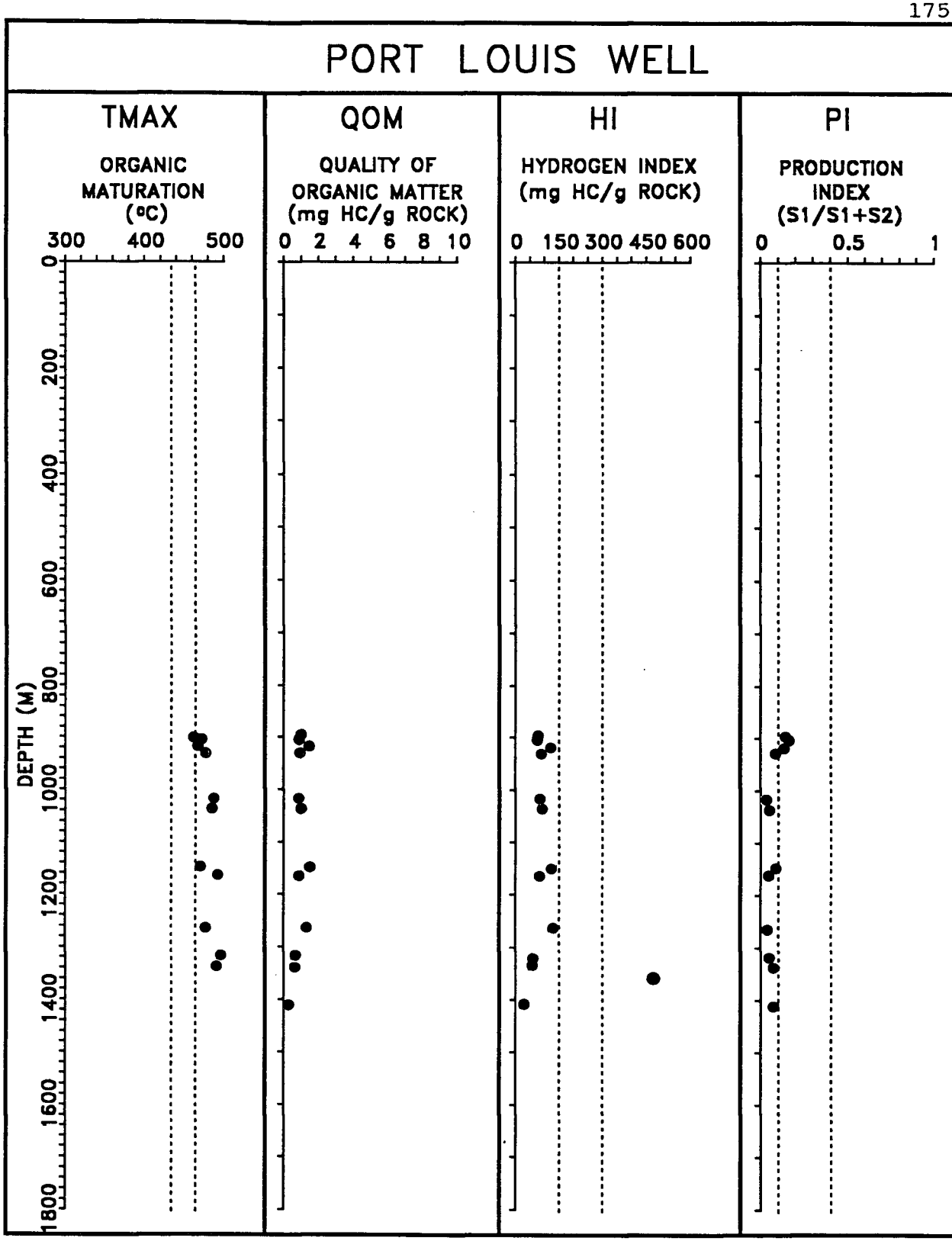

Figure 51. Rock-Eval logs for the Port Louis well which penetrates Tertiary Skonun Formation strata on Graham Island. Tmax, HI, and PI are standard Rock-Eval parameters (Espitalie et al., 1977), QOM = (S1 + S2)/TOC. 430 (435) ^{o}C to 465 ^{o}C T_{max} defines the oil window. HI from 0-150 mg HC/gm C_{org} defines a gas source, HI from 150-300 mg HC/gm C_{org} defines a oil and gas source, HI from 300+ defines an oil source. PI values between 0.1 and 0.4 define the oil window. Samples are predominantly coal and lignite with minor siltstone/sandstone from cuttings and core.

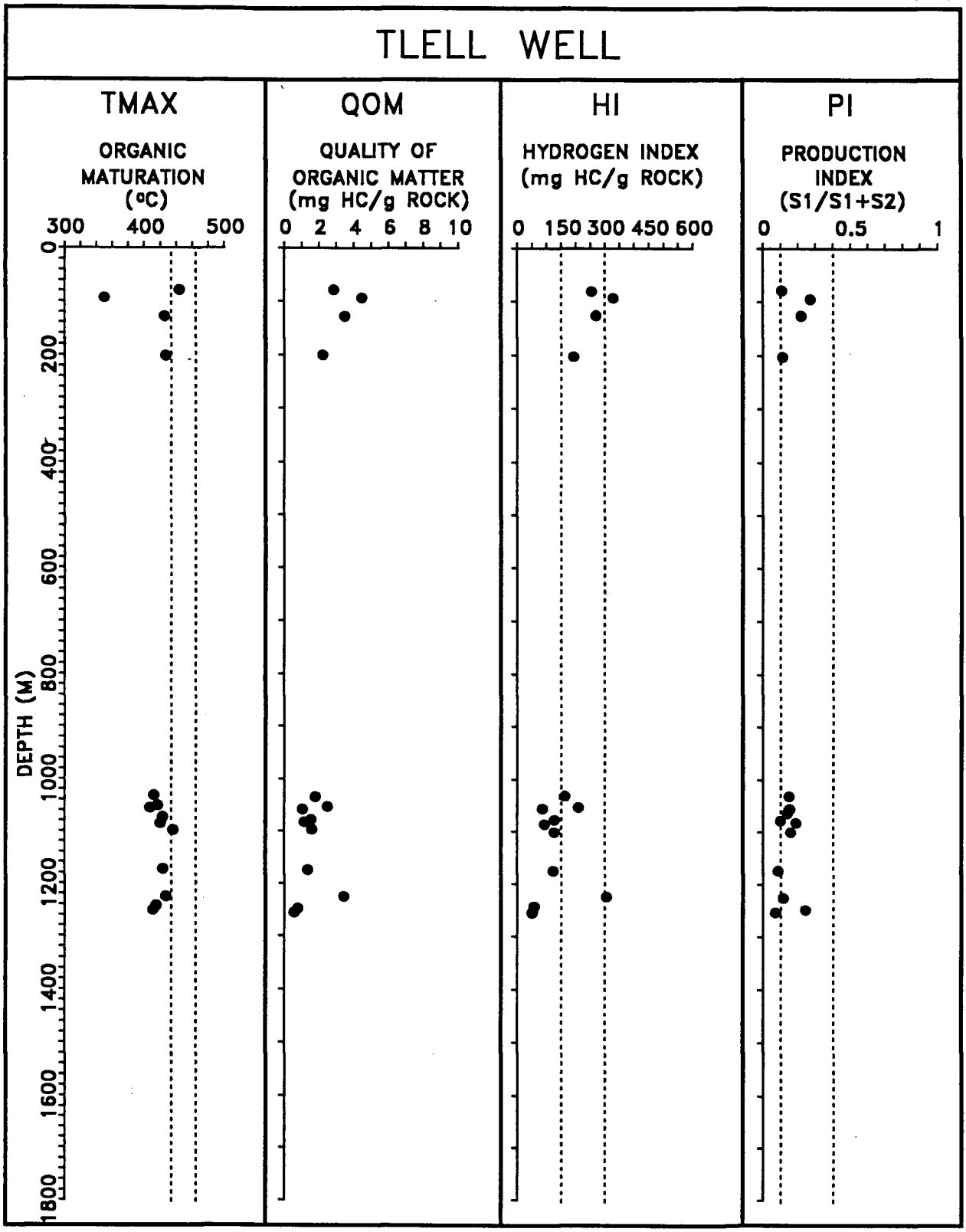

Figure 52. Rock-Eval logs for the Tlell well which penetrates Tertiary Skonun Formation strata on Graham Island. Tmax, HI, and PI are standard Rock-Eval parameters (Espitalie et al., 1977), QOM = (S1 + S2)/TOC. 430 (435) ^{o}C to 465 ^{o}C T_{max} defines the oil window. HI from 0-150 mg HC/gm C_{org} defines a gas source, HI from 150-300 mg HC/gm C_{org} defines a oil and gas source, HI from 300+ defines an oil source. PI values between 0.1 and 0.4 define the oil window. Samples are predominantly coal and lignite with minor siltstone/sandstone from cuttings and core.

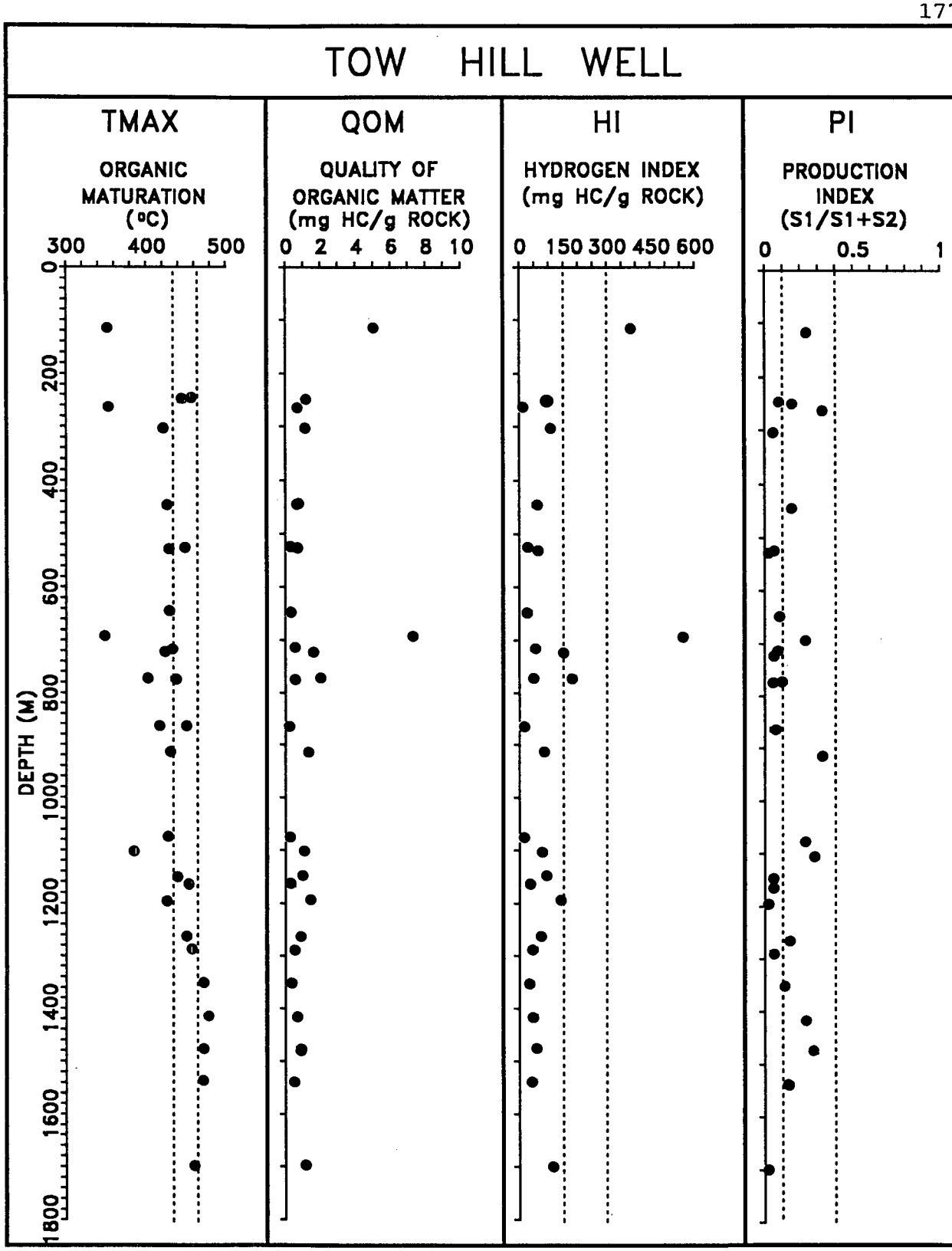

Figure 53. Rock-Eval logs for the Tow Hill well which penetrates Tertiary Skonun Formation strata on Graham Island. Tmax, HI, and PI are standard Rock-Eval parameters (Espitalie et al., 1977), QOM = (S1 + S2)/TOC. 430 (435) ^{o}C to 465 ^{o}C T_{max} defines the oil window. HI from 0-150 mg HC/gm C_{org} defines a gas source, HI from 150-300 mg HC/gm C_{org} defines a oil and gas source, HI from 300+ defines an oil source. PI values between 0.1 and 0.4 define the oil window. Samples are predominantly coal and lignite with minor siltstone/sandstone from cuttings and core.

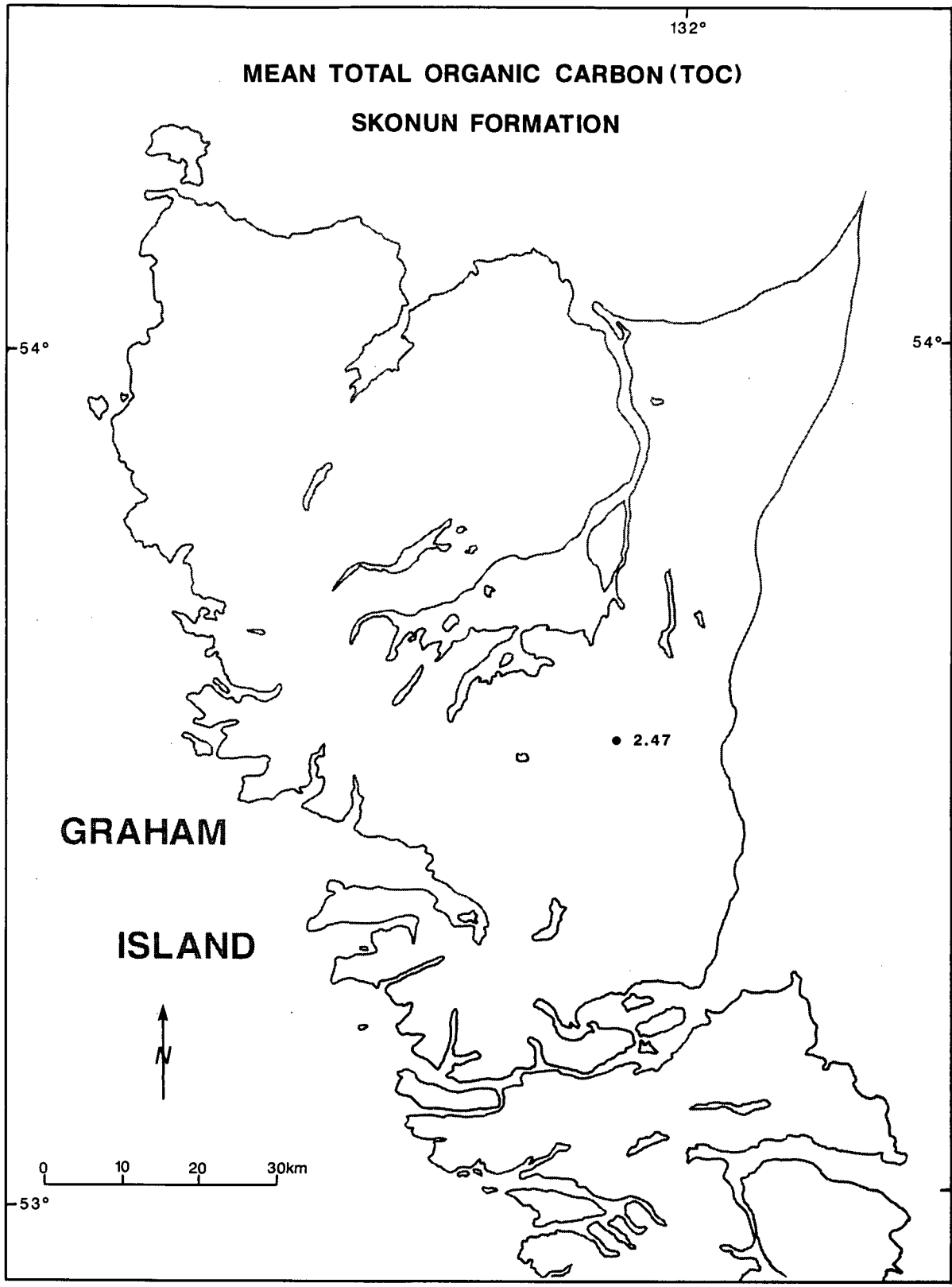

Figure 54. Regional distribution of the mean TOC content for the Skonun Formation. Values are mean TOC calculated across the thickness of the formation at each outcrop location.

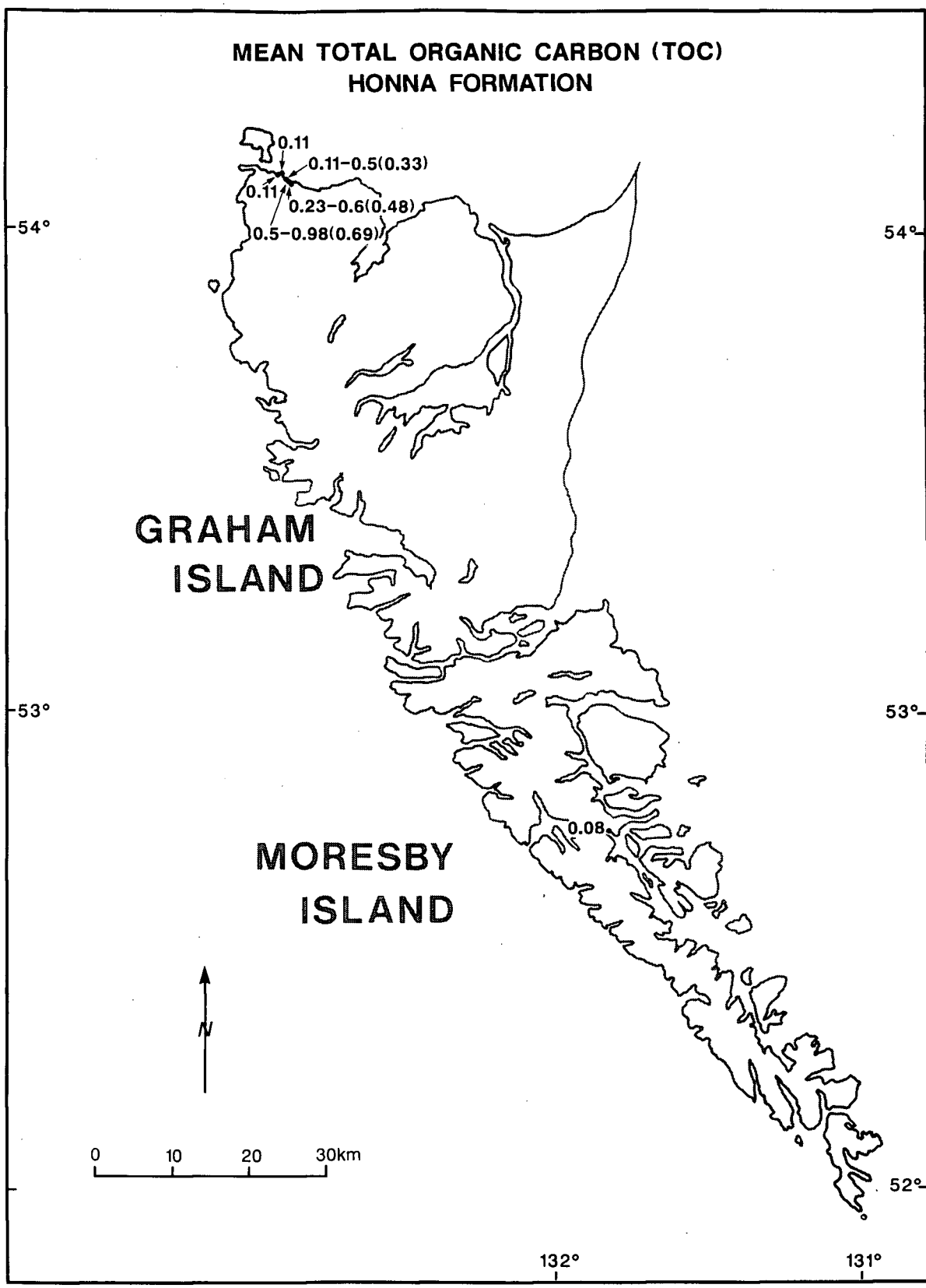

Figure 55. Regional distribution of the mean TOC content for the Honna Formation. Values are mean TOC calculated across the thickness of the formation at each outcrop location. Value in brackets are mean vitrinite reflectance values. Dashed values are minimum and maximum vitrinite reflectance values.

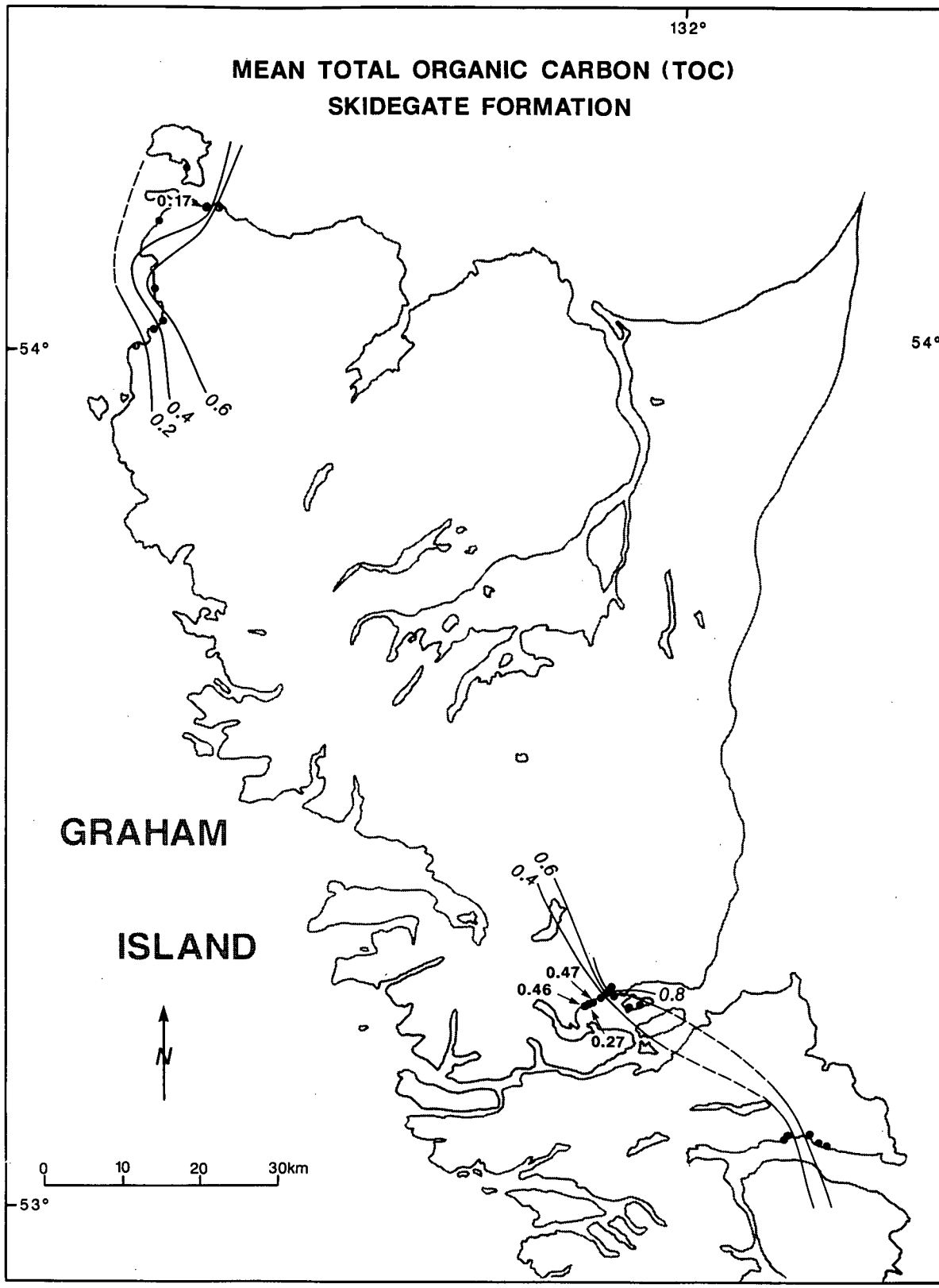

Figure 56. Regional distribution of the mean TOC content for the Skidegate Formation. Values are mean TOC calculated across the thickness of the formation at each outcrop location. Dashed line represents an inferred contour. Labelled values do not fit regional trends and are not contoured.

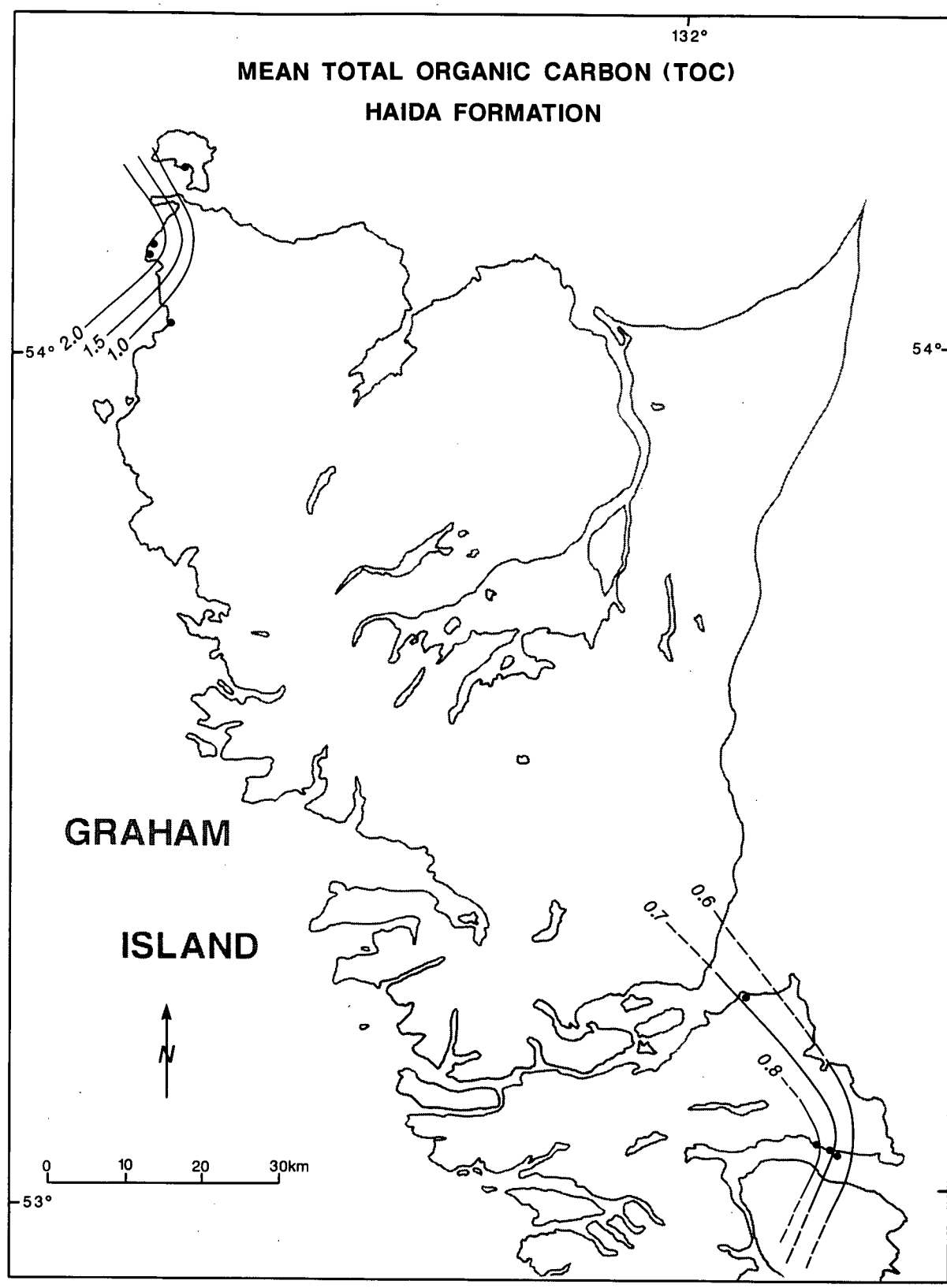

Figure 57. Regional distribution of the mean TOC content for the Haida Formation. Values are mean TOC calculated across the thickness of the formation at each outcrop location. Dashed line represents an inferred contour.

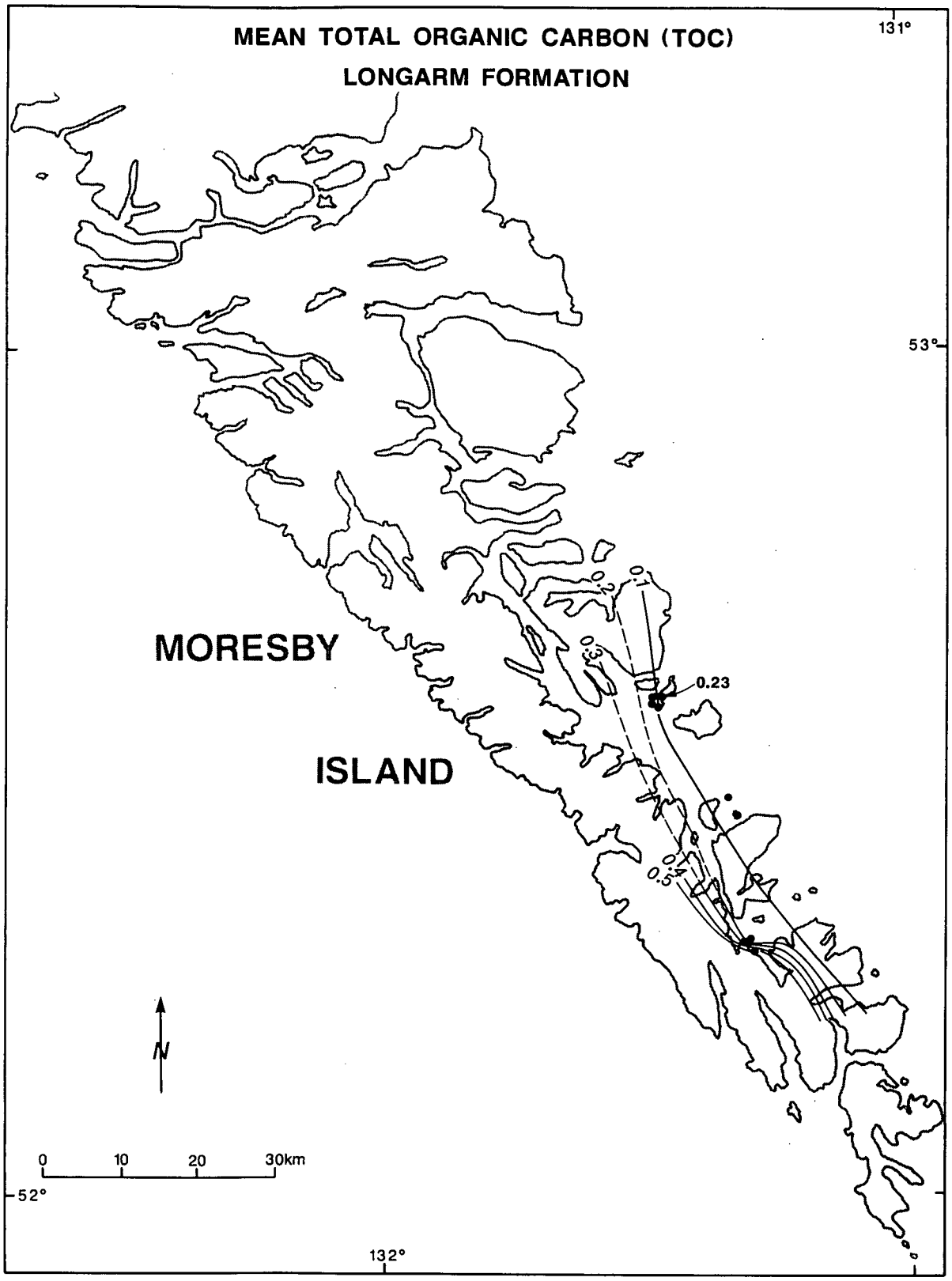

Figure 58. Regional distribution of the mean TOC content for the Longarm Formation. Values are mean TOC calculated across the thickness of the formation at each outcrop location. Dashed line represents an inferred contour. Labelled values do not fit regional trends and are not contoured.

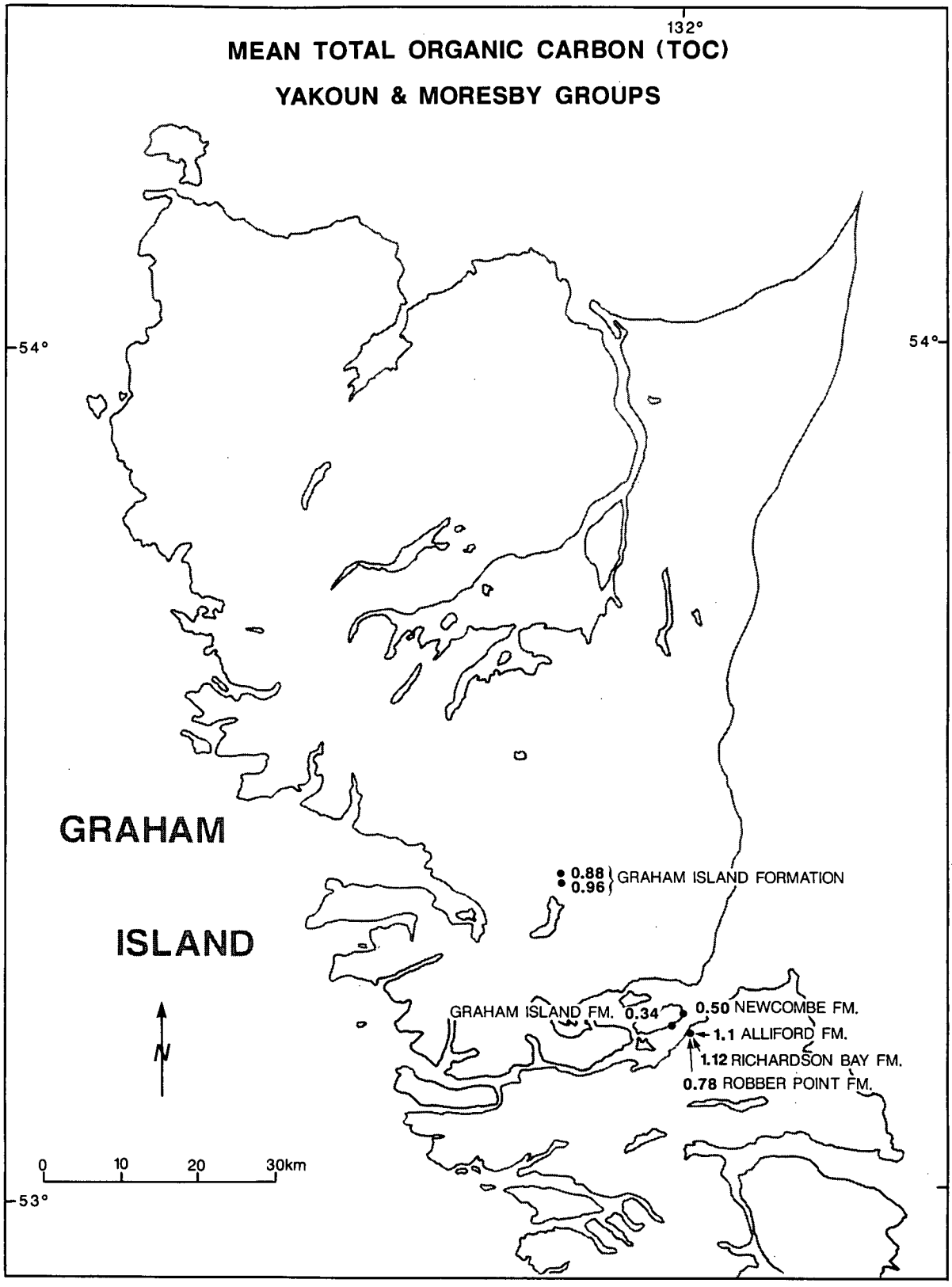

Figure 59. Regional distribution of the mean TOC content for the Yakoun and Moresby Groups. Values are mean TOC calculated across the thickness of the formation at each outcrop location.

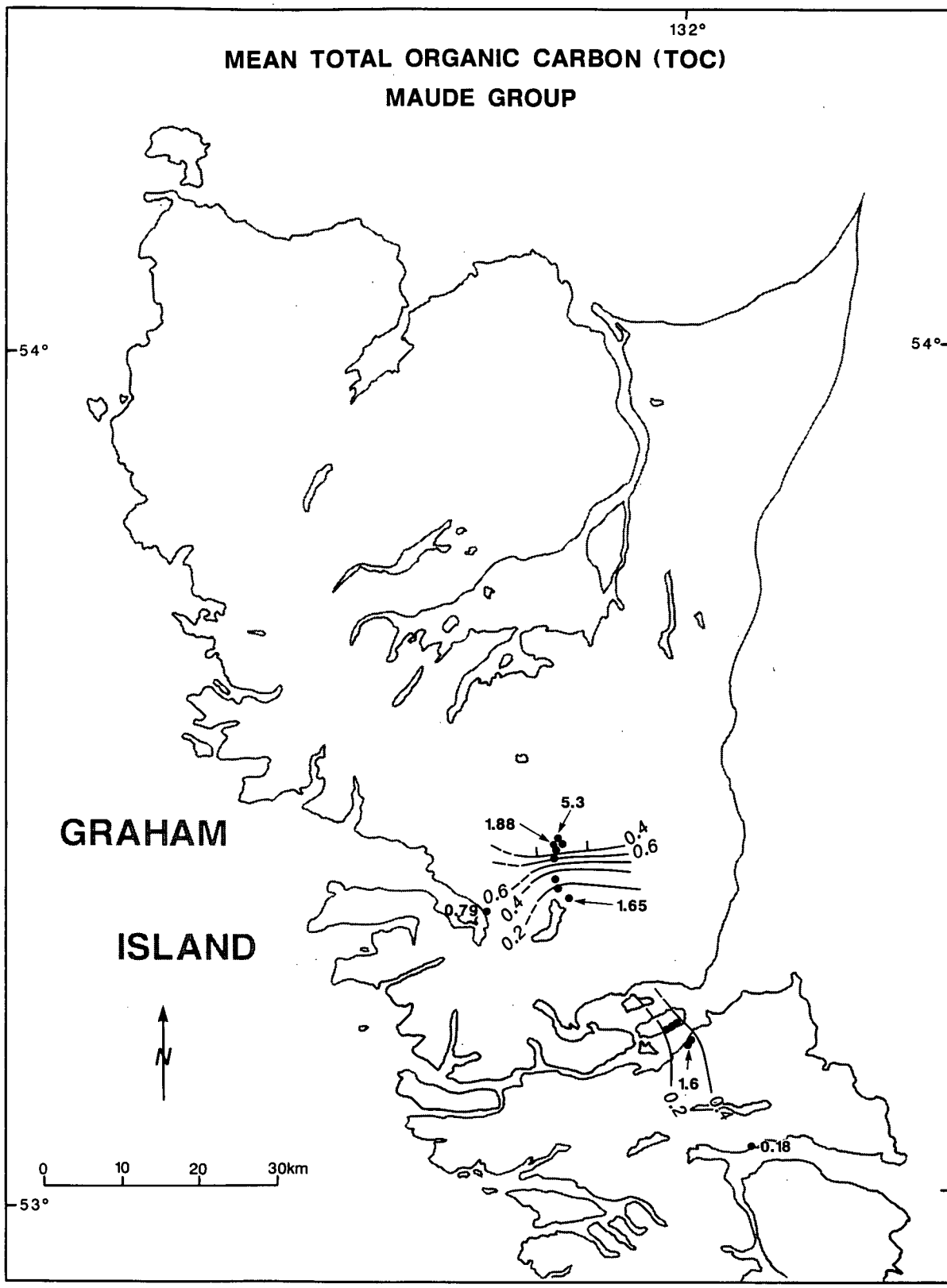

Figure 60. Regional distribution of the mean TOC content for the Maude Group. Values are mean TOC calculated across the thickness of the formation at each outcrop location. Dashed line represents an inferred contour. Labelled values do not fit regional trends and are not contoured.

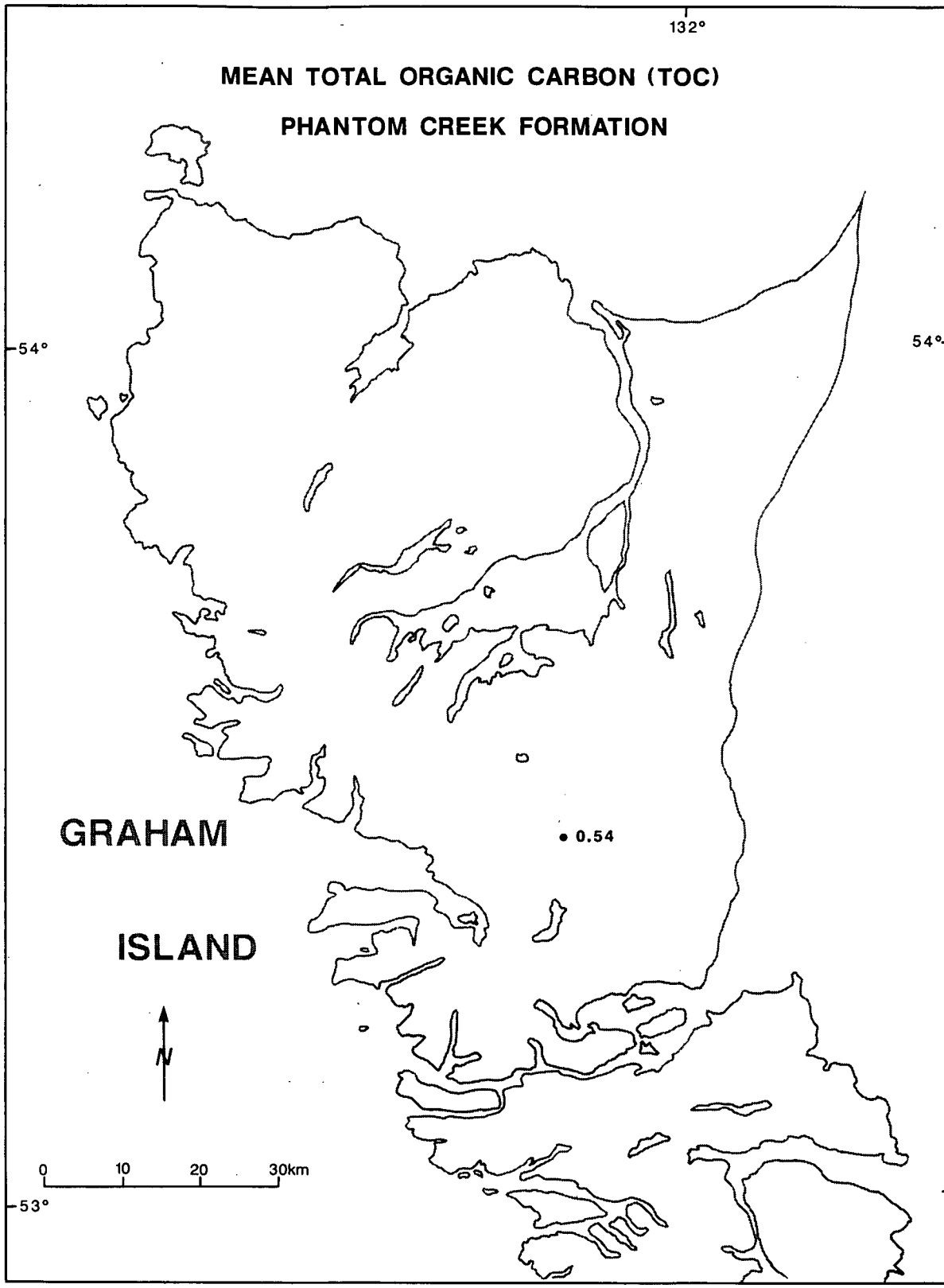

Figure 61. Regional distribution of the mean TOC content for the Phantom Creek Formation. Values are mean TOC calculated across the thickness of the formation at each outcrop location.

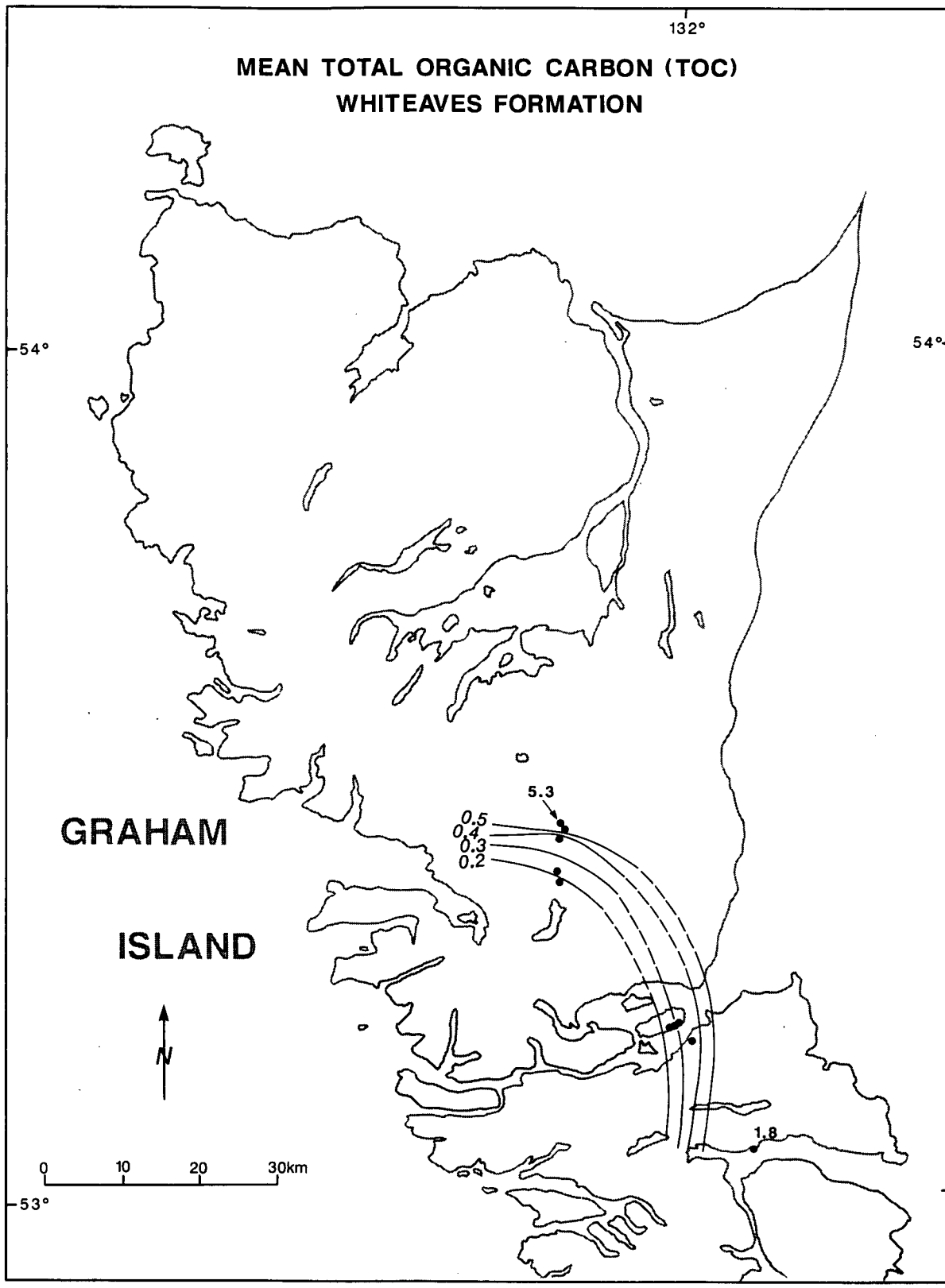

Figure 62. Regional distribution of the mean TOC content for the Whiteaves Formation. Values are mean TOC calculated across the thickness of the formation at each outcrop location. Dashed line represents an inferred contour. Labelled values do not fit regional trends and are not contoured.

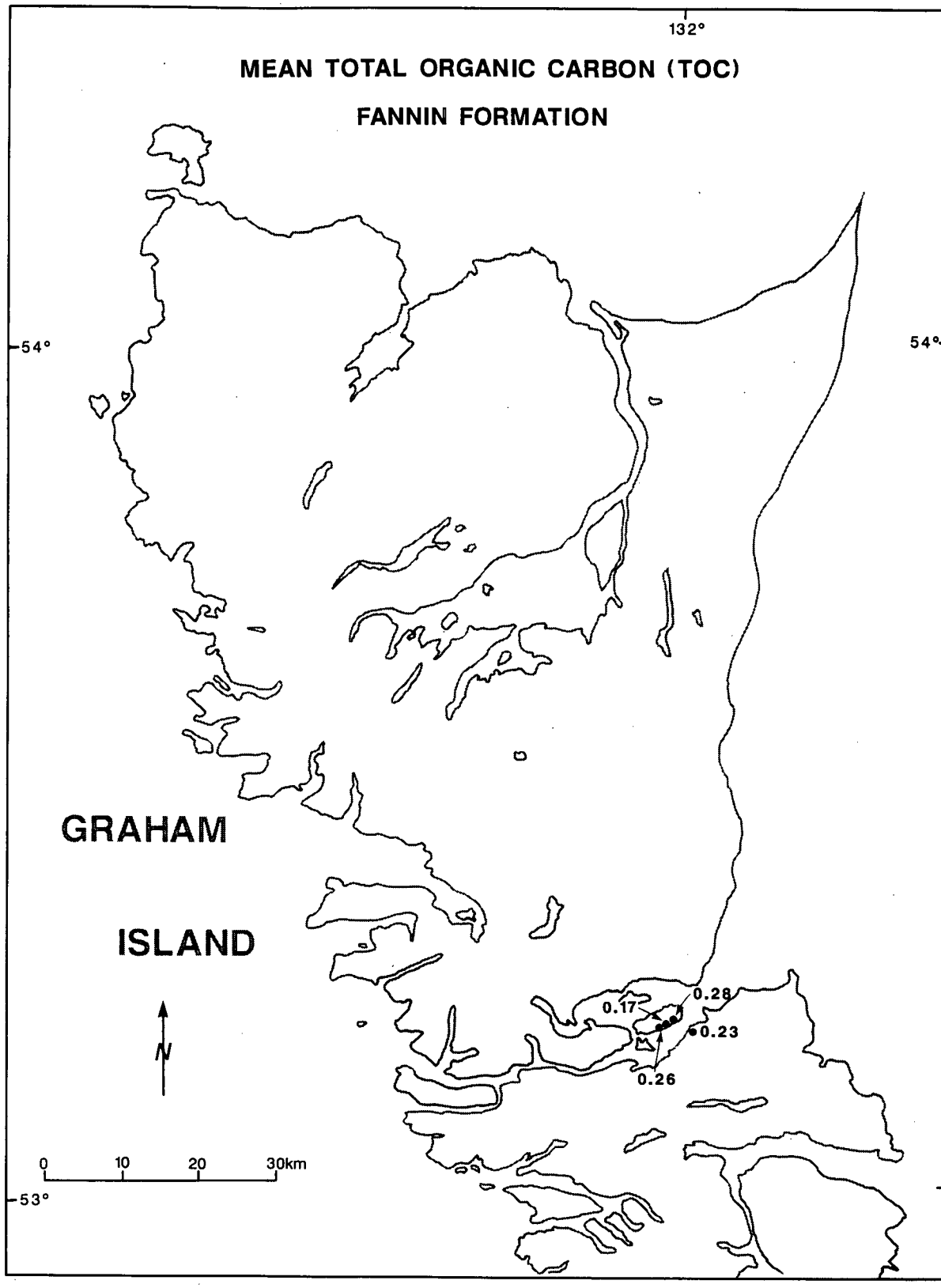

Figure 63. Regional distribution of the mean TOC content for the Fannin Formation. Values are mean TOC calculated across the thickness of the formation at each outcrop location.

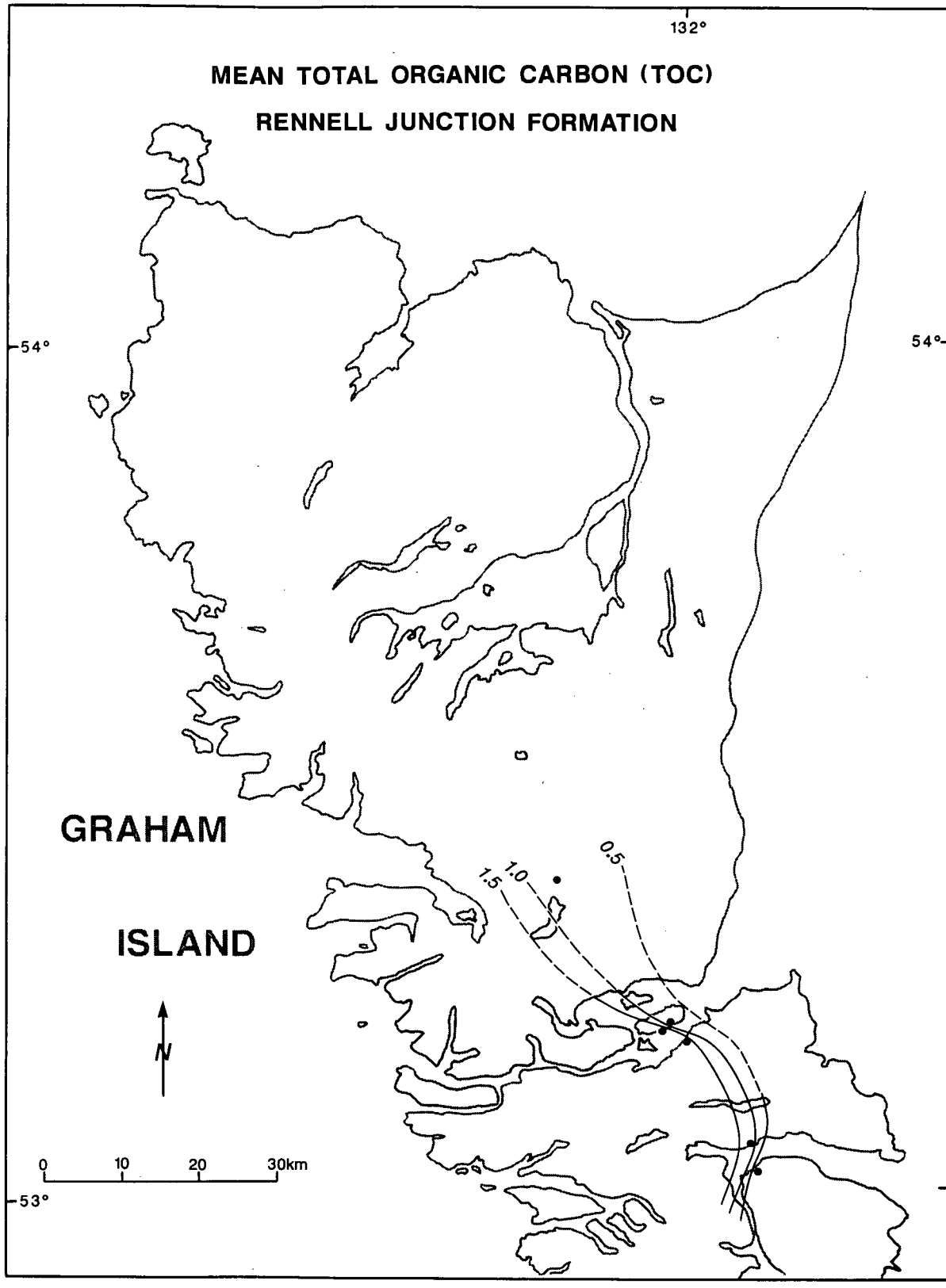

Figure 64. Regional distribution of the mean TOC content for the Rennell Formation. Values are mean TOC calculated across the thickness of the formation at each outcrop location. Dashed line represents an inferred contour. Labelled values do not fit regional trends and are not contoured.

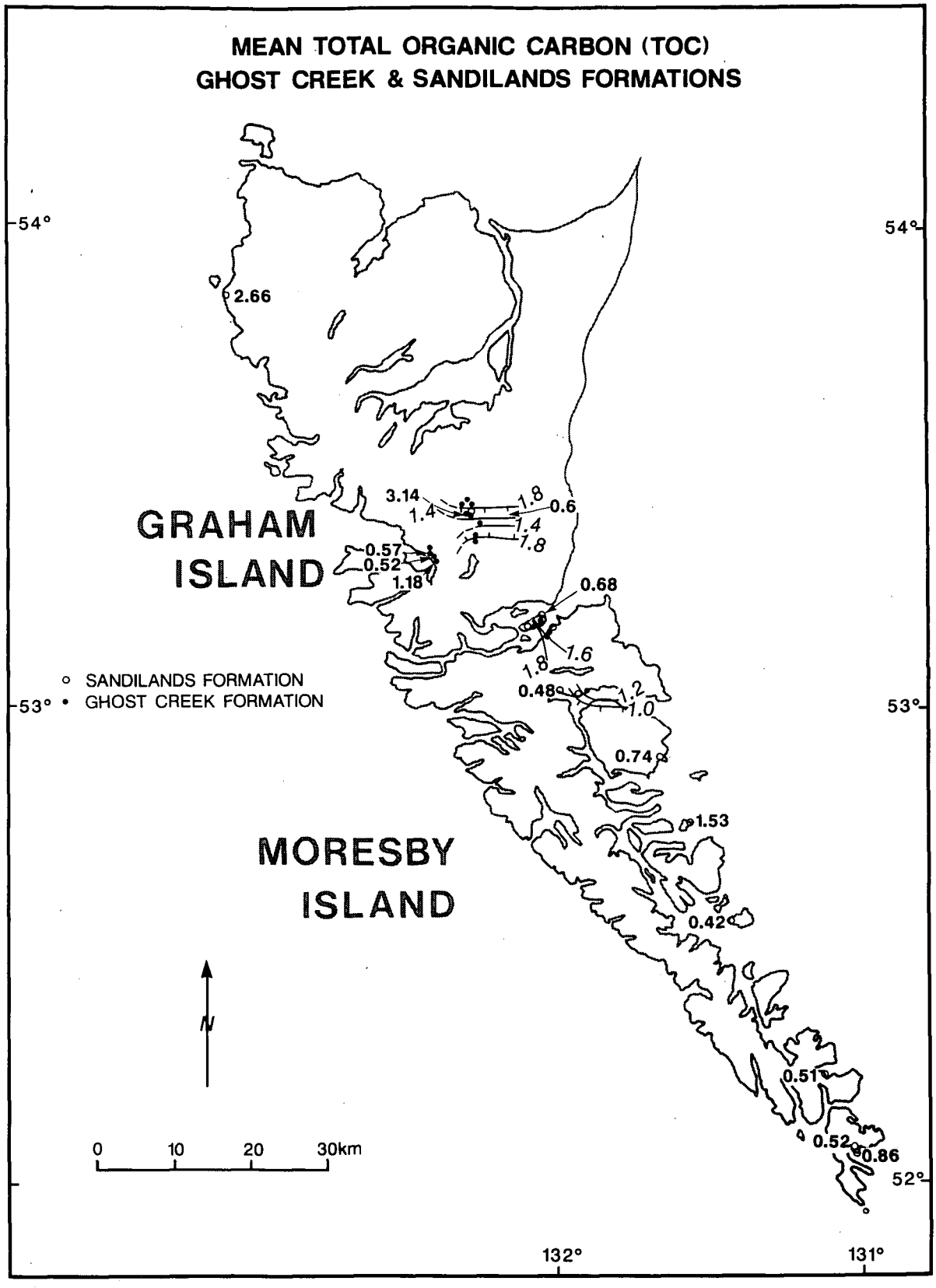

Figure 65. Regional distribution of the mean TOC content for the Ghost Creek and Sandilands Formations. Values are average TOC calculated across the thickness of the formation at each outcrop location. Dashed line represents an inferred contour. Labelled values do not fit regional trends and are not contoured. Tick marks on contour indicate decreasing TOC.

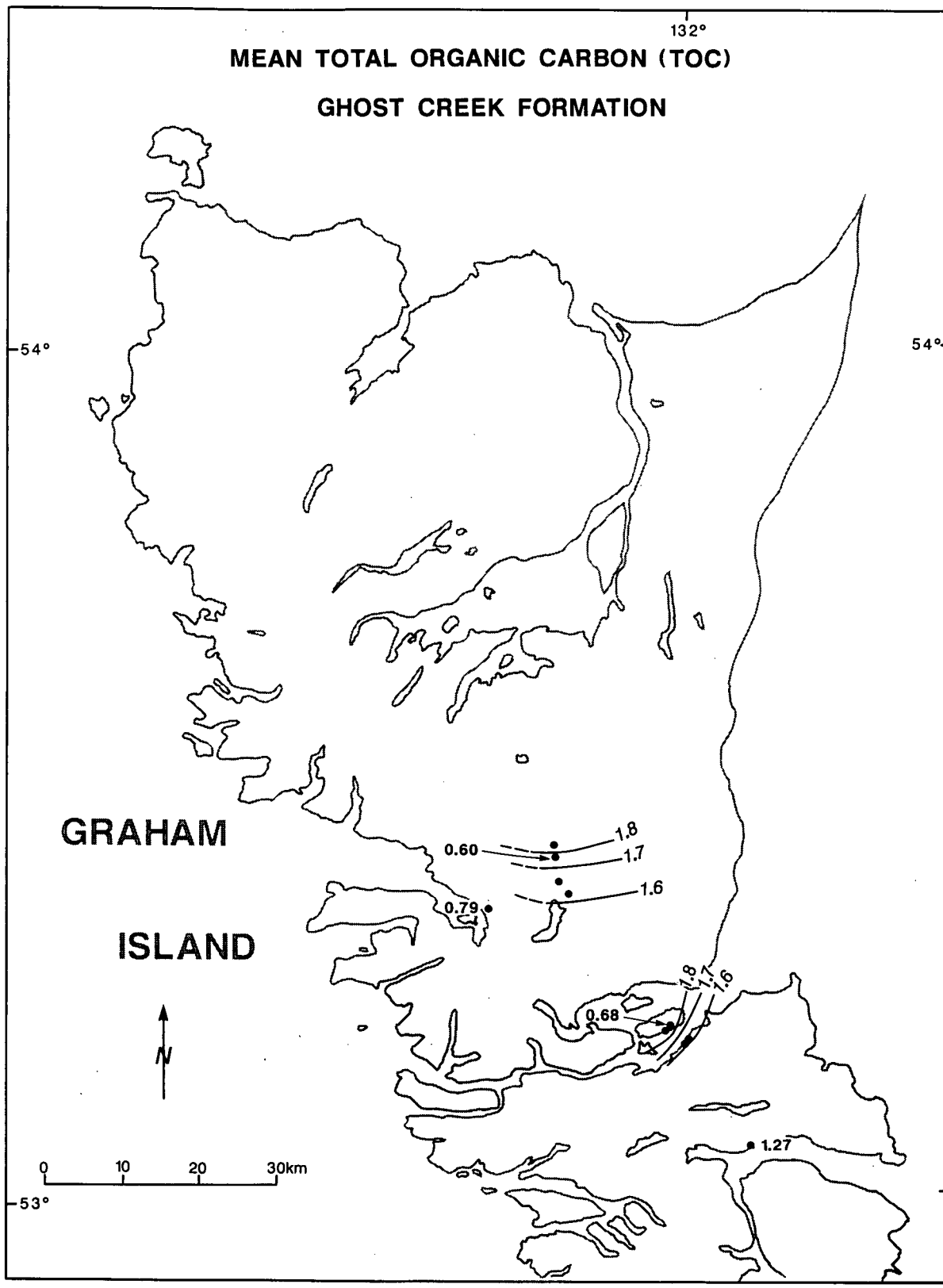

Figure 66. Regional distribution of the average TOC content for the Ghost Creek Formation. Values are average TOC calculated across the thickness of the formation at each outcrop location. Dashed line represents an inferred contour. Labelled values do not fit regional trends and are not contoured.

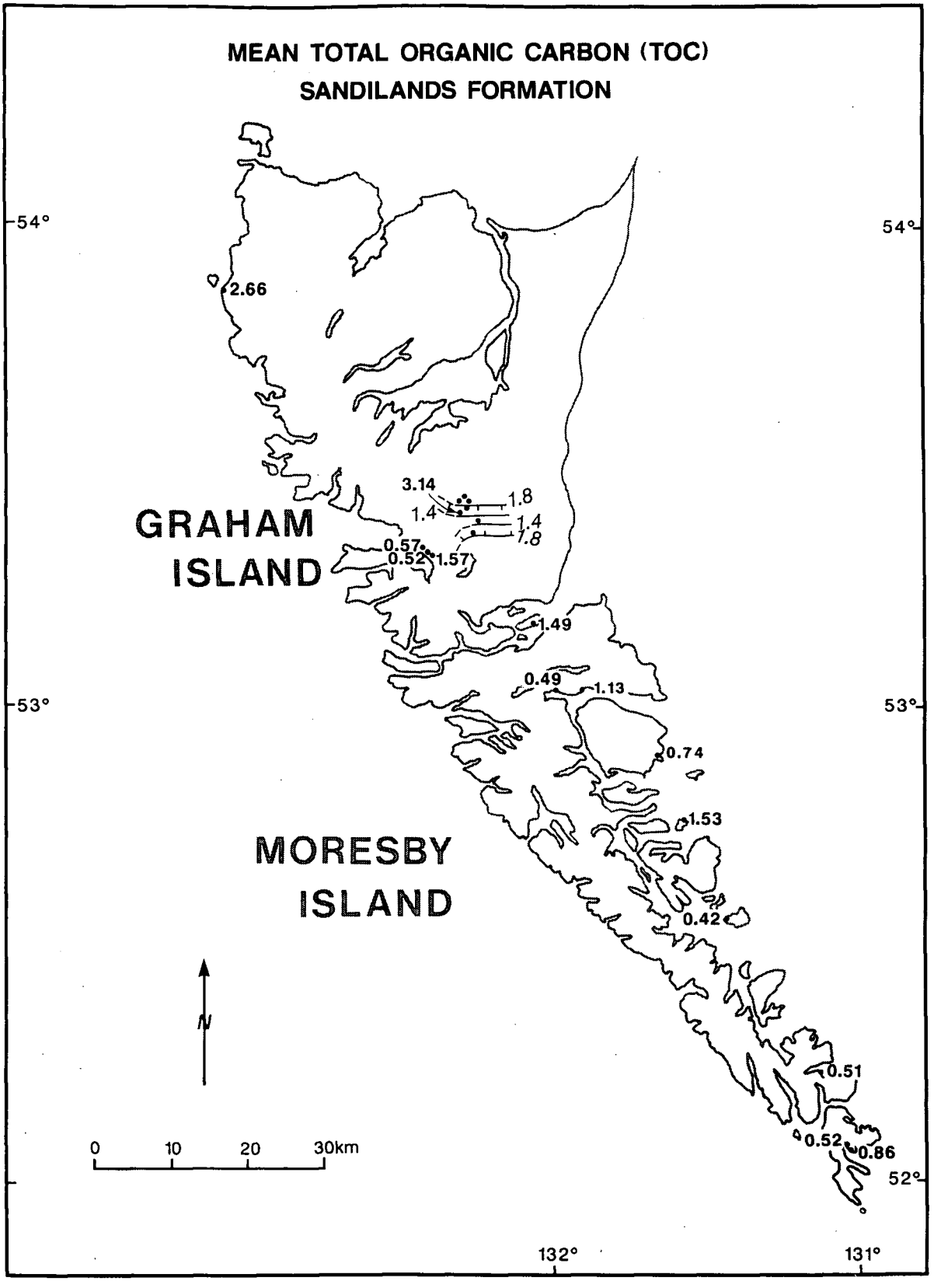

Figure 67. Regional distribution of the average TOC content for the Sandilands Formation. Values are average TOC calculated across the thickness of the formation at each outcrop location. Dashed line represents an inferred contour. Labelled values do not fit regional trends and are not contoured. Tick marks on contour indicate decreasing TOC.

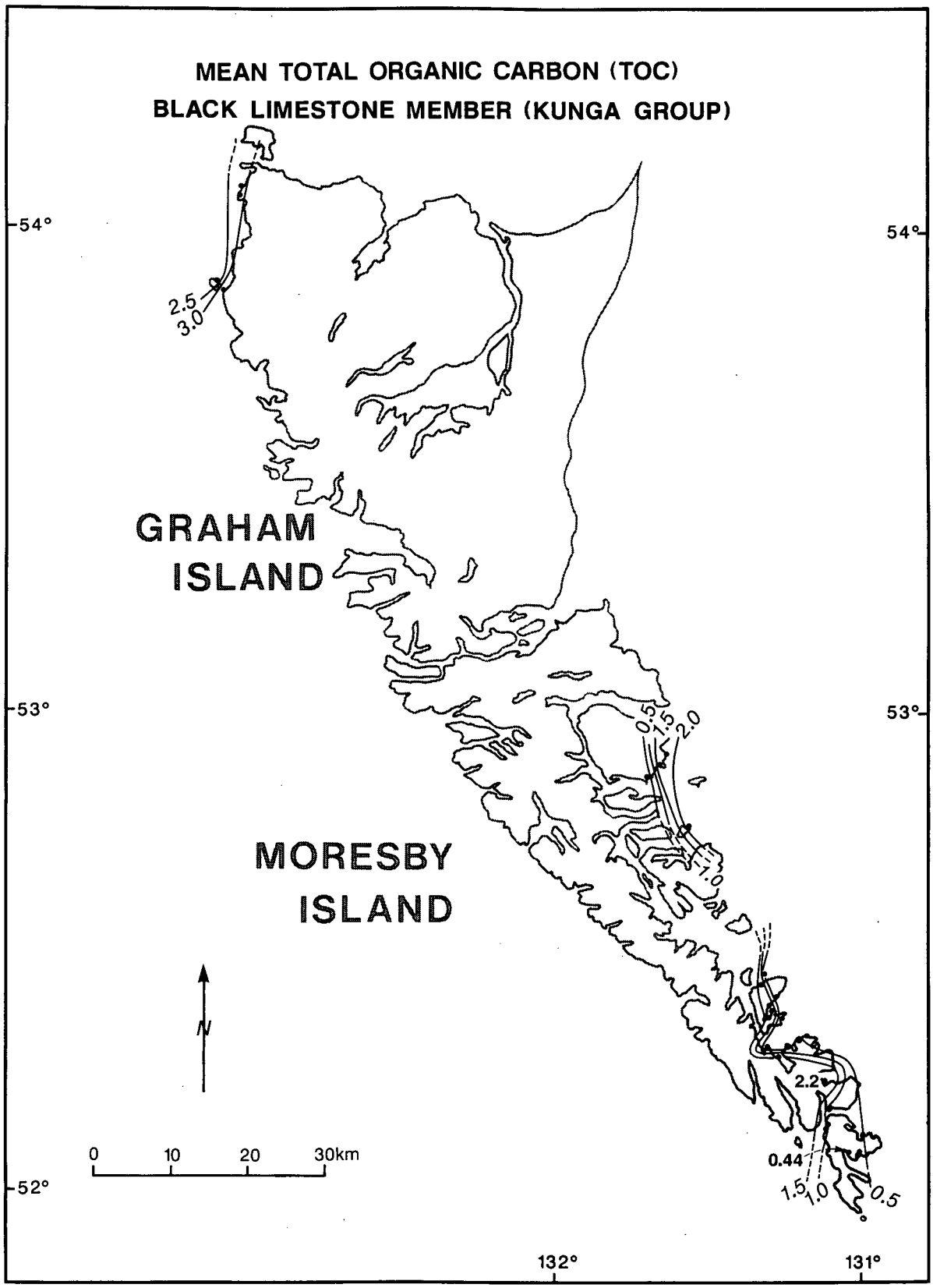

Figure 68. Regional distribution of the average TOC content for the black limestone member (Kunga Group). Values are average TOC calculated across the thickness of the formation at each outcrop location. Dashed line represents an inferred contour. Labelled values do not fit regional trends and are not contoured.

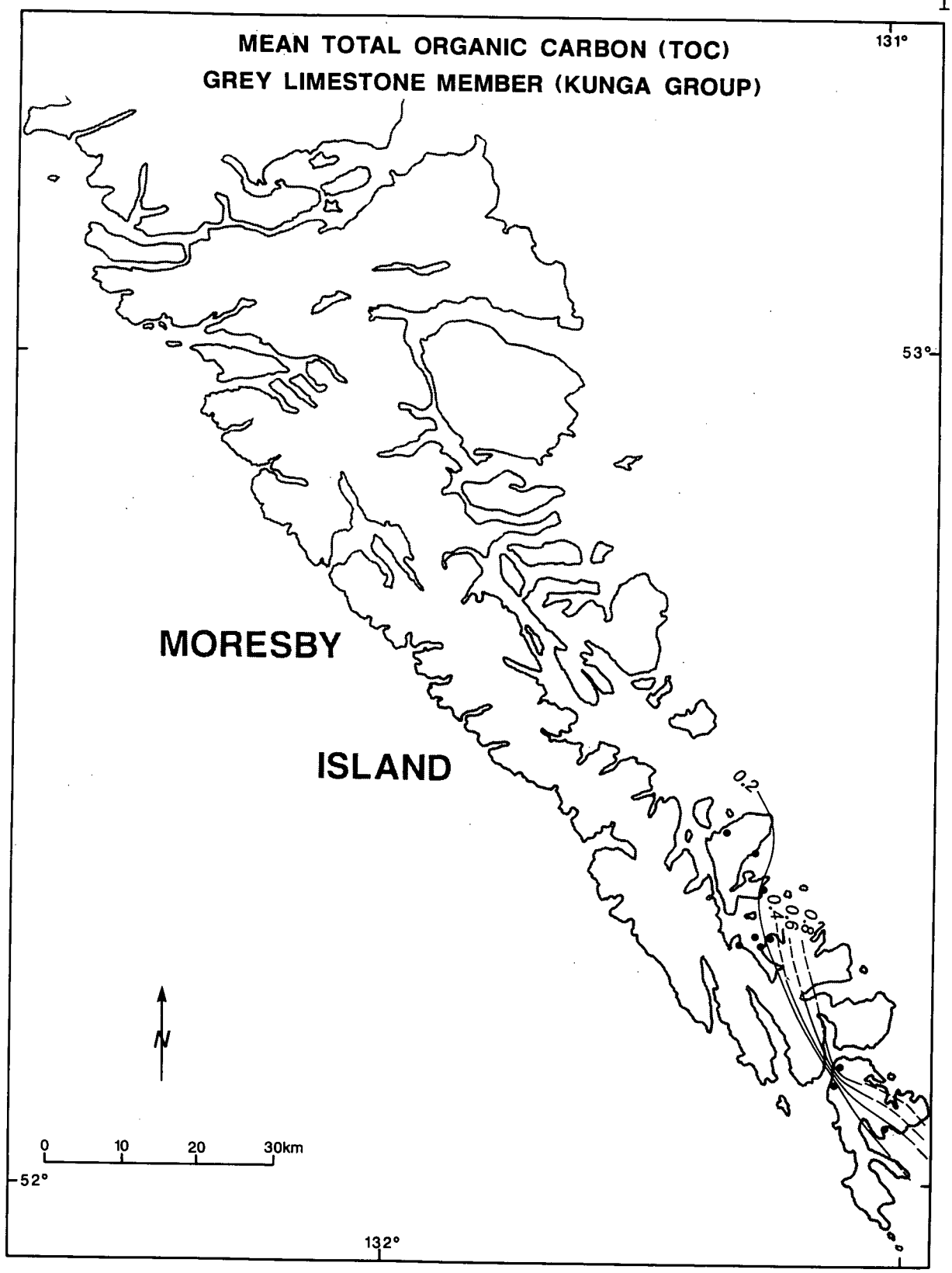

Figure 69. Regional distribution of the average TOC content for the grey limestone member (Kunga Group). Values are average TOC calculated across the thickness of the formation at each outcrop location. Dashed line represents an inferred contour.

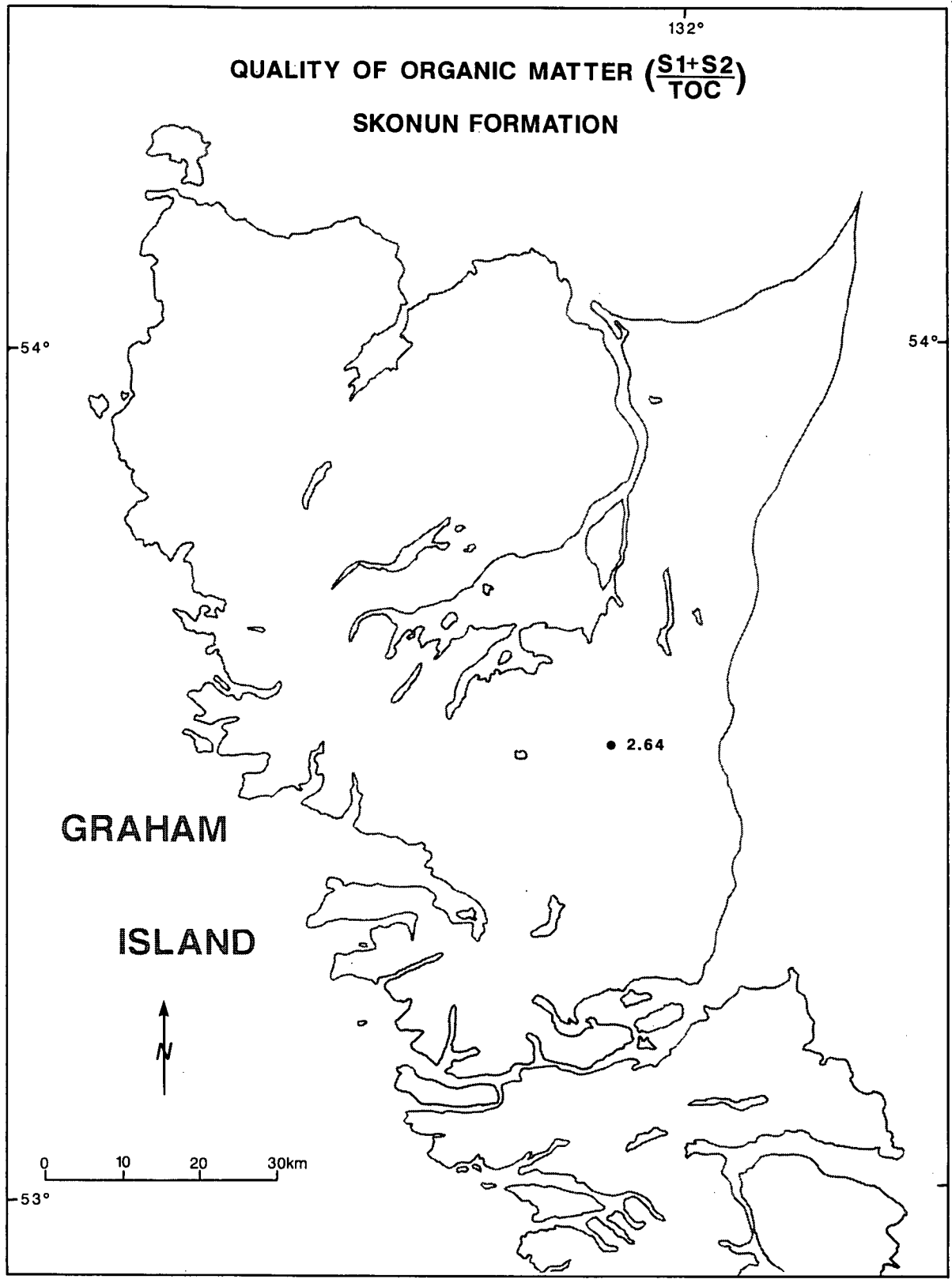

Figure 70. Regional distribution of the average QOM [(S1+S2)/TOC] for the Skonun Formation. Values are average QOM calculated across the thickness of the formation at each outcrop location.

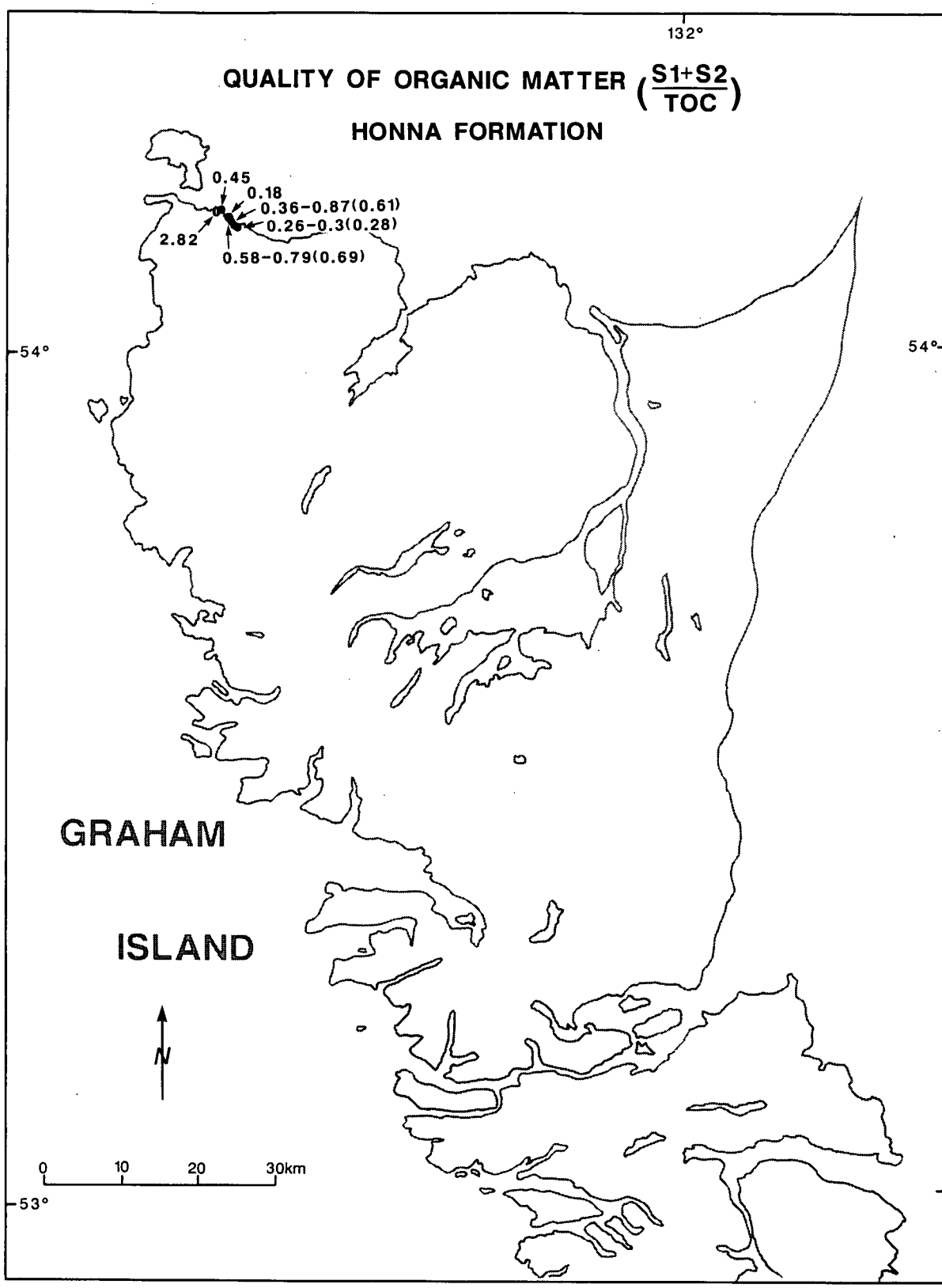

Figure 71. Regional distribution of the average QOM [(S1+S2)/TOC] for the Honna Formation. Values are average QOM calculated across the thickness of the formation at each outcrop location. Values in brackets are mean QOM. Dashed values are minimum and maximum QOM.

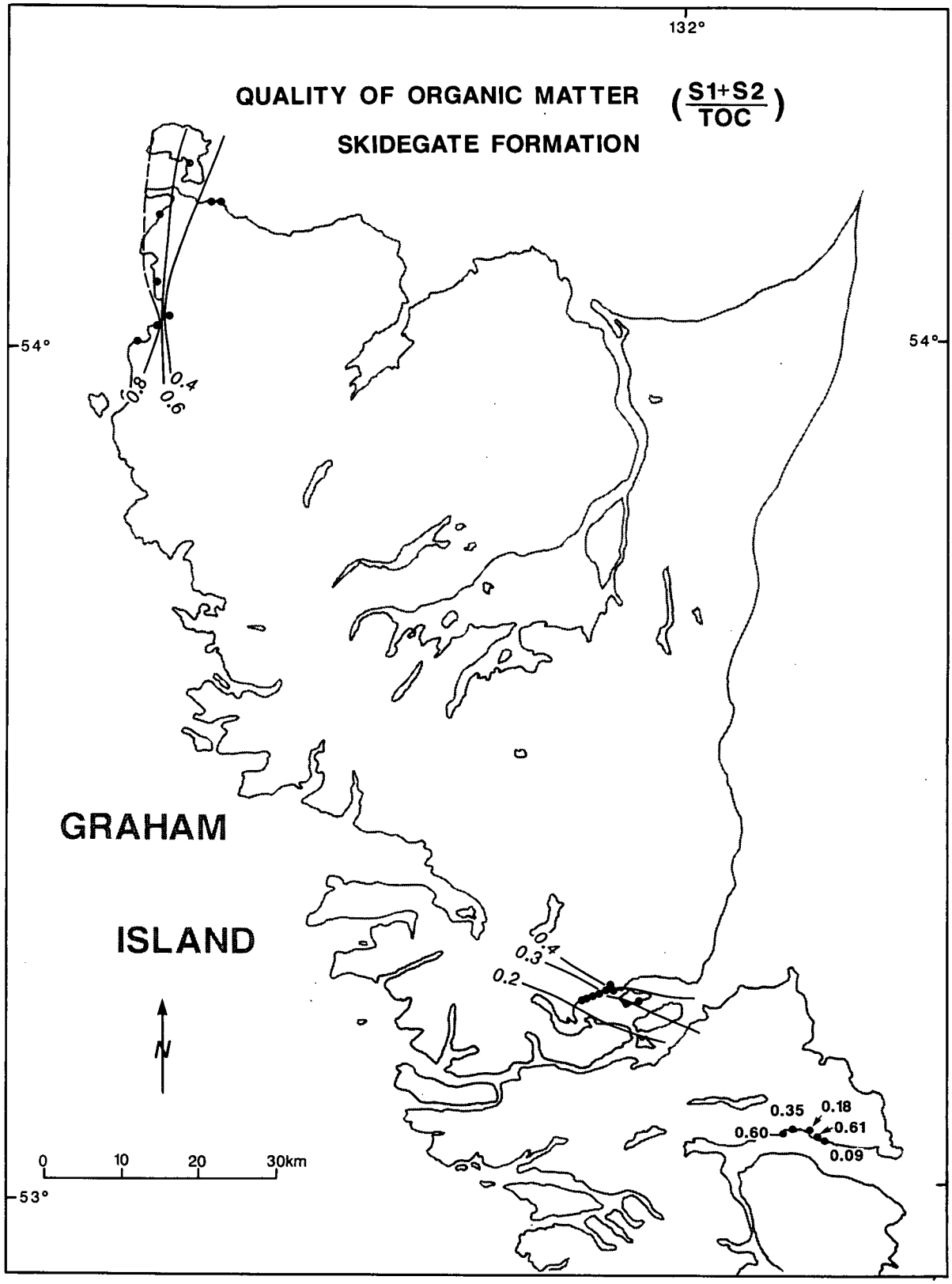

Figure 72. Regional distribution of the average QOM [(S1+S2)/TOC] for the Skidegate Formation. Values are average QOM calculated across the thickness of the formation at each outcrop location. Dashed line represents inferred contour.

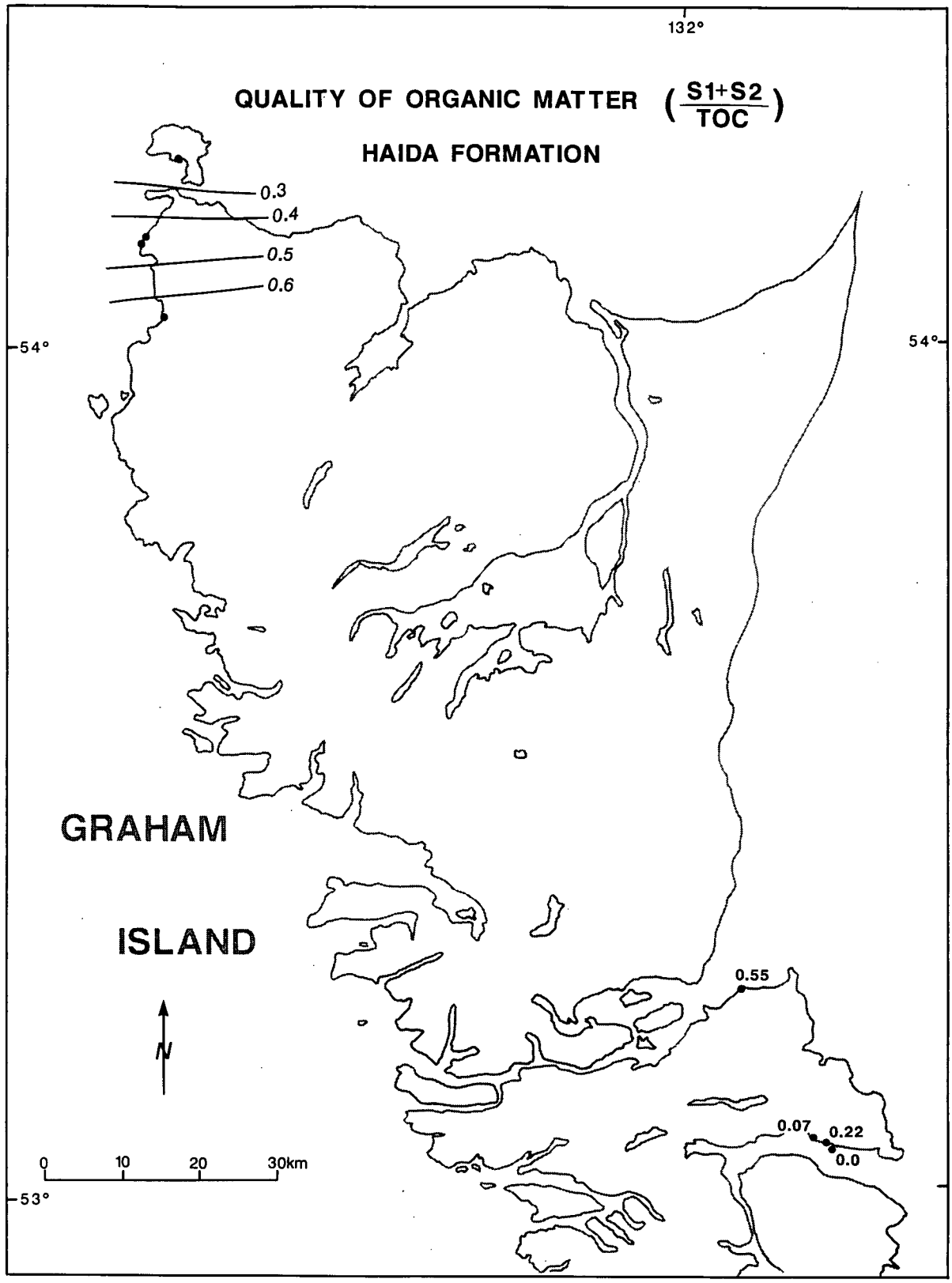

Figure 73. Regional distribution of the average QOM [(S1 + S2)/TOC] for the Haida Formation. Values are average QOM calculated across the thickness of the formation at each outcrop location.

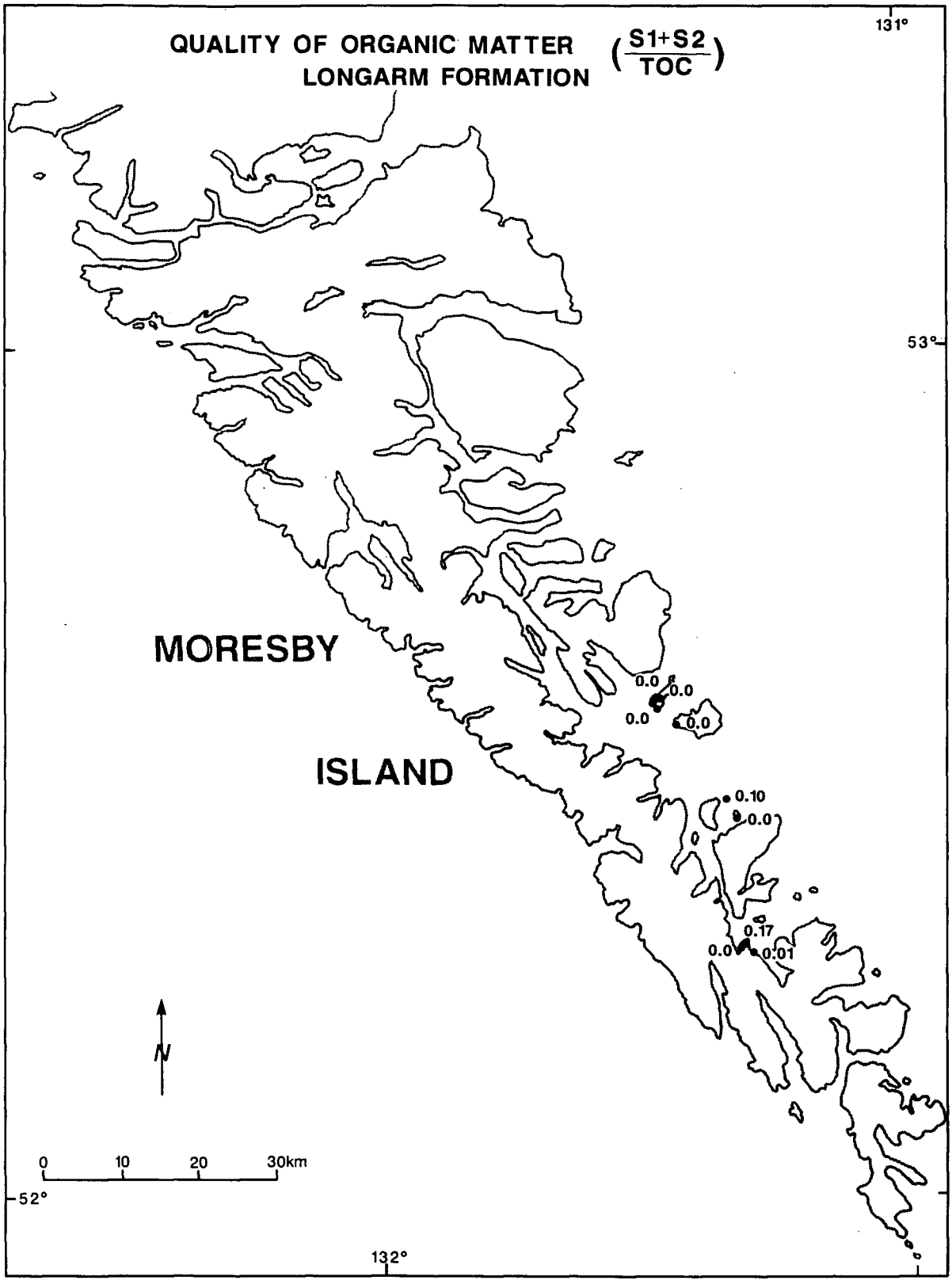

Figure 74. Regional distribution of the average QOM [(S1+S2)/TOC] for the Longarm Formation. Values are average QOM calculated across the thickness of the formation at each outcrop location.

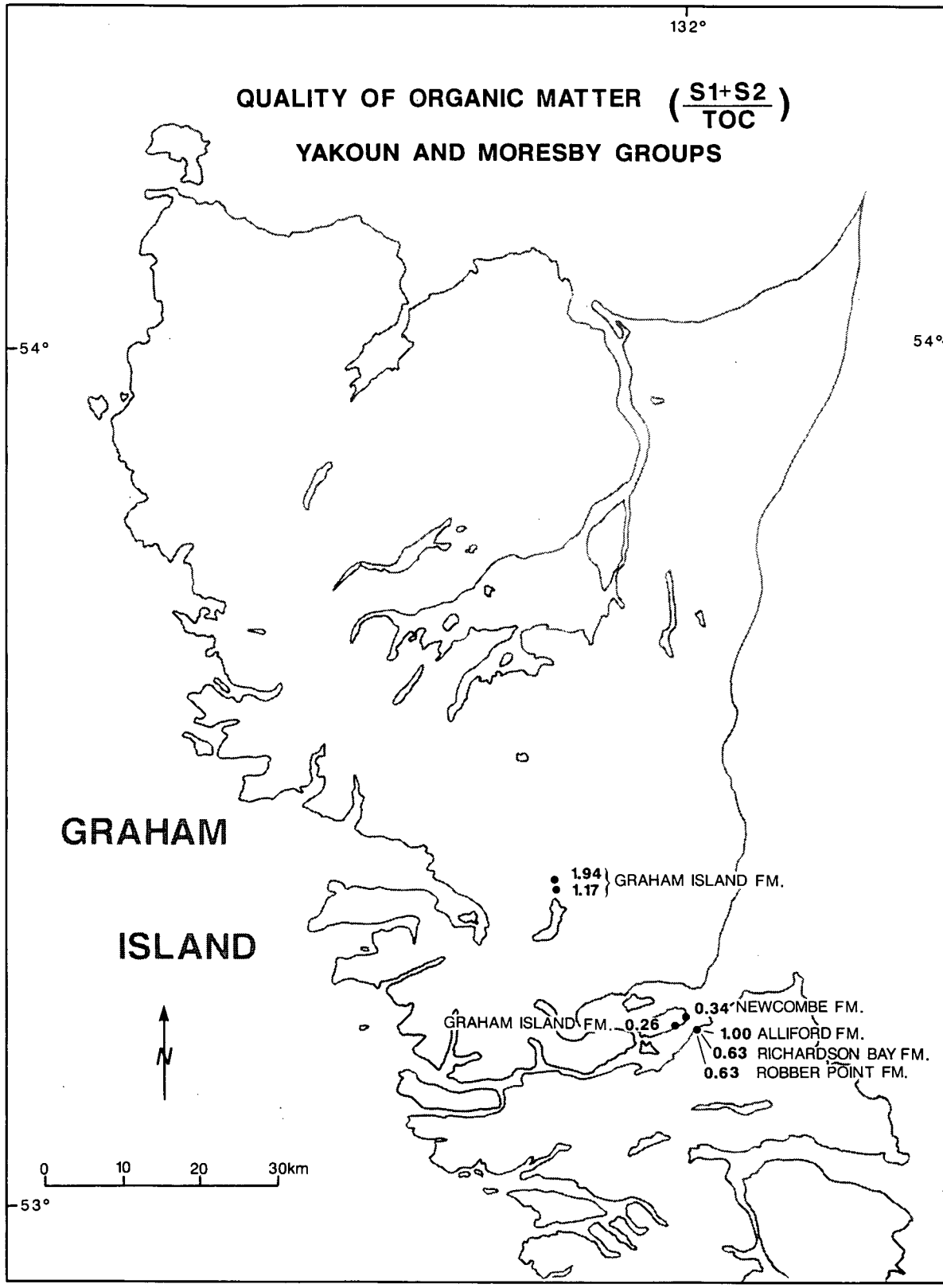

Figure 75. Regional distribution of the average QOM [(S1+S2)/TOC] for the Yakoun and Moresby Groups. Values are average QOM calculated across the thickness of the formation at each outcrop location.

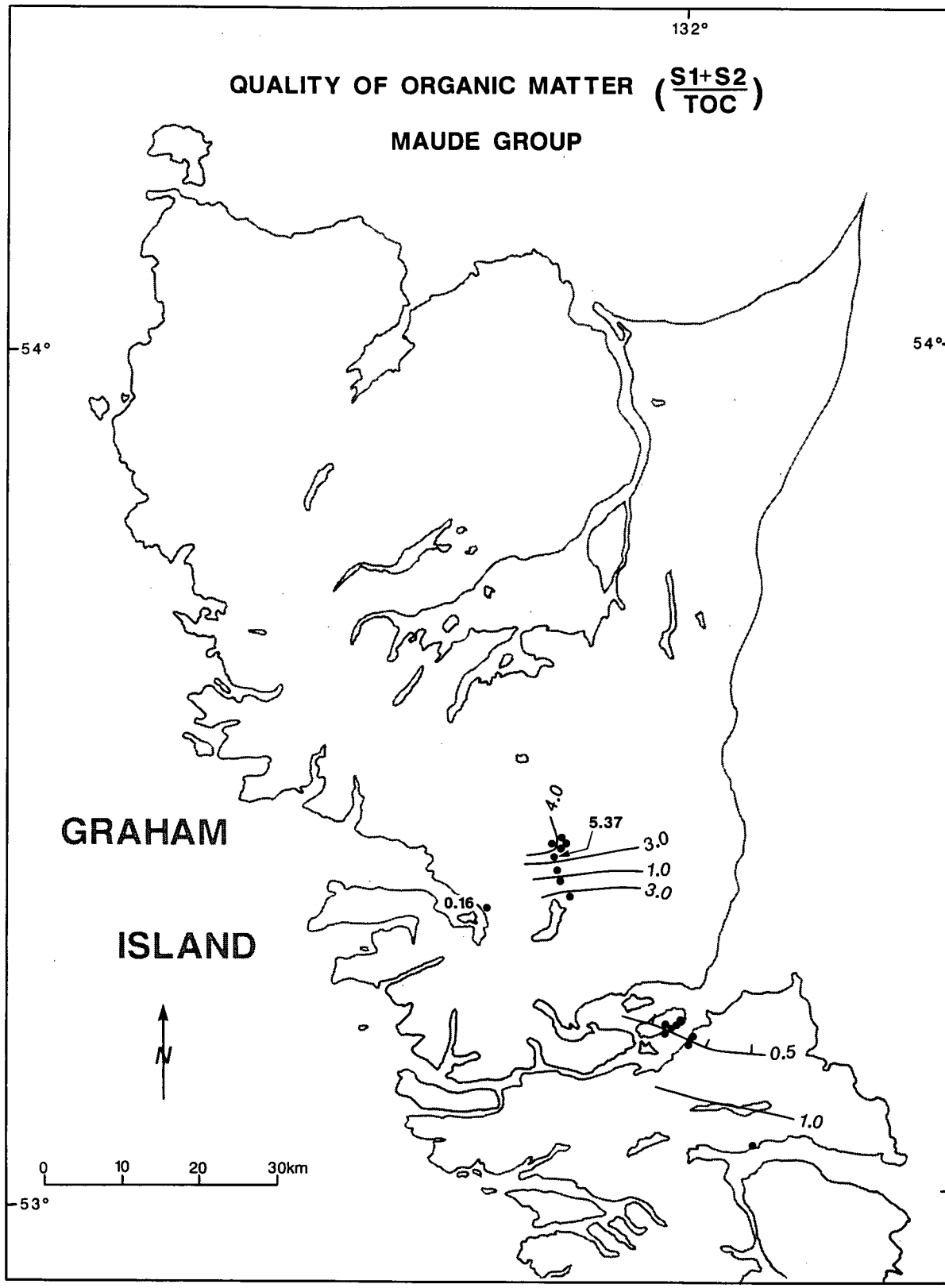

Figure 76. Regional distribution of the average QOM [(S1+S2)/TOC] for the Maude Group. Values are average QOM calculated across the thickness of the formation at each outcrop location. Tick marks on contour line indicate decreasing QOM.

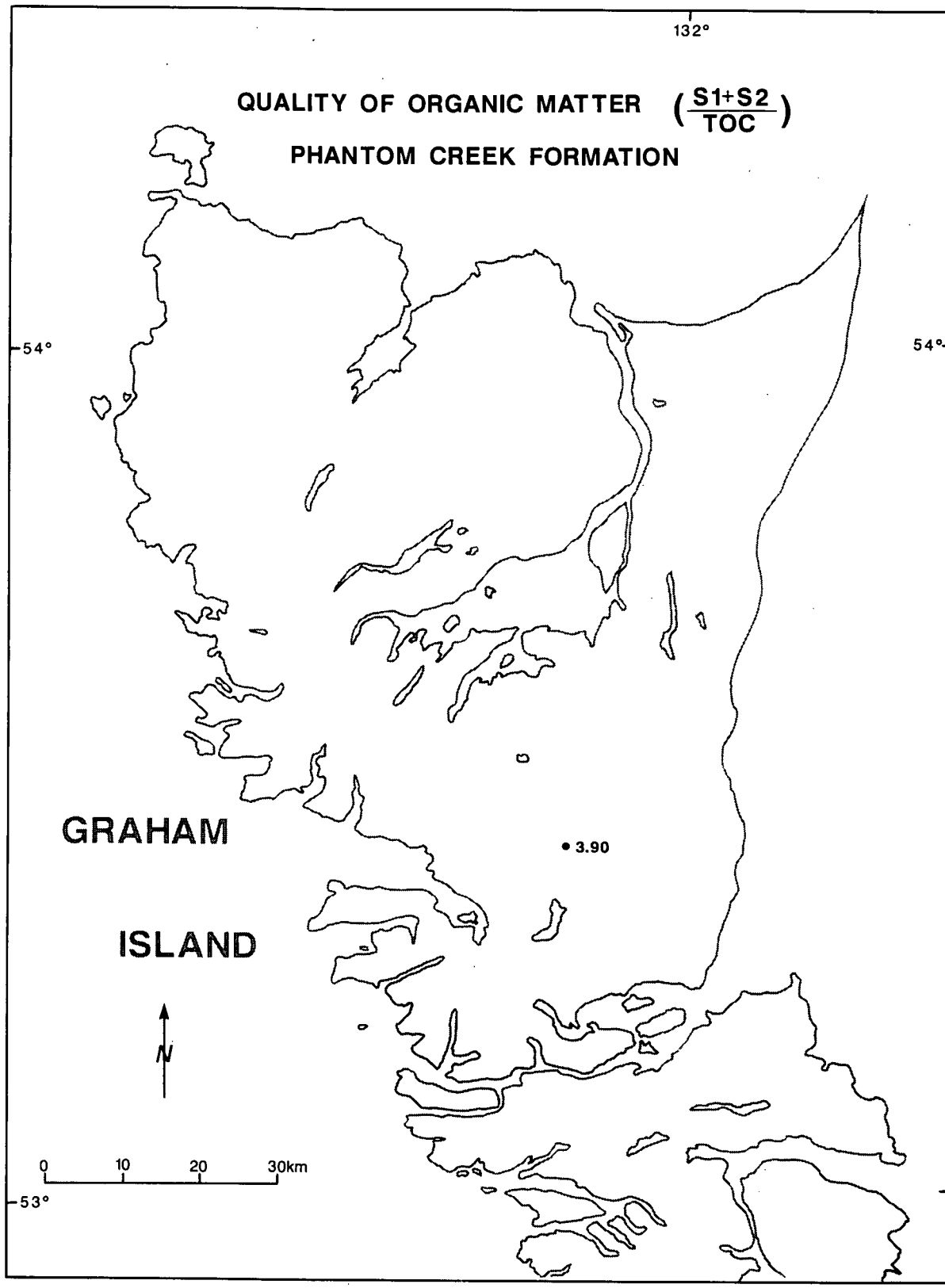

Figure 77. Regional distribution of the average QOM [(S1+S2)/TOC] for the Phantom Creek Formation. Values are average QOM calculated across the thickness of the formation at each outcrop location.

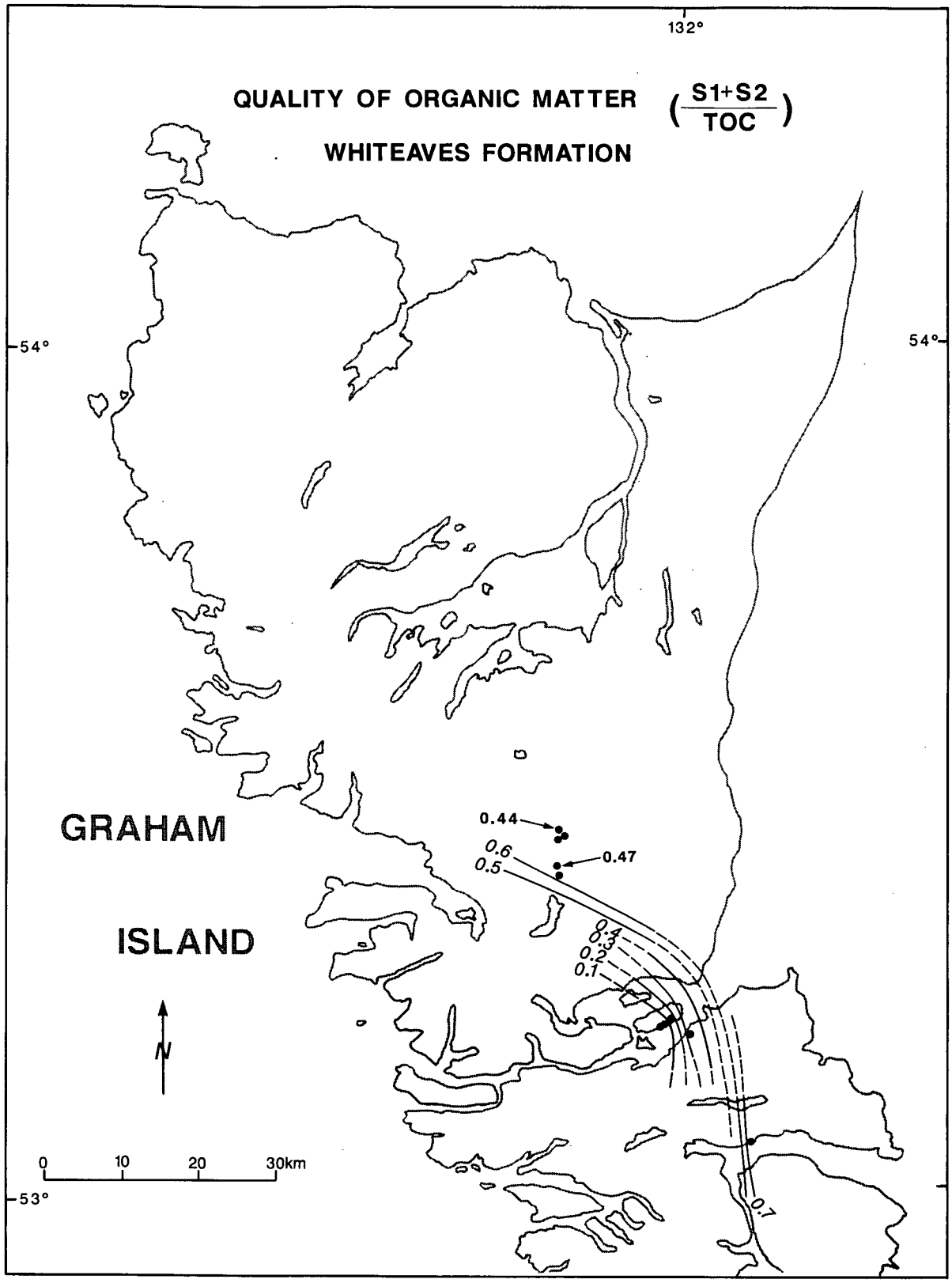

Figure 78. Regional distribution of the average QOM [(S1+S2)/TOC] for the Whiteaves Formation. Values are average QOM calculated across the thickness of the formation at each outcrop location. Dashed line represents inferred contour. Labelled values do not fit regional trends and are not contoured.

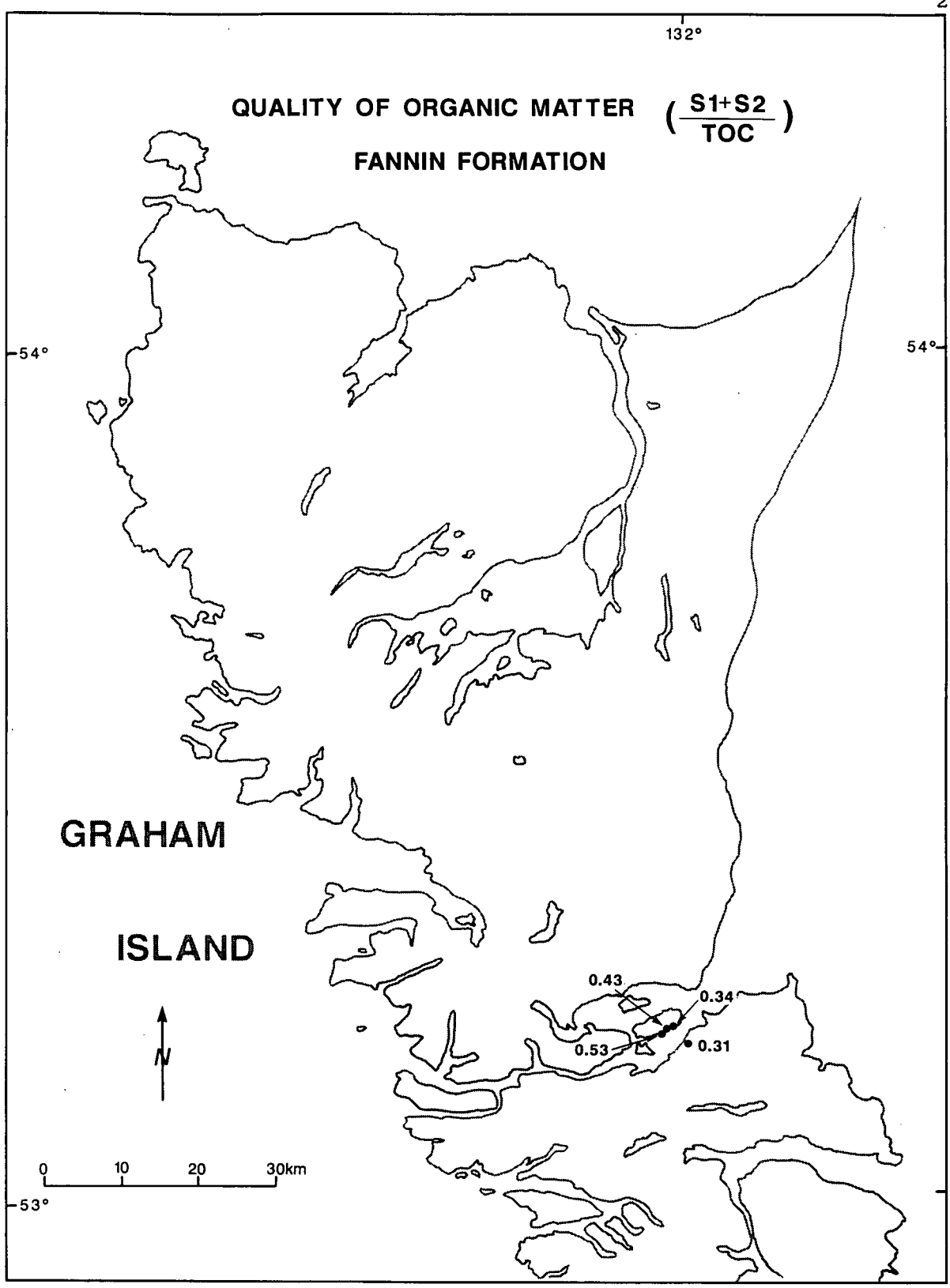

Figure 79. Regional distribution of the average QOM [(S1+S2)/TOC] for the Fannin Formation. Values are average QOM calculated across the thickness of the formation at each outcrop location.

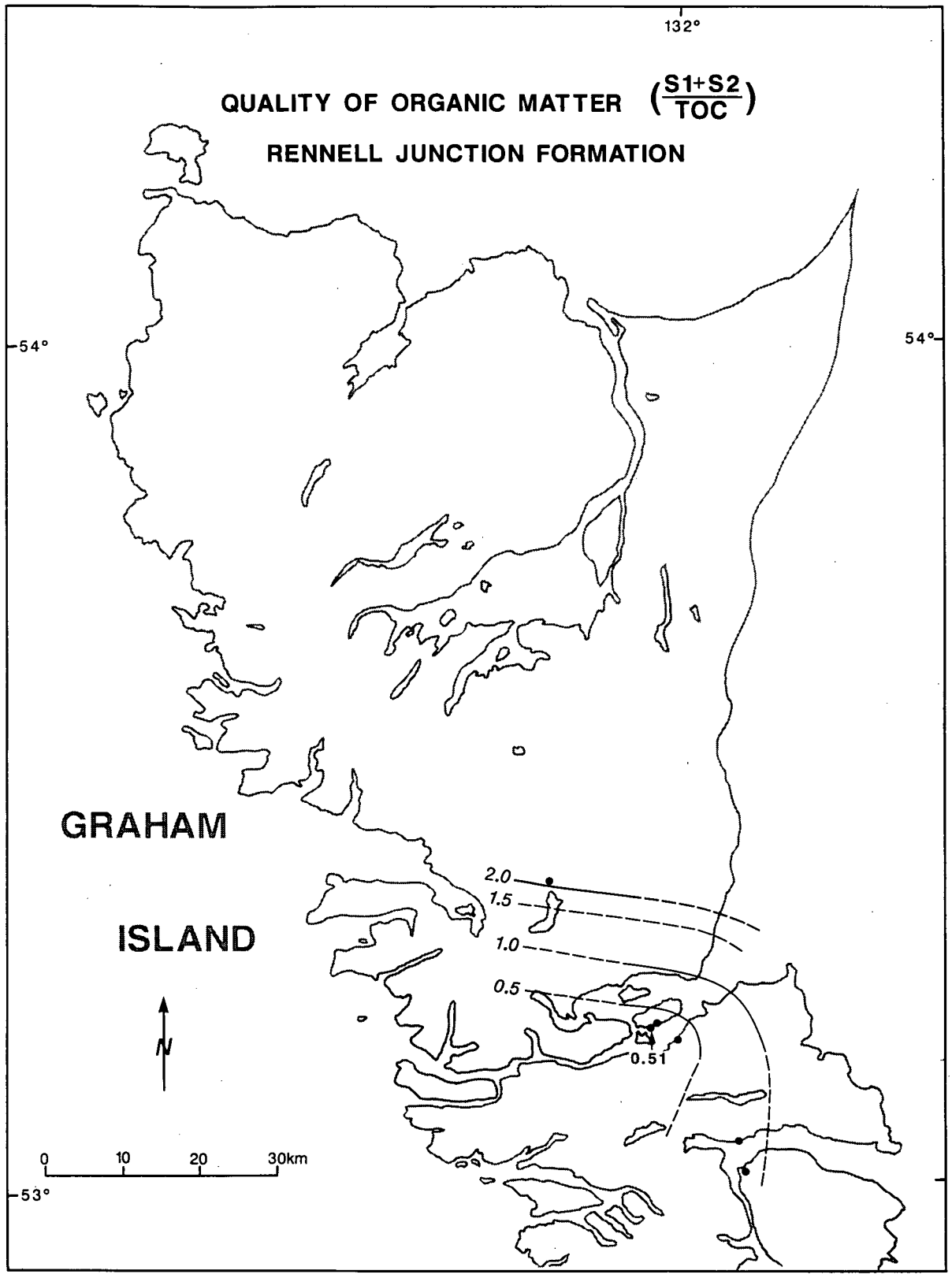

Figure 80. Regional distribution of the average QOM [(S1+S2)/TOC] for the Rennell Junction Formation. Values are average QOM calculated across the thickness of the formation at each outcrop location. Dashed line represents inferred contour. Labelled values do not fit regional trends and are not contoured.

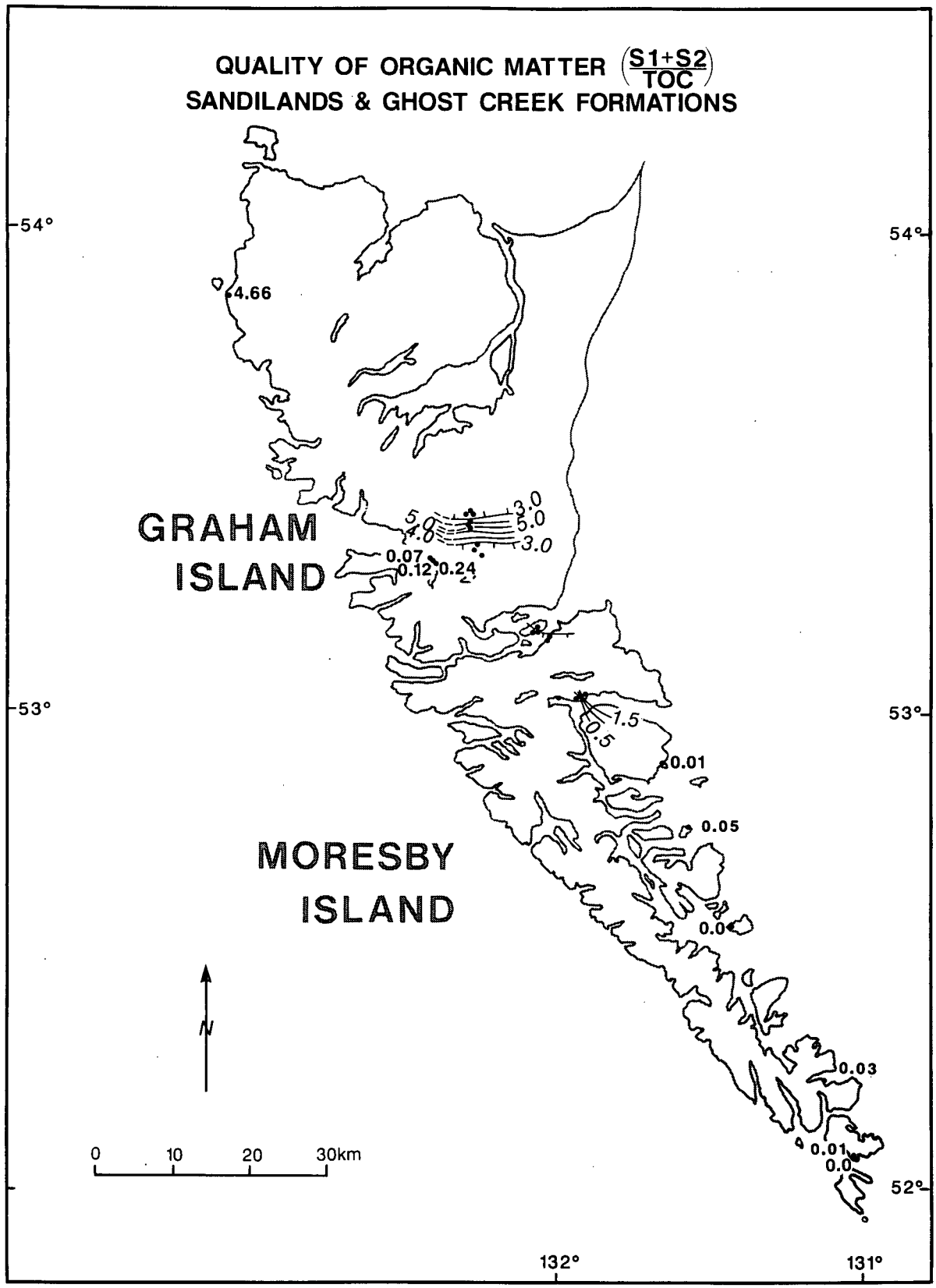

Figure 81. Regional distribution of the average QOM [(S1+S2)/TOC] for the Sandilands and Ghost Creek Formations. Values are average QOM calculated across the thickness of the formation at each outcrop location. Dashed line represents inferred contour. Labelled values do not fit regional trends and are not contoured. Tick mark on contour line indicates decreasing QOM.

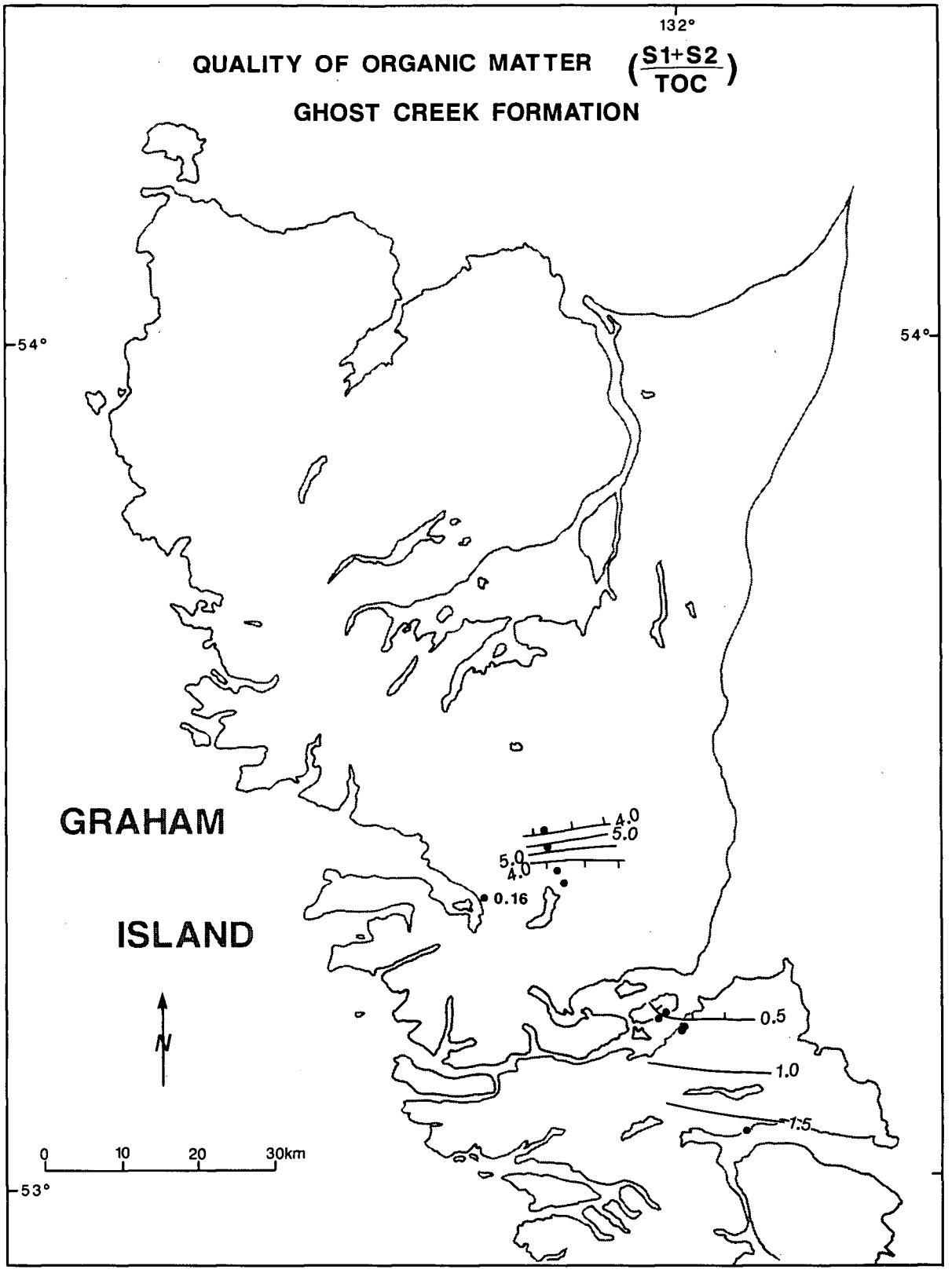

Figure 82. Regional distribution of the average QOM [(S1+S2)/TOC] for the Ghost Creek Formation. Values are average QOM calculated across the thickness of the formation at each outcrop location. Dashed line represents inferred contour. Labelled values do not fit regional trends and are not contoured. Tick mark on contour line indicates decreasing QOM.

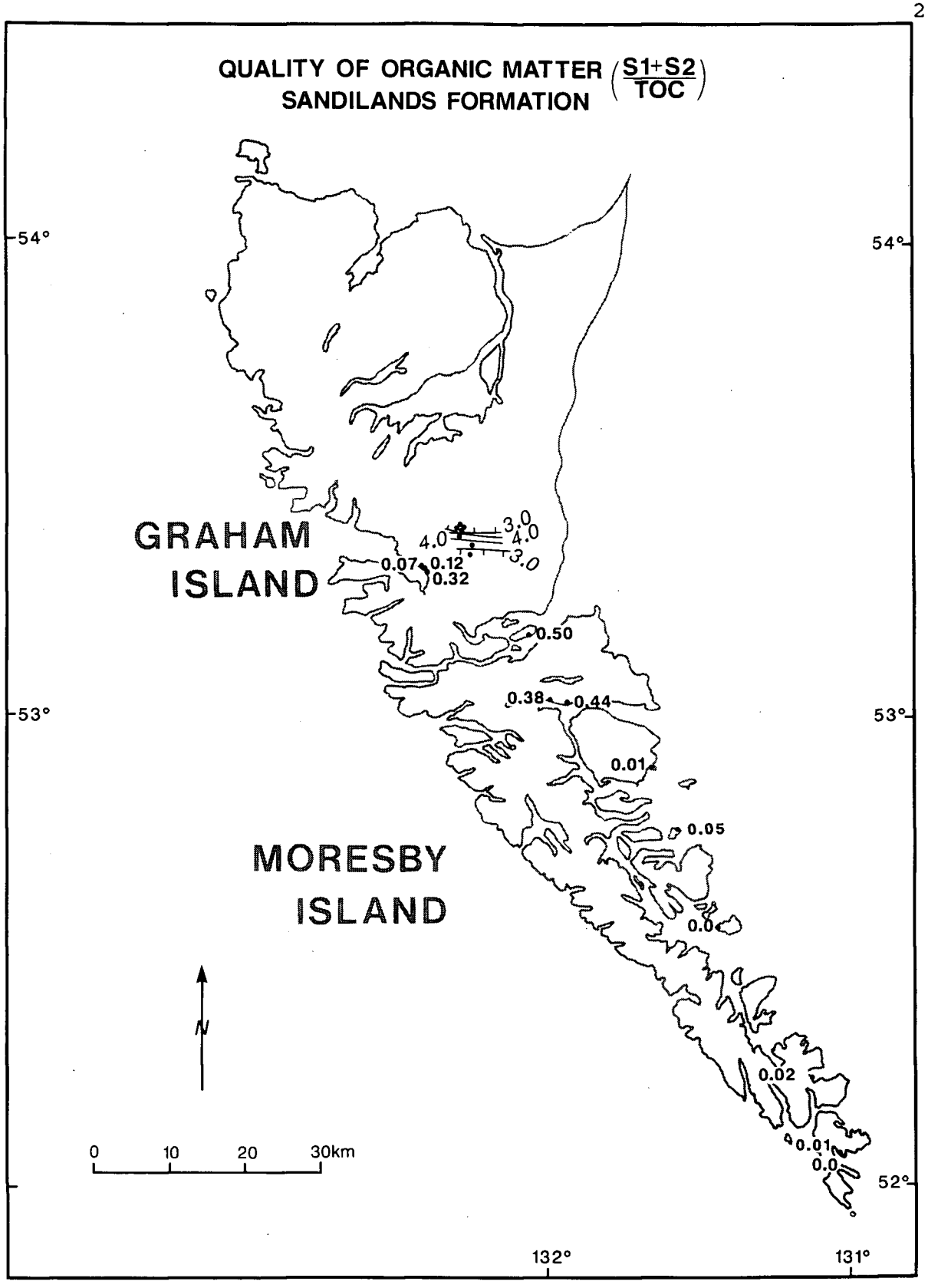

Figure 83. Regional distribution of the average QOM [(S1 + S2)/TOC] for the Sandilands Formation. Values are average QOM calculated across the thickness of the formation at each outcrop location. Dashed line represents inferred contour. Labelled values do not fit regional trends and are not contoured. Tick mark on contour line indicates decreasing QOM.

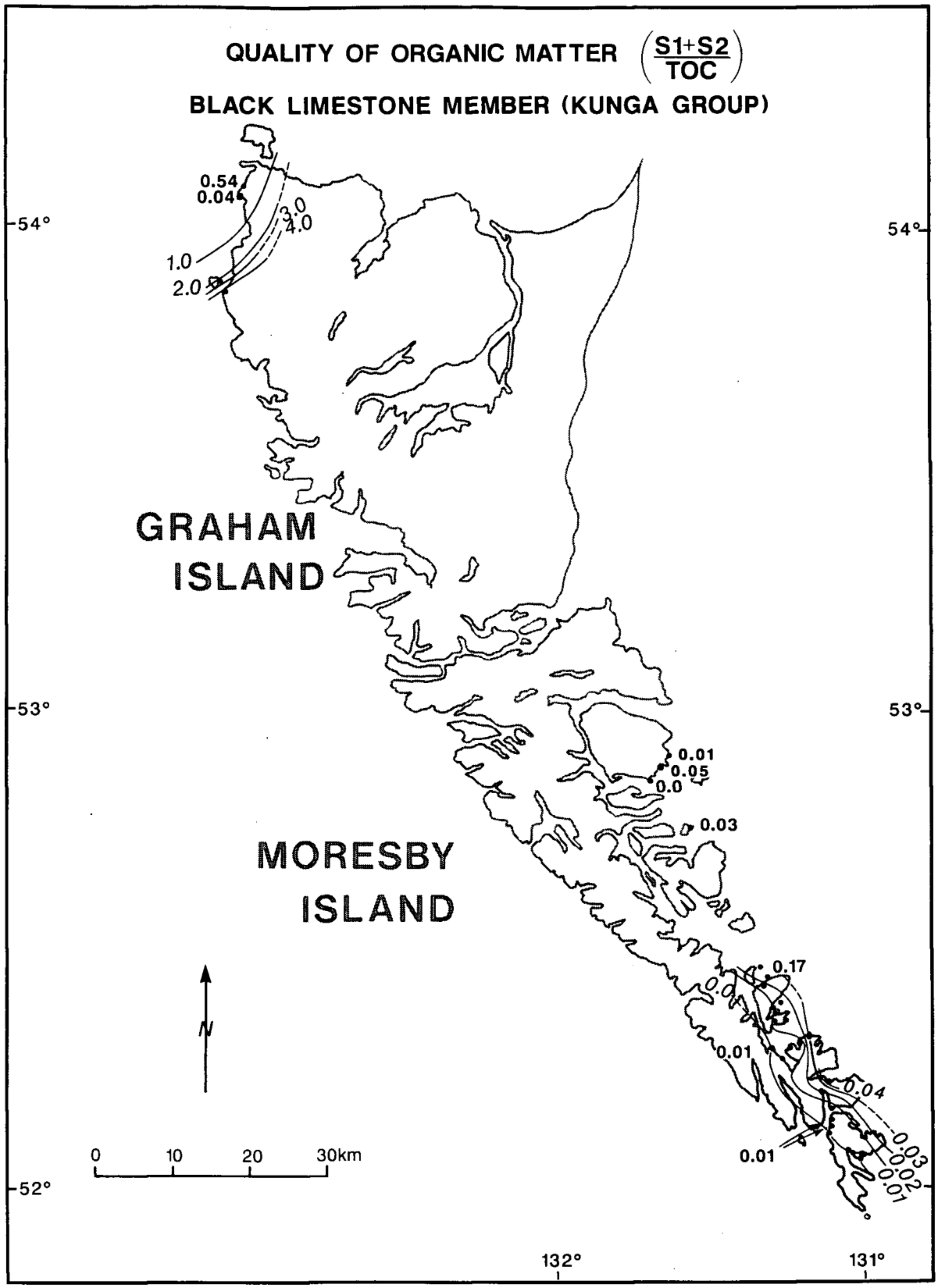

Figure 84. Regional distribution of the average QOM [(S1 + S2)/TOC] for the black limestone member (Kunga Group). Values are average QOM calculated across the thickness of the formation at each outcrop location. Dashed line represents inferred contour. Labelled values do not fit regional trends and are not contoured.

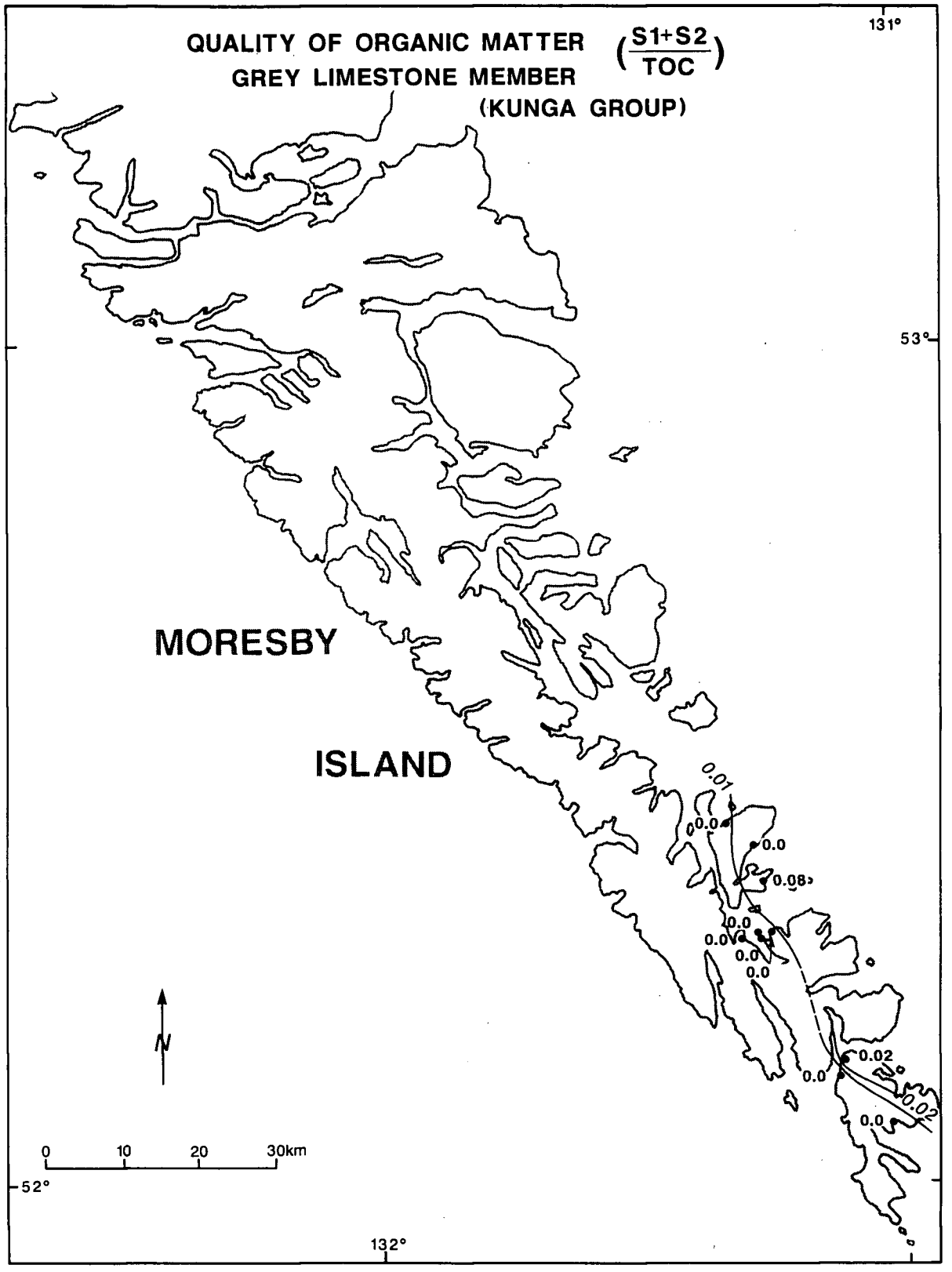

Figure 85. Regional distribution of the average QOM [(S1 + S2)/TOC] for the grey limestone member (Kunga Group). Values are average QOM calculated across the thickness of the formation at each outcrop location. Dashed line represents inferred contour. Labelled values do not fit regional trends and are not contoured.

hydrocarbon generation (see Part I). Mesozoic strata on Morseby Island south of Cumshewa Inlet are overmature and the DOM increases proximal to Jurassic-Cretaceous plutonic suites. The regional level of organic maturation of Triassic and Cretaceous strata on northwest Graham Island ranges from immature to mature with local, anomalous overmature strata. Jurassic and Cretaceous strata on central Graham Island are marginally mature to mature, whereas in the Skidegate and Cumshewa Inlet areas the strata are mature to overmature.

DISCUSSION

The following section documents the hydrocarbon source potential for selected Mesozoic and Tertiary strata. Geochemical parameters from Rock-Eval pyrolysis describing organic maturation, hydrocarbon generative potential, and type of generated hydrocarbons are outlined in Table 5. T_{max} values are not reported in Table 6 for samples with S2 values lower than the minimum 0.2 mg HC/gm C_{org} considered necessary for accurate T_{max} determination (Peters, 1986). In very overmature samples, the HI and OI values are too low to ascertain the type of original organic matter.

KUNGA GROUP

Grey Limestone Member

Low QOM (<0.08 mg HC/gm C_{org}), low HI (<8 mg HC/gm C_{org}), low PI (<0.08) and high maturation (2.35 to 5.28 $\%Ro_{rand}$) values indicate that the massive carbonates of the grey limestone member exposed on Moresby Island have poor oil source potential but are possibly gas source rocks. Some residual organic carbon (<1.1 % TOC), and low PI values (<0.08) from south Moresby Island suggest hydrogen depletion and that the strata may have been source rocks and previously generated hydrocarbons. High maturation values preclude the determination of the initial type of organic matter (Figure 47R).

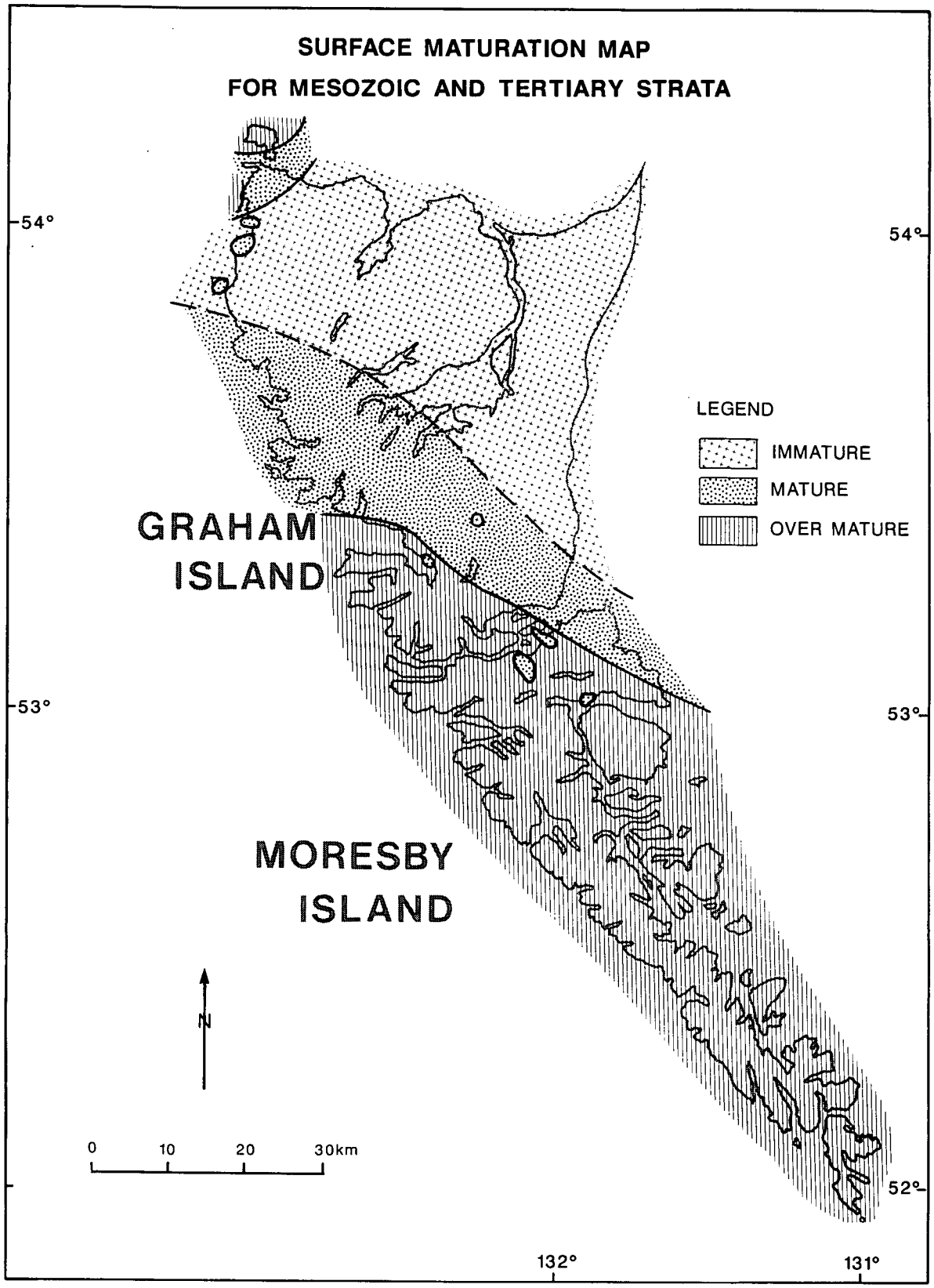

Figure 86. Surface maturation trends for Mesozoic and Tertiary strata derived from vitrinite reflectance data (%Ro_{rand}-see Part I). Oil window is between 0.50 %Ro_{rand} and 1.35 %Ro_{rand}

TABLE 5

GEOCHEMICAL PARAMETERS DESCRIBING LEVEL OF THERMAL MATURATION

MATURATION	PI S1/(S1+S2)	Tmax* (°C)	Ro (%)
TOP OF OIL WINDOW	0.1	430-435	0.5
BOTTOM OF OIL WINDOW	0.4	465	1.35

(*Maturation parameter may depend on type of organic matter)

GEOCHEMICAL PARAMETERS DESCRIBING SOURCE ROCK GENERATIVE POTENTIAL

QUANTITY	TOC (weight %)	S1 (mg HC/gm C_{org})	S2 (mg HC/gm C_{org})
POOR	0.0-0.5	0.0-0.5	0.0-2.5
FAIR	0.5-1.0	0.5-1.0	2.5-5.0
GOOD	1.0-2.0	1.0-2.0	5.0-10.0
VERY GOOD	2+	2+	10+

GEOCHEMICAL PARAMETERS DESCRIBING TYPE OF HYDROCARBON GENERATED

TYPE	HI (mg HC/gm C_{org})*	S2/S3*
GAS	0-150	0-3
GAS AND OIL	150-300	3-5
OIL	300+	5+

(*Assumes a DOM equivalent to R_o=0.6%)

TABLE 6A

GREY LIMESTONE MEMBER (KUNGA GROUP)

SECTION NAME	$\%Ro_{rand}$	TMAX	TOC	S1	S2	PI	QOM	HI	OI
OF SECTION BB									
MEAN	5.8	*	*	*	*	*	*	*	*
# OF SAMPLES	3.	0.	0.	0.	0.	0.	0.	0.	0.
OF SECTION BI									
MEAN	*	*	*	*	*	*	*	*	*
# OF SAMPLES	0.	0.	0.	0.	0.	0.	0.	0.	0.
OF SECTION BJ									
MEAN	2.35	*	*	*	*	*	*	*	*
# OF SAMPLES	1.	0.	0.	0.	0.	0.	0.	0.	0.
OF SECTION BR									
MEAN	2.72	*	*	*	*	*	*	*	*
# OF SAMPLES	4.	0.	0.	0.	0.	0.	0.	0.	0.
OF SECTION CB									
MEAN	8.	*	*	*	*	*	*	*	*
# OF SAMPLES	2.	0.	0.	0.	0.	0.	0.	0.	0.
OF SECTION CRE									
MEAN	4.59	*	*	*	*	*	*	*	*
# OF SAMPLES	1.	0.	0.	0.	0.	0.	0.	0.	0.
OF SECTION HP									
MEAN	2.61	*	*	*	*	*	*	*	*
# OF SAMPLES	1.	0.	0.	0.	0.	0.	0.	0.	0.
OF SECTION HU									
MEAN	2.91	*	*	*	*	*	*	*	*
# OF SAMPLES	8.	0.	0.	0.	0.	0.	0.	0.	0.
OF SECTION JED									
MEAN	6.56	*	*	*	*	*	*	*	*
# OF SAMPLES	3.	0.	0.	0.	0.	0.	0.	0.	0.
OF SECTION KT									
MEAN	4.39	*	*	*	*	*	*	*	*
# OF SAMPLES	10.	0.	0.	0.	0.	0.	0.	0.	0.
OF SECTION TB									
MEAN	4.38	*	*	*	*	*	*	*	*
# OF SAMPLES	4.	0.	0.	0.	0.	0.	0.	0.	0.

TABLE 6A (CONT.)

GREY LIMESTONE MEMBER (KUNGA GROUP)

SECTION NAME	$\%Ro_{rand}$	TMAX	TOC	S1	S2	PI	QOM	HI	OI
OF SECTION TIT									
MEAN	5.28	*	*	*	*	*	*	*	*
# OF SAMPLES	1.	0.	0.	0.	0.	0.	0.	0.	0.
SECTION 1									
MEAN	*	*	1.1	0.01	0.03	0.08	0.02	2.	35.
# OF SAMPLES	0.	0.	3.	3.	3.	3.	3.	3.	3.
SECTION 3									
MEAN	*	*	0.18	0.	0.	0.	0.	0.	33.
# OF SAMPLES	0.	0.	1.	1.	1.	1.	1.	1.	1.
SECTION 6									
MEAN	*	*	0.06	0.	0.	0.	0.	0.	48.
# OF SAMPLES	0.	0.	6.	6.	6.	6.	6.	6.	6.
SECTION 7									
MEAN	*	*	0.28	0.	0.	0.	0.01	0.	26.
# OF SAMPLES	0.	0.	4.	4.	4.	4.	4.	4.	4.
SECTION 8									
MEAN	*	*	0.24	0.	0.02	0.	0.08	8.	24.
# OF SAMPLES	0.	0.	4.	4.	4.	4.	4.	4.	4.
SECTION 9									
MEAN	*	*	0.06	0.	0.	0.	0.	0.	0.
# OF SAMPLES	0.	0.	1.	1.	1.	1.	1.	1.	1.
SECTION 10									
MEAN	*	*	0.06	0.	0.	0.	0.	0.	0.
# OF SAMPLES	0.	0.	1.	1.	1.	1.	1.	1.	1.
SPOT SAMPLE									
MEAN	*	*	0.10	0.	0.	0.	0.	0.	132.
# OF SAMPLES	0.	0.	5.	5.	5.	5.	5.	5.	5.
TF SPOT SAMPLE									
MEAN	2.95	*	0.	0.	0.	0.	*	0.	0.
# OF SAMPLES	3.	0.	3.	3.	3.	3.	0.	3.	3.

TABLE 6B

BLACK LIMESTONE MEMBER (KUNGA GROUP)

SECTION NAME	$\%Ro_{rand}$	TMAX	TOC	S1	S2	PI	QOM	HI	OI
OF SECTION B1									
MEAN	4.56	*	*	*	*	*	*	*	*
# OF SAMPLES	28.	0.	0.	0.	0.	0.	0.	0.	0.
OF SECTION BJ									
MEAN	4.09	*	*	*	*	*	*	*	*
# OF SAMPLES	10.	0.	0.	0.	0.	0.	0.	0.	0.
OF SECTION CB									
MEAN	8.31	*	*	*	*	*	*	*	*
# OF SAMPLES	1.	0.	0.	0.	0.	0.	0.	0.	0.
OF SECTION CRE									
MEAN	4.59	*	*	*	*	*	*	*	*
# OF SAMPLES	1.	0.	0.	0.	0.	0.	0.	0.	0.
OF SECTION DP									
MEAN	4.84	*	*	*	*	*	*	*	*
# OF SAMPLES	2.	0.	0.	0.	0.	0.	0.	0.	0.
OF SECTION EPO									
MEAN	4.81	*	*	*	*	*	*	*	*
# OF SAMPLES	1.	0.	0.	0.	0.	0.	0.	0.	0.
OF SECTION FUN									
MEAN	5.05	*	*	*	*	*	*	*	*
# OF SAMPLES	2.	0.	0.	0.	0.	0.	0.	0.	0.
OF SECTION GB									
MEAN	3.13	*	*	*	*	*	*	*	*
# OF SAMPLES	2.	0.	0.	0.	0.	0.	0.	0.	0.
OF SECTION HO									
MEAN	5.08	*	*	*	*	*	*	*	*
# OF SAMPLES	9.	0.	0.	0.	0.	0.	0.	0.	0.
OF SECTION HP									
MEAN	2.94	*	*	*	*	*	*	*	*
# OF SAMPLES	5.	0.	0.	0.	0.	0.	0.	0.	0.
OF SECTION HUX									
MEAN	4.33	*	*	*	*	*	*	*	*
# OF SAMPLES	19.	0.	0.	0.	0.	0.	0.	0.	0.

TABLE 6B (CONT.)

BLACK LIMESTONE MEMBER (KUNGA GROUP)

SECTION NAME	$\%Ro_{rand}$	TMAX	TOC	S1	S2	PI	QOM	HI	OI
OF SECTION JED									
MEAN	4.23	*	*	*	*	*	*	*	*
# OF SAMPLES	1.	0.	0.	0.	0.	0.	0.	0.	0.
OF SECTION KT									
MEAN	4.66	*	*	*	*	*	*	*	*
# OF SAMPLES	18.	0.	0.	0.	0.	0.	0.	0.	0.
OF SECTION KU									
MEAN	4.56	*	*	*	*	*	*	*	*
# OF SAMPLES	12.	0.	0.	0.	0.	0.	0.	0.	0.
OF SECTION LUX									
MEAN	4.63	*	*	*	*	*	*	*	*
# OF SAMPLES	1.	0.	0.	0.	0.	0.	0.	0.	0.
OF SECTION NPO									
MEAN	4.62	*	*	*	*	*	*	*	*
# OF SAMPLES	3.	0.	0.	0.	0.	0.	0.	0.	0.
OF SECTION POO									
MEAN	3.53	*	*	*	*	*	*	*	*
# OF SAMPLES	5.	0.	0.	0.	0.	0.	0.	0.	0.
OF SECTION RH									
MEAN	5.6	*	*	*	*	*	*	*	*
# OF SAMPLES	2.	0.	0.	0.	0.	0.	0.	0.	0.
OF SECTION RI									
MEAN	4.37	*	*	*	*	*	*	*	*
# OF SAMPLES	6.	0.	0.	0.	0.	0.	0.	0.	0.
OF SECTION ROSS									
MEAN	4.87	*	*	*	*	*	*	*	*
# OF SAMPLES	2.	0.	0.	0.	0.	0.	0.	0.	0.
OF SECTION SC									
MEAN	4.35	*	*	*	*	*	*	*	*
# OF SAMPLES	5.	0.	0.	0.	0.	0.	0.	0.	0.
OF SECTION SHU									
MEAN	2.4	*	*	*	*	*	*	*	*
# OF SAMPLES	6.	0.	0.	0.	0.	0.	0.	0.	0.

TABLE 6B (CONT.)

BLACK LIMESTONE MEMBER (KUNGA GROUP)

SECTION NAME	$\%Ro_{rand}$	TMAX	TOC	S1	S2	PI	QOM	HI	OI
OF SECTION SI									
MEAN	4.1	*	*	*	*	*	*	*	*
# OF SAMPLES	4.	0.	0.	0.	0.	0.	0.	0.	0.
OF SECTION SK									
MEAN	3.78	*	*	*	*	*	*	*	*
# OF SAMPLES	3.	0.	0.	0.	0.	0.	0.	0.	0.
OF SECTION SKU									
MEAN	4.58	*	*	*	*	*	*	*	*
# OF SAMPLES	13.	0.	0.	0.	0.	0.	0.	0.	0.
OF SECTION SPO									
MEAN	3.89	*	*	*	*	*	*	*	*
# OF SAMPLES	1.	0.	0.	0.	0.	0.	0.	0.	0.
OF SECTION TB									
MEAN	2.37	*	*	*	*	*	*	*	*
# OF SAMPLES	1.	0.	0.	0.	0.	0.	0.	0.	0.
OF SECTION VP									
MEAN	3.85	*	*	*	*	*	*	*	*
# OF SAMPLES	1.	0.	0.	0.	0.	0.	0.	0.	0.
SECTION 1									
MEAN	*	*	0.82	0.	0.	0.	0.01	0.	32.
# OF SAMPLES	0.	0.	8.	8.	8.	8.	8.	8.	8.
SECTION 2									
MEAN	*	*	0.9	0.	0.01	0.	0.	0.	231.
# OF SAMPLES	0.	0.	5.	5.	5.	5.	5.	5.	5.
SECTION 3									
MEAN	*	*	1.02	0.	0.	0.	0.01	1.	13.
# OF SAMPLES	0.	0.	8.	8.	8.	8.	8.	8.	8.
SECTION 4									
MEAN	3.64	*	2.21	0.	0.05	0.03	0.05	16.	13.
# OF SAMPLES	3.	0.	4.	4.	4.	4.	4.	4.	4.
SECTION 7									
MEAN	*	*	0.41	0.	0.	0.	0.	0.	3.
# OF SAMPLES	0.	0.	3.	3.	3.	3.	3.	3.	3.

TABLE 6B (CONT.)

BLACK LIMESTONE MEMBER (KUNGA GROUP)

SECTION NAME	$\%Ro_{rand}$	TMAX	TOC	S1	S2	PI	QOM	HI	OI
SECTION 8									
MEAN	*	*	0.25	0.	0.	0.	0.02	0.	50.
# OF SAMPLES	0.	0.	5.	5.	5.	5.	5.	5.	5.
SECTION 9									
MEAN	*	*	0.22	0.	0.	0.	0.01	1.	9.
# OF SAMPLES	0.	0.	9.	9.	9.	9.	9.	9.	9.
SECTION 10									
MEAN	4.29	*	1.16	0.	0.01	0.07	0.01	1.	24.
# OF SAMPLES	14.	0.	15.	15.	15.	15.	15.	15.	15.
SECTION 11									
MEAN	5.11	*	2.56	0.07	0.01	0.87	0.03	0.	11.
# OF SAMPLES	1.	0.	1.	1.	1.	1.	1.	1.	1.
SECTION 12									
MEAN	0.51	440.	3.6	1.21	14.08	0.08	4.19	385.	9.
# OF SAMPLES	6.	6.	6.	6.	6.	6.	6.	6.	6.
SECTION 13									
MEAN	3.19	587.	2.9	0.04	0.08	0.33	0.04	2.	24.
# OF SAMPLES	16.	1.	18.	18.	18.	18.	18.	18.	18.
SECTION 14									
MEAN	1.59	*	*	*	*	*	*	*	*
# OF SAMPLES	2.	0.	0.	0.	0.	0.	0.	0.	0.
SECTION 15									
MEAN	1.47	467.	2.69	0.64	0.83	0.44	0.55	30.	47.
# OF SAMPLES	2.	1.	1.	1.	1.	1.	1.	1.	1.
SECTION 19									
MEAN	1.18	444.	2.17	0.57	4.69	0.12	2.19	192.	14.
# OF SAMPLES	16.	18.	18.	18.	18.	18.	17.	18.	18.
SPOT SAMPLE									
MEAN	4.04	*	1.06	0.	0.01	0.04	0.02	0.	25.
# OF SAMPLES	30.	0.	38.	38.	38.	38.	38.	38.	38.

TABLE 6C

SANDILANDS FORMATION

SECTION NAME	$\%Ro_{rand}$	TMAX	TOC	S1	S2	PI	QOM	HI	OI
SECTION 5									
MEAN	*	*	0.51	0.01	0.03	0.06	0.03	2.	49.
# OF SAMPLES	0.	0.	4.	4.	4.	4.	4.	4.	4.
SECTION 11									
MEAN	3.78	*	1.53	0.04	0.03	0.59	0.05	2.	9.
# OF SAMPLES	18.	0.	21.	21.	21.	21.	21.	21.	21.
SECTION 12									
MEAN	0.45	436.	2.66	0.77	12.9	0.06	4.66	437.	10.
# OF SAMPLES	18.	10.	10.	10.	10.	10.	10.	10.	10.
SPOT SAMPLE									
MEAN	4.	*	0.59	0.	0.	0.	0.01	0.	7.
# OF SAMPLES	5.	0.	8.	8.	8.	8.	8.	8.	8.
CENTRAL GRAHAM ISLAND B-QUARRY									
MEAN	0.40	443.	3.14	1.64	13.85	0.14	4.26	372.	36.
# OF SAMPLES	17.	17.	17.	17.	17.	17.	17.	17.	17.
CENTRAL GRAHAM ISLAND D-QUARRY									
MEAN	0.66	447.	1.32	0.67	3.83	0.16	2.73	229.	525.
# OF SAMPLES	4.	4.	5.	5.	5.	4.	5.	5.	5.
CENTRAL GRAHAM ISLAND BRANCH ROAD 57									
MEAN	0.65	437.	1.25	0.47	3.43	0.16	3.32	264.	42.
# OF SAMPLES	6.	6.	6.	6.	6.	6.	6.	6.	6.
CENTRAL GRAHAM ISLAND MAIN ROAD									
MEAN	0.60	445.	2.08	1.02	4.9	0.15	1.94	159.	68.
# OF SAMPLES	4.	4.	5.	5.	5.	5.	5.	5.	5.
CENTRAL GRAHAM ISLAND WELL I-178									
MEAN	0.60	437.	1.75	1.12	3.86	0.25	2.75	210.	48.
# OF SAMPLES	32.	32.	33.	33.	33.	33.	33.	33.	33.
CENTRAL GRAHAM ISLAND WELL I-179									
MEAN	0.88	447.	9.6	0.50	4.12	0.31	2.71	242.	73.
# OF SAMPLES	40.	37.	40.	40.	40.	38.	39.	39.	39.

TABLE 6C (CONT.)

SANDILANDS FORMATION

SECTION NAME	$\%Ro_{rand}$	TMAX	TOC	S1	S2	PI	QOM	HI	OI
CENTRAL GRAHAM ISLAND WELL I-278									
MEAN	0.65	447.	1.91	0.99	4.60	0.23	2.56	205.	57.
# OF SAMPLES	47.	47.	47.	47.	47.	47.	47.	47.	47.
MAUDE ISLAND									
MEAN	1.35	465.	1.47	0.24	0.52	0.42	0.44	27.	34.
# OF SAMPLES	8.	8.	9.	9.	9.	9.	9.	9.	9.
RENNELL SOUND									
MEAN	1.57	479.	1.47	0.15	0.3	0.40	0.32	17.	18.
# OF SAMPLES	32.	32.	33.	33.	33.	33.	33.	33.	33.
SHIELDS BAY									
MEAN	1.27	*	0.57	0.06	0.0	1.0	0.09	0.0	4.
# OF SAMPLES	7.	0.	7.	7.	7.	7.	7.	7.	7.

TABLE 6D

GHOST CREEK FORMATION

SECTION NAME	%Ro_{rand}	TMAX	TOC	S1	S2	PI	QOM	HI	OI
BC SECTION 10									
MEAN	0.55	448.	1.66	0.39	5.11	0.08	3.19	218.	13.
# OF SAMPLES	3.	4.	4.	4.	4.	4.	4.	4.	4.
BC SECTION 4									
MEAN	1.32	486.	0.68	0.07	0.25	0.22	0.47	36.	29.
# OF SAMPLES	1.	1.	1.	1.	1.	1.	1.	1.	1.
BC SECTION 7									
MEAN	1.51	470.	1.63	0.43	0.63	0.41	0.65	38.	17.
# OF SAMPLES	2.	2.	2.	2.	2.	2.	2.	2.	2.
BC SECTION 8									
MEAN	1.5	480.	1.84	0.44	0.7	0.41	0.66	38.	15.
# OF SAMPLES	4.	4.	4.	4.	4.	4.	4.	4.	4.
BC SECTION CAA-86-2									
MEAN	0.88	454.	1.27	0.43	1.98	0.17	1.73	141.	32.
# OF SAMPLES	6.	4.	5.	5.	5.	5.	5.	5.	5.
CENTRAL GRAHAM ISLAND A-QUARRY									
MEAN	0.50	438.	0.6	1.46	1.76	0.45	5.37	293.	108.
# OF SAMPLES	1.	1.	1.	1.	1.	1.	1.	1.	1.
MAUDE ISLAND									
MEAN	1.38	442.	1.90	0.55	4.66	0.10	2.43	209.	105.
# OF SAMPLES	5.	5.	5.	5.	5.	5.	5.	5.	5.
RENNELL SOUND									
MEAN	1.57	477.	0.79	0.05	0.09	0.48	0.14	9.	106.
# OF SAMPLES	7.	7.	7.	7.	7.	7.	7.	7.	7.
CENTRAL GRAHAM ISLAND WELL I-179									
MEAN	0.88	444.	1.73	0.36	6.64	0.07	3.73	349.	76.
# OF SAMPLES	36.	36.	36.	36.	36.	33.	34.	34.	34.
WHITEAVES BAY									
MEAN	1.35	448.	1.6	0.46	0.60	0.49	0.62	32.	6.
# OF SAMPLES	6.	6.	6.	6.	6.	6.	6.	6.	6.

TABLE 6E

RENNELL JUNCTION FORMATION

SECTION NAME	%Ro_{rand}	TMAX	TOC	S1	S2	PI	QOM	HI	OI
BC SECTION 10									
MEAN	0.52	445.	0.71	0.25	1.27	0.16	2.14	178.	46.
# OF SAMPLES	1.	1.	1.	1.	1.	1.	1.	1.	1.
BC SECTION 4									
MEAN	1.17	467.	0.58	0.05	0.16	0.12	0.33	28.	288.
# OF SAMPLES	2.	1.	2.	2.	2.	2.	2.	2.	2.
BC SECTION 7									
MEAN	1.5	488.	1.57	0.27	0.35	0.44	0.39	22.	8.
# OF SAMPLES	1.	1.	1.	1.	1.	1.	1.	1.	1.
BC SECTION 8									
MEAN	1.45	471.	1.96	0.4	0.59	0.41	0.51	30.	21.
# OF SAMPLES	1.	1.	1.	1.	1.	1.	1.	1.	1.
BC SECTION CAA-86-2									
MEAN	0.88	458.	1.07	0.05	0.3	0.14	0.84	93.	78.
# OF SAMPLES	3.	4.	4.	4.	4.	4.	4.	4.	4.

TABLE 6F

FANNIN FORMATION

SECTION NAME	$\%Ro_{rand}$	TMAX	TOC	S1	S2	PI	QOM	HI	OI
BC SECTION 4									
MEAN	1.31	*	0.18	0.01	0.01	0.25	0.13	8.	74.
# OF SAMPLES	2.	0.	2.	2.	2.	2.	2.	2.	2.
BC SECTION 7									
MEAN	1.45	*	0.23	0.02	0.05	0.22	0.31	25.	27.
# OF SAMPLES	3.	0.	3.	3.	3.	3.	3.	3.	3.
BC SECTION 8									
MEAN	1.47	*	0.26	0.03	0.09	0.24	0.53	42.	88.
# OF SAMPLES	3.	0.	3.	3.	3.	3.	3.	3.	3.
BC SECTION 8									
MEAN	1.51	*	0.28	0.02	0.08	0.2	0.34	28.	136.
# OF SAMPLES	5.	0.	5.	5.	5.	5.	5.	5.	5.
BC SECTION CAA-86-2									
MEAN	0.85	*	*	*	*	*	*	*	*
# OF SAMPLES	2.	0.	0.	0.	0.	0.	0.	0.	0.
NORTH MORESBY									
MEAN	1.42^{*}	*	*	*	*	*	*	*	*
# OF SAMPLES	1.	*	*	*	*	*	*	*	*

($^{*}Ro_{max}$)

TABLE 6G

WHITEAVES FORMATION

SECTION NAME	%Ro_{rand}	TMAX	TOC	S1	S2	PI	QOM	HI	OI	
BC SECTION 10										
MEAN	0.64	448.	0.18	0.01	0.10	0.03	0.62	60.	51.	
# OF SAMPLES	5.	1.	5.	5.	5.	5.	5.	5.	5.	
BC SECTION 11										
MEAN	0.43	440	0.33	0.01	0.18	0.07	0.62	57.	6.	
# OF SAMPLES	5.	1.	5.	5.	5.	5.	5.	5.	5.	
BC SECTION 12										
MEAN	0.46	442.	5.27	0.02	0.24	0.09	0.43	88.	14.	
# OF SAMPLES	2.	1.	2.	2.	2.	2.	2.	2.	2.	
BC SECTION 14										
MEAN	0.78	*	0.26	0.01	0.11	0.11	0.47	42.	10.	
# OF SAMPLES	4.	0.	4.	4.	4.	4.	4.	4.	4.	
BC SECTION 15										
MEAN	0.63	440.	0.59	0.04	0.36	0.11	0.65	58.	5.	
# OF SAMPLES	5.	4.	5.	5.	5.	5.	5.	5.	5.	
BC SECTION 4										
MEAN	1.26	*	0.23	0.	0.01	0.17	0.07	5.	125.	
# OF SAMPLES	3.	0.	3.	3.	3.	3.	3.	3.	3.	
BC SECTION 5										
MEAN	1.5	*	0.34	0.01	0.05	0.26	0.18	14.	88.	
# OF SAMPLES	4.	0.	3.	3.	3.	3.	3.	3.	3.	
BC SECTION 6										
MEAN	1.49	*	0.27	0.	0.02	0.13	0.08	7.	54.	
# OF SAMPLES	3.	0.	4.	4.	4.	4.	4.	4.	4.	
BC SECTION 7										
MEAN	1.42	*	0.32	0.02	0.08	0.2	0.32	25.	18.	
# OF SAMPLES	3.	0.	3.	3.	3.	3.	3.	3.	3.	
BC SECTION CAA-86-2										
MEAN	0.82	464.	1.8	0.16	1.13	0.13	0.73	64.	16.	
# OF SAMPLES	2.	2.	2.	2.	2.	2.	2.	2.	2.	
NORTH MORESBY										
MEAN	1.51*	*	*	*	*	*	*	*	*	# OF
SAMPLES	1.	*	*	*	*	*	*	*	*	
(*Ro_{max})										

TABLE 6H

PHANTOM CREEK FORMATION

SECTION NAME	$\%Ro_{rand}$	TMAX	TOC	S1	S2	PI	QOM	HI	OI
BC SECTION 12									
MEAN	0.46	440.	0.55	0.38	1.85	0.16	3.9	322.	10.
# OF SAMPLES	4.	4.	4.	4.	4.	4.	4.	4.	4.

TABLE 6I

GRAHAM ISLAND FORMATION

SECTION NAME	$\%Ro_{rand}$	TMAX	TOC	S1	S2	PI	QOM	HI	OI
BC SECTION 10									
MEAN	0.48	446.	0.96	0.08	1.57	0.06	1.17	111.	86.
# OF SAMPLES	8.	5.	8.	8.	8.	8.	8.	8.	8.
BC SECTION 14									
MEAN	0.77	443.	0.88	0.14	2.22	0.23	1.94	127.	14.
# OF SAMPLES	6.	4.	7.	7.	7.	7.	7.	7.	7.
BC SECTION 6									
MEAN	1.5	*	0.34	0.01	0.08	0.08	0.26	24.	43.
# OF SAMPLES	3.	0.	3.	3.	3.	3.	3.	3.	3.

TABLE 6J

RICHARDSON BAY FORMATION

SECTION NAME	$\%Ro_{rand}$	TMAX	TOC	S1	S2	PI	QOM	HI	OI
BC SECTION 16									
MEAN	1.13	396.	1.13	0.20	0.52	0.28	0.63	45.	11.
# OF SAMPLES	6.	6.	6.	6.	6.	6.	6.	6.	6.

TABLE 6K

ROBBER POINT FORMATION

SECTION NAME	$\%Ro_{rand}$	TMAX	TOC	S1	S2	PI	QOM	HI	OI
BC SECTION 16									
MEAN	1.10	468.	0.78	0.14	0.35	0.29	0.63	44.	15.
# OF SAMPLES	1.	1.	1.	1.	1.	1.	1.	1.	1.

TABLE 6L

NEWCOMBE FORMATION

SECTION NAME	%Rorand	TMAX	TOC	S1	S2	PI	QOM	HI	OI
BC SECTION 17									
MEAN	1.08	*	0.51	0.02	0.15	0.12	0.34	30.	14.
# OF SAMPLES	3.	0.	3.	3.	3.	3.	3.	3.	3.

TABLE 6M

ALLIFORD FORMATION

SECTION NAME	%Ro_{rand}	TMAX	TOC	S1	S2	PI	QOM	HI	OI
BC SECTION 16									
MEAN	1.04	320.	1.10	0.22	0.89	0.20	1.01	80.	13.
# OF SAMPLES	3.	3.	3.	3.	3.	3.	3.	3.	3.

TABLE 6N

LONGARM FORMATION

SECTION NAME	%Ro_{rand}	TMAX	TOC	S1	S2	PI	QOM	HI	OI
SPOT SAMPLE									
MEAN	3.18	*	0.26	0.	0.	0.03	0.03	5.	44.
# OF SAMPLES	20.	0.	33.	33.	33.	33.	33.	33.	33.
NORTH MORESBY									
MEAN	2.07*	*	*	*	*	*	*	*	*
# OF SAMPLES	5.	*	*	*	*	*	*	*	*

(*Ro_{max})

TABLE 6O

HAIDA FORMATION

SECTION NAME	%Ro_{rand}	TMAX	TOC	S1	S2	PI	QOM	HI	OI
BC SECTION CAA-86-1									
MEAN	0.98	701.	0.68	0.05	0.36	0.1	0.56	49.	5.
# OF SAMPLES	26.	17.	26.	26.	26.	26.	26.	26.	26.
BC SECTION CAA-86-5									
MEAN	0.36	439.	0.73	0.01	0.48	0.02	0.67	65.	29.
# OF SAMPLES	10.	10.	11.	11.	11.	11.	11.	11.	11.
SECTION 14									
MEAN	1.51	504.	2.23	0.35	0.74	0.27	0.48	34.	36.
# OF SAMPLES	8.	2.	3.	3.	3.	3.	3.	3.	3.
SECTION 15									
MEAN	0.77	449.	2.49	0.07	0.9	0.08	0.43	39.	50.
# OF SAMPLES	40.	2.	2.	2.	2.	2.	2.	2.	2.
SECTION 17									
MEAN	0.68	*	*	*	*	*	*	*	*
# OF SAMPLES	11.	0.	0.	0.	0.	0.	0.	0.	0.
SECTION 18									
MEAN	0.43	*	*	*	*	*	*	*	*
# OF SAMPLES	14.	0.	0.	0.	0.	0.	0.	0.	0.
SPOT SAMPLE									
MEAN	4.04	*	0.13	0.	0.	0.14	0.02	0.	33.
# OF SAMPLES	3.	0.	7.	7.	7.	7.	7.	7.	7.
NORTH MORESBY									
MEAN	1.13*	*	*	*	*	*	*	*	*
# OF SAMPLES	2.	*	*	*	*	*	*	*	*

(* Ro_{max})

TABLE 6P

SKIDEGATE FORMATION

SECTION NAME	$\%Ro_{rand}$	TMAX	TOC	S1	S2	PI	QOM	HI	OI
SECTION 20									
MEAN	1.91	497.	0.6	0.01	0.08	0.16	0.24	33.	74.
# OF SAMPLES	14.	1.	11.	11.	11.	11.	11.	11.	11.
BC SECTION CAA-86-3									
MEAN	0.96	433.	0.26	0.03	0.18	0.15	0.95	79.	68.
# OF SAMPLES	35.	11.	32.	32.	32.	32.	32.	32.	32.
BC SECTION CAA-86-4									
MEAN	*	*	*	*	*	*	*	*	*
# OF SAMPLES	0.	0.	0.	0.	0.	0.	0.	0.	0.
BC SECTION CAA-86-6									
MEAN	0.4	439.	0.73	0.02	0.54	0.03	0.73	70.	26.
# OF SAMPLES	23.	25.	25.	25.	25.	25.	25.	25.	25.
BC SECTION CAA-86-T-3									
MEAN	1.09	464.	0.17	0.01	0.10	0.07	0.85	65.	146.
# OF SAMPLES	7.	2.	7.	7.	7.	7.	6.	7.	7.
BC SECTION CAA-86-T-4									
MEAN	0.47	437.	0.43	0.	0.19	0.	0.32	31.	70.
# OF SAMPLES	8.	2.	5.	5.	5.	5.	5.	5.	5.
BC SPOT SAMPLE									
MEAN	1.8	470.	0.51	0.02	0.18	0.06	0.4	37.	28.
# OF SAMPLES	66.	10.	53.	53.	53.	53.	53.	53.	53.
SECTION 16									
MEAN	0.71	442.	0.3	0.01	0.19	0.04	0.71	67.	81.
# OF SAMPLES	10.	2.	8.	8.	8.	8.	8.	8.	8.
SECTION 21									
MEAN	1.39	456.	0.32	0.02	0.12	0.11	0.44	36.	14.
# OF SAMPLES	11.	1.	10.	10.	10.	10.	10.	10.	10.
SECTION 22									
MEAN	0.87	436.	0.63	0.	0.17	0.	0.25	24.	76.
# OF SAMPLES	3.	1.	2.	2.	2.	2.	2.	2.	2.
SPOT SAMPLE									
MEAN	2.94	*	0.13	0.	0.02	0.04	0.31	20.	95.
# OF SAMPLES	3.	0.	4.	4.	4.	4.	3.	4.	4.

TABLE 6Q

HONNA FORMATION

SECTION NAME	$\%Ro_{rand}$	TMAX	TOC	S1	S2	PI	QOM	HI	OI
SECTION 22									
MEAN	1.14	436.	0.43	0.03	0.24	0.09	0.7	60.	125.
# OF SAMPLES	16.	7.	12.	12.	12.	12.	12.	12.	12.
SPOT SAMPLE									
MEAN	*	*	0.08	0.	0.	0.	0.	0.	87.
# OF SAMPLES	0.	0.	1.	1.	1.	1.	1.	1.	1.
NORTH MORESBY									
MEAN	0.80^{*}	*	*	*	*	*	*	*	*
# OF SAMPLES	4.	*	*	*	*	*	*	*	*

($^{*}Ro_{max}$)

TABLE 6R

SKONUN FORMATION

SECTION NAME	%Ro_{rand}	TMAX	TOC	S1	S2	PI	QOM	HI	OI
CAPE BALL WELL									
MEAN	0.32	403.	41.68	16.3	81.42	0.15	2.2	179.	38.
# OF SAMPLES	22.	16.	16.	16.	16.	16.	16.	16.	16.
GOLD CREEK WELL									
MEAN	0.27	418.	24.44	0.97	14.42	0.08	0.70	64.	68.
# OF SAMPLES	7.	4.	4.	4.	4.	4.	4.	4.	4.
LOG CREEK									
MEAN	0.39	420.	2.47	1.32	5.2	0.2	2.64	210.	14.
# OF SAMPLES	1.	1.	1.	1.	1.	1.	1.	1.	1.
MILLER CREEK									
MEAN	0.19	*	*	*	*	*	*	*	*
# OF SAMPLES	1.	0.	0.	0.	0.	0.	0.	0.	0.
NADU RIVER WELL									
MEAN	0.29	400.	6.67	1.36	7.72	0.46	0.9	64.	199
# OF SAMPLES	10.	4.	8.	8.	8.	8.	8.	8.	8.
PORT LOUIS WELL									
MEAN	1.05	486.	10.45	0.73	10.3	0.07	0.87	79.	9.
# OF SAMPLES	24.	13.	14.	14.	14.	14.	14.	14.	14.
TLELL WELL									
MEAN	0.27	417.	22.88	7.27	39.12	0.15	1.91	161.	74.
# OF SAMPLES	17.	14.	15.	15.	15.	15.	15.	15.	15.
TOW HILL WELL									
MEAN	0.48	430.	36.18	7.17	31.76	0.17	1.19	93.	28.
# OF SAMPLES	45.	36.	40.	40.	40.	40.	40.	40.	39.

Black Limestone Member

High DOM (2.37 to 8.31 $\%Ro_{rand}$), and low QOM (<0.05 mg HC/gm C_{org}), PI (0.03 to 0.07), and HI (<16 mg HC/gm C_{org}) values for the interbedded shale and calcarenite of the black limestone member exposed on Moresby Island indicate that the strata are presently poor oil source rocks. Low PI, high DOM, low HI, and variable TOC (<2.56 %) values suggest hydrocarbon depletion and indicate that hydrocarbons may have been previously generated. Moderate amounts of residual carbon (<2.56 % TOC) and low HI values suggest some gas generation potential.

Mature to overmature strata (0.51 to 3.19 $\%Ro_{rand}$; 440 ^{o}C to 587 ^{o}C T_{max}) from northwest Graham Island are good oil and gas source rocks as is evident from high TOC (2.17 % to 3.6 %), QOM (<4.19 mg HC/gm C_{org}), moderate to high HI (192 to 385 mg HC/gm c_{org}), and moderate PI (0.08 to 0.33) values (Tables 5 and 6). Solid bitumen observed in hand specimen accounts for the anomalously high TOC values, and indicates that the strata have previously generated liquid hydrocarbons. Low to moderate PI values in some areas suggest depletion and possible migration of hydrocarbons.

The HI/OI diagram for the black limestone member (Figure 47Q) shows two populations of organic matter: Types I and II with high HI and low OI values with very good oil and gas generative potential from northwest Graham Island; and, overmature Type III with very low HI and high OI values resulting in fair gas but no oil generative potential at Morseby Island.

Sandilands Formation

The DOM for the argillites of the Sandilands Formation exposed on Moresby Island is too high (3.78 to 4.00 $\%Ro_{rand}$) to consider the strata as oil source rocks. Low QOM (<0.05 mg HC/gm C_{org}), low HI (<2 mg HC/gm C_{org}) and high maturation values (Tables 5 and 6) indicate hydrocarbon depletion suggesting that hydrocarbons may have been previously generated. High PI values (<0.59) at Kunga Island

suggest that hydrocarbons have possibly migrated into overmature strata. Moderate amounts of residual TOC (0.51 to 1.56 %) and low HI values suggest some potential for gas generation.

Mature Type I and Type II organic matter of the Sandilands Formation in central Graham Island has good oil and gas source potential as is evident by high TOC (1.25 to 9.6 %), QOM (1.94 to 4.26 mg HC/gm C_{org}), and moderate to high HI (159 to 372 mg HC/gm C_{org}) values (Tables 5 and 6). Moderate PI values (0.14 to 0.42) and free hydrocarbons (S1 < 1.64 mg HC/gm C_{org}) suggest some conversion of kerogen to petroleum.

Marginally immature strata on northwest Graham Island at Kennecott Point are good oil and gas source rocks with high TOC (2.66 %), QOM (4.66 mg HC/gm C_{org}), and HI (437 mg HC/gm C_{org}) values (Tables 5 and 6). Low PI (0.06) and vitrinite reflectance (0.45 $\%Ro_{rand}$) values suggest a low degree of kerogen conversion to petroleum. The Sandilands Formation at depth is probably more mature and may have generated substantial amounts of petroleum.

MAUDE GROUP

Ghost Creek Formation

Marginally mature (0.55 $\%Ro_{rand}$) strata of the Ghost Creek Formation exposed on central Graham Island and locally in Skidegate Inlet have good oil and gas source potential as indicated by moderate TOC (1.66 to 1.73 %), high QOM (3.19 to 3.73 mg HC/gm C_{org}), and moderate HI (218.0 to 349 mg HC/gm C_{org}) values (Tables 5 and 6). A low PI (0.07) suggest a low degree of kerogen conversion to petroleum.

Marginally overmature to overmature strata (1.32 to 1.51 $\%Ro_{rand}$) in Skidegate Inlet (Maude Island) and Rennell Sound are currently poor oil source rocks as suggested by low QOM (0.14 to 0.66 mg

HC/gm C_{org}) and HI (9 to 38 mg HC/gm C_{org}). Moderate PI (0.48) values from Rennell Sound suggest that the strata are overmature.

Rennell Junction Formation

Mature to overmature (0.52 to 1.5 $\%Ro_{rand}$) sandstone, siltstone, and shale from Cumshewa Inlet and Skidegate Inlet are generally poor source rocks (TOC < 1.96 %; QOM = 0.33 mg HC/gm Corg; and HI < 93 mg HC/gm Corg) values. Type III organic matter (Figures 46K and 47N) suggests that the strata are possible gas source rocks.

Marginally mature strata in central Graham Island have fair gas source potential as indicated by low TOC (0.71 %), high QOM (2.14 mg HC/gm C_{org}), and low HI (178 mg HC/gm C_{org}) values (Tables 5 and 6).

Fannin Formation

Generally overmature (0.85 to 1.51 $\%Ro_{rand}$) tuffaceous siltstone in central Graham Island and Skidegate Inlet are poor source rocks as indicated by low TOC (<0.28 %), QOM (<0.53 mg HC/gm C_{org}), and HI (<42 mg HC/gm C_{org}) values (Tables 5 and 6). The HI/OI diagram (Figure 47M) suggests that the Fannin Formation contains terrestrially derived Type III organic matter.

Whiteaves Formation

Low TOC (<0.59 %), QOM (<0.73 mg HC/gm C_{org}) and HI (<60 mg HC/gm C_{org}) values (Tables 5 and 6) suggest a poor petroleum source potential for marginally mature to overmature strata (0.43 to 1.5 $\%Ro_{rand}$) on central Graham Island and Skidegate Inlet. Strata in Cumshewa Inlet have some gas source potential (TOC = 1.8 %; QOM = 0.73 mg HC/gm C_{org}; PI = 0.13; HI = 64 mg HC/gm C_{org}). Very high TOC values (10.28 %) indicate reflect organic rich (Type III) horizons in central Graham Island.

Phantom Creek Formation

Limited data suggests that the marginally immature (0.46 $\%Ro_{rand}$) fine grained sandstones and shales of the Phantom Creek Formation are poor to fair oil and gas source rocks (TOC = O.55 %; QOM = 3.9 mg HC/gm C_{org}; PI = 0.16; and HI = 322 mg HC/gm C_{org}). Low PI values suggest partial conversion of kerogen to petroleum (Tables 5 and 6).

YAKOUN GROUP

Graham Island Formation

Marginally mature to overmature (0.48 to 1.5 $\%Ro_{rand}$) shales and siltstones in central Graham Island have low TOC (0.88 to 0.96 %), moderately high QOM (1.17 to 1.94 mg HC/gm C_{org}), and moderately high HI (<385 mg HC/gm C_{org}) values (Tables 5 and 6) suggesting fair oil and gas source potential.

Strata in the Skidegate Inlet area are poor source rocks (TOC = 0.34 %; QOM = 0.26 mg HC/gm C_{org}).

Richardson Bay Formation

The Richardson Bay Formation consists predominantly of volcanic strata with some sedimentary facies of limited lateral extent. The sedimentary strata contain moderate amounts (1.13 % TOC) of Type III organic matter (HI = 45 mg HC/gm C_{org}). Mature strata (1.13 $\%Ro_{rand}$) in Skidegate Inlet have gas

generative potential as suggested by moderate TOC (1.13 %), low QOM (0.63 mg HC/gm c_{org}) and low HI (45 mg HC/gm C_{org}) values (Tables 5 and 6).

MORESBY GROUP

Robber Point Formation

Mature (1.10 $\%Ro_{rand}$) coarse clastics in Skidegate Inlet generally have insufficient amounts of organic carbon (0.78 % TOC), low QOM (0.63 mg HC/gm C_{org}), and low HI (44 mg HC/gm C_{org}) values to be considered hydrocarbon source rocks (Tables 5 and 6).

Newcombe Formation

Mature, massive volcanic sandstone (1.08 $\%Ro_{rand}$) exposed in Skidegate Inlet generally do not have a sufficient TOC (0.51 %) to generate significant amounts of hydrocarbons. Low QOM (0.34 mg HC/gm Corg) and HI (30 mg HC/gm Corg) values suggest poor oil and gas potential (Tables 5 and 6).

Alliford Formation

Mature (1.04 $\%Ro_{rand}$) siltstones exposed in Skidegate Inlet have fair gas source potential as is indicated by moderate TOC (1.1 %), moderate QOM (1.01 mg HC/gm C_{org}), and low HI (80 mg HC/gm C_{org}) and PI (0.2) values (Tables 5 and 6).

LONGARM FORMATION

Low TOC (0.26 %), QOM (0.03 mg HC/gm C_{org}), HI (5 mg HC/gm C_{org}), PI (0.03), and high maturation (3.18 $\%Ro_{rand}$) values suggest poor oil and gas source potential on Moresby Island (Tables 5 and 6). Data is not available for Graham Island.

QUEEN CHARLOTTE GROUP

Haida Formation

Immature to overmature (0.36 to 1.51 $\%Ro_{rand}$) carbonaceous sandstones of the Haida Formation, rich in terrestrial organic matter (0.68 to 2.49 % TOC), have fair gas source potential on Graham Island (QOM <0.67 mg HC/gm C_{org}; HI <65 mg HC/gm C_{org}; and PI <0.27). Generally overmature (4.04 $\%Ro_{rand}$) strata on Morseby Island have poor oil or gas generative potential (TOC = 0.13 %;QOM = 0.02 mg HC/gm C_{org}; and HI = 0 mg HC/gm C_{org}) but may have previously generated gas pre- or syn- plutonic emplacement in the Cretaceous or Tertiary (see Part I).

Skidegate Formation

Generally low TOC (<0.73 %) and QOM (<0.95 mg HC/gm C_{org}) values suggest that immature to overmature (0.4 to 2.94 $\%Ro_{rand}$) Type III (HI <79 mg HC/gm C_{org}) organic matter of the Skidegate Formation has poor to fair gas generative potential on Graham Island (Tables 5 and 6). Low PI values (<0.16) for mature strata suggest partial kerogen conversion to petroleum.

Honna Formation

Conglomerate, sandstone, and shale facies of the Honna Formation on northwest Graham Island contain mature Type III organic matter and have poor hydrocarbon source potential due to low TOC (<0.43 %). Low QOM (0.7 mg HC/gm C_{org}), HI (<60 mg HC/gm C_{org}), and PI (0.09) values suggest no oil source potential, but possible gas source potential (Tables 5 and 6).

SKONUN FORMATION

Siltstone and shale in the Skonun Formation exposed in central Graham Island contain Type II organic matter and have good oil and gas generative potential (TOC=2.47 %; QOM=2.64 mg HC/gm C_{org}; HI=210 mg HC/gm C_{org}; and PI=0.2). Petrographic analysis of coal and lignite samples from six onshore wells penetrating the Skonun Formation indicates that the organic matter is predominantly Type III and composed of vitrinite. Some coals (Type III organic matter) respond differently to Rock-Eval pyrolysis than dispersed Type III organic matter and have HI values which plot between Types II and III organic matter (Peters, 1986). The liquid hydrocarbon generative potential calculated from HI data, therefore, can be overestimated for coals (Peters, 1986). Generally immature (0.27 to 0.48 $\%Ro_{rand}$) Skonun Formation coals have low to moderate QOM values (0.7 to 2.2 mg HC/gm C_{org}) and hence are fair source rocks.

Generally low HI values (64 to 179 mg HC/gm C_{org}) for marginally mature to mature strata suggest that generated hydrocarbons would consist predominantly of gas and some oil. Hydrogen rich resinite (HI > 500 mg HC/gm C_{org}) was observed petrographically which suggests some horizons with good oil source potential. Coals at west Graham Island (Port Louis well) are mature (1.05 $\%Ro_{rand}$); however, low QOM (0.87 mg HC/gm C_{org}), HI (79 mg HC/gm C_{org}), and PI (0.07) values suggest poor hydrocarbon source potential.

Snowdon et al. (in prep.) have correlated bitumens from oil seeps associated with Masset volcanic rocks with Jurassic, Cretaceous, and Tertiary source strata predominantly from Graham Island. Bitumens from Otard and Tian Bay (northwest Graham Island) and from Tar Island (east Moresby Island) contain 18alpha(H)oleanane correlated with Tertiary, Type III organic matter derived from terrestrial higher plant material. Bitumens associated with fractures in Masset volcanics near Lawn Hill on the east coast of Graham Island have also been correlated with Tertiary source strata. Bitumen samples from the King Creek area in central Graham Island appear to be derived from Lower Jurassic source rocks. Bitumens from Cretaceous strata have not yet been systematically studied.

Factors Affecting Lateral Variations in Source Rock Quality

Source rock quality is controlled primarily by the quality, quantity, and DOM of the organic matter. In the Queen Charlotte Islands, the dominant control on the lateral variation in source rock quality for Triassic and Jurassic strata is the DOM of the organic matter, whereas depositional environments are the primary control for Cretaceous and Tertiary strata.

Upper Triassic and Lower Jurassic source strata may have been deposited in Hecate Strait and Dixon Entrance but have not yet been confirmed. Even if the strata were deposited, increased burial depths have probably resulted in the levels of organic maturation exceeding the oil window. Any hydrocarbons that were generated may have migrated into less mature strata and preserved.

High levels of organic maturation due to high heat flow associated with the San Christoval (SCPS), Burnaby Island (BIPS), and Carpenter Bay (CBPS) Plutonic Suites have resulted in hydrocarbon depletion of the organic matter for the grey limestone member of the Kunga Group. Figure 69 illustrates increasing TOC from west to east on south Moresby Island suggesting that the SCPS was the dominant thermal event. Figure 85 shows very low QOM values with no apparent trend.

TOC values for the black limestone member of the Kunga Group increase from east to west (Figure 68) suggesting that pluton emplacement of the BIPS and CBPS were the dominant thermal events on south Moresby Island. TOC values measured on the east side of the BIPS increases from west to east on central Moresby Island suggesting that the pluton emplacement of the BIPS was also the dominant thermal event on central Moresby Island. TOC and QOM (Figure 84) values on northwest Moresby Island increase to the southeast suggesting an offshore source of high heat flow possibly associated with the Langara Island pluton.

The Sandilands Formation on Moresby Island is overmature and has low TOC (Figure 67) and QOM (Figure 83) values with no apparent lateral trend (due to sparse data distribution). High TOC and QOM values in central Graham Island suggest that the strata are very good source rocks. The strata near Rennell Sound are overmature and have significantly reduced TOC and QOM values as a result of high heat flow associated with plutonic activity south of Rennell Sound.

The Ghost Creek Formation has high TOC (Figure 66) and QOM (Figure 82) values indicating very good source potential. High heat flow associated with plutonism near Rennell Sound has increased the level of organic maturation and decreased the hydrocarbon generative potential of the strata near Rennell Sound as suggested by increasing QOM values from north to south and increasing TOC values from south to north.

The Ghost Creek Formation is not exposed south of Cumshewa Inlet and north of Rennell Sound on central Graham Island. Sandilands and Longarm Formations strata are stratigraphically below and

above the Ghost Creek Formation (respectively) are exposed on south Moresby Island and northwest Graham Island suggesting that deposition of the Ghost Creek Formation (and possibly the entire Maude Group) was restricted to central Graham Island and north Moresby Island. If such is the case, the limited areal extent of Ghost Creek Formation source rocks suggests a limited potential for hydrocarbon generation and accumulation.

TOC (Figure 62) and QOM (Figure 78) values for the Whiteaves Formation tend to increase from southwest to northeast in response to high heat flow from plutonism near Rennell Sound. There is insufficient TOC and QOM data to determine trends for the Fannin (Figures 63 and 79), and Phantom Creek (Figures 61 and 77) Formations.

Higher TOC (Figure 59) and QOM (Figure 75) values were obtained from Skidegate Inlet and central Graham Island respectively for the Yakoun and Moresby Groups; however, the paucity of data precludes determination of TOC and QOM trends.

TOC values for the Longarm Formation on Moresby Island (Figure 58) increase from east to west. However, there is no apparent trend in QOM (Figure 74). The paucity of data, however, precludes accurate interpretation.

The Haida Formation increases in TOC from east to west (Figure 57) suggesting decreased amounts of transported terrestrial organic matter basinward from the western edge of Haida deposition. QOM values from northwest Graham Island (Figure 73) increase towards the south away from plutonism on Langara Island. TOC values are generally lower and HI values are generally higher for the Skidegate Formation relative to the Haida Formation (Figure 56). TOC and HI values increase from west to east for the Skidegate Formation suggesting that there was decreased input of terrestrial organic matter and possibly increased input of marine organic matter in a basinward direction. Higher HI values (Figures 46C and 47C) are observed for the Skidegate Formation than in the Haida Formation (Figures 46D and 47D) suggesting

an increased marine component in Skidegate Formation organic matter. QOM values (Figure 72) increase with increasing distance from plutons on Langara Island and Rennell Sound.

TOC (Figure 55) and QOM (Figure 71) values are low for the Honna Formation and the paucity of data precludes the determination of TOC or QOM trends. Similarly, lateral trends in TOC (Figure 54) and QOM (Figure 70) for the Skonun Formation cannot be ascertained due to the paucity of data.

SUMMARY AND CONCLUSIONS

1. For the most part, Cretaceous and Tertiary strata in the Queen Charlotte Islands contain gas prone Type III organic matter with varying degrees of hydrocarbon source potential. The source rock quality is related primarily to the depositional patterns and the level of organic maturity. Triassic and Jurassic strata (where mature) generally contain a mixture of Type II and Type III organic matter with varying degrees of hydrocarbon source potential related to the level of organic maturation. The Kunga Group and Ghost Creek Formation on central and northwest Moresby Island contain abundant oil and gas prone Type II and significant amounts of oil prone Type I organic matter and have very good petroleum generative potential.

2. Triassic strata from Moresby Island presently have poor oil source potential (QOM < 0.08 mg HC/gm Corg; HI < 16 mg HC/gm Corg; PI < 0.08) due to high levels of organic maturation (2.35 to 8.31 $\%Ro_{rand}$) but may have sourced substantial hydrocarbons in the past. High PI (< 0.59) values for overmature strata at Kunga Island suggest hydrocarbon migration into overmature strata. Moderate amounts of residual TOC (< 2.56 %) suggest some gas generative potential remains. The level of organic maturity increases, and TOC decreases from west to east proximal to the BIPS as a result of high heat flow during pluton emplacement.

Mature to overmature Triassic strata from central and northwest Graham Island have very good oil and gas source potential as indicated by high TOC (2.17 to 9.6 %), QOM (< 4.26 mg HC/gm C_{org}), and HI (< 385 mg HC/gm C_{org}) values. Moderate PI values (0.14 to 0.42) and free hydrocarbons suggest partial

conversion of kerogen to petroleum. The hydrocarbon source potential diminishes from east to west with decreasing distance to plutons near Rennell Sound.

3. Jurassic strata from Graham Island and north Moresby Island generally have poor to fair gas generative potential and poor oil source potential. The marginally mature (0.55 $\%Ro_{rand}$) Ghost Creek Formation is a notable exception and has very good oil and gas source potential as evident by moderate TOC (<1.73 %), high QOM (<3.73 mg HC/gm Corg), moderately high HI values (<349 mg HC/gm Corg). Low PI (0.07) values, however, suggest minimal kerogen conversion to petroleum.

4. Cretaceous strata of the Longarm, Haida, and Honna Formations on Moresby Island have poor hydrocarbon source potential due to high levels of organic maturity (<4.04 $\%Ro_{rand}$). Depositional patterns are an important factor controlling the source potential for Cretaceous strata. The Haida Formation on Graham Island contain Type III dispersed organic matter (<2.49 % TOC; HI<79 mg HC/gm C_{org}) and has poor to fair gas source potential but no oil generative potential. The Skidegate Formation contains a greater component of marine Type II organic matter than the Haida Formation and has poor to fair gas potential. The Honna Formation on Graham Island has poor hydrocarbon source potential due to low TOC (<0.43 %).

5. Type II organic matter from siltstone and shale horizons in Skonun Formation strata have good oil and gas generative potential (TOC=2.47 %; QOM=2.64 mg HC/gm Corg; HI=210 mg HC/gm Corg; and PI=0.2). Coals from the Skonun Formation generally have poor hydrocarbon source potential due to low levels of organic maturity (0.27 to 0.48 $\%Ro_{rand}$). Low to moderate HI (64 to 179 mg HC/gm Corg) values for marginally mature to mature coals suggest some gas source potential and oil generative potential. Mature coals at the Port Louis well are poor hydrocarbon sources due to low QOM values (0.87 mg HC/gm Corg). Resinites observed petrographically and associated high HI values (>500 mg HC/gm Corg) suggest some coal horizons have fair to good oil and gas source potential.

REFERENCES

Bustin, R.M. and Gunther, P.R. 1977
Implications of coalification levels, Eureka Sound Formation, northeastern Arctic Canada; Canadian Journal of Earth Sciences, vol. 14, pp. 1588-1597.

Bustin, B.E.B. and Macauley, G., 1988
Organic petrology and Rock-Eval pyrolysis of the Jurassic Sandilands and Ghost Creek Formations, Queen Charlotte Islands; Bulletin of the Canadian Society of Petroleum Geologists (in press).

Cameron, B.E.B. and Tipper, H.W. 1985
Jurassic stratigraphy of the Queen Charlotte Islands, British Columbia; Geological Survey of Canada, Bulletin, v. 365, 49 p.

Cameron, B.E.B. 1987
Significance of lower Jurassic hydrocarbon source rocks in the Cumshewa Inlet area, Queen Charlotte Islands, British Columbia; *in* Current Research, Part A, Geological Survey of Canada, Paper 87-1A, p. 925-928.

Conford, C. 1984
Source rocks and hydrocarbons of the North Sea; *in* Introduction to the Petroleum Geology of the North Sea. ed. K.W. Glennie, London, 1984, 236 pp.

Espitalie, R., Madec, M. and Tissot, B. 1977
Source rock characterization method for petroleum exploration; 9th Annual Offshore Technology Conference, Houston, Texas, p. 439-444.

Espitalie, R., Deroo, G. and Marquis, F. 1985
Rock-Eval pyrolysis and its applications; Institut Francais du Petrole, reprint No. 27299, 132 p.

Peters, K.E. 1986
Guidelines for evaluating petroleum source rocks using programmed pyrolysis; American Association of Petroleum Geologists, 70, p. 318-329.

Tissot, B.P. and Welte, D.H. 1984
Petroleum Occurrence and Formation; Springer-Verlag, Berlin, 699 p.

PART III
APPENDICES

APPENDIX A

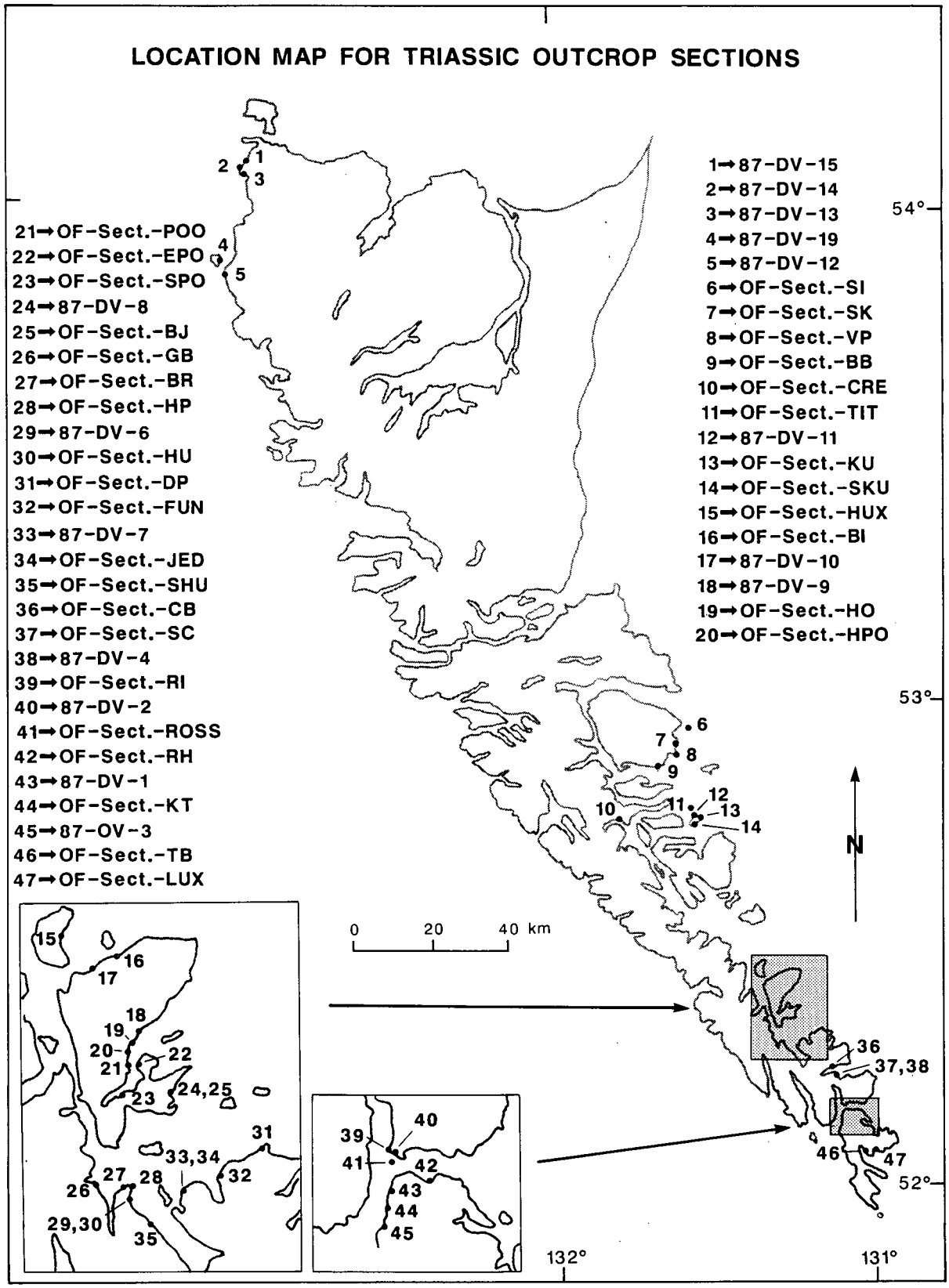

Location map for Triassic outcrop sections

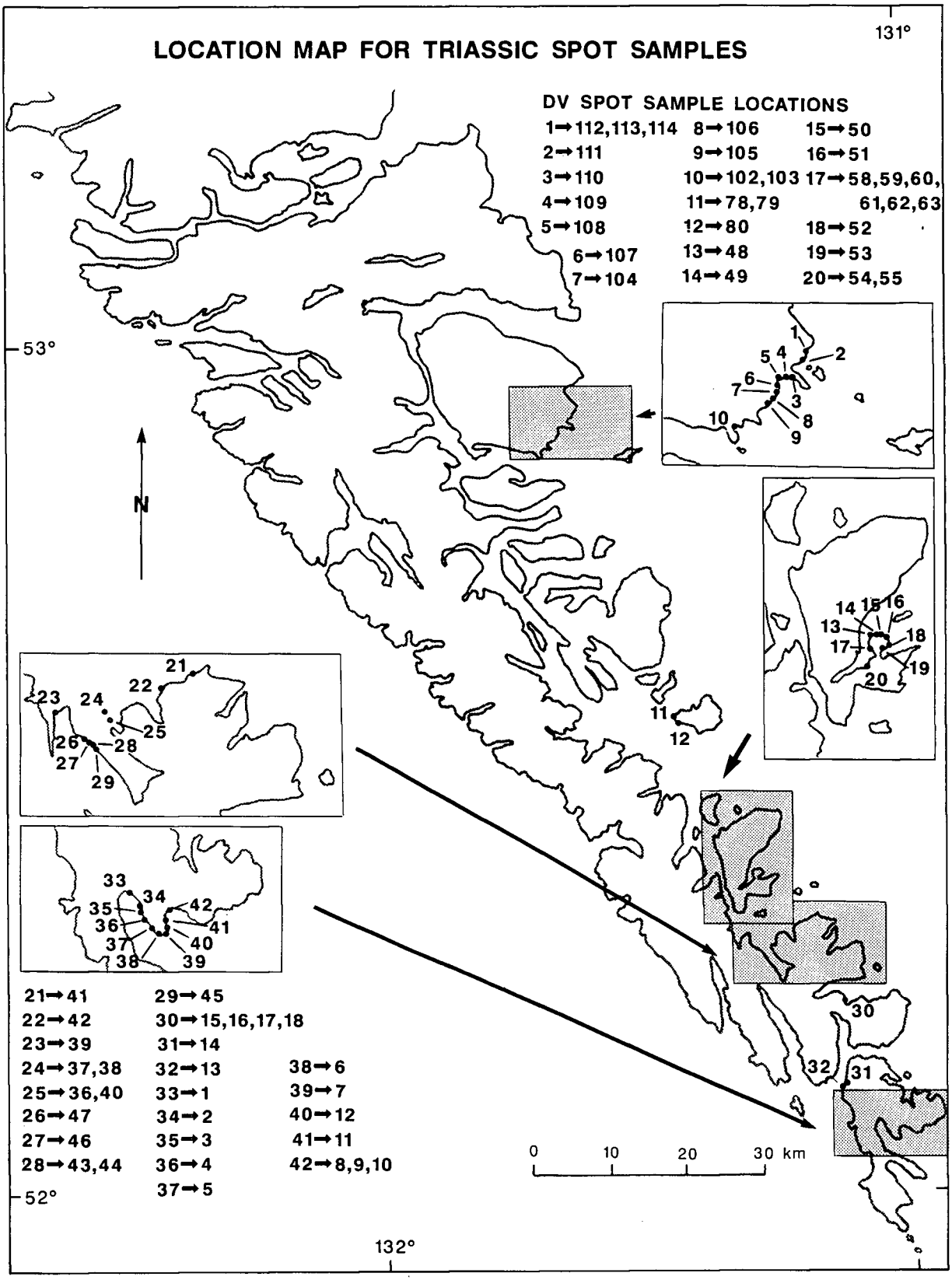

Location map for Triassic spot samples

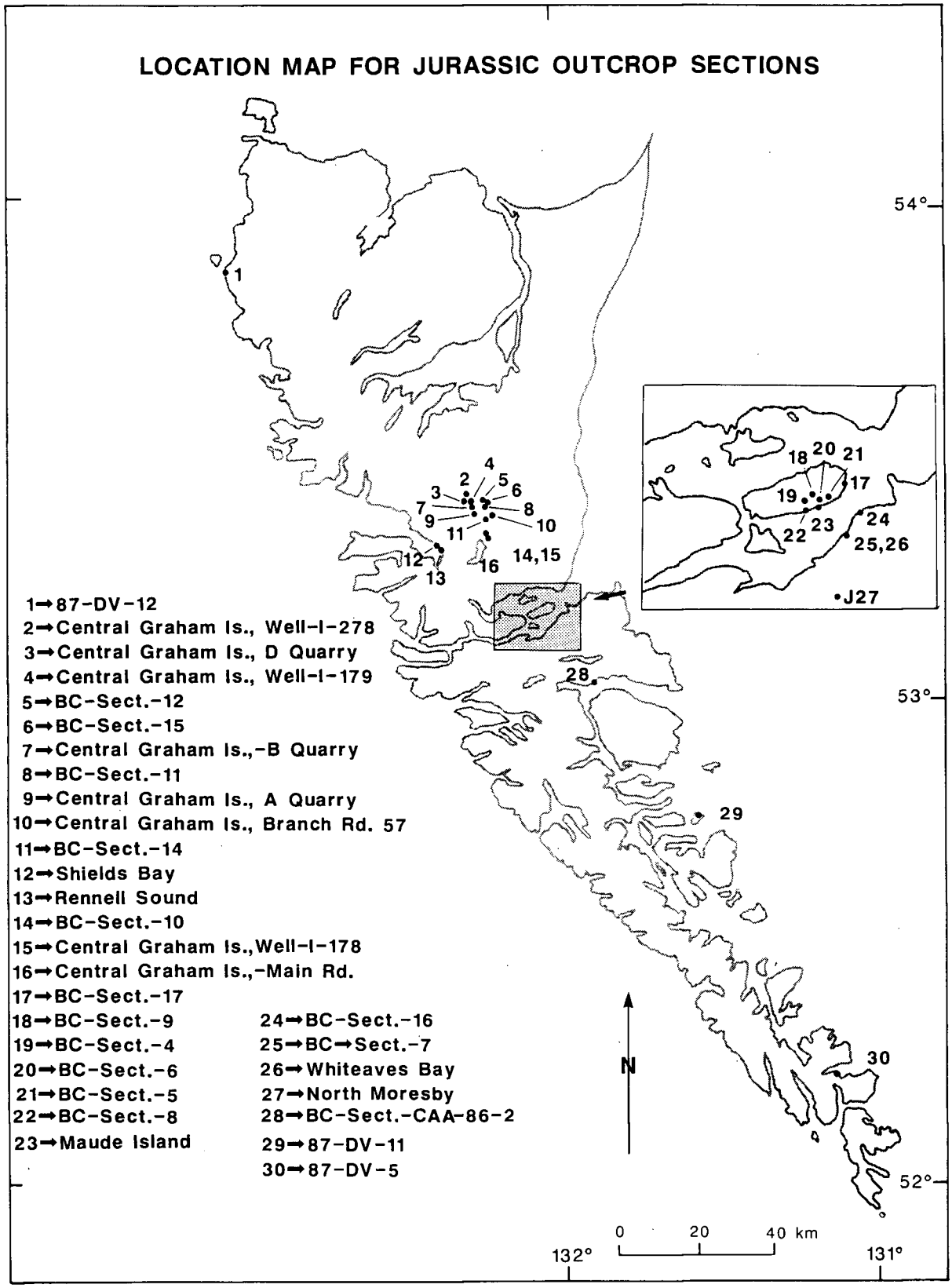

Location map for Jurassic outcrop sections

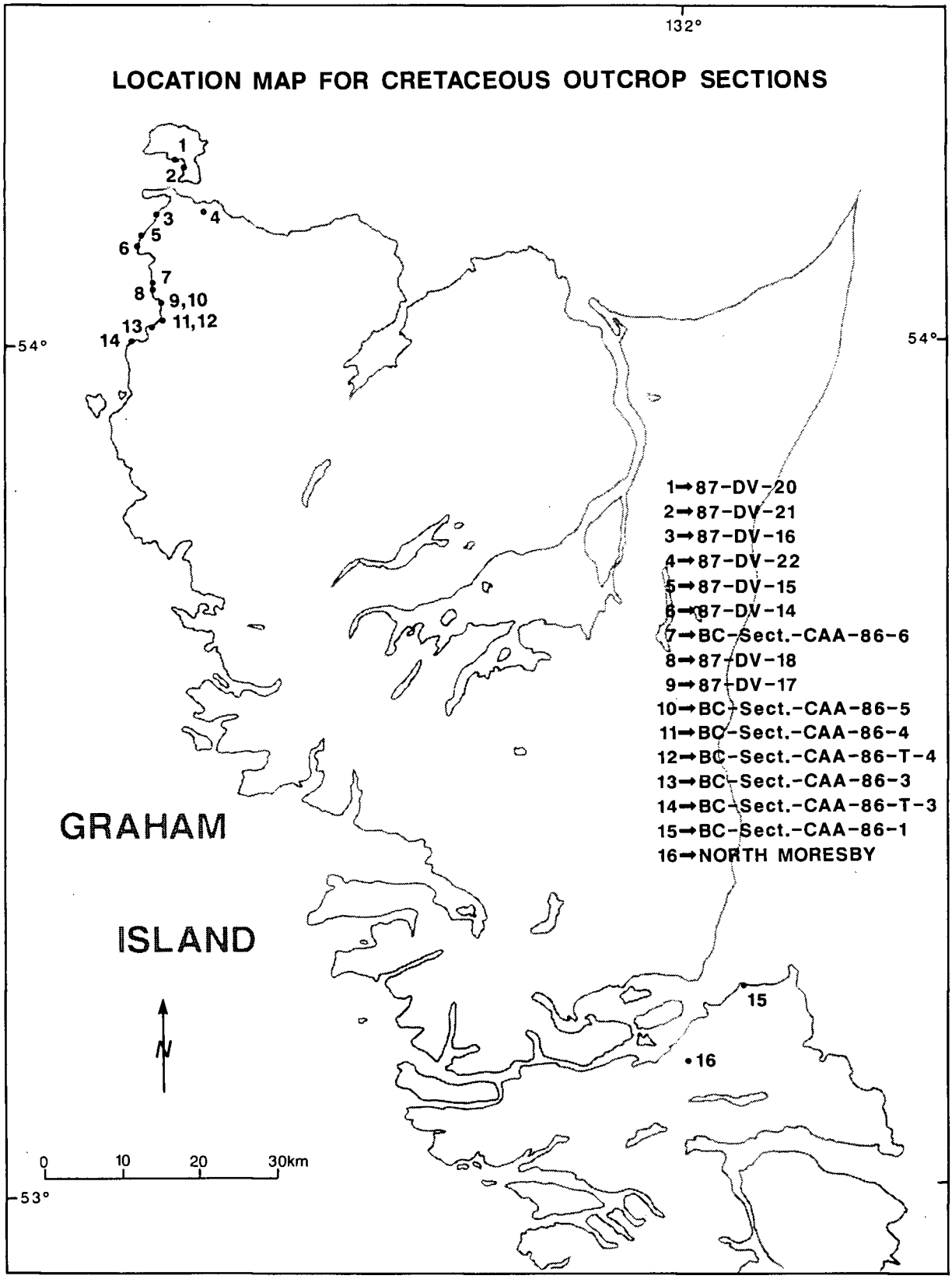

Location map for Cretaceous outcrop sections

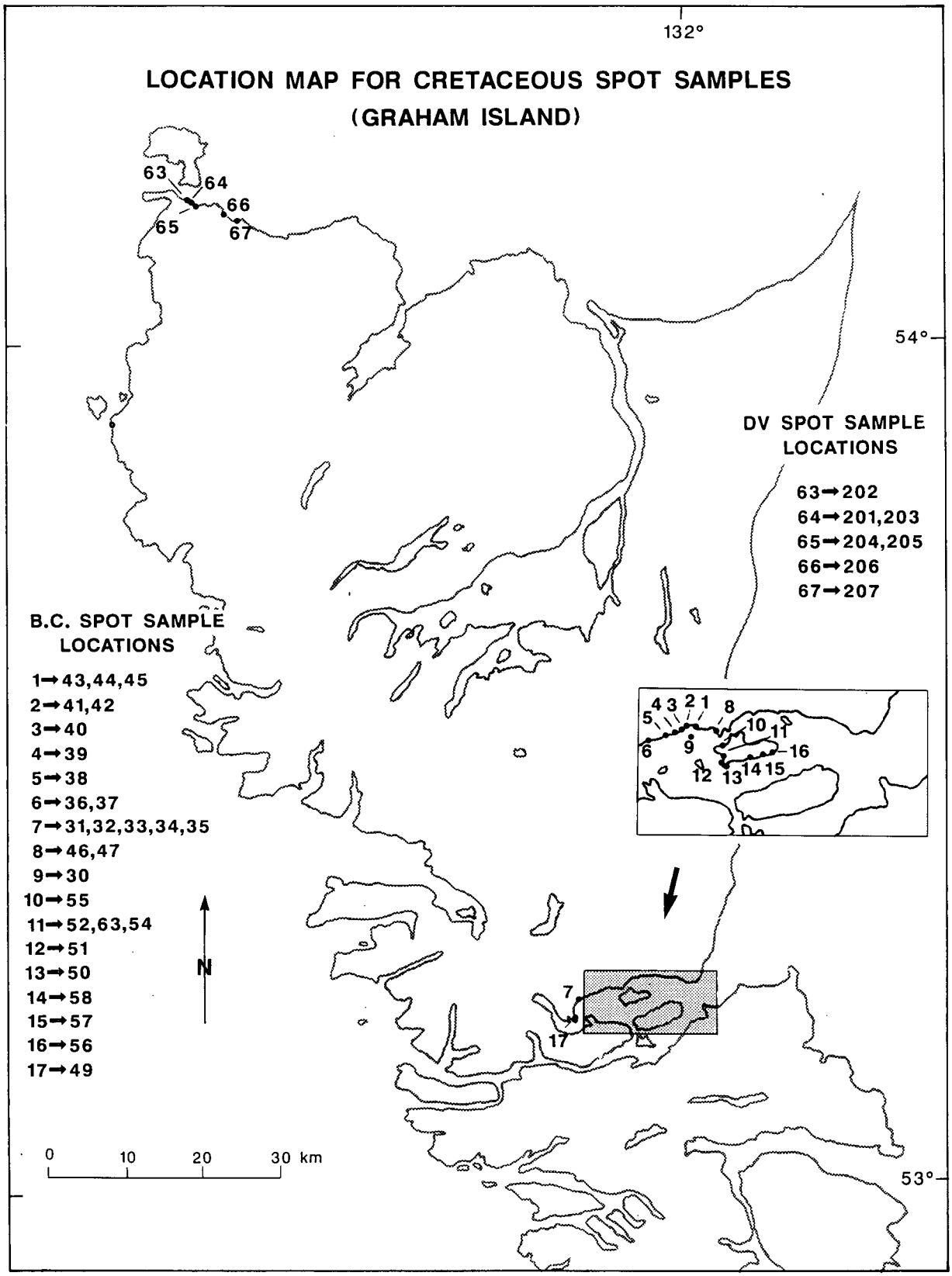

Location map for Cretaceous spot samples (Graham Island)

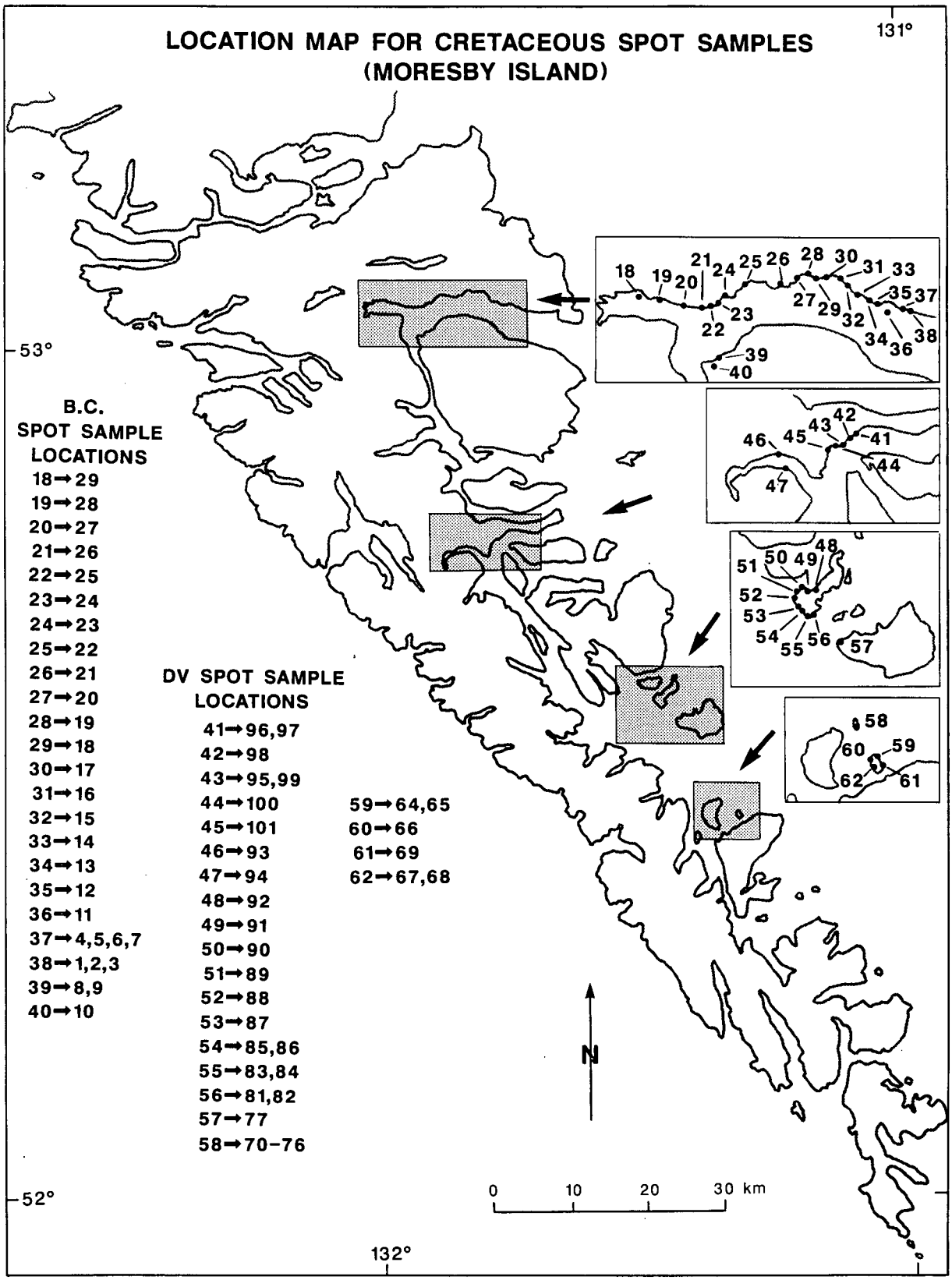

Location map for Cretaceous spot samples (Moresby Island)

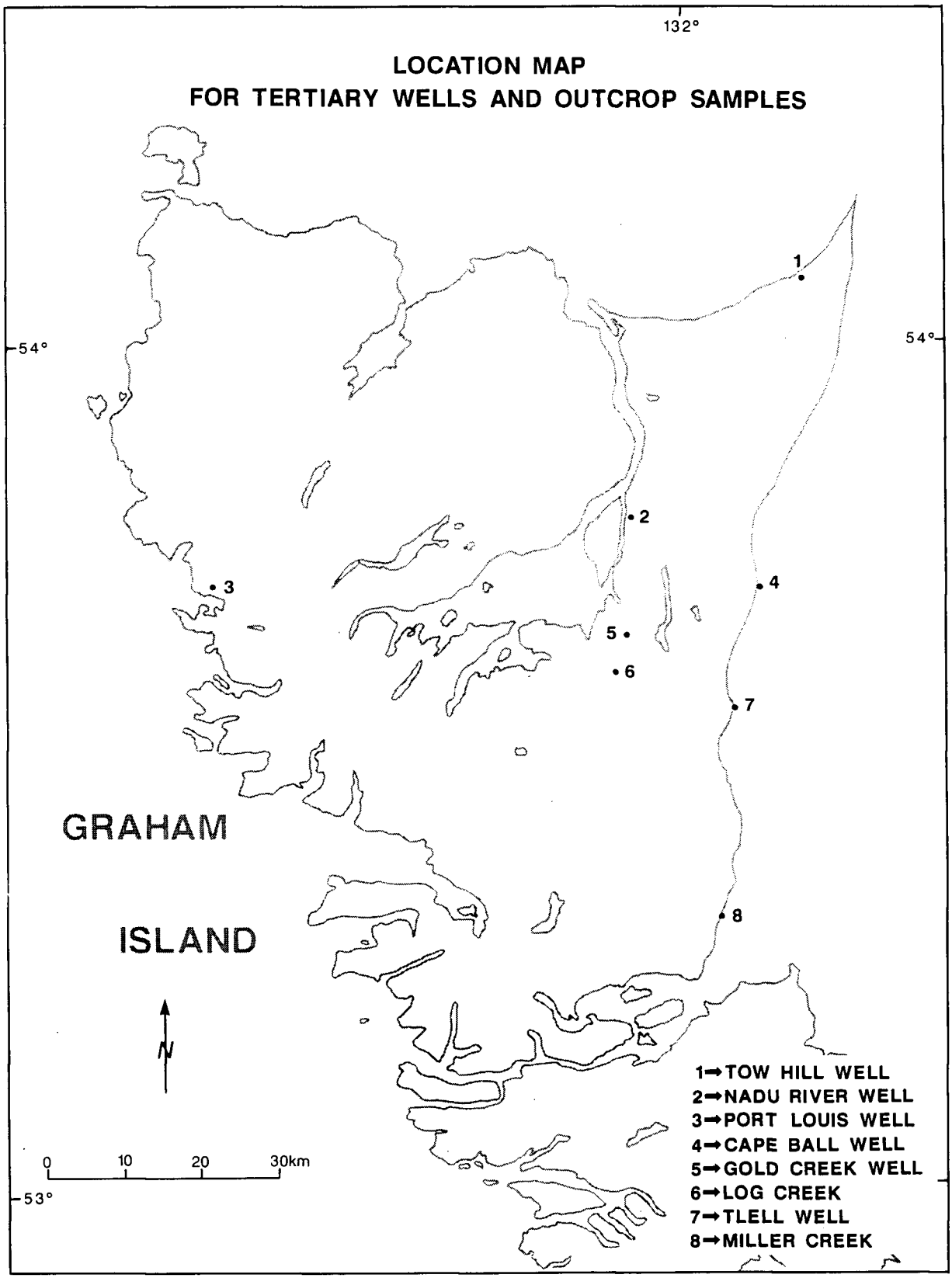

Location map for Tertiary Well and outcrop sections

APPENDIX B

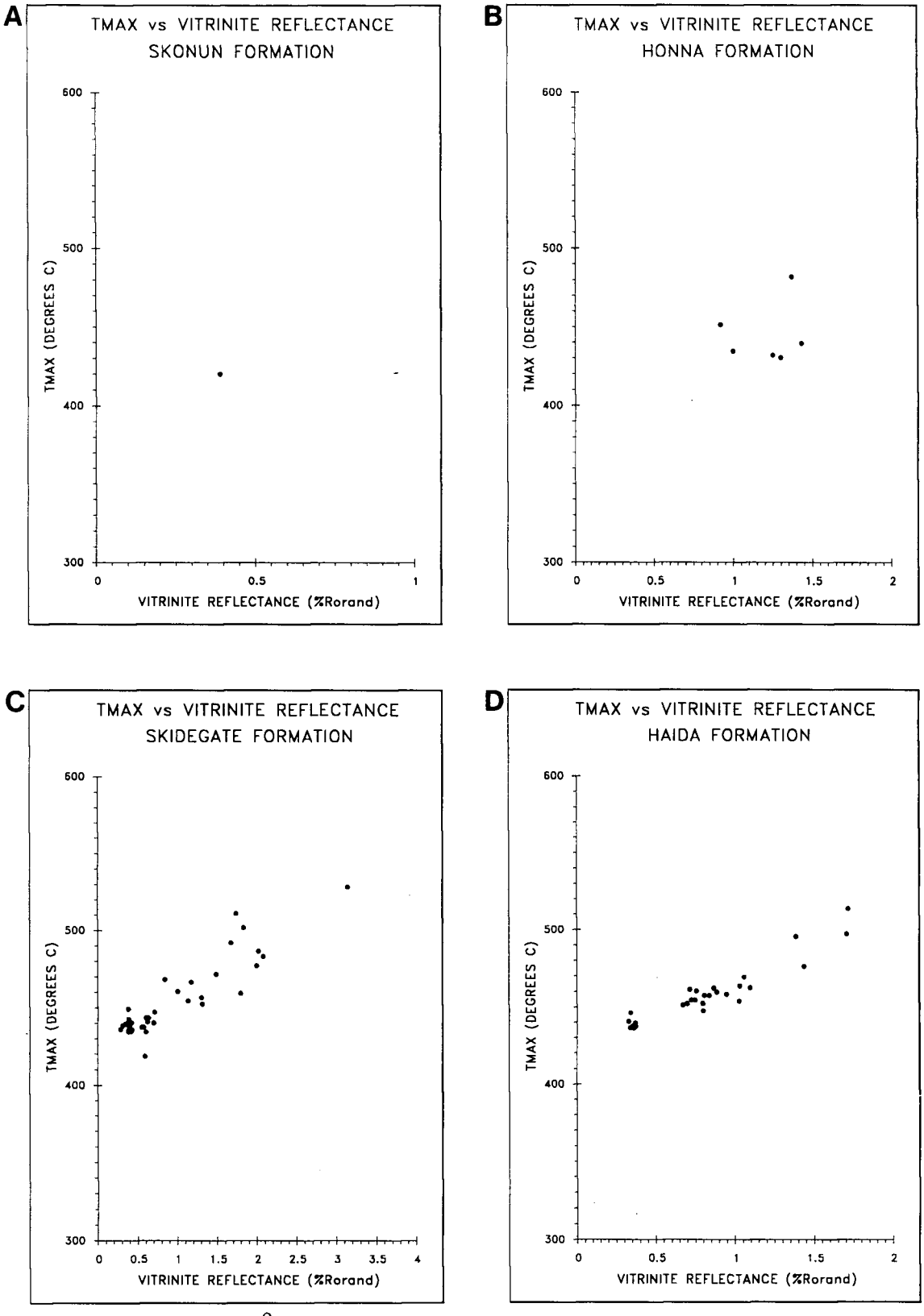

Figure showing the variation of T_{max} (^{O}C) with vitrinite reflectance (%Ro_{rand}): a) Skonun Formation; b) Honna Formation; c) Skidegate Formation; d) Haida Formation

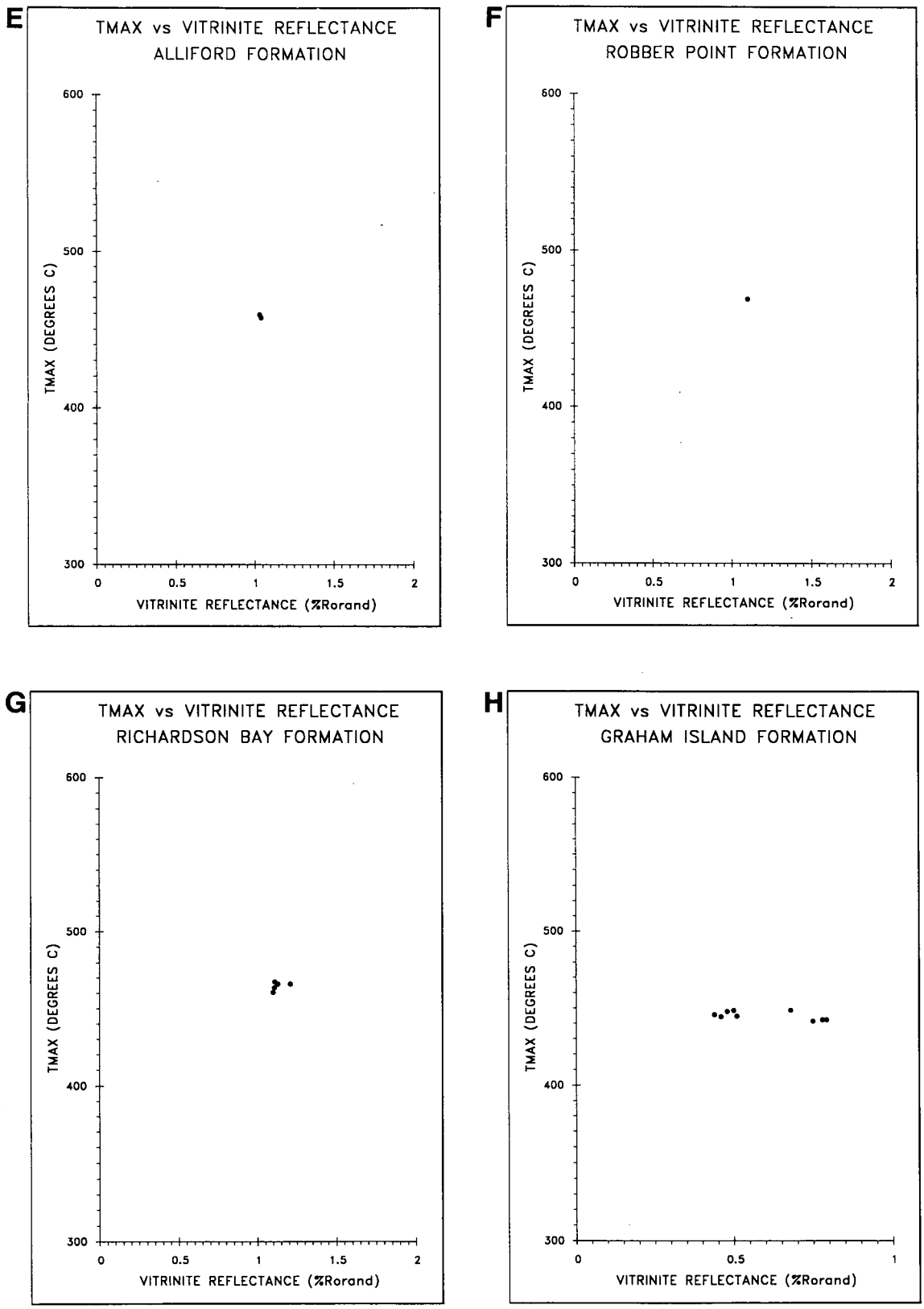

Figure showing the variation of T_{max} (^{O}C) with vitrinite reflectance ($\%Ro_{rand}$): e) Alliford Formation; f) Robber Point Formation; g) Richardson Bay Formation; h) Graham Island

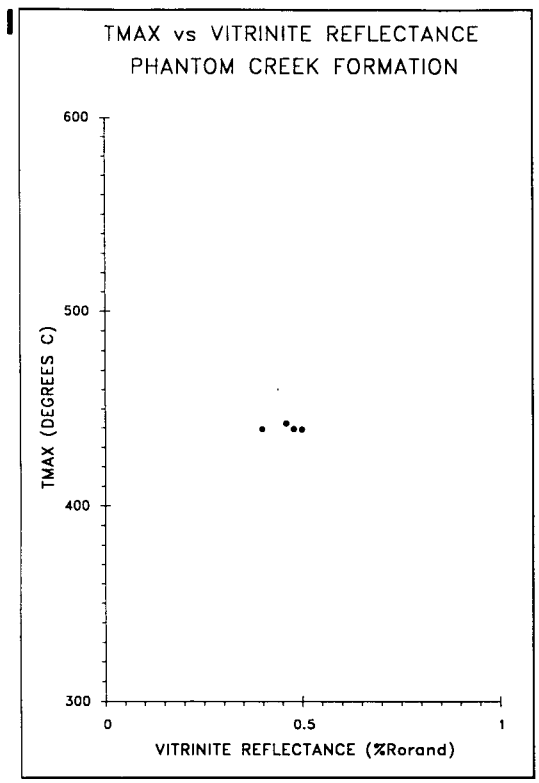

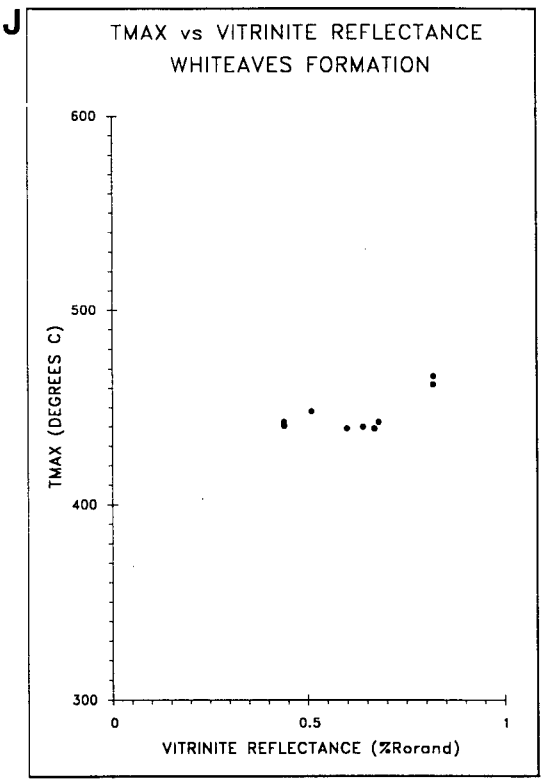

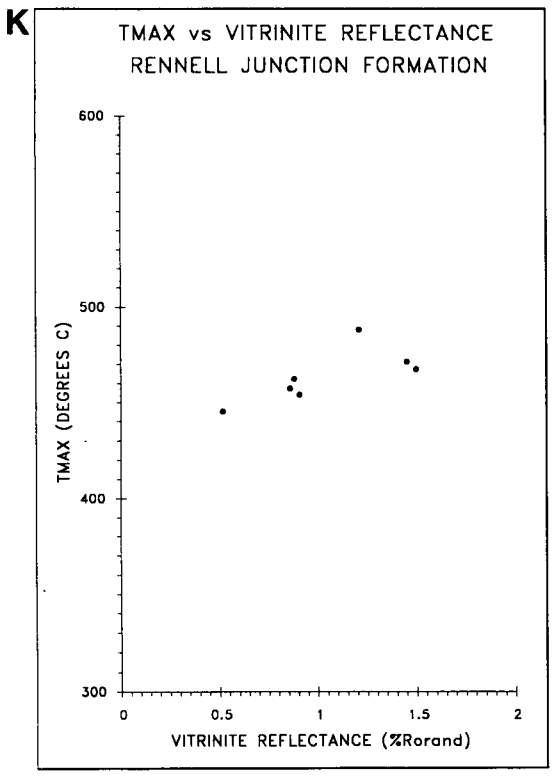

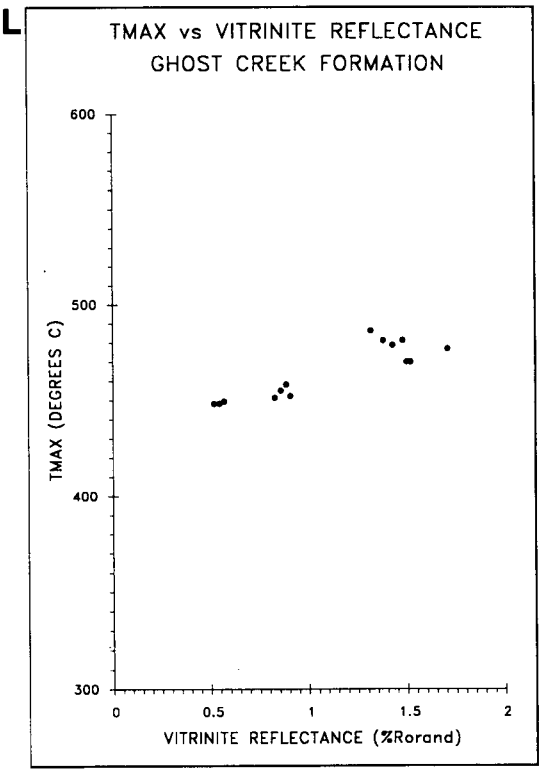

Figure showing the variation of T_{max} (^{O}C) with vitrinite reflectance (%Ro_{rand}): i) Phantom Creek Formation; j) Whiteaves Formation; k) Rennell Junction Formation; l) Ghost Creek Formation

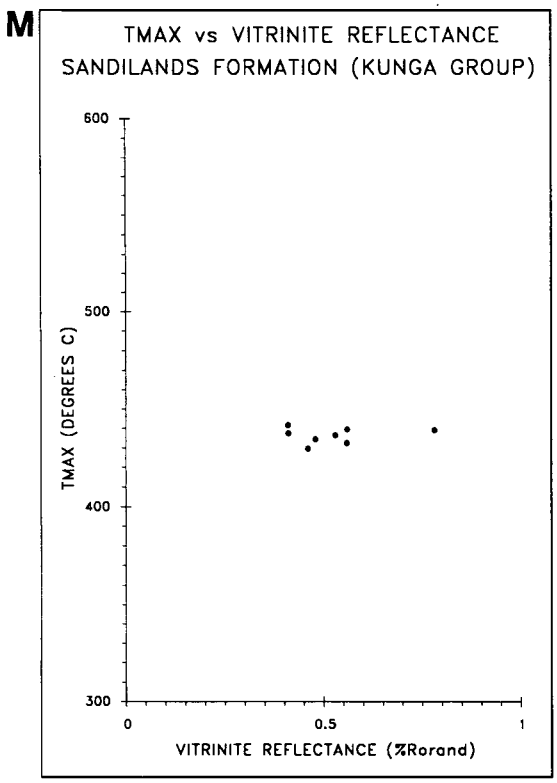

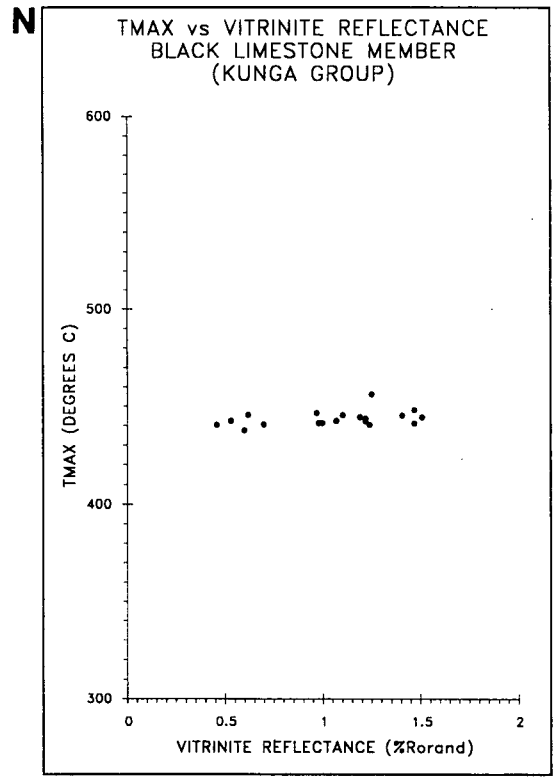

Figure showing the variation of T_{max} (^{o}C) with vitrinite reflectance (%Ro_{rand}): m) Sandilands Formation; n) black limestone member (Kunga Group)